A Graph Theoretic Approach to Matrix Functions and Quantum Dynamics

Pierre-Louis Samuel Benoit Giscard
Keble College, Oxford

A thesis submitted in partial fulfilment of
the requirements for the degree of
Doctor of Philosophy at the University of Oxford

Trinity Term, 2013

Atomic and Laser Physics,
University of Oxford

A graph theoretic approach to matrix functions and quantum dynamics

Pierre-Louis Samuel Benoit Giscard, Keble College, University of Oxford
Trinity Term 2013

Abstract

Many problems in applied mathematics and physics are formulated most naturally in terms of matrices, and can be solved by computing functions of these matrices. For example, in quantum mechanics, the coherent dynamics of physical systems is described by the matrix exponential of their Hamiltonian. In state of the art experiments, one can now observe such unitary evolution of many-body systems, which is of fundamental interest in the study of many-body quantum phenomena. On the other hand the theoretical simulation of such non-equilibrium many-body dynamics is very challenging. In this thesis, we develop a symbolic approach to matrix functions and quantum dynamics based on a novel algebraic structure we identify for sets of walks on graphs.

We begin by establishing the graph theoretic equivalent to the fundamental theorem of arithmetic: all the walks on any finite digraph uniquely factorise into products of prime elements. These are the simple paths and simple cycles, walks forbidden from visiting any vertex more than once. We give an algorithm that efficiently factorises individual walks and obtain a recursive formula to factorise sets of walks. This yields a universal continued fraction representation for the formal series of all walks on digraphs. It only involves simple paths and simple cycles and is thus called a path-sum.

In the second part, we recast matrix functions into path-sums. We present explicit results for a matrix raised to a complex power, the matrix exponential, matrix inverse, and matrix logarithm. We introduce generalised matrix powers which extend desirable properties of the Drazin inverse to all powers of a matrix.

In the third part, we derive an intermediary form of path-sum, called walk-sum, relying solely on physical considerations. Walk-sum describes the dynamics of a quantum system as resulting from the coherent superposition of its histories, a discrete analogue to the Feynman path-integrals. Using walk-sum we simulate the dynamics of quantum random walks and of Rydberg-excited Mott insulators. Using path-sum, we demonstrate many-body Anderson localisation in an interacting disordered spin system. We give two observable signatures of this phenomenon: localisation of the system magnetisation and of the linear magnetic response function.

Lastly we return to the study of sets of walks. We show that one can construct as many representations of series of walks as there are ways to define a walk product such that the factorisation of a walk always exist and is unique. Illustrating this result we briefly present three further methods to evaluate functions of matrices. Regardless of the method used, we show that graphs are uniquely characterised, up to an isomorphism, by the prime walks they sustain.

Acknowledgements

This thesis would not have been possible without my Scatcherd European Scholarship and further financial support from EPSRC. To my advisor Dieter Jaksch, I owe the intellectual freedom necessary to explore such different subjects as graph theory, matrix functions and quantum dynamics. I realise I must have been quite difficult to supervise given my tendency to do only what I have in mind !

I would like to warmly thank Professor Michele Benzi for the many inspiring discussions I have had with him regarding the method of path-sum and the exponential decay of matrix functions. His help played an important role in shaping the SIAM article reporting on the method of path-sums. I also had the chance to meet and discuss with Stefan Güttel, Nick Higham and Nick Trefethen, all of whom greatly expanded my mathematics horizon. I am particularly thankful to Professor Higham's Numerical Analysis Group of the University of Manchester for twice inviting me to present and discuss my work.

During my time in Dieter's group, I have enjoyed the company of many people, some of whom I have had the opportunity to work with: Sarah Al-Assam, Felix Binder, Stephen Clark, Giovanni Cotugno, Samuel Denny, Uwe Dorner, Tom Grujic, Tomi Johnson, Martin Kiffner, Juan-Jose Mendoza Arenas, Sebastian Meznaric (I liked his essay), Mark Mitchison, Edward Owen and Dimitrios Trypogeorgos. I have particularly enjoyed working with Simon Thwaite and Vince Choo. With Simon, I shared the awe of seeing path-sums work for the first time, when the why and how were still enshrouded in mystery. I sincerely wish he would consider staying in academia. Vince has a very communicating enthusiasm for mathematics: I urge him to cultivate it and to stubbornly develop his many ideas ! I look forward to further work with him on *the project*.

Finally, I most indebted to my wife Marlène for her unfailing support and her many sacrifices so I could work in the very best conditions. To her and to my son Armand, I dedicate the present thesis.

Contents

List of Figures

Chapter 1
Introduction

The underlying physical laws necessary for the mathematical theory of a large part of physics and the whole of chemistry are completely known, and the difficulty is only that the exact application of these laws leads to equations much too complicated to be soluble.

P. A. M. Dirac

This thesis is concerned with the development of a novel technique to evaluate matrix functions and its applications to the simulation of quantum dynamics. In this chapter we present the motivations and origins of our approach and present an outline of the thesis.

1.1 Simulating quantum systems

The quality of control over atomic systems in state of the art experiments is such that one can now address and observe quantum evolutions of individual atoms in optical-lattices [1, 2, 3, 4]. Additionally, coherent inter-atomic and light-matter interactions can be made strong enough to occur on short time-scales compared to incoherent processes. This reveals the system's unitary evolution at the individual constituent level which is of fundamental interest in the study of quantum many-body phenomena. Several applications like quantum simulation and quantum computing schemes also rely on this information [5]. On the other hand, the theoretical simulation on a classical computer of such non-equilibrium many-body dynamics is very challenging, mainly due to the exponentially large number of relevant degrees of freedom.

Indeed, consider a "simple" quantum many-body systems comprising N motionless particles, each with 2 energy levels. Then a full description of the system wavefunction ψ requires 2^N complex numbers. This means that a direct exact solution of Schrödinger's equation, which describes the coherent dynamics of non-relativistic quantum systems, is not accessible above $N \gtrsim 20$. Even worse, for $N \gtrsim 250$, this number exceeds the number of atoms in the observable universe so even storing ψ on a computer memory is impossible. For these reasons the problem of simulating the time evolution of quantum many-body systems is believed to be intractable. Pondering on this difficulty, R. Feynman proposed the idea of using quantum systems to simulate other quantum systems, thereby turning the exponential scaling of ψ to our advantage [6]. The validity of this idea was firmly established by S. Lloyd some 14 years later when he showed that universal quantum computation was possible [7]. This means that it is in principle possible to simulate any quantum system relying

on a few universal quantum operations. The same year A. Steane presented the first quantum error correcting code [8], demonstrating that quantum computation was not fundamentally impaired by decoherence. Finally the recognition that quantum computers could efficiently solve problems beyond the scope of classical computers [9, 10] initiated a strong research effort toward physical realisation of quantum computers.

In the mean time, nothing precludes in principle the existence of a small set of parameters, whose cardinality scales polynomially with N, and from which one could construct a good description of ψ. This observation in conjunction with the recent experimental advances has led to the rise of an active area of research focused on the development of theoretical methods to approximate the coherent dynamics of quantum systems. Among the most well known techniques are the Density Matrix Renormalisation Group method [11], related Tensor Network approaches [12] and the Time-Evolving Block Decimation method [13]. These techniques have proven very successful in their respective domains of applicability (e.g. [14, 15, 16]), i.e. mostly 1D systems with nearest neighbour interactions. On the contrary, and in spite of extensive work in the field, very few techniques exist in 2D and 3D [17, 18] and for systems exhibiting long-range interactions.

As part of this ongoing effort, we develop in this thesis a new technique which aims at simulating the coherent time dynamics of quantum systems, termed path-sum, and which is not limited by the system geometry. This technique is based on novel results concerning the algebraic structure of sets of walks on graphs. Below, we explain the origins of this approach.

1.2 Of graphs and matrices

The *"most basic result of algebraic graph theory"* [19] states that the powers of the adjacency matrix of a graph generate all the walks on this graph [20]. This extends to weighted graphs, with matrix powers giving the sum of the weights of the walks on the graph [19]. To clarify these notions, consider the following example:

$$\mathsf{A} = \begin{pmatrix} a_{11} & a_{12} \\ a_{21} & a_{22} \end{pmatrix} \longrightarrow (\mathsf{A}^3)_{11} = \underbrace{a_{11}^3} + \underbrace{a_{12}a_{22}a_{21}} + \underbrace{a_{12}a_{21}a_{11}} + \underbrace{a_{11}a_{12}a_{21}}$$

Each term contributing to $(\mathsf{A}^3)_{11}$ can be seen as the weight of a walk whose trajectory we read off the subscripts. For example, $a_{11}a_{12}a_{21}$ is the weight of the walk $w : 1 \to 2 \to 1 \to 1$, which is illustrated above. Note how the ordering of the walk (left-to-right) differs from the ordering of the weights (right-to-left). In this representation, individual entries of the matrix A represent the weight of an edge of the graph, e.g. a_{12} is the weight of the edge from vertex 2 to vertex 1. The weight of a walk is then the product of the weights of the edges it traverses.

The fundamental equivalence between walks on graphs and matrix powering illustrated above, bore many fruits over the years, in particular in combinatorics [19, 21, 22] and probability theory [23, 24]. In quantum mechanics, it manifests itself most simply through Schrödinger's equation. This equation is

$$\mathsf{H}|\psi(t)\rangle = i\hbar \frac{d}{dt}|\psi(t)\rangle,$$

where $\hbar$ is the reduced Planck constant, $|\psi(t)\rangle$ is a vector describing the instantaneous state of the system at time t written here in Dirac notation and H is the Hamiltonian matrix, a representation of the system energy, which we shall always consider to be finite and discrete. The Schrödinger equation is formally solved by the matrix exponential $\mathsf{U}(t) = \exp(-i\mathsf{H}t/\hbar)$ and $|\psi(t)\rangle = \mathsf{U}(t)|\psi(0)\rangle$. The matrix exponential $\mathsf{U}(t)$ has a power series representation which naturally involves powers of the Hamiltonian H^n, $n \geq 0$. By virtue of the equivalence between walks and matrix powers, the matrix exponential $\mathsf{U}(t)$ is thus seen to be equivalent to a series of walks.

The observation underlying this thesis is that if sets of walks can be endowed with an algebraic structure such that there exists a small set of objects generating all the walks, then one might accelerate the convergence of a walk series by expressing it using these generators. By the equivalence between walks and matrix powers, this would in turn imply novel representations for functions of matrices, and in particular for the matrix exponential $\mathsf{U}(t)$ which describes the dynamics of quantum systems. This is what we achieve in the thesis.

1.3 Thesis overview

The thesis is organised as follows. We begin in Chapter 2 by constructing an algebraic structure for sets of walks on arbitrary finite graphs. In particular, we demonstrate that all the walks factorise uniquely into nesting products of prime walks. Nesting is a product operation between walks which we introduce. It follows that these primes are the generators of all walks. By factoring sets of walks into products of sets of primes, we obtain a recursive formula which describes the set of all walks using only the prime generators. Thanks to this result we derive a universal continued fraction representation for the formal series of all walks between any two vertices of a graph. We give illustrating examples and applications for these results.

In Chapter 3 we present the main application of the prime factorisation of walks: the method of path-sums. By relying on the correspondence between matrix multiplications and walks on graphs, we show that any primary matrix function $f(\mathsf{M})$ of a finite matrix M can be expressed solely in terms of the prime walks sustained by a graph $\mathcal{G}$ describing the sparsity structure of M. We give explicit formulae for the matrix raised to a complex power, the matrix exponential, the inverse and the matrix logarithm. We then provide examples and mathematical applications of these results in the realm of matrix computations.

In Chapter 4, we present a largely self-contained approach to the dynamics of quantum systems, called walk-sum. Walk-sum is equivalent to an intermediate result obtained in the derivation of the path-sum expression for the matrix exponential. In this chapter however it is derived using solely physical arguments. These provide a physical meaning to the methods of walk-sums and path-sums. We illustrate walk-sum by determining analytically the dynamics of continuous time quantum random walks. Our results remain valid for non-Abelian walks, where the internal and external dynamics of the 'walking' particle are coupled. Finally, we investigate the dynamics of systems of strongly interacting Rydberg-excited Mott insulators using walk-sums.

In Chapter 5 we use the method of path-sums to demonstrate Anderson localisation in a strongly interacting quantum many-body system. We present two observable manifestations of many-body localisation over the real-lattice: i) localisation of the number of up-spins present at any time on certain finite sets of sites in the lattice; and ii) localisation of the correlations between the spins at these sites.

In Chapter 6 we construct the meta theory which encompasses the results of Chapter 2. More precisely, we demonstrate that as long as the factorisation of walks into irreducible walks always exists and is unique, then one is free to design new, arbitrary, walk products which lead to novel representations of functions of matrices. We obtain three further methods to evaluate formal series of walks and matrix functions using prime factorisations: the primitive series, the edge-sums and the language equations for matrix functions. Using the connection between walks on graphs and words of formal languages underpinning the language equations, we conclude the chapter by showing that the prime walks sustained by a graph uniquely characterise it.

Finally, in Chapter 7 we summarise the results of the present thesis and discuss their potential future applications.

Reading guide

The present thesis covers and connects three different fields of research: graph theory, linear algebra and quantum physics. We therefore give a brief guide of the thesis for the reader to access his or her chapters of interest.

▶ The reader interested in the graph theoretic aspects of the thesis can read Chapters 2 and 6 for an exposition of the prime factorisation of walks.

▶ The reader interested in the computation of matrix functions and the applications of the prime factorisation of walks in linear algebra can directly read Chapter 3 upon accepting Theorem 2.3.4, p. 17.

▶ The reader interested in the dynamics of quantum systems will read Chapters 4 and 5. In particular, Chapter 4 is largely self-contained and gives physical meanings to the various mathematical expressions appearing in our approach. In contrast, Chapter 5 which is devoted to many-body localisation in interacting quantum systems, make strong use of the results of Chapters 2, 3 and 4 and cannot be understood without the concepts introduced in these chapters.

Chapter 2
Prime Factorisation on Graphs

Everyone engaged in research must have had the experience of working with feverish and prolonged intensity to write a paper which no one else will read or to solve a problem which no one else thinks important and which will bring no conceivable reward – which may only confirm a general opinion that the researcher is wasting his time on irrelevancies.

N. Chomsky

In this chapter we show that the formal series of all walks between any two vertices of any finite digraph or weighted digraph $\mathcal{G}$ is given by a universal continued fraction of finite depth involving the simple paths and simple cycles of $\mathcal{G}$. A simple path is a walk forbidden to visit any vertex more than once, a simple cycle is a cycle whose internal vertices are all distinct and different from the initial vertex. We obtain an explicit formula giving this continued fraction. Our results are based on an equivalent to the fundamental theorem of arithmetic: we demonstrate that arbitrary walks on $\mathcal{G}$ *uniquely* factorise into nesting products of simple paths and simple cycles. Nesting is a walk product which we define. We show that the simple paths and simple cycles are the prime elements of the set of all walks on $\mathcal{G}$ equipped with the nesting product. We give an algorithm producing the prime factorisation of individual walks. We obtain a recursive formula producing the prime factorisation of sets of walks.

The work in this chapter forms the basis of an article that is currently under review for publication in *Forum of mathematics Sigma*, Cambridge University Press.

2.1 Introduction

Walks on graphs are pervasive mathematical objects that appear in a wide range of fields from mathematics and physics to engineering, biology and social sciences [22, 19, 25, 26, 27, 28, 29]. Walks are perhaps most extensively studied in the context of random walks on lattices [30], e.g. because they model physical processes [31]. At the same time, it is difficult to find general 'context-free' results concerning walks and their sets. Indeed, properties obeyed by walks are almost always strongly dependent on the graph on which the walks take place. For this reason, many results concerning walks on graphs are dependent on the specific context in which they appear.

In this chapter, we study walks and their sets on digraphs and weighted digraphs as separate mathematical entities and with minimal context. We demonstrate that they obey non-trivial properties that are largely *independent* of the digraph on which the walks take place. Foremost amongst these properties is the existence and uniqueness of the factorisation of walks into products of primes, which we show are the simple paths and simple cycles of the digraph, also known as self-avoiding walks and self-avoiding polygons, respectively. Another such property is the existence of a universal form for the formal series of all walks between any two vertices of any finite (weighted) digraph: it is a continued fraction of finite depth, which we provide. This universal continued fraction has already found applications in the fields of matrix functions and quantum dynamics, which we present in Chapters 3, 4 and 5. We believe that the unique factorisation property will also find applications in the field of graph characterisation as we show in Chapter 6. Indeed, a digraph is, up to an isomorphism, uniquely determined by the set of all walks on it [32]. The prime factorisation of walk sets which we provide will reduce the difficulty of comparing walk sets to comparing sets of primes, of which there is only a finite number on any finite digraph.

Usually, the product operation on the set $W_{\mathcal{G}}$ of all walks on a digraph $\mathcal{G}$ is the concatenation. It is a very liberal operation: the concatenation $a \circ b$ of two walks is non-zero whenever the final vertex of a is the same as the initial vertex of b. This implies that both the irreducible and the prime elements of the set of all walks equipped with the concatenation product, denoted $(W_{\mathcal{G}}, \circ)$, are the walks of length 1, i.e. the edges of $\mathcal{G}$. Consequently, the factorisation of a walk w on $\mathcal{G}$ into concatenations of prime walks is somewhat trivial. For this reason, we abandon the operation of concatenation and introduce instead the nesting product, symbol $\odot$, as the product operation between walks on $\mathcal{G}$. Nesting is a much more restrictive operation than concatenation, in that the nesting of two walks is non-zero only if the walks satisfy certain constraints. As a result of these constraints, the irreducible and prime elements of $(W_{\mathcal{G}}, \odot)$, obtained upon replacing the concatenation with the nesting product, are the simple paths and simple cycles of $\mathcal{G}$, rather than its edges. The rich structure that is consequently induced on walk sets is at the origin of the universal continued fraction formula for formal series of walks.

This chapter is organised as follows. In §2.2, we present the notation and terminology used throughout the chapter. In particular we define the nesting product and establish its properties in §2.2.2. In §2.3 we give the main results of the present chapter: (i) existence and uniqueness of the factorisation of any walk into nesting products of primes, the simple paths and simple cycles; (ii) an algorithm producing the prime factorisation of individual walks; (iii) a recursive formula factorising walk sets into nested sets of primes; (iv) a universal continued fraction representing factorised formal series of walks on digraphs and weighted digraphs; and (v) identification of the depth of this continued fraction with the length of the longest prime. The results of this section are proven in sections 2.5.2, 2.5.3 and 2.5.4. Finally, in §2.4 we present examples illustrating our results.

2.2 Required Concepts

2.2.1 Notation and terminology

A *directed graph* or *digraph* is a set of *vertices* connected by *directed edges* also known as arrows. An arrow e starts at vertex $s(e)$ and terminates at vertex $t(e)$, which we write $e:\ s(e) \to t(e)$ or $(s(e)t(e))$. Throughout this thesis, we let $\mathcal{G} = \big(\mathcal{V}(\mathcal{G}), \mathcal{E}(\mathcal{G})\big)$ be a finite digraph with $\mathcal{V}(\mathcal{G})$ its vertex set and $\mathcal{E}(\mathcal{G})$ its edge set. This digraph may contain self-loops but not multiple edges, i.e. we restrict ourselves to at most one directed edge from $\alpha \in \mathcal{V}(\mathcal{G})$ to $\omega \in \mathcal{V}(\mathcal{G})$. The latter restriction is solely for the purpose of notational clarity, and all of our results can be straightforwardly extended to cases where $\mathcal{G}$ contains multiple edges. We denote the vertices of $\mathcal{G}$ by numbers or Greek letters $\alpha, \beta, \ldots$. The digraph obtained by deleting vertices $\alpha, \beta, \ldots$ and all edges incident on these vertices from $\mathcal{G}$ is written $\mathcal{G}\backslash\{\alpha, \beta, \ldots\}$.

A *walk* w of length $\ell(w) = n \geq 1$ from μ_0 to μ_n on $\mathcal{G}$ is a left-to-right sequence $(\mu_0\mu_1)(\mu_1\mu_2)\cdots(\mu_{n-1}\mu_n)$ of n contiguous directed edges. This walk starts at μ_0 and terminates at μ_n We describe w by its vertex string $(\mu_0\,\mu_1\,\mu_2\,\cdots\,\mu_n)$ or by its vertex-edge sequence $(\mu_0)(\mu_0\mu_1)(\mu_1)\cdots(\mu_{n-1}\mu_n)(\mu_n)$. If $\mu_0 = \mu_n$, w is termed a *cycle* or closed walk; otherwise, w is an open walk. When necessary, the initial vertex of w will be denoted by $h(w)$, and the final vertex by $t(w)$. The set of all walks on $\mathcal{G}$ is denoted by $W_{\mathcal{G}}$, and the set of all walks from vertex μ_0 to vertex μ_n on $\mathcal{G}$ is denoted by $W_{\mathcal{G};\,\mu_0\mu_n}$.

A *simple path* is an open walk whose vertices are all distinct. The set of all the simple paths on $\mathcal{G}$ is denoted by $\Pi_{\mathcal{G}}$. The set of simple paths from α to ω is denoted by $\Pi_{\mathcal{G};\,\alpha\omega}$. On any finite digraph $\mathcal{G}$, these sets are finite.

A *simple cycle* is a cycle whose internal vertices are all distinct and different from the initial vertex. The set of all the simple cycles on $\mathcal{G}$ is denoted by $\Gamma_{\mathcal{G}}$, while the set of simple cycles off a specific vertex α is denoted by $\Gamma_{\mathcal{G};\,\alpha}$. On any finite digraph $\mathcal{G}$, these sets are finite.

A *trivial walk* is a walk of length 0 off any vertex $\mu \in \mathcal{V}(\mathcal{G})$, denoted by (μ). A trivial walk is both a simple path and a simple cycle. Note, trivial walks are different from the *empty walk*, denoted 0, whose length is undefined.

The *concatenation* is a non-commutative product operation between walks. Let $w_1 = (\alpha_1 \cdots \alpha_\ell) \in W_{\mathcal{G}}$ and $w_2 = (\beta_1 \cdots \beta_{\ell'}) \in W_{\mathcal{G}}$. Then the concatenation of w_1 with w_2 is defined as

$$w_1 \circ w_2 = \begin{cases} (\alpha_1 \cdots \alpha_\ell\, \beta_2 \cdots \beta_{\ell'}), & \text{if } \alpha_\ell \equiv \beta_1, \\ 0, & \text{otherwise.} \end{cases} \tag{2.1}$$

The empty walk is absorbing for the concatenation, i.e. $\forall w \in W_{\mathcal{G}},\ w \circ 0 = 0 \circ w = 0$.

Remark 2.2.1 (Concatenating sets)**.** Let A and B be two sets of walks on $\mathcal{G}$. Then we write $A \circ B$ for the set obtained by concatenating every element of B into every element of A.

Let $\mathfrak{V} = \{V\}$ be a collection of vector spaces, each of arbitrary finite dimension, such that $\mathfrak{V}$ is in one to one correspondence with the vertex set $\mathcal{V}(\mathcal{G})$ of a finite directed graph $\mathcal{G}$. For simplicity we designate by $V_\mu \in \mathfrak{V}$ the vector space associated to vertex $\mu \in \mathcal{V}(\mathcal{G})$. Let $\mathfrak{F} = \{\varphi_{\mu\to\nu} : V_\mu \to V_\nu\}$ be a collection of linear mappings in one to one correspondence with the edge set $\mathcal{E}(\mathcal{G})$ of $\mathcal{G}$. We associate the linear mapping $\varphi_{\nu\leftarrow\mu} \in \mathfrak{F}$ to the directed edge from μ to ν. Then $\mathfrak{G} = (\mathfrak{V}, \mathfrak{F})$ is a representation of the directed graph $\mathcal{G}$, which in this context is also called a *quiver* [33, 34]. The representation of a walk $w = (\alpha_1\alpha_2\cdots\alpha_\ell) \in W_\mathcal{G}$ is the linear mapping φ_w obtained from the composition of the linear mappings representing the successive edges traversed by the walk $\varphi_w = \varphi_{\alpha_\ell\leftarrow\alpha_{\ell-1}} \circ \cdots \circ \varphi_{\alpha_3\leftarrow\alpha_2} \circ \varphi_{\alpha_2\leftarrow\alpha_1}$. The representation of a trivial walk (μ) is the identity map 1_μ on V_μ and the representation of the empty walk 0 is the 0 map.

Remark 2.2.2. The utility of the quiver as a representation of a digraph is explained in Remark 2.2.5, p. 12.

A *weighted digraph* $(\mathcal{G}, \mathrm{W})$ is a digraph $\mathcal{G}$ paired with a weight function W that assigns a weight $\mathrm{W}[e]$ to each directed edge e of $\mathcal{G}$. We let the weight of a directed edge from μ to ν, denoted $\mathsf{w}_{\nu\mu} = \mathrm{W}[(\mu\nu)]$, be a d_ν-by-d_μ complex matrix representing the linear mapping $\varphi_{\nu\leftarrow\mu}$. Furthermore, we impose that $\mathrm{W}[0] = 0$ and $\mathrm{W}[(\mu)] = \mathsf{I}_\mu$, the identity matrix of dimension d_μ. For two directed edges e_1 and e_2 such that $e_1 \circ e_2 \neq 0$, we let

$$\mathrm{W}[e_1 \circ e_2] = \mathrm{W}[e_2]\mathrm{W}[e_1]. \tag{2.2}$$

Note that the ordering of the weights when two edges are concatenated is suitable for the multiplication of their weights to be carried out. The *weight of a walk* $w \in W_\mathcal{G}$, denoted $\mathrm{W}[w]$, is the right-to-left product of the weights of the edges it traverses. Since walks are in one to one correspondence with linear mappings, for any two walks w, w' satisfying $h(w) = h(w')$ and $t(w) = t(w')$ we define the sum $w + w'$ as the object whose representation is the linear mapping which is sum of the two linear maps representing w and w', $\varphi_{w+w'} = \varphi_w + \varphi_{w'}$. It follows that

$$\mathrm{W}\big[w + w'\big] = \mathrm{W}\big[w\big] + \mathrm{W}\big[w'\big]. \tag{2.3}$$

We require the empty walk to be the neutral element of the addition operation $+$, i.e. $w + 0 = w$ and $\mathrm{W}\big[w + 0\big] = \mathrm{W}[w]$.

The *characteristic series* of $W_{\mathcal{G};\,\alpha\omega}$ is the formal series [35]

$$\Sigma_{\mathcal{G};\,\alpha\omega} = \sum_{w \in W_{\mathcal{G};\,\alpha\omega}} w. \tag{2.4}$$

In other words, the coefficient of w in $\Sigma_{\mathcal{G};\,\alpha\omega}$, denoted $(\Sigma_{\mathcal{G};\,\alpha\omega}, w)$, is 1 if $w \in W_{\mathcal{G};\,\alpha\omega}$ and 0 otherwise. If it exists, the weighted characteristic series $\mathrm{W}[\Sigma_{\mathcal{G};\,\alpha\omega}]$ is the series of all walk weights.

Remark 2.2.3 (More general weights)**.** It is possible to generalise the definitions of quiver and of weighted digraph to the case where the weight of an edge from μ

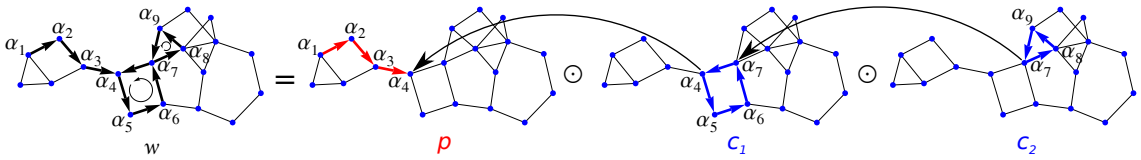

Figure 2.1: An example of nesting: the walk $w = \alpha_1\alpha_2\alpha_3\alpha_4\alpha_5\alpha_6\alpha_7\alpha_8\alpha_9\alpha_7\alpha_4$ is obtained upon inserting the simple cycle $c_2 = \alpha_7\alpha_8\alpha_9\alpha_7$ into $c_1 = \alpha_4\alpha_5\alpha_6\alpha_7\alpha_4$ and then into the simple path $p = \alpha_1\alpha_2\alpha_3\alpha_4$, that is $w = p \odot \big(c_1 \odot c_2\big)$.

to ν is any morphism $\phi_{\nu\leftarrow\mu} : V_\mu \to V_\nu$ in an additive category $\mathcal{C}$ from an object V_μ, associated with the vertex μ, to an object V_ν, associated with the vertex ν. Then all the results of this chapter hold upon requiring that the matrix of morphisms $(\mathsf{M})_{\nu\mu} = \phi_{\nu\leftarrow\mu}$ be invertible. This remark is based on an observation of [36].

2.2.2 The nesting product

We now turn to the definition and properties of the nesting product. Nesting is more restrictive than concatenation; in particular, the nesting of two walks will be non-zero only if they obey the following property:

Definition 2.2.1 (Canonical property)**.** Consider $(a, b) \in W_{\mathcal{G}}^2$ with $b = \beta\,\beta_2\,\cdots\,\beta_q\,\beta$ a cycle off β, and $a = \alpha_1\,\alpha_2\,\cdots\beta\cdots\,\alpha_k$ a walk that visits β at least once. Let $\alpha_j = \beta$ be the last appearance of β in a. Then the couple (a, b) is canonical if and only if one of the following conditions holds:

(i) a and b are cycles off the same vertex β; or

(ii) $\{\alpha_{i<j} \neq \beta\} \cap b = \emptyset$; that is, no vertex other than β that is visited by a before α_j is also visited by b.

Definition 2.2.2 (Nesting product)**.** Let $(w_1, w_2) \in W_{\mathcal{G}}^2$. If the couple (w_1, w_2) is not canonical, we define the nesting product to be $w_1 \odot w_2 = 0$. Otherwise, let $w_1 = (\eta_1\,\eta_2\cdots\beta\cdots\eta_{\ell_1})$ be a walk of length ℓ_1 and let $w_2 = (\beta\,\kappa_2\cdots\kappa_{\ell_2}\,\beta)$ be a cycle of length ℓ_2 off β. Then the operation of nesting is defined by

$$\odot : W_{\mathcal{G}} \times W_{\mathcal{G}} \;\to\; W_{\mathcal{G}}, \tag{2.5a}$$

$$(w_1, w_2) \;\to\; w_1 \odot w_2 = (\eta_1\,\eta_2\cdots\beta\,\kappa_2\cdots\kappa_{\ell_2}\,\beta\cdots\eta_{\ell_1}). \tag{2.5b}$$

The walk $w_1 \odot w_2$ of length $\ell_1 + \ell_2$ is said to consist of w_2 nested into w_1. The vertex sequence of $w_1 \odot w_2$ is formed by replacing the *last* appearance of β in w_1 by the entire vertex sequence of w_2.

▶ Nesting is non-commutative and non-associative: for example, $11 \odot 131 = 1131$, while $131 \odot 11 = 1311$, and $\big(12 \odot 242\big) \odot 11 = 11242$, while $12 \odot \big(242 \odot 11\big) = 0$.

▶ Nesting coincides with concatenation for cycles off the same vertex. Let $(c_1, c_2) \in W^2_{\mathcal{G};\alpha\alpha}$, then $c_1 \odot c_2 = c_1 \circ c_2$. Consequently nesting is associative over the cycles, $(c_1 \odot c_2) \odot c_3 = c_1 \odot (c_2 \odot c_3) = c_1 \odot c_2 \odot c_3$ where $c_3 \in W_{\mathcal{G};\alpha\alpha}$. This in turn implies power-associativity over the cycles and we simply write c^p for the nesting of a cycle c with itself p times, e.g. $1212121 = 121 \odot 121 \odot 121 = 121^3$. We interpret c^0 as the trivial walk off $h(c)$.

▶ Let $\mu \in \mathcal{V}(\mathcal{G})$. Consider the trivial walk (μ) and observe that for any cycle $w \in W_{\mathcal{G}}$ visiting μ we have $(\mu) \odot w = w \odot (\mu) = w$. Therefore we say that a trivial walk is a local identity element on the cycles. For any open walk $w' \in W_{\mathcal{G}}$ visiting μ, we have $w' \odot (\mu) = w'$ and we say that a trivial walk is a local right-identity element on the open walks.

Remark 2.2.4 (Nesting sets)**.** Let A and B be two sets of walks on $\mathcal{G}$. Then we write $A \odot B$ for the set obtained by nesting every element of B into every element of A.

Definition 2.2.3 (Kleene star and nesting Kleene star)**.** Let $\alpha \in \mathcal{V}(\mathcal{G})$ and let $E_\alpha \subseteq W_{\mathcal{G};\alpha\alpha}$. Set $E^0_\alpha = \{(\alpha)\}$ and $E^i_\alpha = E^{i-1}_\alpha \circ E_\alpha$ for $i \geq 1$. Then the *Kleene star* of E_α, denoted E^*_α, is the set of walks formed by concatenating any number of elements of E_α, that is $E^*_\alpha = \bigcup_{i=0}^{\infty} E^i_\alpha$ [37]. The *nesting Kleene star* of E_α, denoted $E^{\odot *}_\alpha$, is the equivalent of the Kleene star with the concatenation replaced by the nesting product: $E^{\odot *}_\alpha = \bigcup_{i=0}^{\infty} E^{\odot i}_\alpha$ where $E^{\odot 0}_\alpha = \{(\alpha)\}$ and $E^{\odot i}_\alpha = E^{\odot(i-1)}_\alpha \odot E_\alpha$ for $i \geq 1$. Since nesting coincides with concatenation for cycles off the same vertex, the nesting Kleene star coincide with the usual Kleene star $E^{\odot *}_\alpha = E^*_\alpha$. Thus, from now on we do not distinguish between the two.

Finally, with the nesting product comes a notion of divisibility. This notion plays a fundamental role in the identification of irreducible and prime walks:

Definition 2.2.4 (Divisibility)**.** Let $(w, w') \in W^2_{\mathcal{G}}$. We say that w' divides w, and write $w' \,|\, w$, if and only if $\exists\, (a, b) \in W^2_{\mathcal{G}}$ such that either $w = (a \odot w') \odot b$ or $w = a \odot (w' \odot b)$.

2.2.3 The nesting near-algebra

Having established the properties of the nesting product, we now turn to determining the structure it induces on the sets of walks and their characteristic series. In order for the latter to be defined, we need to equip walk sets with an addition. To this end, and in the spirit of the path algebra $K\mathcal{G}$ [38], we want to construct a K-algebra with the set of walks $W_{\mathcal{G}}$ as basis but equipped with the nesting product instead of the concatenation. However left-distributivity of the nesting product with respect to addition does not hold (§2.5.1). Therefore, we define instead a near K-algebra equipped with the nesting product.

Definition 2.2.5 (Near K-algebra [38])**.** Let K be an algebraic closed field and A a set. Let $+$ and $\bullet$ be an addition and a product operation defined between elements

Layer 1	**Layer 2**	**Layer 3**
Near-algebra $K\mathcal{G}_{\odot}$	Quiver $\mathfrak{V}$	Matrix space $\mathbb{C}^{n\times n}$
Walk w	Mapping φ_w	Matrix M_{φ_w}
$w_{1+2} = w_1 + w_2$	$\varphi_{w_{1+2}} = \varphi_{w_1} + \varphi_{w_2}$	$\mathsf{M}_{\varphi_{w_{1+2}}} = \mathsf{M}_{\varphi_{w_1}} + \mathsf{M}_{\varphi_{w_2}}$
Concatenation $w_{1\circ 2} = w_1 \circ w_2$	Composition $\varphi_{w_{1\circ 2}} = \varphi_{w_2} \circ \varphi_{w_1}$	Multiplication $\mathsf{M}_{\varphi_{w_{1\circ 2}}} = \mathsf{M}_{\varphi_{w_2}} . \mathsf{M}_{\varphi_{w_1}}$
Formal inverse w^{-1}	Composition inverse $\varphi_{w^{-1}} = \varphi_w^{(-1)}$	Matrix inverse $\mathsf{M}_{\varphi_{w^{-1}}} = \mathsf{M}_{\varphi_w}^{-1}$

Table 2.1: Correspondences between the three layers of representation used in this thesis.

of A, respectively. Then we say that $(A, +, \bullet)$ forms a near K-algebra if and only if $(A, +)$ is an abelian group, the $\bullet$ product is compatible with the elements of K and right distributive with respect to $+$.

Definition 2.2.6 (Nesting near-algebra)**.** Let K be an algebraically closed field. The nesting near-algebra $K\mathcal{G}_{\odot} = (W_{\mathcal{G}}, +, \odot)$ is a near K-algebra. Its support set is the set of walks on $\mathcal{G}$ and with the product of two walks w, w' given by the nesting product $w \odot w'$.

Remark 2.2.5 (Three layers of representation)**.** While we have defined an addition and a product operation between walks on digraphs, these operations can give rise to rather abstract objects. For example, let w_1 and w_2 be two walks with identical end points. Then, the object $w_{1,2} = w_1 + w_2$ exists but seems rather difficult to comprehend. To resolve this difficulty, we use the notion of quiver, introduced in §2.2.1 and which facilitates the rigorous manipulation of sums and products of walks. For example, it is easier to understand $w_{1,2}$ as the object whose representation on the quiver $\mathfrak{V}$ is the linear map $\varphi_{w_{1,2}} = \varphi_{w_1} + \varphi_{w_2}$. In turn, the linear mappings of the quiver have representations in terms of matrices, which allow direct manipulation of sums, products and inverse of mappings. In the present study we therefore use these three layers: i) the basic layer is the near K-algebra $K\mathcal{G}_{\odot}$ and comprises the walks, their sums, products and we will see, their formal inverses; ii) these objects are then represented by linear mappings on the quiver, which constitutes our second layer; and finally iii) the third layer comprises the matrix representations of these mappings. Correspondences between these layers are given on Table 2.1.

2.2.4 Irreducible and prime walks

We are now ready to identify the irreducible and prime elements of $(W_{\mathcal{G}}, \odot)$. Following standard definitions [39, 40], a walk $w \in W_{\mathcal{G}}$ is *irreducible* if, whenever $\exists\, a \in W_{\mathcal{G}}$ with $a \,|\, w$, then either a is trivial, or $a = w$ up to nesting with trivial walks (i.e. local identities). In the opposite situation, we say that w is *reducible*. A walk $w \in W_{\mathcal{G}}$ is *prime* with respect to nesting if and only if for all $(a, b) \in W_{\mathcal{G}}^2$ such that $w \,|\, a \odot b$ then $w \,|\, a$ or $w \,|\, b$. The irreducible and prime elements of $(W_{\mathcal{G}}, \odot)$ are identified by the following result:

Proposition 2.2.1. *The set of irreducible walks is exactly* $\Pi_{\mathcal{G}} \cup \Gamma_{\mathcal{G}}$. *The irreducible walks are the prime elements of* $(W_{\mathcal{G}}, \odot)$.

Remark 2.2.6 (Identifying the simple paths and simple cycles)**.** The simple paths and simple cycles of the digraph $\mathcal{G}$ can be systematically obtained via the powers of its nilpotent adjacency matrix [41, 42]. The nilpotent adjacency matrix $\bar{\mathsf{A}}_{\mathcal{G}}$ is constructed by weighting the adjacency matrix A of $\mathcal{G}$ with formal variables ζ_e, one for each directed edge e and such that: i) $[\zeta_e, \zeta_{e'}] = 0$ for any two edges $(e, e') \in \mathcal{E}(\mathcal{G})$; and ii) $\zeta_e^2 = 0$ for all edges $e \in \mathcal{E}(\mathcal{G})$. From this last property, it follows that only the simple paths and simple cycles a non-zero coefficient in powers of $\bar{A}_{\mathcal{G}}$.

We defer the proof of Proposition 2.2.1 to §2.5.2. Having established the definition and properties of the nesting product as well as the irreducible and prime elements it induces in $(W_{\mathcal{G}}, \odot)$, we turn to the factorisation of individual walks and walk sets.

2.3 Prime Factorisation on Digraphs

In this section, we present the main results of this chapter. First, we present the equivalent to the fundamental theorem of arithmetic on digraphs and we give an algorithm factoring walks into nesting products of primes. Second, we give a formula for factoring the set of walks $W_{\mathcal{G};\,\alpha\omega}$ between any two vertices of $\mathcal{G}$ into nesting products of sets of primes. Third, we give a universal form for the prime factorisation of the characteristic series of all walks between any two vertices of any finite digraphs. Fourth, we give an equivalent relation for weighted digraphs. As we will see, these two universal forms are continued fractions of finite depth over the simple paths and simple cycles of the digraph. Finally, we relate the depth of the continued fractions with the length of the longest simple path. All the results of this section are proven in §2.5.2–2.5.4 and examples illustrating their use are provided in §2.4.

2.3.1 The fundamental theorem of arithmetic on digraphs

The fundamental theorem of arithmetic is arguably the most important result in the field of number theory [43]. It establishes the central role played by the prime numbers and has many profound consequences on the properties of integers. We

now present its analogue for individual walks on arbitrary digraphs. We begin by stating the conditions under which two factorisations of a walk into nesting products of shorter walks are equivalent.

Definition 2.3.1 (Factorisation of a walk)**.** Let $w \in W_{\mathcal{G}}$. A factorisation of the walk w, denoted $\mathfrak{f}(w)$, is a way of writing w using nesting products of at least two walks, called the factors.

Definition 2.3.2 (Equivalent factorisations)**.** Let $w \in W_{\mathcal{G}}$. We say that two factorisations $\mathfrak{f}_1(w)$ and $\mathfrak{f}_2(w)$ of a walk w are equivalent, denoted $\mathfrak{f}_1(w) \equiv \mathfrak{f}_2(w)$, if and only if one can be obtained from the other through the reordering of parentheses and factors, and up to nesting with trivial walks, without modifying w. Equivalent factorisations have the same non-trivial factors.

Definition 2.3.3 (Prime factorisation)**.** A prime factorisation $\hat{\mathfrak{f}}(w)$ of a walk $w \in W_{\mathcal{G}}$ is a factorisation of w into nesting products of simple paths and simple cycles.

The relation $\equiv$ between factorisations of Definition 2.3.2 is clearly an equivalence relation. Thus, for each walk w on $\mathcal{G}$, it defines an equivalence class on the set of all prime factorisations of this walk, $F_w = \{\hat{\mathfrak{f}}(w)\}$. It is a central result of this chapter that all prime factorisations of w belong to the same equivalence class $[\mathcal{F}_{\odot}(w)] = \{\hat{\mathfrak{f}}(w) \in F_w, \hat{\mathfrak{f}}(w) \equiv \mathcal{F}_{\odot}(w)\}$ and the set of irreducible factors of w is uniquely determined by w:

Theorem 2.3.1 (Fundamental theorem of arithmetic on digraphs)**.** *Any walk on $\mathcal{G}$ factorises uniquely, up to equivalence, into nesting products of primes, the simple paths and simple cycles on $\mathcal{G}$.*

From now on we shall thus speak of *the* prime factorisation $\mathcal{F}_{\odot}(w)$ of a walk w. Below we give an algorithm that produces $\mathcal{F}_{\odot}(w)$ for an arbitrary walk.

An algorithm to factorise individual walks

Let $w \in W_{\mathcal{G}}$ and $\mathsf{F}\big(\mathfrak{f}(w)\big)$ be the set of *reducible* factors appearing in a factorisation $\mathfrak{f}(w)$ of w.

Algorithm 1, presented on p. 15, picks an arbitrary reducible factor of $a \in \mathsf{F}\big(\mathfrak{f}(w)\big)$ (initially we let $\mathfrak{f}(w) = w$) and factorises a into nesting products of strictly shorter walks, yielding $\mathfrak{f}(a)$. The algorithm then updates $\mathfrak{f}(w)$, replacing a with its factorisation in $\mathfrak{f}(w)$, denoted $\mathfrak{f}(w) \to \mathfrak{f}(w)\,/\,\{a \to \mathfrak{f}(a)\}$. At this point, the above procedure starts again, with the algorithm picking an arbitrary reducible factor appearing in the updated factorisation $\mathfrak{f}(w)$. At each round, reducible factors are decomposed into nesting products of shorter walks. The algorithm stops when $\mathsf{F}\big(\mathfrak{f}(w)\big)$ is the empty set $\varnothing$, at which point $\mathfrak{f}(w)$ is the prime factorisation $\mathcal{F}_{\odot}(w)$ of w. We demonstrate the validity of the algorithm in §2.5.3.

▶ A detailed example of the use of Algorithm 1 is provided in §2.4.1.

Input : A walk $w \in W_{\mathcal{G}}$
Output : The prime factorisation $\mathcal{F}_{\odot}(w)$

$\mathfrak{f}(w) = w$;
while $\mathsf{F}\big(\mathfrak{f}(w)\big) \neq \varnothing$ **do**
  Choose any $a \in \mathsf{F}\big(\mathfrak{f}(w)\big)$;
  if $h(a) = t(a) = \mu$ *and* a *visits vertex* μ a *total of* $k > 2$ *times* **then**
    Let $c_0, \cdots, c_k$ be the $k+1$ cycles off μ identified by splitting the vertex string of a at each internal appearance of μ.
    $\mathfrak{f}(w) \to \mathfrak{f}(w) \,/\, \{a \to (c_0 \odot \cdots \odot c_k)\}$;
      % Replace a with $(c_0 \odot \cdots \odot c_k)$ in $\mathfrak{f}(w)$
  else
    $w_0 = a$; $\mathfrak{f}_0(a) = w_0$;
    $j = 0$;
    while $w_j \notin \Pi_{\mathcal{G}} \cup \Gamma_{\mathcal{G}}$ **do**
      Traverse w_j from start to finish
      if w_j *is open* **then**
        Start the traversal on $h(w_j)$
      else
        Start the traversal on the first internal vertex of w_j
      end
      Upon arriving at the earliest vertex η that w_j visits at least twice, define :
      $s_{j+1} = (\eta_{\text{first}} \cdots \eta_{\text{last}})$;
        % Cycle from the first to the last occurrence of η in w_j
      $w_{j+1} = w_j \,/\, \{s_{j+1} \to (\eta)\}$;
        % Replace s_{j+1} with (η) in w_j
      $\mathfrak{f}_{j+1}(a) = \mathfrak{f}_j(a) \,/\, \{w_j \to (w_{j+1} \odot s_{j+1})\}$;
        % Replace w_j with $w_{j+1} \odot s_{j+1}$ in $\mathfrak{f}_j$
      $j = j + 1$;
    end
    Let $m = j$ and $r = w_m \in \Pi_{\mathcal{G}} \cup \Gamma_{\mathcal{G}}$. Observe that
    $\mathfrak{f}_m(a) = \Big(\big((r \odot s_m) \odot s_{m-1}\big) \odot \cdots \Big) \odot s_1$.
    $\mathfrak{f}(w) \to \mathfrak{f}(w) \,/\, \{a \to \mathfrak{f}_m(a)\}$;
      % Replace a with $\mathfrak{f}_m(a)$ in $\mathfrak{f}(w)$
  end
end
$\mathcal{F}_{\odot}(w) \equiv \mathfrak{f}(w)$;
  % All the factors appearing in $\mathfrak{f}(w)$ are now irreducible

Algorithm 1: Prime factorisation of individual walks

2.3.2 Prime factorisation of walk sets

In this section we present the prime factorisation of walk sets. More precisely, we obtain the set of walks between any two vertices of $\mathcal{G}$ from nested sets of simple paths and simple cycles.

Theorem 2.3.2 (Factorisation of walk sets)**.** *The prime factorisation of $W_{\mathcal{G}}$, is achieved by the following recursive relations:*

$$W_{\mathcal{G};\,\nu_0\nu_p} = \left(\left(\left(\Pi_{\mathcal{G};\,\nu_0\nu_p} \odot A^*_{\mathcal{G}\setminus\{\nu_0,\cdots,\nu_{p-1}\};\,\nu_p} \right) \odot \cdots \odot A^*_{\mathcal{G}\setminus\{\nu_0\};\,\nu_1} \right) \odot A^*_{\mathcal{G};\,\nu_0} \right), \tag{2.6a}$$

where $(\nu_0\,\nu_1\cdots\nu_{p-1}\,\nu_p) \in \Pi_{\mathcal{G};\,\nu_0\nu_p}$ and

$$A_{\mathcal{G};\,\mu_c} = \left(\left(\left(\Gamma_{\mathcal{G};\,\mu_c} \odot A^*_{\mathcal{G}\setminus\{\mu_c,\,\mu_1,\cdots,\,\mu_{c-2}\};\,\mu_{c-1}} \right) \odot \cdots \odot A^*_{\mathcal{G}\setminus\{\mu_c,\,\mu_1\};\,\mu_2} \right) \odot A^*_{\mathcal{G}\setminus\{\mu_c\};\,\mu_1} \right), \tag{2.6b}$$

with $(\mu_c\,\mu_1\cdots\mu_{c-1}\,\mu_c) \in \Gamma_{\mathcal{G};\,\mu_c}$.

Note that if $\nu_0 = \nu_p$, then $\Pi_{\mathcal{G};\,\nu_0\nu_p} = (\nu_0)$ and $W_{\mathcal{G};\,\nu_0\nu_0} = A^*_{\mathcal{G};\,\nu_0}$ with $A_{\mathcal{G};\,\nu_0}$ given by Eq. (2.6b). This gives the factorisation for sets of cycles on $\mathcal{G}$.

The set $A_{\mathcal{G};\,\mu_c}$ is defined recursively through Eq. (2.6b). Indeed $A_{\mathcal{G};\,\mu_c}$ is expressed in terms of $A_{\mathcal{G}\setminus\{\mu_c,\,\mu_1,\cdots,\,\mu_{j-1}\};\,\mu_j}$ which is in turn defined through Eq. (2.6b) but on the subgraph $\mathcal{G}\setminus\{\mu_c,\ldots,\mu_{j-1}\}$ of $\mathcal{G}$. The recursion stops when vertex μ_j has no neighbour on this subgraph, in which case $A_{\mathcal{G}\setminus\{\mu_c,\,\mu_1,\cdots,\,\mu_{j-1}\};\,\mu_j} = \Gamma_{\mathcal{G}\setminus\{\mu_c,\,\mu_1,\cdots,\,\mu_{j-1}\};\,\mu_j} = \{(\mu_j\mu_j)\}$ if the loop $(\mu_j\mu_j)$ exists and $A_{\mathcal{G}\setminus\{\mu_c,\,\mu_1,\cdots,\,\mu_{j-1}\};\,\mu_j} = (\mu_j)$ otherwise. The maximum depth at which this recursion stops is discussed in §2.3.4.

2.3.3 Prime factorisation of characteristic series of walks

An essential consequence of the existence and uniqueness of the prime factorisation of walks, Theorem 2.3.1, is that additive arithmetic functions of walks are completely determined by their values on the primes, the simple paths and simple cycles of $\mathcal{G}$. Here we exploit this property to express the characteristic series $\Sigma_{\mathcal{G};\,\alpha\omega}$ of all the walks $w \in W_{\mathcal{G};\,\alpha\omega}$ solely in terms of prime walks.

Specifically, by using the fact that every open walk can be factorised into a simple path and a collection of nested cycles, we rewrite the characteristic series of $W_{\mathcal{G};\,\alpha\omega}$ as a series over simple paths by modifying each path in the series to include all collections of cycles that can be nested off the vertices it visits. We implement this modification by replacing each vertex α in a simple path by a 'dressed vertex' $(\alpha)'_{\mathcal{G}}$ representing the characteristic series of all cycles nested off α on $\mathcal{G}$:

$$(\alpha)'_{\mathcal{G}} = \sum_{c \in W_{\mathcal{G};\,\alpha\alpha}} c. \tag{2.7}$$

In turn, we rewrite the characteristic series above as a series over simple cycles $\gamma \in \Gamma_{\mathcal{G};\,\alpha}$ upon replacing each vertex μ traversed by a simple cycle γ by a dressed

vertex representing the characteristic series of all the cycles that can be nested off μ on the appropriate subgraph of $\mathcal{G}$. Using the vertex-edge notation of walks, the dressed vertex is therefore

$$\begin{aligned}(\alpha)'_{\mathcal{G}} &= \sum_{p\in\mathbb{N}} \left(\sum_{(\alpha\mu_2\cdots\mu_m\alpha)\,\in\,\Gamma_{\mathcal{G};\,\alpha}} (\alpha)(\alpha\mu_2)(\mu_2)'_{\mathcal{G}\setminus\{\alpha\}}\cdots(\mu_m)'_{\mathcal{G}\setminus\{\alpha,\,\mu_2,\cdots,\mu_{m-1}\}}(\mu_m\alpha)(\alpha) \right)^p, \\ &= \sum_{p\in\mathbb{N}} \Big(\sum_{\gamma\in\Gamma_{\mathcal{G};\,\alpha}} \gamma' \Big)^p, \end{aligned} \tag{2.8}$$

where the sums over $p \in \mathbb{N}$ account for cycles made of a single repeated simple cycle, e.g. γ^p, and γ' is a notation for a simple cycle γ with dressed vertices. Finally, we show in §2.5.4 that the linear mapping representing a dressed vertex on the quiver is the inverse mapping $\varphi_{(\alpha)'_{\mathcal{G}}} = \big(1_\alpha - \sum_{\gamma\in\Gamma_{\mathcal{G};\,\alpha}} \varphi_{\gamma'}\big)^{-1}$ and from now on we represent dressed vertices using the inverse notation.

Theorem 2.3.3 (Path-sum)**.** *Let $\Sigma_{\mathcal{G};\,\alpha\omega}$ denote the characteristic series of all walks from α to ω on $\mathcal{G}$. Then $\Sigma_{\mathcal{G};\,\alpha\omega}$ is given in vertex-edge notation by*

$$\Sigma_{\mathcal{G};\,\alpha\omega} = \sum_{\Pi_{\mathcal{G};\,\alpha\omega}} (\alpha)'_{\mathcal{G}}\,(\alpha\nu_2)\,(\nu_2)'_{\mathcal{G}\setminus\{\alpha\}}\cdots(\nu_p\omega)\,(\omega)'_{\mathcal{G}\setminus\{\alpha,\nu_2,\ldots,\nu_p\}}\,, \tag{2.9a}$$

where p is the length of the simple path $(\alpha\nu_2\cdots\nu_p\omega) \in \Pi_{\mathcal{G};\,\alpha\omega}$, and $(\alpha)'_{\mathcal{G}}$ denotes the dressed vertex α on $\mathcal{G}$, given by

$$(\alpha)'_{\mathcal{G}} = \left[(\alpha) - \sum_{\Gamma_{\mathcal{G};\,\alpha}} (\alpha)\,(\alpha\mu_2)\,(\mu_2)'_{\mathcal{G}\setminus\{\alpha\}}\,(\mu_2\mu_3)\cdots(\mu_m)'_{\mathcal{G}\setminus\{\alpha,\mu_2,\ldots,\mu_{m-1}\}}\,(\mu_m\alpha)\,(\alpha) \right]^{-1}, \tag{2.9b}$$

where m is the length of the simple cycle $(\alpha\mu_2\cdots\mu_m\alpha) \in \Gamma_{\mathcal{G};\,\alpha}$.

The dressed vertex $(\alpha)'_{\mathcal{G}}$ is defined recursively through Eq. (2.9b) since it is expressed in terms of dressed vertices $(\mu_j)'_{\mathcal{G}\setminus\{\alpha,\mu_2,\ldots,\mu_{j-1}\}}$. These are in turn defined through Eq. (2.9b) but on the subgraph $\mathcal{G}\setminus\{\alpha,\mu_2,\ldots,\mu_{j-1}\}$ of $\mathcal{G}$. The recursion stops when vertex μ_j has no neighbour on this subgraph, in which case $(\mu_j)'_{\mathcal{G}\setminus\{\alpha,\mu_2,\ldots,\mu_{j-1}\}} = [(\mu_j)-(\mu_j\mu_j)]^{-1}$ if the loop $(\mu_j\mu_j)$ exists and $(\mu_j)'_{\mathcal{G}\setminus\{\alpha,\mu_2,\ldots,\mu_{j-1}\}} = (\mu_j)$ otherwise.

The recursive definition of dressed vertices implies that the formula of Theorem 2.3.3 for $\Sigma_{\mathcal{G};\,\alpha\omega}$ yields a formal continued fraction. On finite digraphs, the depth of this continued fraction is finite, see §2.3.4. The formal factorisation of $\Sigma_{\mathcal{G};\,\alpha\omega}$ achieved by Theorem 2.3.3 yields a factorised form for series of walks on *weighted* digraphs. This directly leads to applications in the field of matrix computations, as shown in the next chapter.

Theorem 2.3.4 (Weighted path-sum)**.** *Let* M *be an invertible matrix defined through* $(\mathsf{M})_{\nu\mu} = \mathsf{w}_{\nu\mu}$*. Then as long as all of the required inverses exist, the weight of the sum of all walks from* α *to* ω *on the weighted digraph* $(\mathcal{G}, \mathrm{W})$ *is given by*

$$\mathrm{W}\big[\Sigma_{\mathcal{G};\,\alpha\omega}\big] = \sum_{\Pi_{\mathcal{G};\,\alpha\omega}} \mathsf{F}_{\mathcal{G}\setminus\{\alpha,\ldots,\nu_p\};\,\omega}\,\mathsf{w}_{\omega\nu_p}\cdots\mathsf{F}_{\mathcal{G}\setminus\{\alpha\};\,\nu_2}\,\mathsf{w}_{\nu_2\alpha}\,\mathsf{F}_{\mathcal{G};\alpha}\,, \tag{2.10a}$$

where p *is the length of the simple path,* $\mathsf{w}_{\nu\mu} = \mathrm{W}[(\mu\nu)]$ *is the weight of the edge* $(\mu\nu)$*, and*

$$\mathsf{F}_{\mathcal{G};\,\alpha} \equiv \mathrm{W}\big[(\alpha)'_{\mathcal{G}}\big] = \Bigg[\mathsf{I}_\mu - \sum_{\Gamma_{\mathcal{G};\,\alpha}} \mathsf{w}_{\alpha\mu_m}\,\mathsf{F}_{\mathcal{G}\setminus\{\alpha,\ldots,\mu_{m-1}\};\,\mu_m}\,\mathsf{w}_{\mu_m\mu_{m-1}}\cdots\mathsf{F}_{\mathcal{G}\setminus\{\alpha\};\,\mu_2}\,\mathsf{w}_{\mu_2\alpha}\Bigg]^{-1}, \tag{2.10b}$$

with m *the length of the simple cycle and* I_μ *the* $d_\mu \times d_\mu$ *identity matrix.* $\mathsf{F}_{\mathcal{G};\,\alpha}$ *is the effective weight of the vertex* α *on* $\mathcal{G}$ *once it is dressed by all the cycles off it.*

The expression of $\mathrm{W}\big[\Sigma_{\mathcal{G};\,\alpha\omega}\big]$ is a continued fraction of finite depth, which results from the recursive definition of the $\mathsf{F}_{\mathcal{G};\,\alpha}$. Theorem 2.3.4 thus expresses the sum of the weights of all walks from α to ω on any finite digraph as a *finite matrix-valued continued fraction* over the simple paths and simple cycles of $\mathcal{G}$. As we will see with the examples, this allows direct verifications using matrix computations of the results of Theorem 2.3.3 and 2.3.4, which look otherwise very abstract. But before we give examples illustrating the Theorems above, we determine the depth at which the continued fraction terminates.

2.3.4 Complexity of the prime factorisation

The prime factorisation of a walk set $W_{\mathcal{G};\,\alpha\omega}$ reduces this set to nested sets of prime walks. Since these primes – the simple cycles and simple paths of $\mathcal{G}$ – are difficult to identify, we expect the factorised form of $W_{\mathcal{G};\alpha\omega}$ to be difficult to construct. For example, if the digraph is Hamiltonian, the Hamiltonian cycle or path must appear in the factorisation of at least one walk set. Consequently, we expect that factoring *all* the walk sets requires determining the existence of such a cycle or path, a problem which is known to be NP-complete.

In order to formalise this observation, we now determine the star-height of the prime factorisation, as given by Theorem 2.3.2, of any set $W_{\mathcal{G};\,\alpha\omega}$. The star-height $h(\mathfrak{E})$ of a regular expression $\mathfrak{E}$ was introduced by Eggan [44] as the number of nested Kleene stars in $\mathfrak{E}$. This quantity characterises the structural complexity of formal expressions. As we will see in the examples of §2.4, prime factorisations of walk sets typically have a non-zero star-height. Furthermore, the proofs of Theorems 2.3.3 and 2.3.4 in §2.5.4 demonstrate that the star-height of $W_{\mathcal{G};\,\alpha\omega}$ is equal to the depth of the continued fraction generated by Theorems 2.3.3 and 2.3.4. In §2.5.5 we obtain an exact recursive expression for $h(W_{\mathcal{G};\,\alpha\omega})$. The following result says that the problem of evaluating $h(W_{\mathcal{G};\,\alpha\omega})$ is nonetheless NP-complete on undirected connected graphs:

Theorem 2.3.5. *Let $\mathcal{G}$ be a finite undirected connected graph, possibly with self-loops. Let $(\alpha,\omega)\in\mathcal{V}(\mathcal{G})^2$ and let $\mathrm{L}\Pi_{\mathcal{G};\,\alpha}$ be the set of longest simple paths starting at α, with ℓ_α their length. Then*

$$h\big(W_{\mathcal{G};\,\alpha\omega}\big)=h\big(W_{\mathcal{G};\,\alpha\alpha}\big)=\begin{cases}\ell_\alpha+1, & \text{if } \exists\,(\alpha\nu_2\cdots\nu_{\ell_\alpha})\in\mathrm{L}\Pi_{\mathcal{G};\,\alpha} \text{ such that there}\\ & \text{is a self-loop on vertex } \nu_{\ell_\alpha},\\ \ell_\alpha, & \text{otherwise.}\end{cases}\tag{2.11}$$

The problem of determining $h(W_{\mathcal{G};\,\alpha\omega})$ and $h(W_{\mathcal{G};\,\alpha\alpha})$ is equivalent to determining the existence of a Hamiltonian path starting at α. It is therefore NP-complete.

Theorem 2.3.5 means that just determining the complexity of prime factorisations on ordinary graphs is already quite hard. This result may be considered unsurprising in view of the fact that prime factorisations are known to be difficult to obtain, e.g. in the case of integers. Here, however, the origin of the difficulty is different from that in the case of integer factorisation: it resides in factoring *all* the sets of *all* the walks between any two vertices of a connected graph or in computing the star-heights of the factorised forms. At the opposite, factoring an individual walk using Algorithm 1 is surprisingly easy: we can show that the time complexity of the algorithm scales quadratically with the length $\ell(w)$ of the walk w being factorised in the worst case scenario, and only linearly with $\ell(w)$ in the typical case scenario.

2.4 Illustrative Examples

The main application of the results presented in this chapter concerns the calculation of matrix functions and, by extension, the simulation of quantum systems. This is presented in details in details in Chapters 3, 4 and 5. Two further applications of the prime factorisation of walks that are being developed are: i) a probabilistic algorithm for finding all the shortest paths between all pairs of vertices on random graphs; and ii) solving the graph isomorphism problem using prime walks, this is briefly discussed in Chapter 6. Here we provide simple examples illustrating Algorithm 1, Theorems 2.3.2, 2.3.3 and 2.3.4.

2.4.1 Short examples

Example 2.4.1 (The prime factorisation of a walk)**.** In this example we give a detailed step-by-step example illustrating Algorithm 1. Let $\mathcal{G}$ be the complete undirected graph on 4 vertices with vertex labels {1,2,3,4}, and consider the factorising the walk $w=(133112343442333)$.

Initially, the walk factorisation is simply $\mathfrak{f}(w)=w$ and its set of irreducible factors is therefore $\mathsf{F}\big(\mathfrak{f}(w)\big)=w$. Since w is the only factor in $\mathfrak{f}(w)$, we let $a=w$. The algorithm runs as follows:

(1) Walk a is open, define $w_0 = a$ and $\mathfrak{f}_0(a) = w_0$. Traversing w_0 from its first vertex onwards, vertex 1 is the earliest vertex visited at least twice by w_0. Then $s_1 = 13311$, $w_1 = 12343442333$ and $\mathfrak{f}_1(a) = w_1 \odot s_1$.

(1a) $w_1 \notin \Pi_{\mathcal{G}} \cup \Gamma_{\mathcal{G}}$ and w_1 is open. Traversing w_1 from its first vertex onwards, vertex 2 is the earliest vertex visited at least twice by w_1. Then $s_2 = 2343442$, $w_2 = 12333$ and $\mathfrak{f}_2(a) = (w_2 \odot s_2) \odot s_1$.

(1b) $w_2 \notin \Pi_{\mathcal{G}} \cup \Gamma_{\mathcal{G}}$ and w_2 is open. Traversing w_2 from its first vertex onwards, vertex 3 is the earliest vertex visited at least twice by w_2. Then $s_3 = 333$, $w_3 = 123$ and $\mathfrak{f}_3(a) = \big((w_3 \odot s_3) \odot s_2\big) \odot s_1$.

(1c) $w_3 \in \Pi_{\mathcal{G}} \cup \Gamma_{\mathcal{G}}$, we exit the while loop, and update $\mathfrak{f}(w)$, replacing a by $\mathfrak{f}_3(a)$. We obtain,

$$\mathfrak{f}(w) = \Big((w_3 \odot s_3) \odot s_2\Big) \odot s_1 = \Big((123 \odot 333) \odot 2343442\Big) \odot 13311.$$

(2) Now $\mathsf{F}\big(\mathfrak{f}(w)\big) = \{333,\, 2343442\,, 13311\}$. We choose $a = 333$. This walk is a cycle off 3 and visits vertex 3 one further time. Define $c_0 = 33$, $c_1 = 33$ and update $\mathfrak{f}(w)$, replacing 333 by $33 \odot 33 = 33^2$, that is,

$$\mathfrak{f}(w) = \Big((123 \odot 33^2) \odot 2343442\Big) \odot 13311.$$

(3) $\mathsf{F}\big(\mathfrak{f}(w)\big) = \{2343442\,, 13311\}$. We choose $a = 13311$, a is a cycle off 1 and visits vertex 1 one further time. Define $c_0 = 1331$ and $c_1 = 11$, and update $\mathfrak{f}(w)$, replacing a with $c_0 \odot c_1$,

$$\mathfrak{f}(w) = \Big((123 \odot 33^2) \odot 2343442\Big) \odot (1331 \odot 11).$$

(4) $\mathsf{F}\big(\mathfrak{f}(w)\big) = \{2343442\,, 1331\}$. Choosing $a = 1331$, a is a cycle off 1 but does not have 1 as internal vertex. Then $s_1 = 33$, $w_1 = 131$ and $\mathfrak{f}_1(a) = w_1 \odot s_1$.

(4a) $w_1 \in \Pi_{\mathcal{G}} \cup \Gamma_{\mathcal{G}}$, we exit the while loop, and update $\mathfrak{f}(w)$, replacing a with $\mathfrak{f}_1(a)$. We obtain

$$\mathfrak{f}(w) = \Big((123 \odot 33^2) \odot 2343442\Big) \odot \Big((131 \odot 33) \odot 11\Big).$$

(5) $\mathsf{F}\big(\mathfrak{f}(w)\big) = \{2343442\}$, then $a = 2343442$. Walk a is a cycle off 2 but does not have 2 as internal vertex. Then $s_1 = 343$, $w_1 = 23442$ and $\mathfrak{f}_1(a) = w_1 \odot s_1$.

(5a) $w_1 \notin \Pi_{\mathcal{G}} \cup \Gamma_{\mathcal{G}}$, w_1 is a cycle off 2 but does not have 2 as internal vertex. Then $s_2 = 44$, $w_2 = 2342$ and $\mathfrak{f}_2(a) = (w_2 \odot s_2) \odot s_1$.

(5b) $w_2 \in \Pi_{\mathcal{G}} \cup \Gamma_{\mathcal{G}}$, we exit the while loop and update $\mathfrak{f}(w)$, replacing a with $\mathfrak{f}_2(a)$. We obtain

$$\mathfrak{f}(w) = \Big((123 \odot 33^2) \odot \big((2342 \odot 44) \odot 343 \big) \Big) \odot \big((131 \odot 33) \odot 11 \big). \quad (2.12)$$

At this point $\mathsf{F}\big(\mathfrak{f}(w)\big) = \varnothing$. Eq. (2.12) is therefore the prime factorisation $\mathcal{F}_{\odot}(w)$ of w into nesting products of prime walks. A pictorial representation of the operations performed by the algorithm is given below:

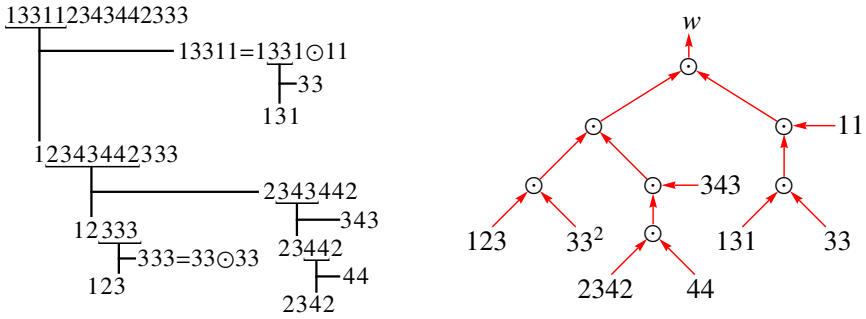

For illustrative purposes, we show on the right a tree T_w representing the prime factorisation of w. Each node corresponds to a nesting product, the leaves are the irreducible factors of w, and the root is the walk w itself. The tree T_w is in fact a subgraph of the Hasse diagram of the set of walks partially ordered by the divisibility relation of Definition 2.2.4. This observation lies at the heart of a "number theory" of prime walks, which we cannot report here due to length concerns.

Example 2.4.2 (Prime factorisation of all the walks of a digraph)**.** In this example we produce the prime factorisation of an set of walks thanks to Theorem 2.3.2. We consider the complete ordinary graph on three vertices 1, 2 and 3 with a self-loop on each vertex, denoted by $\mathcal{LK}_3$. We are interested in factorising $W_{\mathcal{LK}_3;\,11}$.

This is an set of cycles and Eq. (2.6a) thus yields $W_{\mathcal{LK}_3;\,11} = A^*_{\mathcal{LK}_3;\,11}$. To factorise $A^*_{\mathcal{LK}_3;\,11}$, we note that $\Gamma_{\mathcal{LK}_3;\,1} = \{1, 11, 121, 131, 1231, 1321\}$. Thus Eq. (2.6b) gives

$$W_{\mathcal{LK}_3;\,11} = \Big\{ 11,\ 121 \odot A^*_{\mathcal{LK}_3\setminus\{1\};\,22},\ 131 \odot A^*_{\mathcal{LK}_3\setminus\{1\};\,33}, \quad (2.13)$$
$$\big(1231 \odot A^*_{\mathcal{LK}_3\setminus\{1,2\};\,33}\big) \odot A^*_{\mathcal{LK}_3\setminus\{1\};\,22},\ \big(1321 \odot A^*_{\mathcal{LK}_3\setminus\{1,3\};\,22}\big) \odot A^*_{\mathcal{LK}_3\setminus\{1\};\,33} \Big\}^*.$$

We now factor all $A^*_{\mathcal{G}\ldots}$ sets by using Eq. (2.6b) once more. Since $\Gamma_{\mathcal{LK}_3\setminus\{1\};\,2} = \{2, 22, 232\}$ and $\Gamma_{\mathcal{LK}_3\setminus\{1,3\};\,2} = \{2, 22\}$, we have

$$A^*_{\mathcal{LK}_3\setminus\{1\};\,22} = \{22, 232 \odot A^*_{\mathcal{LK}_3\setminus\{1,2\};\,33}\}^* \quad \text{and} \quad A^*_{\mathcal{LK}_3\setminus\{1,3\};\,22} = \{22\}^*, \quad (2.14)$$

and the analogous expressions produced by exchanging the labels 2 and 3. Inserting

these expressions into Eq. (2.13), we arrive at

$$W_{\mathcal{LK}_3;\,11} = \Big\{ 11, 121 \odot \Big\{ 22, 232 \odot \{33\}^* \Big\}^*, 131 \odot \Big\{ 33, 323 \odot \{22\}^* \Big\}^*, \tag{2.15}$$
$$\big(1231 \odot \{33\}^*\big) \odot \Big\{ 22, 232 \odot \{33\}^* \Big\}^*, \big(1321 \odot \{22\}^*\big) \odot \Big\{ 33, 323 \odot \{22\}^* \Big\}^* \Big\}^*.$$

This set contains the prime factorisation of any cycle off 1 on $\mathcal{LK}_3$. The star height of the prime factorisation of $W_{\mathcal{LK}_3;\,11}$ is 3, as predicted by Theorem 2.3.5.

Example 2.4.3 (Summing walks on $\mathcal{K}_3$)**.** To illustrate Theorem 2.3.3 we produce the prime factorisation of $\Sigma_{\mathcal{K}_3;11}$, the characteristic series of all the walks from vertex 1 to itself on the complete ordinary graph on three vertices with no self-loops, denoted by $\mathcal{K}_3$.

Since the only simple path from a vertex to itself is the trivial path, Eq. (2.9a) simply gives $\Sigma_{\mathcal{K}_3;11} = (1)'_{\mathcal{K}_3}$. According to Eq. (2.9b) the dressed vertex is given by

$$(1)'_{\mathcal{K}_3} = \Big[(1) - (12)(2)'_{\mathcal{K}_3\setminus\{1\}}(21) - (13)(3)'_{\mathcal{K}_3\setminus\{1\}}(31) -$$
$$(12)(2)'_{\mathcal{K}_3\setminus\{1\}}(23)(3)'_{\mathcal{K}_3\setminus\{1,2\}}(31) - (13)(3)'_{\mathcal{K}_3\setminus\{1\}}(32)(2)'_{\mathcal{K}_3\setminus\{1,3\}}(21) \Big]^{-1}, \tag{2.16}$$

which follows from the observation that the only non-trivial simple cycles off vertex 1 on $\mathcal{K}_3$ are the two backtracks (121) and (131) and the two triangles (1231) and (1321). Now we use Eq. (2.9b) again to evaluate the required dressed vertices. We observe that there are no non-trivial simple cycles off vertex 2 on $\mathcal{K}_3\setminus\{1,3\}$, and no non-trivial simple cycles off vertex 3 on $\mathcal{K}_3\setminus\{1,2\}$. Thus $(2)'_{\mathcal{K}_3\setminus\{1,3\}}$ is just the trivial walk (2), and $(3)'_{\mathcal{K}_3\setminus\{1,2\}} = (3)$. Furthermore, since the only non-trivial simple cycle off vertex 2 on $\mathcal{K}_3\setminus\{1\}$ is (232), we obtain

$$(2)'_{\mathcal{K}_3\setminus\{1\}} = \big[(2) - (23)(3)'_{\mathcal{K}_3\setminus\{1,2\}}(32)\big]^{-1} = \big[(2) - (232)\big]^{-1}. \tag{2.17}$$

Similarly we have $(3)'_{\mathcal{K}_3\setminus\{1\}} = \big[(3) - (323)\big]^{-1}$. Inserting these results in Eq. (2.16) yields

$$\Sigma_{\mathcal{K}_3;\,11} = \Big[(1) - (12)\big[(2) - (232)\big]^{-1}(21) - (13)\big[(3) - (323)\big]^{-1}(31)$$
$$- (12)\big[(2) - (232)\big]^{-1}(231) - (13)\big[(3) - (323)\big]^{-1}(321) \Big]^{-1}. \tag{2.18}$$

This result may alternatively be obtained from the prime factorisation of $W_{\mathcal{K}_3;\,11}$

$$W_{\mathcal{K}_3;\,11} = \Big\{ 121 \odot \{232\}^*, 131 \odot \{323\}^*, 1231 \odot \{232\}^*, 1321 \odot \{323\}^* \Big\}^*, \tag{2.19}$$

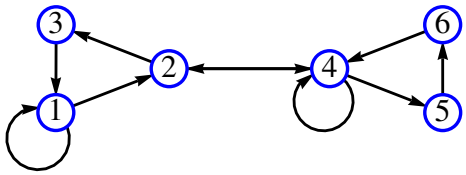

Figure 2.2: The digraph $\mathcal{G}$ of Example 2.4.4.

by following the procedure described in the proof of Theorem 2.3.3: we sum the elements of the factorised form of $W_{\mathcal{K}_3;11}$, with the sums over the Kleene stars yielding formal inverses.

The best way to convince oneself of the correctness of the prime factorisation of a characteristic series such as Eq. (2.18) is to give weights to the graph edges. In this situation, and if the factorisation is correct, the weight of the continued fraction representing the prime factorisation of the characteristic series is directly identifiable with a matrix inverse. This inverse can often be calculated through direct matrix computations, allowing a direct verification of the factorisation. This is what we show in the next example.

Example 2.4.4 (Walk generating function)**.** Consider the digraph $\mathcal{G}$ illustrated on Fig. 2.2, and let A be its adjacency matrix. Let $g_{\mathcal{G};11}(z) = \sum_{n=0}^{\infty} z^n(\mathsf{A}^n)_{11}$ be the walk generating function for all the walks on $\mathcal{G}$ from vertex 1 back to itself [20]. This can be computed by noting that $g_{11}(z)$ is the sum of the weights of all the walks $w \in W_{\mathcal{G};11}$ on a weighted version of $\mathcal{G}$, which has an edge weight of z assigned to every edge.
Theorem 2.3.3 yields $\Sigma_{\mathcal{G};11}$, the sum of all walks on the unweighted digraph $\mathcal{G}$, as

$$\Sigma_{\mathcal{G};11} = \Big[(1) - (11) - (12)(2)'_{\mathcal{G}\setminus\{1\}}(231)\Big]^{-1}, \tag{2.20a}$$

$$(2)'_{\mathcal{G}\setminus\{1\}} = \Big[(2) - (24)(4)'_{\mathcal{G}\setminus\{1,2\}}(42)\Big]^{-1}, \quad (4)'_{\mathcal{G}\setminus\{1,2\}} = \Big[(4) - (44) - (4564)\Big]^{-1}, \tag{2.20b}$$

which corresponds to summing over the factorised form

$$W_{\mathcal{G};11} = \Big\{11,\ 1231 \odot \big\{242 \odot \{44,\ 4564\}^*\big\}^*\Big\}^*. \tag{2.21}$$

According to Theorem 2.3.4, the sum over the walks of the weighted digraph is obtained upon replacing each edge by its weight in Eq. (2.20). This yields

$$\mathrm{W}\big[\Sigma_{\mathcal{G};11}\big] = \frac{1}{1 - z - z\frac{1}{1-z\frac{1}{1-z-z^3}z}z^2} = -\frac{z^3 + z^2 + z - 1}{z^6 + 2z^4 - z^3 - 2z + 1}. \tag{2.22}$$

We can verify that $\mathrm{W}\big[\Sigma_{\mathcal{G};11}\big]$ is equal to $g_{\mathcal{G};11}(z) = \big([\mathsf{I} - z\mathsf{A}]^{-1}\big)_{11}$, where I is the 6×6 identity matrix, provided $|z| < \rho(\mathsf{A})^{-1}$ with $\rho(\mathsf{A})$ the spectral radius of A, as

expected [20]. This shows that all the walks off 1 on $\mathcal{G}$ are indeed present in the factorised form of the walk set Eq. (2.21) and that the prime factorisation of the characteristic series Eq. (2.20) is correct.

Sometimes, the required matrix inverse is too complicated to be calculated, e.g. because the matrix is too large or very ill-behaved such as nearly singular. In these situations, the continued fraction representing the factorised characteristic series of weighted walks is a reliable way of obtaining the matrix inverse. This observation forms the basis of Chapter 3.

2.4.2 Walks on finite graphs

In this section we give a further example of application of Theorem 2.3.4: we obtain the walk generating functions of finite Cayley trees. To this end, we first determine the walk generating functions of finite path-graphs and cycle-graphs[1].

Walks on finite path-graphs and cycle graphs

Let $\mathcal{P}_n$ and $\mathcal{C}_n$ be the n-vertices undirected path-graph and cycle graph, respectively. We are interested in their walk generating functions

$$g_{\mathcal{G};\,\alpha\omega}(z) = \sum_n |W_{\mathcal{G};\,\alpha\omega;n}| z^n, \tag{2.23}$$

where $|W_{\mathcal{G};\,\alpha\omega;n}|$ is the number of walks of length n from vertex α to vertex ω on $\mathcal{G}$.

For convenience, we label the vertices of $\mathcal{P}_n$ from left to right, from 0 to $n-1$. Let α be a vertex of $\mathcal{P}_n$, if $\alpha \neq 0,\, n-1$, then the only simple cycles off α on $\mathcal{P}_n$ are the two back-tracks $(\alpha\,\alpha \pm 1\,\alpha)$ with weight z^2 and, if $\alpha = 0$ or $n-1$, then only one back-track exists. According to Theorem 2.3.4, the path-sum for $g_{\mathcal{G};\,\alpha\alpha}(z)$ thus reads

$$g_{\mathcal{G};\,\alpha\alpha}(z) = \frac{1}{1 - z^2 F_\alpha(z) - z^2 F_{n-\alpha-1}(z)}, \tag{2.24}$$

where F_α is the continued fraction of depth $\alpha - 1$ which represents the weight of the dressed neighbour of α,

$$F_\alpha(z) = \mathrm{W}\big[(\alpha-1)'_{\mathcal{P}_n \setminus \{\alpha\}}\big] = \cfrac{1}{1 - \cfrac{z^2}{1 - \cfrac{z^2}{\cdots}}} = \frac{Q_{\alpha-1}(z)}{Q_\alpha(z)}, \tag{2.25}$$

with $Q_x(u) = {}_2F_1\left(\frac{1}{2} - \frac{x}{2}, -\frac{x}{2}; -x; 4u^2\right)$ the Gauss hypergeometric function. Then,

$$g_{\mathcal{P}_n;\,\alpha\alpha}(z) = \frac{Q_{n-\alpha-1}(z) Q_\alpha(z)}{Q_n(z)}, \tag{2.26}$$

[1] Contrary to the generating functions of finite Cayley trees, those of finite path-graphs and cycle-graphs are already known thanks to direct diagonalisation. We derive them again to illustrate our results.

which follows from the identity $Q_n(z) = Q_{n-\alpha-1}(z)Q_\alpha(z) - z^2Q_{n-\alpha-2}(z)Q_\alpha(z) - z^2Q_{n-\alpha-1}(z)Q_{\alpha-1}(z)$. Now let ω be another vertex of $\mathcal{P}_n$. The graph is symmetric and we may assume without loss of generality that $d = \alpha - \omega \geq 0$. Since there is only one simple path from α to ω, Theorem 2.3.4 yields

$$g_{\mathcal{P}_n;\,\alpha\omega}(z) = z^d g_{\mathcal{P}_{\alpha-d};00} \cdots g_{\mathcal{P}_{\alpha-1};00}(z) g_{\mathcal{P}_n;\,\alpha\alpha}(z). \tag{2.27}$$

With the result Eq. (2.26) we find

$$g_{\mathcal{P}_n;\,\alpha\omega}(z) = z^d \frac{Q_{n-\alpha-1}(z)Q_{\alpha-d}(z)}{Q_n(z)}. \tag{2.28}$$

This gives all the walk generating functions on all finite path-graphs.

We now derive the walk generating functions of cycle graphs. For convenience, we label the vertices of $\mathcal{C}_n$ clockwise from 0 to $n-1$. We begin with the walk generating function $g_{\mathcal{C}_n;\,00}(z)$ for all the cycles off vertex 0. This is the sum of all cycle weights on a weighted version of $\mathcal{C}_n$ where all edges have weight z. The only simple cycles off 0 are the two backtracks to its neighbours, with weight z^2, and the two simple cycles of length n (the two directions count as different simple cycles), with weight z^n. Then

$$g_{\mathcal{C}_n;\,00}(z) = \frac{1}{1 - 2z^2\, g_{\mathcal{P}_{n-1};\,00}(z) - 2z^n\, g_{\mathcal{P}_1;\,00}(z) \cdots g_{\mathcal{P}_{n-2};\,00}(z) g_{\mathcal{P}_{n-1};\,00}(z)}, \tag{2.29a}$$

$$= \frac{Q_{n-1}(z)}{Q_{n-1}(z) - 2z^2Q_{n-2}(z) - 2z^n}. \tag{2.29b}$$

To obtain Eq. (2.29a), we first used the symmetry of $\mathcal{C}_n$, noting that $\mathrm{W}\big[(1)'_{\mathcal{C}_n\setminus\{0\}}\big] = \mathrm{W}\big[(n)'_{\mathcal{C}_n\setminus\{0\}}\big]$ etc. Second, we remarked that $\mathcal{C}_n\setminus\{0\} \equiv \mathcal{P}_{n-1}$ and similarly, $\mathcal{C}_n\setminus\{0,1,\cdots,j\} \equiv \mathcal{P}_{n-j-1}$, $0 \leq j \leq n-1$. Then Eq. (2.29b) follows from Eq. (2.26). Now we turn to the walk generating function $g_{\mathcal{C}_n;\,0d}(z)$ for all walks from 0 to a vertex located at distance d, which we assume without loss of generality to be positive $0 \leq d \leq \lfloor n/2 \rfloor$. There are two simple paths from 0 to d: one of length d and one of length $n-d$. Thanks to Theorem 2.3.4 we get

$$g_{\mathcal{C}_n;\,0d}(z) = z^{n-d} g_{\mathcal{P}_d;\,00}(z) \cdots g_{\mathcal{P}_{n-1};\,00}(z) g_{\mathcal{C}_n;\,00}(z) + z^d g_{\mathcal{P}_{n-d};\,00}(z) \cdots g_{\mathcal{P}_{n-1};\,00}(z) g_{\mathcal{C}_n;\,00}(z), \tag{2.30a}$$

$$= \frac{Q_{d-1}(z)z^{n-d} + z^d Q_{n-d-1}(z)}{Q_{n-1}(z) - 2z^2Q_{n-2}(z) - 2z^n}. \tag{2.30b}$$

Walks on finite Cayley trees

A finite Cayley tree $\mathcal{T}_n^\Delta$ is an undirected rooted tree where every vertex within distance $d < \Delta$ from the root 0 is connected to n other vertices, while vertices at distance Δ from the root have $n-1$ neighbours, see Fig. 2.3. The quantities Δ and n are called the radius and bulk connectivity of $\mathcal{T}_n^\Delta$, respectively. Finite Cayley trees

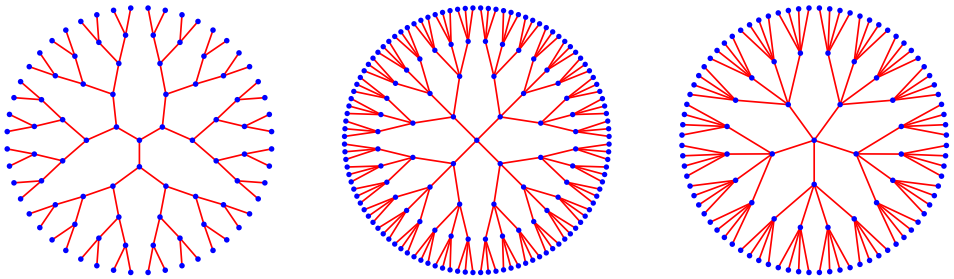

Figure 2.3: Illustration of three finite Cayley trees with, from left to right, $\mathcal{T}_3^5$, $\mathcal{T}_4^4$ and $\mathcal{T}_5^3$. The corresponding Bethe lattices are infinite in the radial direction.

and their infinite counterparts, the Bethe lattices $\mathcal{B}_n \equiv \mathcal{T}_n^\infty$, have found widespread applications in mathematics, physics and even in biology [45, 46, 47, 48].

Even though the finite Cayley tree appears at least as often as the infinite Bethe lattice in applications, the former is usually approximated by the latter which is easier to handle. Indeed, the walk generating functions of the Bethe lattices satisfy easily solvable relations[2]

$$g_{\mathcal{B}_n;00}(z) = \left(1 - n\,z^2\,g_{\mathcal{B}_n\setminus\{0\};11}(z)\right)^{-1}, \tag{2.31a}$$

$$g_{\mathcal{B}_n\setminus\{0\};11}(z) = \left(1 - (n-1)\,z^2\,g_{\mathcal{B}_n\setminus\{0\};11}(z)\right)^{-1}, \tag{2.31b}$$

where 0 and 1 designate any vertex and any vertex neighbouring 0, respectively. These equations are not fulfilled by finite Cayley trees, which exhibit finite size effects that are often neglected for the sake of simplicity. Yet these effects are generally important due to the large fraction of vertices on the outer-rim of the tree. In this section we obtain the exact walk generating functions on any finite Cayley tree.

We begin with the walk generating function $g_{\mathcal{T}_n^\Delta;00}$ for the cycles off the root of the tree. There are n backtracks off the root of the tree with weight z^2 and therefore

$$g_{\mathcal{T}_n^\Delta;\alpha\alpha} = \frac{1}{1 - nz^2 F_\Delta\left(z\sqrt{n-1}\right)}, \tag{2.32}$$

with F_Δ the finite continued fraction of depth Δ defined in Eq. (2.25). Indeed, since there are $n-1$ backtracks off the neighbours of the roots on $\mathcal{T}_n^\Delta\setminus\{0\}$, F_Δ fulfills the recursion relation

$$F_\Delta\left(z\sqrt{n-1}\right) = \frac{1}{1 - z^2(n-1)F_{\Delta-1}\left(z\sqrt{n-1}\right)}, \tag{2.33}$$

with solution $F_\Delta\left(z\sqrt{n-1}\right) = Q_{\Delta-1}\left(z\sqrt{n-1}\right)/Q_\Delta\left(z\sqrt{n-1}\right)$. The walk generating

[2] Called self-consistency relations in the physics literature.

function is therefore

$$g_{\mathcal{T}_n^\Delta;\,00} = \frac{Q_\Delta}{Q_\Delta - nz^2 Q_{\Delta-1}}. \tag{2.34}$$

where the functions Q_x are to be evaluated at $z\sqrt{n-1}$. We are now in position to obtain the walk generating function $g_{\mathcal{T}_n^\Delta;\,0d}$ for the walks from the root to a vertex located at distance d from it, $0 \leq d \leq \Delta$. Since there is only one simple path from 0 to d, we have

$$g_{\mathcal{T}_n^\Delta;\,0d} = z^d g_{\mathcal{T}_n^\Delta\setminus\{0,1,\cdots d-1\};\,dd} \cdots g_{\mathcal{T}_n^\Delta\setminus\{0\};\,11} g_{\mathcal{T}_n^\Delta;\,00}. \tag{2.35}$$

This simplifies upon noting that the graphs $\mathcal{T}_n^\Delta\setminus\{0,1\cdots j-1\}$ are truncated Cayley trees of radius $\Delta+1-j$ and with the root connected to only $n-1$ neighbours. Thus the walk generating functions $g_{\mathcal{T}_n^\Delta\setminus 0,1,\cdots j-1;\,jj}$ are easily found to be $F_{\Delta+1-j}(z\sqrt{n-1})$ and it follows that

$$g_{\mathcal{T}_n^\Delta;\,0d} = z^d \frac{Q_{\Delta-d}}{Q_\Delta} \frac{Q_{\Delta-1}}{Q_{\Delta-1} - nz^2 Q_{\Delta-2}}. \tag{2.36}$$

Again, the functions Q_x of the above expression are to be evaluated at $z\sqrt{n-1}$. In the limit $\Delta \to \infty$, we recover the known results of the Bethe lattice:

$$\lim_{\Delta\to\infty} g_{\mathcal{T}_n^\Delta;\,0d} = \frac{2^{d+1}(n-1)\,z^d \left(\sqrt{1-4(n-1)z^2}+1\right)^{-d}}{n\sqrt{1-4(n-1)z^2}+n-2} \equiv g_{\mathcal{B}_n;\,0d}, \tag{2.37}$$

in particular setting $d = 0$, we see that $\lim_{\Delta\to\infty} g_{\mathcal{T}_n^\Delta;\,00}$ fulfills Eqs. (2.31a), as expected.

On $\mathcal{T}_n^\Delta$ there are a total of $\binom{\Delta+3}{3} - 1$ different walk generating functions and we will consequently not derive them all explicitly here. Any one is nonetheless accessible thanks to Theorem 2.3.4. For example, consider the walk generating function $g_{\mathcal{T}_n^\Delta;\,dd}$ for a vertex located at distance d, $0 \leq d \leq \Delta$, of the root. We obtain $g_{\mathcal{T}_n^\Delta;\,dd}$ as the continued fraction of depth d

$$\begin{aligned} g_{\mathcal{T}_n^\Delta;\,dd} = \frac{1\,\big|}{\big|1-z^2(n-1)F_{\Delta-d}} - \frac{z^2\,\big|}{\big|1-z^2(n-2)F_{\Delta-(d-1)}} - \\ \frac{z^2\,\big|}{\big|1-z^2(n-2)F_{\Delta-(d-2)}} - \cdots - \frac{z^2\,\big|}{\big|1-z^2(n-2)F_{\Delta-1}-z^2F_{\Delta+1}}, \end{aligned} \tag{2.38}$$

where all functions F_x are to be evaluated at $z\sqrt{n-1}$. In this expression we used the notation of Pringsheim for continued fractions, i.e. $a_0 + \frac{a_1|}{|a_2} + \frac{a_3|}{|\cdots} = a_0 + \frac{a_1}{a_2+\frac{a_3}{\cdots}}$.

2.5 Proofs for the Prime Factorisation on Graphs

In this section we prove the results presented in the preceding sections without proof. We begin by proving that $(W_\mathcal{G}, +, \odot)$ forms a noncommutative nonassociative near-

algebra. We then prove the results of §2.3 on the prime factorisation of walks.

2.5.1 The nesting near-algebra

For $(W_\mathcal{G}, +, \odot)$ to form a noncommutative nonassociative near K-algebra, we must verify that $(W_\mathcal{G}, +)$ is an abelian group, shown in [38], and that the nesting product is compatible with the scalars and right distributive.

Compatibility with the scalars: let $(k_1, k_2) \in K^2$, $a \in W_{\mathcal{G};\,\alpha\omega}$ and $b \in W_{\mathcal{G};\,\mu\mu}$. We show that $(k_1\, a) \odot (k_2\, b) = k_1 k_2 (a \odot b)$. If $a \odot b = 0$ the property is trivially true. Otherwise, according to Definition 2.2.2, $\exists!\, a_1 \in W_{\mathcal{G};\,\alpha\mu}$, $\exists!\, a_2 \in W_{\mathcal{G};\,\mu\omega}$ with $a \odot b = a_1 \circ b \circ a_2$. Then $(k_1\, a) \odot (k_2\, b) = k_1 a_1 \circ (k_2 b) \circ a_2$. Since concatenation is bilinear, $k_1 a_1 \circ (k_2 b) \circ a_2 = k_1 k_2\, (a_1 \circ b \circ a_2) = k_1 k_2 (a \odot b)$ and nesting is compatible with the scalars.

Right-distributivity : let $(a, b) \in W^2_{\mathcal{G};\,\mu\mu}$ and $c \in W_{\mathcal{G};\,\alpha\omega}$. We show that $c \odot (a + b) = c \odot a + c \odot b$. Walks a and b being cycles off the same vertex μ (otherwise $a + b = 0$ and the property is trivially true), it follows that $c \odot a = 0 \iff c \odot b = 0 \iff c \odot (a + b) = 0$ and the property is true as soon as $c \odot a$ or $b = 0$. Otherwise, definition 2.2.2 implies that $\exists!\, c_1 \in W_{\mathcal{G};\,\alpha\mu}$ and $\exists!\, c_2 \in W_{\mathcal{G};\,\mu\omega}$ such that $c \odot a = c_1 \circ a \circ c_2$ and $c \odot b = c_1 \circ b \circ c_2$. Since concatenation is bilinear we have $c \odot a + c \odot b = c_1 \circ a \circ c_2 + c_1 \circ b \circ c_2 = c_1 \circ (a + b) \circ c_2 = c \odot (a + b)$ and nesting is right distributive.

Failure of left-distributivity : let $(a, b) \in W^2_{\mathcal{G};\,\alpha\omega}$ and $c \in W_{\mathcal{G};\,\mu\mu}$. We show that in general $(a + b) \odot c \neq a \odot c + b \odot c$. Suppose that both a and b visit μ. Then by Definition 2.2.2, $\exists!\, a_1 \in W_{\mathcal{G};\,\alpha\mu}$ and $\exists!\, a_2 \in W_{\mathcal{G};\,\mu\omega}$ with $a \odot c = a_1 \circ c \circ a_2$. Similarly, $b \odot c \neq 0 \Rightarrow \exists!\, b_1 \in W_{\mathcal{G};\,\alpha\mu}$ and $\exists!\, b_2 \in W_{\mathcal{G};\,\mu\omega}$ with $b \odot c = b_1 \circ c \circ b_2$. Now $a \odot c + b \odot c = a_1 \circ c \circ a_2 + b_1 \circ c \circ b_2 \neq (a_1 + b_1) \circ c \circ (a_2 + b_2) = (a + b) \odot c$.

The nesting product is therefore compatible with the scalars and right-distributive with respect to $+$ but not left-distributive. It follows that $K\mathcal{G}_\odot = (W_\mathcal{G}, +, \odot)$ is a noncommutative nonassociative near K-algebra.

2.5.2 Existence and uniqueness of the prime factorisation

We begin by showing that the factorisation of a walk into nesting products of simple paths and simple cycles always exists and is unique in the sense of Definition 2.3.2. We then demonstrate Proposition 2.2.1, i.e. that the simple paths and simple cycles are the prime elements of $(W_\mathcal{G}, \odot)$, thereby establishing Theorem 2.3.1 as an equivalent to the fundamental theorem of arithmetic.

Let $\mathcal{P}(n)$ be the following proposition: *$\forall w \in W_\mathcal{G}$ of length $\ell(w) \leq n$, there exists a unique factorisation, up to equivalence, of w into nesting products of irreducible walks, i.e.* $\exists!\, F(w) \in \mathcal{F}_w / \equiv$.

We demonstrate that $\mathcal{P}(n)$ holds for all $n \geq 1$ by induction on the walk length n.

Firstly, we demonstrate that $\mathcal{P}(1)$ is true. Consider $w \in W_{\mathcal{G}}$ such that $\ell(w) = 1$. Then w is either of the form $(\alpha\alpha)$ or $(\alpha\omega)$, for some vertices α and ω, and is then irreducible. Furthermore, the factorised form of w is w itself and is clearly unique in the sense of Definition 2.3.2, so $\mathcal{P}(1)$ holds.

Secondly, we show that $\forall j \leq n,\ \mathcal{P}(j)$ holds $\Rightarrow \mathcal{P}(n+1)$ holds. Consider $w \in W_{\mathcal{G}}$ such that $\ell(w) = n+1$. If w is irreducible, then its factorisation into nesting product(s) of irreducible walk(s) exists and is unique: $F(w) \equiv w$. If w is not irreducible, then $\exists\,(a,b)$ non-trivial such that $w = a \odot b$. Necessarily $1 \leq \ell(a),\ \ell(b) \leq n$ and, supposing $\forall j \leq n,\ \mathcal{P}(j)$ holds, $\exists!\, F(a)$ and $\exists!\, F(b)$. Then $\mathfrak{f}_1(w) = F(a) \odot F(b)$ is a valid prime factorisation of w. Now suppose that there exists a second prime factorisation $\mathfrak{f}_2(w)$ of w, with $\mathfrak{f}_1(w) \not\equiv \mathfrak{f}_2(w)$. Since $\mathfrak{f}_2(w)$ exists, $\exists\,(c,d)$ a couple of non-trivial walks with $w = c \odot d$, $1 \leq \ell(c),\ \ell(d) \leq n$, and $\mathfrak{f}_2(w) = F(c) \odot F(d)$.

If $a = c$ and $b = d$ then by the induction hypothesis $\ell(a) = \ell(c) \leq n \Rightarrow \exists!\, F(a) \equiv F(c)$ and $\ell(b) = \ell(d) \leq n \Rightarrow \exists!\, F(b) \equiv F(d)$. Thus $\mathfrak{f}_1(w) \equiv \mathfrak{f}_2(w)$ and $\mathcal{P}(n+1)$ holds. Now consider the case $(a,b) \neq (c,d)$. Since $w = a \odot b = c \odot d$, the position of the cycle d in the vertex sequence of w must fall into one of the following three cases:

i) $\underline{d \subseteq a}$. Let $e = a \cap c$ be the vertex sequence common to a and c, see schematic representation below. Note that (a,b) canonical $\Rightarrow (e,b)$ canonical, and (c,d) canonical $\Rightarrow (e,d)$ canonical and $c = e \odot b$ and $a = e \odot d$. It follows that $\mathfrak{f}_1(w) = \big(F(e) \odot F(d)\big) \odot F(b)$ and $\mathfrak{f}_2(w) = \big(F(e) \odot F(b)\big) \odot F(d)$. Now since $1 \leq \ell(e), \ell(b), \ell(d) \leq n$ and since $\mathcal{P}(j)$ holds $\forall j \leq n$, $\exists!\, F(e)$, $\exists!\, F(d)$, and $\exists!\, F(b)$. Consequently $\mathfrak{f}_1(w) \equiv \mathfrak{f}_2(w) \Rightarrow \mathcal{P}(n+1)$ holds.

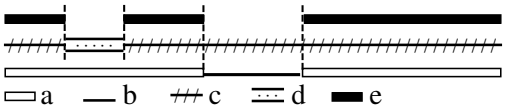

Schematic representation of the vertex sequence of w in the case $d \subseteq a$.

ii) $\underline{d \subseteq b}$. Let $e = b \cap c$. By construction, e is a cycle, (a,b) canonical $\Rightarrow (a,e)$ canonical and (c,d) canonical $\Rightarrow (e,d)$ canonical. Thus $b = e \odot d$ and $c = a \odot e$ and then $\mathfrak{f}_1(w) = F(a) \odot \big(F(e) \odot F(d)\big)$ and $\mathfrak{f}_2(w) = \big(F(a) \odot F(e)\big) \odot F(d)$. Now since $1 \leq \ell(a), \ell(e), \ell(d) \leq n$ and since $\mathcal{P}(j)$ holds $\forall j \leq n$, $\exists!\, F(e)$, $\exists!\, F(d)$, and $\exists!\, F(a)$. Consequently $\mathfrak{f}_1(w) \equiv \mathfrak{f}_2(w) \Rightarrow \mathcal{P}(n+1)$ holds.

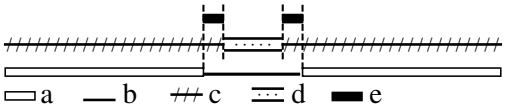

Case $d \subseteq b$.

iii) d straddles a and b. Given that $c \odot d \neq 0$ and $a \odot b \neq 0$ by assumption, d and b must be cycles off vertices δ and β, respectively. Since d straddles over a and b, then δ is visited by both a and b, and β is visited by both c and d.

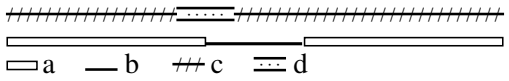

Case d straddles over a and b.

We first examine the situation $\beta \neq \delta$, distinguishing two cases: 1) $a \in W_{\mathcal{G};\,\beta\beta}$. Then c visits β before δ, but β is also visited by d. Thus the couple (c, d) is non-canonical, which is a contradiction. 2) $a \in W_{\mathcal{G};\,\alpha\beta}$, or β appears only as an internal vertex of a. In either situation, a visits δ before the final appearance of β, but δ is also visited by b. Then the couple (a, b) is non-canonical, which is a contradiction.

Secondly, consider the case of $\beta = \delta$. Then the last appearance of β in c must be the last vertex of b (since $a \odot b$ nests b into a off the final appearance of β). However, d straddles a and b, which implies that i) c visits β after the last vertex of d, and ii) d is not nested into c off the last appearance of β. This is a contradiction.

Therefore, in any of the above cases, we found it to be impossible that $w = a \odot b = c \odot d$ with d straddling a and b.

We have demonstrated that $\mathcal{P}(1)$ is true, and upon supposing that $\mathcal{P}(j)$ holds for all $j \leq n$, we have shown that $\mathcal{P}(n+1)$ holds. Consequently $\mathcal{P}(n)$ holds $\forall n \in \mathbb{N}\backslash\{0\}$. The prime factorisation of a walk thus always exists and is unique in the sense of Definition 2.3.2. □

We now establish Proposition 2.2.1 in two steps. First we determine the irreducible walks and then the prime walks.

Proposition 2.5.1. *Let $w \in W_{\mathcal{G}}$. Then w is irreducible if and only if $w \in \Pi_{\mathcal{G}} \cup \Gamma_{\mathcal{G}}$.*

Proof. Clearly $w \in \Pi_{\mathcal{G}} \cup \Gamma_{\mathcal{G}} \Rightarrow w$ irreducible. Now consider an irreducible walk w, and suppose that $w \notin \Pi_{\mathcal{G}} \cup \Gamma_{\mathcal{G}}$. Since w is neither a simple path nor a simple cycle, there exists an earliest vertex μ visited at least twice by w (if w is a cycle, then consider the earliest internal vertex visited at least twice by w). Now let $s_\mu \subset w$ be the vertex sequence joining the first appearance of μ to its final appearance in w, and let w_μ be the vertex sequence obtained from w by replacing s_μ by (μ) in w. Then (w_μ, s_μ) is a canonical couple of non-trivial walks and $w = w_\mu \odot s_\mu$, which is a contradiction. □

Proposition 2.5.2. *Let $w \in W_{\mathcal{G}}$. Then w is prime if and only if $w \in \Pi_{\mathcal{G}} \cup \Gamma_{\mathcal{G}}$.*

Proof. Firstly, we demonstrate $w \in \Pi_{\mathcal{G}} \cup \Gamma_{\mathcal{G}} \Rightarrow w$ prime. Consider $(a, b) \in W_{\mathcal{G}}^2$ such that $w \,|\, a \odot b$. Since $w \in \Pi_{\mathcal{G}} \cup \Gamma_{\mathcal{G}}$ then w is an irreducible factor appearing in the

prime factorisation $\mathcal{F}_{\odot}(a \odot b)$. By uniqueness of this factorisation, w must either be an irreducible factor of $\mathcal{F}_{\odot}(a)$, implying $w \,|\, a$; or an irreducible factor of $\mathcal{F}_{\odot}(b)$, implying $w \,|\, b$; or both. It follows that w is prime. Secondly, we show that w prime $\Rightarrow w \in \Pi_{\mathcal{G}} \cup \Gamma_{\mathcal{G}}$. Suppose that $\exists\, w \in W_{\mathcal{G}}$ prime with $w \notin \Pi_{\mathcal{G}} \cup \Gamma_{\mathcal{G}}$. Then observe that since $w \notin \Pi_{\mathcal{G}} \cup \Gamma_{\mathcal{G}}$, w is not irreducible, and there exists at least one canonical couple of non-trivial walks $(a, b) \in W_{\mathcal{G}}^2$ such that $w = a \odot b$. Clearly $w \,|\, a \odot b$, and a and b are strictly shorter than w. Therefore w does not divide a, $w \nmid a$ and similarly $w \nmid b$, which is a contradiction. □

Propositions 2.5.1 and 2.5.2 yield Proposition 2.2.1. Together with the proof of existence and uniqueness of the prime factorisation, this establishes Theorem 2.3.1.

2.5.3 Validity of the walk factorisation algorithm

We demonstrate the validity of Algorithm 1, first by verifying the correctness of the factorisations it performs and second by showing that for any finite-length walk, the algorithm stops and yields the prime factorisation. Let $\mathfrak{f}(w)$ be any factorisation of a walk $w \in W_{\mathcal{G}}$ of finite length ℓ and let $a \in \mathsf{F}\big(\mathfrak{f}(w)\big)$.

If $a \in W_{\mathcal{G};\mu\mu}$ and μ appears $k > 0$ times as internal vertex of a, then the algorithm splits the vertex string of a at each internal appearance of μ, thus producing $k+1$ cycles $c_{0\leq j\leq k}$ off μ. Clearly, by construction, $a = c_0 \circ \cdots \circ c_k$. Since nesting coincides with concatenation over the cycles, we have $c_j \circ c_{j+1} = c_j \odot c_{j+1}$ and

$$a = c_0 \odot \cdots \odot c_k, \tag{2.39}$$

as claimed in the algorithm. Note that the $c_{0\leq j\leq k}$ cycles are strictly shorter that a and, by construction, do not have μ as internal vertex.

Else, let $(\alpha_1\, \alpha_2 \cdots \alpha_n)$ be the vertex sequence of a. Consider the earliest vertex η of a visited at least twice by a (the earliest internal vertex, if a is a cycle). Let i be the position of the earliest occurrence of η in a (thus $\alpha_i = \eta$) and let s_1 be the associated sequence, as per the algorithm. Let w_1 be the walk obtained from a by deleting s_1 from a. Then the couple $(w_1,\, s_1)$ is canonical, since all vertices $\alpha_{k<i}$ are visited precisely once by w and therefore cannot be visited by s_1. Then, by construction of s_1 and w_1, we have $\mathfrak{f}_1(a) = w_1 \odot s_1$. By applying the same reasoning as above for the earliest vertex λ visited at least twice by w_1 (the earliest internal vertex, if w_1 is a cycle), we construct a canonical couple $(w_2,\, s_2)$ with $w_1 = w_2 \odot s_2$ and thus $\mathfrak{f}_2(a) = (w_2 \odot s_2) \odot s_1$. Proceeding similarly with w_2 and all the subsequent non-irreducible walks w_j thus yields

$$\mathfrak{f}_m(a) = \Big(\big((r \odot s_m) \odot s_{m-1}\big) \odot \cdots \Big) \odot s_1, \tag{2.40}$$

where and $r \equiv w_m$ is irreducible, as claimed in the algorithm.

In both cases a is factorised into nesting products of strictly shorter walks. These are either irreducible, or they will in turn be factorised into nesting products of strictly shorter walks by the algorithm. Thus, if the initial length of the walk

is ℓ, after at most $\ell - 1$ recursive factorisations, all factors obtained are either irreducible or of length 1. Since all walks of length 1 are irreducible, it follows that the algorithm factors finite-length walks into nesting products of irreducible walks in a finite number of steps.

2.5.4 Prime factorisations of $W_{\mathcal{G};\,\alpha\omega}$ and $\Sigma_{\mathcal{G};\,\alpha\omega}$

▶ We first prove Theorem 2.3.2.

Proof. Let $(\nu_0,\, \nu_p) \in \mathcal{V}(\mathcal{G})^2$, and consider $w \in W_{\mathcal{G};\,\nu_0\nu_p}$. For convenience, we define

$$B_{\mathcal{G};\,\nu_0\nu_p} = \left(\left(\left(\Pi_{\mathcal{G};\,\nu_0\nu_p} \odot C^*_{\mathcal{G}\setminus\{\nu_0,\cdots,\nu_{p-1}\};\,\nu_p} \right) \odot \cdots \odot C^*_{\mathcal{G}\setminus\{\nu_0\};\,\nu_1} \right) \odot C^*_{\mathcal{G};\,\nu_0} \right), \tag{2.41}$$

where $C_{\mathcal{G}\setminus\{\nu_0,\cdots,\nu_{j-1}\};\,\nu_j}$ is the set of cycles off ν_j on $\mathcal{G}\setminus\{\nu_0,\cdots,\nu_{j-1}\}$ that do not have ν_j as internal vertex. We demonstrate that $B_{\mathcal{G};\,\nu_0\nu_p} = W_{\mathcal{G};\,\nu_0\nu_p}$ by showing that $W_{\mathcal{G};\,\nu_0\nu_p} \subseteq B_{\mathcal{G};\,\nu_0\nu_p}$ and $B_{\mathcal{G};\,\nu_0\nu_p} \subseteq W_{\mathcal{G};\,\nu_0\nu_p}$. In a second time, we show that $C_{\mathcal{G};\,\mu_c}$ identifies with the set $A_{\mathcal{G};\,\mu_c}$ defined in the Theorem.

By Eq. (2.40), w can be expressed as a simple path $r \in \Pi_{\mathcal{G};\,\nu_0\nu_p}$ with cycles s_j nested into it, that is $\mathfrak{f}(w) = \left(\left((r \odot s_m) \odot s_{m-1} \right) \odot \cdots \right) \odot s_1$. By construction, the s_j are non-trivial cycles nested off different vertices of the simple path r. For all the vertices ν_k of r, we define $s_{\nu_k} = (\nu_k)$ if no s_j is nested off ν_k and $s_{\nu_k} = s_j$ if $h(s_j) = \nu_k$. Then let

$$\tilde{\mathfrak{f}}(w) = \left(\left((r \odot s_{\nu_p}) \odot s_{\nu_{p-1}} \right) \odot \cdots \right) \odot s_{\nu_0}, \tag{2.42}$$

and note that $\tilde{\mathfrak{f}}(w) \equiv \mathfrak{f}(w)$. By the canonical property, s_{ν_j} cannot visit any of the $\nu_0, \cdots, \nu_{j-1}$ vertices and must therefore belong to $W_{\mathcal{G}\setminus\{\nu_0,\cdots,\nu_{j-1}\};\,\nu_j\nu_j}$. By Eq. (2.39), any cycle of $W_{\mathcal{G}\setminus\{\nu_0,\cdots,\nu_{j-1}\};\,\nu_j\nu_j}$ can be decomposed into nesting products of shorter cycles c_i off ν_j that do not have ν_j as internal vertex. Therefore $s_{\nu_j} \in C^*_{\mathcal{G}\setminus\{\nu_0,\cdots,\nu_{j-1}\};\,\nu_j}$ and consequently $w \in B_{\mathcal{G};\,\nu_0\nu_p} \Rightarrow W_{\mathcal{G};\,\nu_0\nu_p} \subseteq B_{\mathcal{G};\,\nu_0\nu_p}$. Furthermore, any element of $B_{\mathcal{G};\,\nu_0\nu_p}$ is a walk on $\mathcal{G}$ from ν_0 to ν_p and $B_{\mathcal{G};\,\nu_0\nu_p} \subseteq W_{\mathcal{G};\,\nu_0\nu_p} \Rightarrow B_{\mathcal{G};\,\nu_0\nu_p} = W_{\mathcal{G};\,\nu_0\nu_p}$.

It remains to show that $C_{\mathcal{G};\,\mu_c}$ is the set $A_{\mathcal{G};\,\mu_c}$ of the Theorem. Let $c \in C_{\mathcal{G};\,\mu_c}$. Applying the same reasoning as above, c factorises as in Eq. (2.42) but with $r \in \Gamma_{\mathcal{G};\,\mu_c}$. Then c is an element of the set :

$$\left(\left(\left(\Gamma_{\mathcal{G};\,\mu_c} \odot C^*_{\mathcal{G}\setminus\{\mu_c,\,\mu_1,\cdots,\,\mu_{c-2}\};\,\mu_{c-1}} \right) \odot \cdots \odot C^*_{\mathcal{G}\setminus\{\mu_c,\,\mu_1\};\,\mu_2} \right) \odot C^*_{\mathcal{G}\setminus\{\mu_c\};\,\mu_1} \right). \tag{2.43}$$

Furthermore any element of the above set is a cycle off μ_c that does not have μ_c as internal vertex. Therefore $C_{\mathcal{G};\,\mu_c}$ identifies with the set of Eq. (2.43). Clearly if μ_c has no neighbour on $\mathcal{G}$, $C_{\mathcal{G};\,\mu_c} = (\mu_c\mu_c)$ if the loop $(\mu_c\mu_c)$ exists and $C_{\mathcal{G};\,\mu_c} = (\mu_c)$ otherwise. It follows that $C_{\mathcal{G};\,\mu_c} = A_{\mathcal{G};\,\mu_c}$ since both fulfill the same recursive relation and value on vertices with no neighbour. This establishes Eq. (2.6b) and, together with $B_{\mathcal{G};\,\nu_0\nu_p} = W_{\mathcal{G};\,\nu_0\nu_p}$, Eq. (2.6a). □

▶ We prove Theorem 2.3.3.

Proof. The theorem follows from Theorem 2.3.2. Consider $W_{\mathcal{G};\,\alpha\omega}$ be the set of walks from α to ω. We first decompose $W_{\mathcal{G};\,\alpha\omega}$ using Eq. (2.6a), identifying α with ν_0 and ω with ν_p for convenience, then sum over the elements of the sets on both sides of the equality. This yields, in vertex-edge notation,

$$\Sigma_{\mathcal{G};\,\alpha\omega} = \sum_{(\alpha\nu_1\cdots\nu_{p-1}\omega)\in\Pi_{\mathcal{G};\,\alpha\omega}} \left(\sum_{\mathfrak{a}_0\in A^*_{\mathcal{G};\,\alpha}} \mathfrak{a}_0\right)(\alpha\nu_1)\left(\sum_{\mathfrak{a}_1\in A^*_{\mathcal{G}\setminus\{\alpha\};\,\nu_1}} \mathfrak{a}_1\right)(\nu_1\nu_2)\cdots \tag{2.44}$$
$$\cdots(\nu_{p-1}\omega)\left(\sum_{\mathfrak{a}_p\in A^*_{\mathcal{G}\setminus\{\alpha,\nu_1,\cdots,\nu_{p-1}\};\,\omega}} \mathfrak{a}_p\right),$$

which we obtain upon nesting the sets $A^*_{\mathcal{G};\,\alpha}$, $A^*_{\mathcal{G}\setminus\{\alpha\};\,\nu_1},\ldots$ into the simple paths of $\Pi_{\mathcal{G};\,\alpha\omega}$ at the appropriate positions. Equation (2.44) shows that the sums over these sets can be seen as effective vertices produced by dressing each vertex of the simple paths by all the cycles that visit these vertices on progressively smaller digraphs $\mathcal{G}$, $\mathcal{G}\setminus\{\alpha\},\ldots$. For example, we define a dressed vertex $(\alpha)'_{\mathcal{G}}$ representing the series of all the cycles off α on $\mathcal{G}$ as

$$(\alpha)'_{\mathcal{G}} = \sum_{\mathfrak{a}_0\in A^*_{\mathcal{G};\,\alpha}} \mathfrak{a}_0. \tag{2.45}$$

It follows that Eq. (2.44) yields Eq. (2.9a), with dressed vertices representing the characteristic series of the $A^*_{\mathcal{G}\setminus\{\alpha,\nu_1\cdots\nu_{j-1}\};\,\nu_j}$ sets. These series are proper [49]: their constant term is a trivial walk, e.g. (α) in Eq. (2.45), which is different from the empty walk 0. Thus the series represents the inverse $(\alpha)'_{\mathcal{G}} = [(\alpha) - \sum_{c\in A_{\mathcal{G};\,\alpha}} c]^{-1}$ [50].

We can verify this explicitly on the quiver: define $\varphi_{\Gamma_{\mathcal{G};\,\alpha}}$ the mapping representing the finite series $\sum_{\gamma\in\Gamma_{\mathcal{G};\,\alpha}}\gamma'$. By linearity, this is simply $\varphi_{\Gamma_{\mathcal{G};\,\alpha}} = \sum_{\gamma\in\Gamma_{\mathcal{G};\,\alpha}}\varphi_{\gamma'}$. Define $\varphi_{(\alpha)'_{\mathcal{G}}} = \sum_{p\in\mathbb{N}}\varphi^{(p)}_{\Gamma_{\mathcal{G};\,\alpha}}$, where $\varphi^{(p)}_{\Gamma_{\mathcal{G};\,\alpha}}$ is the p-th composition of $\varphi_{\Gamma_{\mathcal{G};\,\alpha}}$ with itself, $\varphi^{(0)}_{\Gamma_{\mathcal{G};\,\alpha}}$ being the local identity map 1_α. Then observe that $\varphi_{(\alpha)'_{\mathcal{G}}}\circ\varphi_{\Gamma_{\mathcal{G};\,\alpha}} = \varphi_{\Gamma_{\mathcal{G};\,\alpha}}\circ\varphi_{(\alpha)'_{\mathcal{G}}} = \sum_{p\in\mathbb{N}}\varphi^{(p+1)}_{\Gamma_{\mathcal{G};\,\alpha}} = \varphi_{(\alpha)'_{\mathcal{G}}} - 1_\alpha$. Consequently, $\varphi_{(\alpha)'_{\mathcal{G}}}$ is the compositional inverse

$$\varphi_{(\alpha)'_{\mathcal{G}}} = \left(1_\alpha - \varphi_{\Gamma_{\mathcal{G};\,\alpha}}\right)^{(-1)}, \tag{2.46}$$

which is the quiver representation of the formal inverse $(\alpha)'_{\mathcal{G}} = [(\alpha) - \sum_{c\in A_{\mathcal{G};\,\alpha}} c]^{-1}$. By the same token, the matrix representation of $\varphi_{(\alpha)'_{\mathcal{G}}}$ is the matrix inverse of the matrix representation of $1_\alpha - \varphi_{\Gamma_{\mathcal{G};\,\alpha}}$.

By combining this result with Eq. (2.6b), the dressed vertices are thus seen to

be of the form

$$(\alpha)'_{\mathcal{G}} = \left[(\alpha) - \sum_{\Gamma_{\mathcal{G};\alpha}} (\alpha)\,(\alpha\mu_2)\,(\mu_2)'_{\mathcal{G}\setminus\{\alpha\}}\,(\mu_2\mu_3)\cdots(\mu_m\alpha)\right]^{-1}, \tag{2.47}$$

where m is the length of the simple cycle $(\alpha\mu_2\cdots\mu_m\omega) \in \Gamma_{\mathcal{G};\alpha}$ and (α) is the local identity common to all walks of $W_{\mathcal{G};\alpha\alpha}$, in particular $\forall c \in \Gamma_{\mathcal{G};\alpha}$, we have $c^0 = (\alpha)$. In this expression, the dressed vertices again represent sums over the Kleene stars that appear when $A_{\mathcal{G};\alpha}$ is decomposed using Eq. (2.6b). This establishes Eq. (2.9b). □

▶ We prove Theorem 2.3.4.

Proof. This theorem follows from Theorem 2.3.3 together with the properties of the weight function. □

2.5.5 The star-height of factorised walk sets

We begin by establishing an exact recursive relation yielding the star-height of the prime factorisation of a walk-set. This relation will be necessary to prove Theorem 2.3.5.

Proposition 2.5.3 (Star-height)**.** *Let $(\mu_c, \nu_0, \nu_p) \in \mathcal{V}(\mathcal{G})^3$. Then, the star-height $h\big(W_{\mathcal{G};\mu_c\mu_c}\big)$ of the factorised expression for the set of cycles $W_{\mathcal{G};\mu_c\mu_c}$ is given by the recursive relation*

$$h\big(W_{\mathcal{G};\mu_c\mu_c}\big) = \begin{cases} 0 & \text{if } \Gamma_{\mathcal{G};\mu_c} = \{(\mu_c)\}, \\ 1 + \max\limits_{\Gamma_{\mathcal{G};\mu_c}} \max\limits_{1\le i\le c-1} h\big(W_{\mathcal{G}\setminus\{\mu_c,\mu_1,\cdots,\mu_{i-1}\};\mu_i\mu_i}\big) & \text{otherwise,} \end{cases} \tag{2.48}$$

where $(\mu_c\mu_1\cdots\mu_{c-1}\mu_c) \in \Gamma_{\mathcal{G};\mu_c}$. The star-height $h\big(W_{\mathcal{G};\nu_0\nu_p}\big)$ of the factorised expression for the set of open walks $W_{\mathcal{G};\nu_0\nu_p}$ is

$$h\big(W_{\mathcal{G};\nu_0\nu_p}\big) = \max_{\Pi_{\mathcal{G};\nu_0\nu_p}} \max_{0\le i\le p} h\big(W_{\mathcal{G}\setminus\{\nu_0,\nu_1,\cdots,\nu_{i-1}\};\nu_i\nu_i}\big), \tag{2.49}$$

where $(\nu_0\nu_1\cdots\nu_{p-1}\nu_p) \in \Pi_{\mathcal{G};\nu_0\nu_p}$.

Proof. These results follow from Eqs. (2.6a, 2.6b). We have $W_{\mathcal{G};\mu_c\mu_c} = A^*_{\mathcal{G};\mu_c}$ and thus if $A_{\mathcal{G};\mu_c} = \Gamma_{\mathcal{G};\mu_c} = \{(\mu_c)\}$ is trivial, then $h(W_{\mathcal{G};\mu_c\mu_c}) = 0$. Otherwise, $h(W_{\mathcal{G};\mu_c\mu_c}) = 1 + h(A_{\mathcal{G};\mu_c})$. Now by Eq. (2.6b) we have

$$h\big(A_{\mathcal{G};\mu_c}\big) = \max_{\Gamma_{\mathcal{G};\mu_c}} \max_{1\le i\le c-1} h\big(A_{\mathcal{G}\setminus\{\mu_c,\mu_1,\cdots,\mu_{i-1}\};\mu_i\mu_i}\big), \tag{2.50}$$

and since $W_{\mathcal{G}\setminus\{\mu_c,\mu_1,\cdots,\mu_{i-1}\};\mu_i\mu_i} = A^*_{\mathcal{G}\setminus\{\mu_c,\mu_1,\cdots,\mu_{i-1}\};\mu_i\mu_i}$, Eq. (2.48) follows. By similar reasoning, Eq. (2.49) is obtained from Eq. (2.6a); we omit the details. □

Remark 2.5.1 (Cycle rank)**.** The cycle rank $r(\mathcal{G})$ of a graph $\mathcal{G}$ [44] quantifies the minimum number of vertices that must be removed from $\mathcal{G}$ in order for its largest strongly connected component to be acyclic. Contrary to what one might expect, the star-heights $h(W_{\mathcal{G};\,\nu_0\nu_p})$ and $h(W_{\mathcal{G};\,\mu_c\mu_c})$ are not equal to the cycle rank $r(\mathcal{G})$. This is because of an essential difference between Proposition 2.5.3 and the definition of $r(\mathcal{G})$: when calculating the star-height of a prime factorisation, the removal of vertices takes place along simple paths and simple cycles of $\mathcal{G}$. Conversely, the definition of $r(\mathcal{G})$ allows the removal of non-neighbouring vertices throughout the graph. By this argument we see that the cycle rank is only a lower bound on the star-height of factorised forms of walk sets: $h(W_{\mathcal{G};\,\nu_0\nu_p}) \geq r(\mathcal{G})$ and $h(W_{\mathcal{G};\,\mu_c\mu_c}) \geq r(\mathcal{G})$.

► We now prove Theorem 2.3.5.

Proof. We begin by proving the result for $h(W_{\mathcal{G};\,\alpha\alpha})$. Let $p_\alpha = (\alpha\nu_2\cdots\nu_{\ell_\alpha}) \in \mathrm{L}\Pi_{\mathcal{G};\,\alpha}$. Consider the cycle w_α off α produced by traversing p_α from start to finish, then traversing the loop $(\nu_{\ell_\alpha}\nu_{\ell_\alpha})$ if it exists, then returning to α along p_α. The proof consists of showing that w_α comprises the longest possible chain of recursively nested simple cycles on $\mathcal{G}$.

To this end, consider the factorisation of w_α. Let L_α be equal to $(\nu_{\ell_\alpha}\nu_{\ell_\alpha})$, if this loop exists, or (ν_{ℓ_α}), otherwise. Then observe that

$$w_\alpha = b_0 \odot \Big(b_1 \odot \cdots \odot \big(b_{\ell_\alpha-1} \odot (b_{\ell_\alpha} \odot L_\alpha)\big)\ldots\Big)\,, \tag{2.51}$$

where $b_{0\leq j\leq \ell_\alpha-1}$ is the back-track $b_j = (\nu_j\nu_{j+1}\nu_j) \in \Gamma_{\mathcal{G}\setminus\{\alpha,\nu_2\cdots\nu_{j-1}\};\,\nu_j}$, where we have identified α with ν_0 for convenience. Equation (2.51) shows that w_α is a chain of ℓ_α (or $\ell_\alpha+1$, if the loop $(\nu_{\ell_\alpha}\nu_{\ell_\alpha})$ exists) recursively nested non-trivial simple cycles, and $W_{\mathcal{G};\,\alpha\alpha}$ must involve at least this many nested Kleene stars.

To see that this chain is the longest, suppose that there exists a walk w' involving $n > \ell_\alpha$ $\big($or $n > \ell_\alpha+1$, if the loop $(\nu_{\ell_\alpha}\nu_{\ell_\alpha})$ exists$\big)$ non-trivial recursively nested simple cycles $c_1, \cdots, c_n$; that is, $c_1 \odot \big(\cdots \odot (c_{n-1} \odot c_n)\big) \subseteq w'$. Then, by the canonical property, the vertex sequence $s \subseteq w'$ joining the first vertex of c_1 to the last internal vertex of c_n defines a simple path p' of length $\ell(p') \geq n > \ell_\alpha$. This is in contradiction to the definition of ℓ_α, and thus w' does not exist. Consequently, $h(W_{\mathcal{G};\,\alpha\alpha}) = \ell_\alpha + 1$ if the loop $(\nu_{\ell_\alpha}\nu_{\ell_\alpha})$ exists, or ℓ_α, if there is no self-loop on ν_{ℓ_α}.

We now turn to determining $h(W_{\mathcal{G};\,\alpha\omega})$. Combining Eq. (2.49) with the result for $h(W_{\mathcal{G};\,\alpha\alpha})$ obtained above yields

$$h\big(W_{\mathcal{G};\,\alpha\omega}\big) = \max_{\Pi_{\mathcal{G};\,\nu_0\nu_p}} \max_{0\leq i\leq p} \begin{cases} \ell_{\nu_i}\big(\mathcal{G}\backslash\{\alpha,\ldots,\nu_{i-1}\}\big) + 1 & \text{if there is a self-loop on vertex } \nu_i, \\ \ell_{\nu_i}\big(\mathcal{G}\backslash\{\alpha,\ldots,\nu_{i-1}\}\big) & \text{otherwise,} \end{cases} \tag{2.52}$$

where $\ell_{\nu_i}(\mathcal{G}\backslash\{\alpha,\ldots,\nu_{i-1}\})$ is the length of the longest simple path p_{ν_i} off vertex ν_i on $\mathcal{G}\backslash\{\alpha,\ldots,\nu_{i-1}\}$, and $\nu_{\ell_{\nu_i}}$ is the last vertex of p_{ν_i}. Finally, we note that p_α is the longest of all the simple paths p_{ν_i}: since $\mathcal{G}$ is undirected and connected, it is strongly

connected, and since $\mathcal{G}\backslash\{\alpha,\ldots,\nu_{i-1}\}$ is a subgraph of $\mathcal{G}$ strictly smaller than $\mathcal{G}$, then p_{ν_i} must be shorter than p_α. Therefore Eq. (2.52) yields $h(W_{\mathcal{G};\,\alpha\omega}) = h(W_{\mathcal{G};\,\alpha\alpha})$.

It follows from these results that in order to determine the star-height of the factorised form of any walk set on an undirected connected $\mathcal{G}$, one must determine the existence of a Hamiltonian path on $\mathcal{G}$. Consequently, the problem of determining $h\big(W_{\mathcal{G};\,\alpha\omega}\big)$ and $h\big(W_{\mathcal{G};\,\alpha\alpha}\big)$ is NP-complete. □

2.6 Summary and Outlook

In this chapter we established that walks on any finite digraph $\mathcal{G}$ factorise uniquely into nesting products of prime walks, which are the simple paths and simple cycles on $\mathcal{G}$. We used this result to factorise sets of walks, as well as the characteristic series of all walks between any two vertices of any finite digraph or weighted digraph, thereby obtaining a universal continued fraction expression for these series.

As mentioned in the text, our results can be recast so as to hold for digraphs with multiple directed edges. Less evident, and more interesting, is the extension of the results presented here to other species of graphs, such as hypergraphs and continuous (weighted) graphs. In the latter case, we have already obtained preliminary results which could not report here due to length concerns. We believe that research in this direction will find applications in solving fractional differential equations and might prove useful for quantum field theories, where the evolution of quantum systems can be described as the integral of all the walks on a continuous graph.

The factorisation of walks into products of simple paths and simple cycles is certainly not the only possible construction of this type on digraphs. In particular, the important points in obtaining resummed expressions for series of walks are the *existence* and *uniqueness* of the factorisation of walks into primes. Indeed, provided both properties are verified, there is a unique way to group walks into families generated by their prime factors. Furthermore, we are free to construct different walk factorisations based on different definitions for the walk product, e.g. inducing different prime walks. Consequently, as long as the existence and uniqueness properties hold, we can construct as many representations of walk sets and walk series as there are ways to define a walk product. We formalise these observations in the last chapter of the present thesis.

Chapter 3
The Method of Path-Sums

I regard as quite useless the reading of large treatises of pure analysis: too large a number of methods pass at once before the eyes. It is in the works of applications that one must study them; one judges their ability there and one apprises the manner of making use of them.

J. L. Lagrange

We introduce the method of path-sums which is a tool for analytically evaluating a primary function of a finite square discrete matrix, based on the closed-form resummation of infinite families of terms in the corresponding Taylor series. Provided the required inverse transforms are available, our approach yields the exact result in a finite number of steps. We achieve this by combining a mapping between matrix powers and walks on a weighted directed graph with a universal graph-theoretic result on the structure of such walks. We present path-sum expressions for a matrix raised to a complex power, the matrix exponential, matrix inverse, and matrix logarithm. We present examples of the application of the path-sum method.

The work in this chapter was carried out in collaboration with Simon Thwaite and forms the basis of an article that has been published in the *SIAM Journal on Matrix Analysis and Applications* **34(2)**, 445-469, 2013.

3.1 Introduction

Many problems in applied mathematics, physics, computer science, and engineering are formulated most naturally in terms of matrices, and can be solved by computing functions of these matrices. Two well-known examples are the use of the matrix inverse in the solution of systems of linear equations, and the application of the matrix exponential to the solution of systems of linear ordinary differential equations with constant coefficients. These applications, among many others, have led to the rise of an active area of research in applied mathematics and numerical analysis focusing on the development of methods for the computation of functions of matrices over $\mathbb{R}$ or $\mathbb{C}$ (see e.g. [51]).

As part of this ongoing effort, we introduce in this chapter a novel symbolic method for evaluating primary matrix functions f analytically and in closed form. The method – which we term the method of path-sums – is valid for finite square discrete matrices, and exploits connections between matrix multiplication and graph theory. It is based on the following three central concepts: (i) we describe a method

of partitioning a matrix M into submatrices and associate these with a weighted directed graph $\mathcal{G}$; (ii) we show that the problem of evaluating any submatrix of $f(\mathsf{M})$ is equivalent to summing the weights of all the walks that join a particular pair of vertices in this directed graph; (iii) we use a universal result about the structure of walks on graphs to exactly resum the weights of families of walks to infinite order. This reduces the sum over weighted walks to a sum over weighted simple paths, a simple path being forbidden to visit any vertex more than once. For any finite size matrix, the graph $\mathcal{G}$ is finite and so is the number of simple paths. We apply the method of path-sums to four common matrix functions: a matrix raised to an arbitrary complex power, the matrix inverse, the matrix exponential, and the matrix logarithm. In each case, we obtain an exact closed-form expression that allows the corresponding function $f(\mathsf{M})$ to be analytically evaluated in a finite number of operations, provided the required inverse transform is available.

This chapter is organised as follows. In §3.2 we present the foundational material required by the method of path-sums: in §3.2.1 we describe the partition of a matrix into submatrices; in §3.2.3 we construct the graph corresponding to this partition, and describe the mapping between matrix multiplication and walks on the corresponding graph. In §3.3, we present path-sum expressions for a matrix raised to a complex power, the matrix inverse, the matrix exponential, and the matrix logarithm. These results are proved in §3.5. In §3.4, we provide examples of the application of our results. We summarise our results in §3.6 and briefly discuss the effect of truncations on path-sums expressions.

3.2 Required Concepts

In this section we present the three main concepts that underpin the method of path-sums. We begin by outlining the partition of an arbitrary matrix M into a collection of sub-arrays, and show how this partition leads naturally to the definition of a weighted directed graph $\mathcal{G}$ that encodes the structure of M. We then show that computing any power of M is equivalent to evaluating the weights of a family of walks on $\mathcal{G}$. We conclude by presenting a universal result on the structure of walks on graphs that forms the basis for a closed-form summation of classes of walks on $\mathcal{G}$.

3.2.1 Matrix partitions

A partition of a matrix M is a regrouping of the elements of M into smaller arrays which interpolate between the usual matrix elements of M and M itself. In this section we show how these arrays can be used to compute any function that can be expressed as a power series in M.

Definition 3.2.1 (General matrix partitions)**.** Let M be a $D \times D$ matrix over the complex field $\mathbb{C}$. Let V be a D-dimensional vector space over $\mathbb{C}$ with orthonormal basis $\{v_i\}$ $(1 \leq i \leq D)$. Consider a family of vector spaces $V_1, \ldots, V_n$ such that

$V_1 \oplus V_2 \oplus \cdots \oplus V_n = V$. Let V_j have dimension d_j and basis $\{v_{i_{j,k}}\}$, with $1 \leq k \leq d_j$ and $1 \leq i_{j,k} \leq D$, and let ε_j be the orthogonal projector onto V_j, i.e. $\varepsilon_j = \sum_{k=1}^{d_j} v_{i_{j,k}} v_{i_{j,k}}^\dagger$ where $\dagger$ designates the conjugate transposition. These projectors satisfy $\varepsilon_i \varepsilon_j = \delta_{i,j}\, \varepsilon_i$, and the closure relation $\sum_{j=1}^{n} \varepsilon_j = \mathcal{I}$ with $\mathcal{I}$ the identity operator on V. Consider the restriction-operator $\mathsf{R}_\mu \in \mathbb{C}^{d_\mu \times D}$, such that $\mathsf{R}_\mu^\dagger \mathsf{R}_\mu = \varepsilon_\mu$. A general partition of the matrix M is then defined to be the ensemble of matrices $\{\mathsf{M}_{\mu\nu}\}$ $(1 \leq (\mu, \nu) \leq n)$, where

$$\mathsf{M}_{\mu\nu} = \mathsf{R}_\mu \mathsf{M}\, \mathsf{R}_\nu^\dagger, \tag{3.1}$$

is a $d_\mu \times d_\nu$ matrix that defines a linear map $\varphi_{\mu\nu} : V_\nu \to V_\mu$. For $\mu \neq \nu$, we call $\mathsf{M}_{\mu\nu}$ a flip, while for $\mu = \nu$, we call $\mathsf{M}_{\nu\nu} = \mathsf{M}_\nu$ a static[1]. The projectors ε_μ are called projector-lattices. In general there is no relationship between $\mathsf{M}_{\mu\nu}$ and $\mathsf{M}_{\nu\mu}$. However if M is Hermitian then $\mathsf{M}_{\nu\mu} = \mathsf{M}_{\mu\nu}^\dagger$ and $\mathsf{M}_\nu = \mathsf{M}_\nu^\dagger$. Similar relations can be derived for the case where M is symmetric or antisymmetric.

Remark 3.2.1 (Block matrix representation)**.** For any general partition of M, there exists an invertible matrix P such that all $\mathsf{M}_{\mu\nu}$ are contiguous blocks in $\mathsf{P}\mathsf{M}\mathsf{P}^{-1}$. In other terms, there exists an invertible matrix P and n blocks B_μ of subsequent indices such that $\mathsf{M}_{\mu\nu} = \big((\mathsf{P}\mathsf{M}\mathsf{P}^{-1})_{jk}\big)_{j \in B_\mu,\, k \in B_\nu}$. If the $\{v_i\}$ basis vectors are the canonical ones, then the projector lattices are diagonal and P is a permutation matrix.

Example 3.2.1 (General partition of a matrix)**.** To illustrate a general partition, consider the 4×4 matrix M with elements $(\mathsf{M})_{ij} = m_{ij}$, which can be interpreted as a linear map on the vector space $V = \mathrm{span}\big(v_1, v_2, v_3, v_4\big)$ with $v_1 = (1,0,0,0)^{\mathrm{T}}$ with T the transposition, $v_2 = (0,1,0,0)^{\mathrm{T}}$, etc. Choosing vector spaces $V_1 = \mathrm{span}\big(v_1, v_3, v_4\big)$ and $V_2 = \mathrm{span}\big(v_2\big)$ such that $V_1 \oplus V_2 = V$, yields the following partition of M

$$\mathsf{M}_{11} = \begin{pmatrix} m_{11} & m_{13} & m_{14} \\ m_{31} & m_{33} & m_{34} \\ m_{41} & m_{43} & m_{44} \end{pmatrix},\ \mathsf{M}_{12} = \begin{pmatrix} m_{12} \\ m_{32} \\ m_{42} \end{pmatrix},\ \mathsf{M}_{21} = \begin{pmatrix} m_{21} & m_{23} & m_{24} \end{pmatrix},\ \mathsf{M}_{22} = \big(m_{22}\big). \tag{3.2}$$

Remark 3.2.2 (Number of general partitions)**.** The partition of a matrix M into flips and statics is not unique – any family of vector spaces such that $\bigoplus_{j=1}^{n} V_j = V$ produces a valid partition of M. Consequently, a $D \times D$ matrix admits, up to a change of basis, $S(D,n)$ different partitions on n such vector spaces, where $S(D,n)$ is the Stirling number of the second kind. It follows that the total number of general partitions of M is, up to a change of basis, the D^{th} Bell number $B_D = \sum_n S(D,n)$. Included in this number are the partitions of M into the usual matrix elements (i.e. $\mathsf{M}_{\mu\nu} = (m_{\mu\nu})$) obtained by choosing $\{V_\mu\}$ to be D subspaces of dimension one, and the partition of M into a single static $\mathsf{M}_1 = \mathsf{M}$, obtained by choosing $V_1 = V$. In between these extremes, the subarrays $\mathsf{M}_{\mu\nu}$ interpolate between the normal matrix

[1] These terms originate from quantum many-body physics, see Chapter 4.

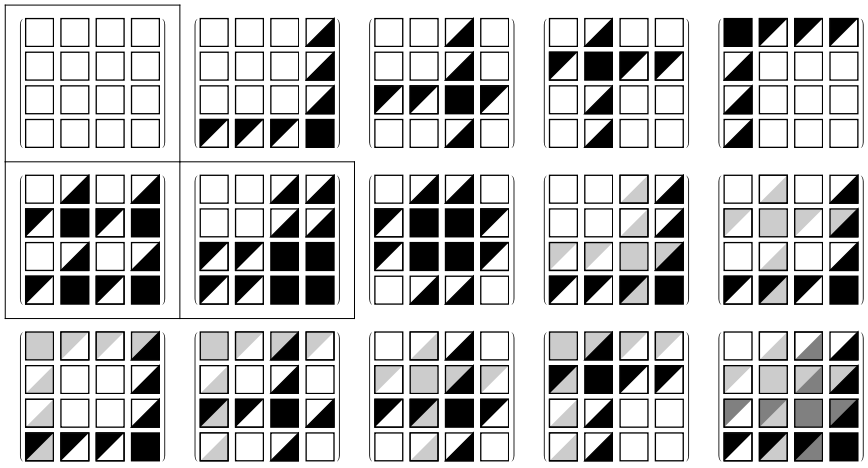

Figure 3.1: The $B_4 = 15$ possible partitions of a 4×4 matrix by diagonal projector lattices, see Remark 3.2.1. Solid and bicolor squares represent the matrix elements of statics and flips, respectively. The three tensor product partitions are framed. The trivial partition is in the upper-left corner, while the partition into the usual matrix elements is in the lower-right corner.

elements of M and the matrix M itself. Figure 3.1 illustrates the whole collection of possible repartitions of a 4×4 matrix into submatrices.

Definition 3.2.2 (Tensor product partitions)**.** An important subclass of matrix partitions are those that correspond to projector-lattices of tensor product form. This subclass of partitions will be referred to as tensor product partitions, and arises when the vector space V is decomposed as the tensor product (instead of the direct sum) of a collection of subspaces. Let V be a D-dimensional vector space over the complex field $\mathbb{C}$, and consider a family of vector spaces $\mathcal{V}_1, \ldots, \mathcal{V}_N$ such that $\mathcal{V}_1 \otimes \cdots \otimes \mathcal{V}_N = V$. Let $\mathcal{V}_i$ have dimension d_i ($2 \leq d_i \leq D$) and orthonormal basis $\{\mu_i\}$ ($1 \leq \mu \leq d_i$), and let $P^{(i)}_{\mu_i} = \mu_i \mu_i^\dagger$ be the orthogonal projector onto the subspace of $\mathcal{V}_i$ spanned by μ_i. Then a projector-lattice of tensor product form is

$$\varepsilon^{(S)}_{\mu} = \bigotimes_{i=1}^{S-1} P^{(i)}_{\mu_i} \otimes \mathcal{I}^{(S)} \otimes \bigotimes_{i=S+1}^{N} P^{(i)}_{\mu_i}, \tag{3.3}$$

where $\mathcal{I}^{(S)}$ is the identity operator on $\mathcal{V}_S$ and $\mu = (\mu_1, \ldots, \mu_{S-1}, \mu_{S+1}, \ldots, \mu_N)$ is an $(N-1)$-dimensional multi-index denoting which orthogonal projectors are present in $\varepsilon^{(S)}_{\mu}$. The projector-lattice $\varepsilon^{(S)}_{\mu}$ acts as a projector on each $\mathcal{V}_i$ ($i \neq S$) while applying the identity operator to $\mathcal{V}_S$. For fixed S there are D/d_S distinct projector-lattices, corresponding to the different choices of the projector indices μ_i. For any $D \times D$ matrix M and pair of projector-lattices $\varepsilon^{(S)}_{\mu}$, $\varepsilon^{(S)}_{\nu}$ there exists a $d_S \times d_S$ matrix $\mathsf{M}^{(S)}_{\mu\nu}$ such that

$$\varepsilon^{(S)}_{\mu} \mathsf{M} \, \varepsilon^{(S)}_{\nu} = \bigotimes_{i=1}^{S-1} T^{(i)}_{\mu_i \nu_i} \otimes \mathsf{M}^{(S)}_{\mu\nu} \otimes \bigotimes_{i=S+1}^{N} T^{(i)}_{\mu_i \nu_i}, \tag{3.4}$$

where $T^{(i)}_{\mu_i\nu_i} = \mu_i\nu_i^\dagger$ is a transition operator from ν_i to μ_i in $\mathcal{V}_i$. The matrix $\mathsf{M}^{(S)}_{\mu\nu}$ defines a linear map on $\mathcal{V}_S$. The ensemble of $(D/d_S)^2$ matrices $\{\mathsf{M}^{(S)}_{\mu\nu}\}$ will be referred to as a tensor product partition of M on $\mathcal{V}_s$. The three possible tensor product partitions of M are illustrated by the framed images in Figure 3.1.

Remark 3.2.3 (Number of tensor product partitions)**.** To count the number of possible tensor product partitions of a $D \times D$ matrix, we note that every factorisation of D into k integers $d_i \geq 2$ contributes k partitions to the total. The total number of tensor product partitions is therefore equal to the total number of elements in all factorisations of D. For $D = 2, 3, 4, 5, 6, 7, 8, \ldots$ this is equal to $1, 1, 3, 1, 3, 1, 6, \ldots$ (sequence A066637 in [52]). A special case arises when D has the form d^N, with d prime. Then the factorisations of D into k parts are in one-to-one correspondence with the additive partitions of N into k parts, and the number of tensor product partitions is equal to the total number of elements in all partitions of N. For example, matrices of dimension $D = 2, 4, 8, 16, 32, \ldots$ admit $1, 3, 6, 12, 20, \ldots$ (sequence A006128 in [52]) tensor product partitions.

3.2.2 The partition of matrix powers and functions

Since the matrix elements of M^k ($k \in \mathbb{N}^* = \mathbb{N}\backslash\{0\}$) are generated from those of M through the rules of matrix multiplication, the partition of a matrix power can be expressed in terms of the partition of the original matrix. Here we present this relationship for the case of a general partition of M; the case of a tensor product partition is identical. The proof of these results is deferred to §3.5. The partition of M^k is given in terms of the partition of M by $\big(\mathsf{M}^k\big)_{\omega\alpha} = \sum_{\eta_k,\ldots,\eta_2} \mathsf{M}_{\omega\eta_k} \cdots \mathsf{M}_{\eta_3\eta_2}\mathsf{M}_{\eta_2\alpha}$, where $\alpha \equiv \eta_1$, $\omega \equiv \eta_{k+1}$, and each of the sums runs over the n values that index the vector spaces of the general partition. It follows that the partition of a matrix function $f(\mathsf{M})$ with power series expansion $f\big(\mathsf{M}\big) = \sum_{k=0}^{\infty} f_k\, \mathsf{M}^k$ is

$$f\big(\mathsf{M}\big)_{\omega\alpha} = \sum_{k=0}^{\infty} f_k \sum_{\eta_k,\ldots,\eta_2} \mathsf{M}_{\omega\eta_k} \cdots \mathsf{M}_{\eta_3\eta_2}\mathsf{M}_{\eta_2\alpha}. \tag{3.5}$$

This equation provides a method of computing individual submatrices of $f\big(\mathsf{M}\big)$ without evaluating the full result. In the next section, we map the infinite sum of Eq. (3.5) into a sum over the contributions of walks on a weighted graph, thus allowing exact resummations of families of terms of Eq. (3.5) by applying results from graph theory.

3.2.3 The graph of a matrix partition

Given an arbitrary partition of a matrix M, we construct a weighted directed graph $\mathcal{G}$ that encodes the structure of this partition. Terms that contribute to the matrix power M^k are then in one-to-one correspondence with walks of length k on $\mathcal{G}$. The infinite sum over walks on $\mathcal{G}$ involved in the evaluation of $f(\mathsf{M})$ is then reduced into a sum over simple paths on $\mathcal{G}$.

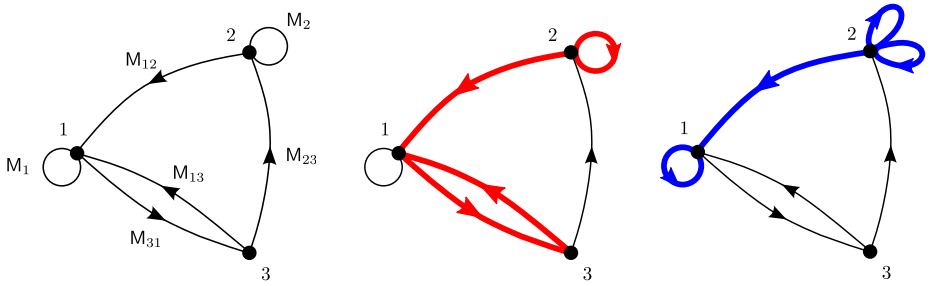

Figure 3.2: (a) The graph of the general partition of the 4×4 matrix in Eq. (3.6) onto the vector spaces V_1, V_2, V_3 defined in the text. Each edge in the graph is labelled by its weight. (b) Two walks of length 4 from vertex 2 to vertex 1 in thick red (left) and blue (right) lines. Their contributions $c_{\text{red}} = \mathsf{M}_{13}\mathsf{M}_{31}\mathsf{M}_{12}\mathsf{M}_2$ and $c_{\text{blue}} = \mathsf{M}_1\mathsf{M}_{12}\left(\mathsf{M}_2\right)^2$ form two of the eight terms that sum up to $(\mathsf{M}^4)_{12}$.

Definition 3.2.3 (Graph of a matrix partition)**.** Let $\{\mathsf{M}_{\mu\nu}\}$ be the partition of M formed by a particular set of n projector-lattices $\{\varepsilon_\mu\}$. Then the graph of this matrix partition is defined to be the weighted directed graph $\mathcal{G} = (\mathcal{V}, \mathcal{E}, \mathrm{w})$, where $\mathcal{V} = \{v_\mu\}$ is a set of $m \leq n$ vertices with the same labels as the projector-lattices, $\mathcal{E} = \{(\nu\mu) : \mathsf{M}_{\mu\nu} \neq \mathbf{0}\}$ is a set of directed edges among these vertices, and w is an edge-weight function that assigns the submatrix M_μ to the loop $(\mu\mu)$ and $\mathsf{M}_{\mu\nu}$ to the link $(\nu\mu)$. From now on, $\mathcal{G}\backslash\{\alpha, \beta, \ldots\}$ denotes the graph obtained by deleting vertices $\alpha, \beta, \ldots$ from $\mathcal{G}$; and $\mathcal{G}_0$ represents the graph obtained by deleting all loops from $\mathcal{G}$.

Remark 3.2.4 (Graph minors)**.** The various graphs that correspond to the different ways of partitioning a matrix M into an ensemble of submatrices are minors of the graph obtained by partitioning M into its usual matrix elements. Note, this implies that the number of minors obtained by merging vertices[2] on a graph with D vertices is at most B_D, with this bound being reached by the complete graph.

Example 3.2.2 (Graph of a matrix partition)**.** Consider decomposing the 4×4 matrix

$$\mathsf{M} = \begin{pmatrix} m_{11} & m_{12} & m_{13} & m_{14} \\ m_{21} & m_{22} & m_{23} & m_{24} \\ 0 & 0 & m_{33} & m_{34} \\ m_{41} & m_{42} & 0 & 0 \end{pmatrix}, \tag{3.6}$$

onto vector spaces $V_1 = \mathrm{span}\big(v_1, v_2\big)$, $V_2 = \mathrm{span}\big(v_3\big)$, $V_3 = \mathrm{span}\big(v_4\big)$ with $v_1 =$

[2]We allow vertex merging regardless of whether vertices share an edge or not.

$(1,0,0,0)^{\mathrm{T}}$, $v_2 = (0,1,0,0)^{\mathrm{T}}$, etc. The corresponding partition of M is

$$\mathsf{M}_1 = \begin{pmatrix} m_{11} & m_{12} \\ m_{21} & m_{22} \end{pmatrix}, \qquad \mathsf{M}_{12} = \begin{pmatrix} m_{13} \\ m_{23} \end{pmatrix}, \qquad \mathsf{M}_{13} = \begin{pmatrix} m_{14} \\ m_{24} \end{pmatrix} \tag{3.7a}$$

$$\mathsf{M}_2 = \begin{pmatrix} m_{33} \end{pmatrix}, \qquad \mathsf{M}_{23} = \begin{pmatrix} m_{34} \end{pmatrix}, \qquad \mathsf{M}_{31} = \begin{pmatrix} m_{41} & m_{42} \end{pmatrix}, \tag{3.7b}$$

and $\mathsf{M}_{21} = \mathsf{M}_{32} = \mathsf{M}_3 = \mathbf{0}$. Figure 3.2 illustrates $\mathcal{G}$, together with two walks of length 4 from vertex 2 to vertex 1 that contribute to $\big(\mathsf{M}^4\big)_{12}$.

The graph $\mathcal{G}$ provides a useful representation of a matrix partition: each vertex represents a vector space in the partition, while each edge represents a linear mapping between vector spaces. The graph $\mathcal{G}$ is thus a quiver and the set of vector spaces $\{V_\mu\}$ together with the set of linear maps $\{\varphi_{\mu\nu}\}$ is a representation of this quiver. Further, the pattern of edges in $\mathcal{G}$ encodes the structure of M: each loop $(\mu\mu)$ represents a non-zero static, while each link $(\nu\mu)$ represents a non-zero flip. The matrix M can therefore be said to be a $\mathcal{G}$-structured matrix. Every walk on $\mathcal{G}$, e.g. $w = (\eta_1)(\eta_1\eta_2)\cdots(\eta_{k-1}\eta_k)(\eta_k)$, is now in one-to-one correspondence with a product $\mathrm{W}[w] = \mathsf{M}_{\eta_k\eta_{k-1}}\cdots\mathsf{M}_{\eta_3\eta_2}\mathsf{M}_{\eta_2\eta_1}$ of submatrices [20, 19]. This matrix product is termed the contribution of the walk w and, being a product of matrices, is written right-to-left. This correspondence allows a matrix power to be expressed as a sum over contributions of walks on $\mathcal{G}$. Equation (3.5) becomes

$$f\big(\mathsf{M}\big)_{\omega\alpha} = \sum_{k=0}^{\infty} f_k \sum_{W_{\mathcal{G};\alpha\omega;k}} \mathrm{W}(w), \tag{3.8}$$

where $W_{\mathcal{G};\alpha\omega;k}$ is the set of all walks of length k from α to ω on $\mathcal{G}$. We do not know if such a formulation of $f(\mathsf{M})$ would be possible for a nonprimary matrix function and thus we only consider primary matrix functions in this thesis.

Thanks to Theorem 2.3.4 we reduce a sum of walk contributions, such as the one of Eq. (3.8), into a sum of weighted simple paths and simple cycles. If $\mathcal{G}$ is a finite graph, there is only a finite number of simple paths and simple cycles and the resulting representation of $f\big(\mathsf{M}\big)$ presents finitely many terms.

3.3 Path-Sum Expressions for Common Matrix Functions

In §3.2 we showed that projector-lattices can be used to evaluate the partition of a matrix function $f\big(\mathsf{M}\big)$, and further, that the resulting expression can be interpreted as a sum over walks on a directed graph $\mathcal{G}$ (Eq. (3.8)). This mapping enables results from graph theory to be applied to the evaluation of matrix power series. In this section we exploit this connection by using Theorem 2.3.4 to resum, in closed form, certain families of terms in the power series for the partition of some common matrix functions. For each function we resum all terms in the power series

that correspond to closed walks on $\mathcal{G}$, and thereby obtain a closed-form expression for the submatrices $f(\mathsf{M})_{\omega\alpha}$. Since this expression takes the form of a finite sum over simple paths on $\mathcal{G}$, we refer to it as a path-sum result. The existence of a form involving finitely many terms and giving exactly a matrix function may seem unsurprising in view of the existence of the Cayley-Hamilton Theorem (CHT) [51]. Indeed the Theorem entails that any analytical function f of a matrix M is given by a polynomial in M. The CHT is limited to matrices over a commutative ring however, while the graph-theoretic origin of the path-sum result means that it is not. As a consequence, the CHT does not have an immediate generalisation that holds for arbitrary matrix partitions. For these reasons, if there exists a relation between the CHT and the path-sum representation of matrix functions, it must be that the CHT follows from the path-sum formula when all walks weights commute. More precisely, the determinant of a matrix M has a unique expansion in terms of simple cycles on the graph whose adjacency matrix has the same structure than M [175]. However, this expansion, which arises from the cycle representation of permutations, is (precisely for this reason) invariant under cyclic permutations of the vertices visited by the simple cycles, e.g. (1231) and (2312) represent the same term. Evidently, this holds for weighted walks if and only if all walk weights commute, which is only true for matrices over commutative rings. This explains why there is no block formula for the determinant and thus why the CHT fails for matrices with non-commuting elements. One could insist on constructing a non-commutative determinant by removing the invariance under cyclic permutations, which requires to make the determinant entry-specific. In fact, this new object also has a path-sum representation: it is the quasideterminant, see §3.4.5.

Below we present path-sum results for a matrix raised to a general complex power, the matrix inverse, matrix exponential, and matrix logarithm. The results are proved in §3.5, and examples illustrating their use are provided in §3.4.

3.3.1 A matrix raised to a complex power

Theorem 3.3.1 (**Path-sum result for a matrix raised to a complex power**). *Let $\mathsf{M} \in \mathbb{C}^{D\times D}$ be a non-nilpotent matrix, $\{\mathsf{M}_{\mu\nu}\}$ be an arbitrary partition of M and $q \in \mathbb{C}$. Then the partition of M^q is given by*

$$(\mathsf{M}^q)_{\omega\alpha} = -\mathcal{Z}_u^{-1}\left\{\sum_{\Pi_{\mathcal{G}_0;\alpha\omega}} \mathsf{F}_{\mathcal{G}\setminus\{\alpha,\ldots,\nu_\ell\}}[\omega]\,\mathsf{M}_{\omega\nu_\ell}\cdots\mathsf{F}_{\mathcal{G}\setminus\{\alpha\}}[\nu_2]\,\mathsf{M}_{\nu_2\alpha}\,\mathsf{F}_{\mathcal{G}}[\alpha]\right\}[n]\Big|_{n=-q-1}, \quad (3.9a)$$

where $\mathcal{G}$ is the graph of $\{(\mathsf{M}-\mathsf{I})_{\mu\nu}\}$, ℓ is the length of the simple path, and

$$\mathsf{F}_{\mathcal{G}}[\alpha] = \left[\mathsf{I}z^{-1} - \mathsf{M}_\alpha - \sum_{\Gamma_{\mathcal{G}_0;\alpha}} \mathsf{M}_{\alpha\mu_m}\mathsf{F}_{\mathcal{G}\setminus\{\alpha,\ldots,\mu_{m-1}\}}[\mu_m]\cdots\mathsf{F}_{\mathcal{G}\setminus\{\alpha\}}[\mu_2]\mathsf{M}_{\mu_2\alpha}\right]^{-1}, \quad (3.9b)$$

with m the length of the simple cycle.

Here $\mathcal{Z}_u^{-1}\{g(z)\}[n]$ denotes the inverse unilateral Z-transform of $g(z)$ [53]. The quantity $\mathsf{F}_{\mathcal{G}}[\alpha]$ is defined recursively through Eq. (3.9b). Indeed $\mathsf{F}_{\mathcal{G}}[\alpha]$ is expressed in terms of $\mathsf{F}_{\mathcal{G}\setminus\{\alpha,\ldots,\mu_{j-1}\}}[\mu_j]$ which is in turn defined through Eq. (3.9b) but on the subgraph $\mathcal{G}\setminus\{\alpha,\ldots,\mu_{j-1}\}$ of $\mathcal{G}$. The recursion stops when vertex μ_j has no neighbour on this subgraph, in which case $\mathsf{F}_{\mathcal{G}\setminus\{\alpha,\ldots,\mu_{j-1}\}}[\mu_j] = (\mathsf{I}z^{-1} - \mathsf{M}_{\mu_j})^{-1}$ if the loop $(\mu_j\mu_j)$ exists and $\mathsf{F}_{\mathcal{G}\setminus\{\alpha,\ldots,\mu_{j-1}\}}[\mu_j] = \mathsf{I}z$ otherwise. $\mathsf{F}_{\mathcal{G}}[\alpha]$ is thus a matrix continued fraction which terminates at a finite depth. It is an effective weight associated to vertex α resulting from the dressing of α by all the closed walks off α on $\mathcal{G}$.

Remark 3.3.1 (Matrix p^{th}-roots)**.** When analytically computing the p^{th}-root, $p \in \mathbb{N}^*$, of a matrix M using Theorem 3.3.1 one can obtain all the primary p^{th}-roots of that matrix. Indeed remark first that whenever a number $\lambda = |\lambda|e^{i\theta}$ appears raised to the power $q = 1/p$ in the analytical result, one is free to choose any one of its p^{th}-roots $\lambda^q|_{q=1/p} \equiv |\lambda|^{1/p}e^{i\theta/p}e^{2in\pi/p}$, $n \in \{0, 1, \cdots, p-1\}$. Second, λ is necessarily an eigenvalue of M since, by the Jordan decomposition, $\mathsf{M}^q = \mathsf{P}\mathsf{J}^q\mathsf{P}^{-1}$, and thus any number raised to the power q in M^q is one that appears on the diagonal of J. It follows that all the primary p^{th}-roots of M are indeed obtained from Theorem 3.1 upon choosing different p^{th}-roots for the numbers $\lambda^{1/p}$ [51].

3.3.2 The matrix inverse

Theorem 3.3.2 (**Path-sum result for the matrix inverse**)**.** *Let $\mathsf{M} \in \mathbb{C}^{D\times D}$ be an invertible matrix, and $\{\mathsf{M}_{\mu\nu}\}$ be an arbitrary partition of M. Then as long as all of the required inverses exist, the partition of M^{-1} is given by the path-sum*

$$\left(\mathsf{M}^{-1}\right)_{\omega\alpha} = \sum_{\Pi_{\mathcal{G}_0;\alpha\omega}} (-1)^{\ell}\, \mathsf{F}_{\mathcal{G}\setminus\{\alpha,\ldots,\nu_\ell\}}[\omega]\mathsf{M}_{\omega\nu_\ell}\cdots\mathsf{F}_{\mathcal{G}\setminus\{\alpha\}}[\nu_2]\,\mathsf{M}_{\nu_2\alpha}\,\mathsf{F}_{\mathcal{G}}[\alpha], \tag{3.10a}$$

where $\mathcal{G}$ is the graph of $\{(\mathsf{M}-\mathsf{I})_{\mu\nu}\}$, ℓ is the length of the simple path, and

$$\mathsf{F}_{\mathcal{G}}[\alpha] = \left[\mathsf{M}_\alpha - \sum_{\Gamma_{\mathcal{G}_0;\alpha}} (-1)^m\, \mathsf{M}_{\alpha\mu_m}\mathsf{F}_{\mathcal{G}\setminus\{\alpha,\ldots,\mu_{m-1}\}}[\mu_m]\cdots\mathsf{F}_{\mathcal{G}\setminus\{\alpha\}}[\mu_2]\mathsf{M}_{\mu_2\alpha}\right]^{-1}, \tag{3.10b}$$

with m the length of the simple cycle.

If α has no neighbours in $\mathcal{G}$ then $\mathsf{F}_{\mathcal{G}}[\alpha] = \mathsf{M}_\alpha^{-1}$ counts the contributions of all loops on α.

Remark 3.3.2 (Known inversion formulae)**.** Two known matrix inversion results can be straightforwardly recovered as special cases of Theorem 3.3.2. Firstly, by considering the complete directed graph on two vertices, we obtain the well-known block inversion formula

$$\begin{pmatrix}\mathsf{A} & \mathsf{B}\\ \mathsf{C} & \mathsf{D}\end{pmatrix}^{-1} = \begin{pmatrix}(\mathsf{A}-\mathsf{B}\mathsf{D}^{-1}\mathsf{C})^{-1} & -\mathsf{A}^{-1}\mathsf{B}\,(\mathsf{D}-\mathsf{C}\mathsf{A}^{-1}\mathsf{B})^{-1}\\ -\mathsf{D}^{-1}\mathsf{C}\,(\mathsf{A}-\mathsf{B}\mathsf{D}^{-1}\mathsf{C})^{-1} & (\mathsf{D}-\mathsf{C}\mathsf{A}^{-1}\mathsf{B})^{-1}\end{pmatrix}. \tag{3.11}$$

Secondly, by applying Theorem 3.3.2 to the path-graph on $N \leq D$ vertices (denoted here $\mathcal{P}_N$), we obtain known continued fraction formulae for the inverse of a $D \times D$ block tridiagonal matrix [54, 55, 56, 57]. This follows from the observation that a $\mathcal{P}_N$-structured matrix is a block tridiagonal matrix. We provide a general formula for the exponential and inverse of arbitrary $\mathcal{P}_N$-structured matrices in §3.4.3.

Remark 3.3.3 (Path-sum results via the Cauchy integral formula)**.** A path-sum expression can be derived for any matrix function upon using Theorem 3.3.2 together with the Cauchy integral formula

$$f(\mathsf{M}) = \frac{1}{2\pi \mathrm{i}} \oint_{\Gamma} f(z)\,(z\mathsf{I} - \mathsf{M})^{-1}\,\mathrm{d}z, \tag{3.12}$$

where $\mathrm{i}^2 = -1$, f is an holomorphic function on an open subset U of $\mathbb{C}$ and Γ is a closed contour completely contained in U that encloses the eigenvalues of M. However, for certain matrix functions (including all four we consider in this section) a path-sum expression can be derived independently of the Cauchy integral formula by using Theorem 2.3.4 directly on the power series for the function. This method is the one we use to prove the results of this section (see §3.5) and can be extended to matrices over division rings.

Remark 3.3.4 (Schur decomposition)**.** Let $\mathsf{M} \in \mathbb{C}^{D\times D}$, $\mathsf{M} = \mathsf{U}\mathsf{T}\mathsf{U}^{-1}$ be its Schur decomposition, i.e. T is upper triangular, and let $\{\mathsf{M}_{\mu\nu}\}$ a partition of M. The difficulty of evaluating $f(\mathsf{M})$ if M is full can be alleviated upon using the Schur decomposition of M in conjunction with the method of path-sums. Indeed observe that

$$\big(f(\mathsf{M})\big)_{\omega\alpha} = \sum_{\mu,\,\nu} \mathsf{U}_{\omega\mu}\,\big(f(\mathsf{T})\big)_{\mu\nu}\,(\mathsf{U}_{\alpha\nu})^{\dagger}, \tag{3.13}$$

where we have used $\mathsf{U}^{-1} = \mathsf{U}^{\dagger}$ and $(\mathsf{U}^{\dagger})_{\nu\alpha} = (\mathsf{U}_{\alpha\nu})^{\dagger}$. Thus the problem of evaluating any $(f(\mathsf{M}))_{\omega\alpha}$ is reduced to that of evaluating $f(\mathsf{T})$. Now remark that regardless of the partition $\{\mathsf{T}_{\mu\nu}\}$ considered, the graph $\mathcal{G}$ of that partition has no simple cycle of length $m > 1$. Thus the path-sum formula for any matrix function $f(\mathsf{T})$ is especially simple. For example consider obtaining $f(\mathsf{T})$ via the Cauchy integral formula Eq. (3.12). Then the resolvent matrix $\mathsf{R}_{\mathsf{T}}(z) = (z\mathsf{I} - \mathsf{T})^{-1}$ of T is given by the path-sum

$$\big(\mathsf{R}_{\mathsf{T}}(z)\big)_{\mu\nu} = \sum_{\Pi_{\mathcal{G}_0;\nu\mu}} (z\mathsf{I} - \mathsf{T}_{\mu})^{-1}\,\mathsf{M}_{\mu\eta_{\ell}} \cdots \mathsf{M}_{\eta_2\nu}\,(z\mathsf{I} - \mathsf{T}_{\nu})^{-1}, \tag{3.14a}$$

$$\big(\mathsf{R}_{\mathsf{T}}(z)\big)_{\mu} = (z\mathsf{I} - \mathsf{T}_{\mu})^{-1}, \tag{3.14b}$$

where $\mathcal{G}$ is the graph of $\{\mathsf{T}_{\mu\nu}\}$ and ℓ is the length of the simple path.

3.3.3 The matrix exponential

Theorem 3.3.3 (**Path-sum result for the matrix exponential**). *Let* $\mathsf{M} \in \mathbb{C}^{D\times D}$ *and* $\{\mathsf{M}_{\mu\nu}\}$ *be an arbitrary partition of* M*, with* $\mathcal{G}$ *the corresponding graph. Then for* $\tau \in \mathbb{C}$ *the partition of* $\exp(\tau\mathsf{M})$ *is given by the path-sum*

$$\exp(\tau\mathsf{M})_{\omega\alpha} = \mathfrak{L}^{-1}\left\{\sum_{\Pi_{\mathcal{G}_0;\alpha\omega}} \mathsf{F}_{\mathcal{G}\setminus\{\alpha,\ldots,\nu_\ell\}}[\omega]\mathsf{M}_{\omega\nu_\ell}\cdots\mathsf{F}_{\mathcal{G}\setminus\{\alpha\}}[\nu_2]\,\mathsf{M}_{\nu_2\alpha}\,\mathsf{F}_{\mathcal{G}}[\alpha]\right\}(t)\Bigg|_{t=\tau}, \tag{3.15a}$$

where ℓ *is the length of the simple path and*

$$\mathsf{F}_{\mathcal{G}}[\alpha] = \left[s\mathsf{I} - \mathsf{M}_\alpha - \sum_{\Gamma_{\mathcal{G}_0;\alpha}} \mathsf{M}_{\alpha\mu_m}\mathsf{F}_{\mathcal{G}\setminus\{\alpha,\ldots,\mu_{m-1}\}}[\mu_m]\cdots\mathsf{F}_{\mathcal{G}\setminus\{\alpha\}}[\mu_2]\mathsf{M}_{\mu_2\alpha}\right]^{-1}, \tag{3.15b}$$

with m *the length of the simple cycle.*

Here s is the Laplace variable conjugate to t, and $\mathfrak{L}^{-1}\{g(s)\}(t)$ denotes the inverse Laplace transform of $g(s)$. The quantity $\mathsf{F}_{\mathcal{G}}[\alpha]$ is a matrix continued fraction which terminates at a finite depth. It is an effective weight associated to vertex α resulting from the dressing of α by all the closed walks off α on $\mathcal{G}$. If α has no neighbours in $\mathcal{G}$ then $\mathsf{F}_{\mathcal{G}}[\alpha] = [s\mathsf{I} - \mathsf{M}_\alpha]^{-1}$ counts the contributions of all loops off α.

Lemma 3.3.1 (Walk-sum result for the matrix exponential). *Let* $\mathsf{M} \in \mathbb{C}^{D\times D}$ *and* $\{\mathsf{M}_{\mu\nu}\}$ *be an arbitrary partition of* M*, with* $\mathcal{G}$ *the corresponding graph. Then for* $\tau \in \mathbb{C}$ *the partition of* $\exp(\tau\mathsf{M})$ *is given by the walk-sum*

$$\exp(\tau\mathsf{M})_{\omega\alpha} = \sum_{W_{\mathcal{G}_0;\alpha\omega}} \int_0^\tau \mathrm{d}t_m \cdots \int_0^{t_2} \mathrm{d}t_1\, \exp\big[(t-t_m)\mathsf{M}_\omega\big]\mathsf{M}_{\omega\mu_m}\cdots$$
$$\cdots\exp\big[(t_2-t_1)\mathsf{M}_{\mu_2}\big]\mathsf{M}_{\mu_2\alpha}\exp\big[t_1\mathsf{M}_\alpha\big]. \tag{3.16}$$

This result corresponds to dressing the vertices only by loops, instead of by all closed walks. An infinite sum over all walks from α to ω on the loopless graph $\mathcal{G}_0$ therefore remains to be carried out.

3.3.4 The matrix logarithm

Theorem 3.3.4 (**Path-sum result for the principal logarithm**). *Let* $\mathsf{M} \in \mathbb{C}^{D\times D}$ *be a matrix with no eigenvalues on the negative real axis, and* $\{\mathsf{M}_{\mu\nu}\}$ *be a partition of* M*. Then as long as all of the required inverses exist, the partition of the*

principal matrix logarithm of M *is given by the path-sum*

$$\big(\log \mathsf{M}\big)_{\omega\alpha} = \tag{3.17a}$$
$$\begin{cases} \displaystyle\int_0^1 \mathrm{d}x\; x^{-1}\,(\mathsf{I}-\mathsf{F}_{\mathcal{G}}[\alpha])\,, & \omega=\alpha, \\ \displaystyle\sum_{\Pi_{\mathcal{G}_0;\alpha\omega}} \int_0^1 \mathrm{d}x\; (-x)^{\ell-1}\,\mathsf{F}_{\mathcal{G}\setminus\{\alpha,\ldots,\nu_\ell\}}[\omega]\mathsf{M}_{\omega\nu_\ell}\cdots\mathsf{F}_{\mathcal{G}\setminus\{\alpha\}}[\nu_2]\,\mathsf{M}_{\nu_2\alpha}\,\mathsf{F}_{\mathcal{G}}[\alpha], & \omega\neq\alpha, \end{cases}$$

where $\mathcal{G}$ *is the graph of* $\{(\mathsf{I}-\mathsf{M})_{\mu\nu}\}$*,* ℓ *the length of the simple path and*

$$\mathsf{F}_{\mathcal{G}}[\alpha] = \tag{3.17b}$$
$$\left[\mathsf{I}-x(\mathsf{I}-\mathsf{M}_\alpha)-\sum_{\Gamma_{\mathcal{G}_0;\alpha}}(-x)^m\,\mathsf{M}_{\alpha\mu_m}\mathsf{F}_{\mathcal{G}\setminus\{\alpha,\ldots,\mu_{m-1}\}}[\mu_m]\;\cdots\;\mathsf{M}_{\mu_3\mu_2}\mathsf{F}_{\mathcal{G}\setminus\{\alpha\}}[\mu_2]\mathsf{M}_{\mu_2\alpha}\right]^{-1},$$

with m *the length of the simple cycle.*

The quantity $\mathsf{F}_{\mathcal{G}}[\alpha]$ is a matrix continued fraction which terminates at a finite depth. It is an effective weight associated to vertex α resulting from the dressing of α by all the closed walks off α on $\mathcal{G}$. If α has no neighbours in $\mathcal{G}$ then $\mathsf{F}_{\mathcal{G}}[\alpha] = [\mathsf{I}-x(\mathsf{I}-\mathsf{M}_\alpha)]^{-1}$ counts the contributions of all loops off α.

Remark 3.3.5 (Richter relation)**.** The path-sum expression of Theorem 3.3.4 is essentially the well-known integral relation for the matrix logarithm [58, 59, 51]

$$\log \mathsf{M} = \int_0^1 (\mathsf{M}-\mathsf{I})\big[x(\mathsf{M}-\mathsf{I})+\mathsf{I}\big]^{-1}\mathrm{d}x, \tag{3.18}$$

with a path-sum expression of the integrand. However, the proof of Theorem 3.3.4 that we present in 3.5.5 does not make explicit use of Eq. (3.18).

3.4 Applications

In this section we present some examples of the application of the path-sum method. In the first part we provide numerical examples for a matrix raised to a complex power, the matrix inverse, exponential, and logarithm. In the second part, we provide exact results for the matrix exponential and matrix inverse of block tridiagonal matrices and evaluate the computational cost of path-sum on arbitrary tree-structured matrices.

3.4.1 Short examples

Example 3.4.1 (Singular and defective matrix raised to an arbitrary complex power)**.** To illustrate the result of Theorem 3.3.1, we consider raising the matrix

$$\mathsf{M} = \begin{pmatrix} -4 & 0 & -1 & 0 & -1 \\ -2 & -2 & 6 & -2 & 4 \\ 6 & 2 & 1 & -2 & 3 \\ 0 & 0 & -1 & -4 & -1 \\ -6 & -2 & -5 & 2 & -7 \end{pmatrix}, \tag{3.19}$$

to an arbitrary complex power q. Note that M has a spectral radius $\rho(\mathsf{M}) = 4$ and is both singular and defective; i.e. non-diagonalisable. We partition M onto vector space $V_1 = \mathrm{span}\big(v_1, v_2\big)$ and $V_2 = \mathrm{span}\big(v_3, v_4, v_5\big)$ with $v_1 = (1,0,0,0)^{\mathrm{T}}$ etc., such that $V_1 \oplus V_2 = V$. The corresponding graph $\mathcal{G}$ is the complete graph on two vertices, denoted $\mathcal{K}_2$. Following Theorem 3.3.1, the elements of M^q are given by,

$$(\mathsf{M}^q)_{ii} = -\mathcal{Z}_u^{-1}\big\{\mathsf{F}_{\mathcal{K}_2}[i]\big\}[n]\Big|_{n=-q-1} \quad \text{and} \quad (\mathsf{M}^q)_{ij} = -\mathcal{Z}_u^{-1}\big\{\mathsf{F}_{\mathcal{K}_2\setminus j}[i]\mathsf{M}_{12}\mathsf{F}_{\mathcal{K}_2}[j]\big\}[n]\Big|_{n=-q-1}, \tag{3.20}$$

where $(i,j) = 1,2$, $i \neq j$, $\mathsf{F}_{\mathcal{K}_2}[i] = \big[\mathsf{I}z^{-1} - \mathsf{M}_i - \mathsf{M}_{ij}\mathsf{F}_{\mathcal{K}_2\setminus i}[j]\mathsf{M}_{ji}\big]^{-1}$ and $\mathsf{F}_{\mathcal{K}_2\setminus i}[j] = [\mathsf{I}z^{-1} - \mathsf{M}_j]^{-1}$. We thus find in the Z-domain

$$\tilde{\mathsf{M}}(z) = z(4z+1)^{-2}\times \tag{3.21}$$
$$\begin{pmatrix} 4z+1 & 0 & -z & 0 & -z \\ 2z(4z-1) & 8z^2+6z+1 & \frac{88z^3+50z^2+6z}{4z+1} & -2z(4z+1) & \frac{56z^3+34z^2+4z}{4z+1} \\ 2z(4z+3) & 2z(4z+1) & \frac{88z^3+54z^2+13z+1}{4z+1} & -2z(4z+1) & \frac{56z^3+22z^2+3z}{4z+1} \\ 0 & 0 & -z & 4z+1 & -z \\ -2z(4z+3) & -2z(4z+1) & -\frac{88z^3+38z^2+5z}{4z+1} & 2z(4z+1) & \frac{-56z^3-6z^2+5z+1}{4z+1} \end{pmatrix}.$$

and finally $\mathsf{M}^q = -\mathcal{Z}_u^{-1}\{\tilde{\mathsf{M}}(z)\}[n]|_{n=-q-1}$, which is

$$\mathsf{M}^q = \frac{(-4)^q}{8}\begin{pmatrix} 8 & 0 & 2q & 0 & 2q \\ 8q-4 & 4 & q(q-2)-11 & 4 & q(q-2)-7 \\ -8q-4 & -4 & -q(q-2)-3 & 4 & -q(q-2)-7 \\ 0 & 0 & 2q & 8 & 2q \\ 8q+4 & 4 & q(q-2)+11 & -4 & q(q-2)+15 \end{pmatrix}. \tag{3.22}$$

This expression is valid for any $q \in \mathbb{C}$ and fulfills $\mathsf{M}^{q+q'} = \mathsf{M}^q\mathsf{M}^{q'}$, $\forall (q,q') \in \mathbb{C}^2$. Setting $q = 1/2$, we obtain

$$\mathsf{M}^{1/2} = \frac{\mathrm{i}}{16}\begin{pmatrix} 32 & 0 & 4 & 0 & 4 \\ 0 & 16 & -47 & 16 & -31 \\ -32 & -16 & -9 & 16 & -25 \\ 0 & 0 & 4 & 32 & 4 \\ 32 & 16 & 41 & -16 & 57 \end{pmatrix}, \tag{3.23}$$

with $\mathrm{i}^2 = -1$, for which it is easily verified that $(\mathsf{M}^{1/2})^2 = \mathsf{M}$. Any p^{th} root of M, with $p \in \mathbb{N}^*$, can also be calculated and verified. Further, we note that although M is not invertible, setting $q = -1$ in Eq. (3.22) yields the Drazin inverse $\mathsf{M}^\sharp$ of M [60], while setting $q = 0$ yields a left and right identity $\mathsf{M}^\flat$ on M

$$\mathsf{M}^\sharp = \frac{1}{16}\begin{pmatrix} -4 & 0 & 1 & 0 & 1 \\ 6 & -2 & 4 & -2 & 2 \\ -2 & 2 & 3 & -2 & 5 \\ 0 & 0 & 1 & -4 & 1 \\ 2 & -2 & -7 & 2 & -9 \end{pmatrix}, \quad \mathsf{M}^\flat = \frac{1}{8}\begin{pmatrix} 8 & 0 & 0 & 0 & 0 \\ -4 & 4 & -11 & 4 & -7 \\ -4 & -4 & -3 & 4 & -7 \\ 0 & 0 & 0 & 8 & 0 \\ 4 & 4 & 11 & -4 & 15 \end{pmatrix}. \tag{3.24}$$

The above Drazin inverse satisfies indeed $\mathsf{M}\mathsf{M}^\sharp\mathsf{M} = \mathsf{M}$, $\mathsf{M}^\sharp\mathsf{M}\mathsf{M}^\sharp = \mathsf{M}^\sharp$ and $\mathsf{M}^\sharp\mathsf{M}^q = \mathsf{M}^q\mathsf{M}^\sharp = \mathsf{M}^{q-1}$. We also have M: $\mathsf{M}^\flat\mathsf{M}^q = \mathsf{M}^q\mathsf{M}^\flat = \mathsf{M}^q$ for any $q \in \mathbb{C}$ and finally $\mathsf{M}^\sharp\mathsf{M} = \mathsf{M}\mathsf{M}^\sharp = \mathsf{M}^\flat$ as expected of the Drazin inverse. These properties imply that $\mathsf{M}^\flat$ is the projector onto $\mathrm{im}(\mathsf{M})$, the image of M. We demonstrate in §3.4.2 that Theorem 3.3.1 always produces the Drazin inverse.

In addition to the examples with $q = -1$, 0, and $1/p$ with $p \in \mathbb{N}^*$ presented here, the formula of Eq. (3.22) also holds for any complex value of q and is well behaved. For example, we verify analytically using Theorem 3.3.1 to calculate $(\mathsf{M}^{\pm\mathrm{i}})^q$ that $(\mathsf{M}^{\pm\mathrm{i}})^{\mp\mathrm{i}} = \mathsf{M}$. Finally, it is noteworthy that numerical methods implemented by standard softwares such as MATLAB and *Mathematica* suffer from serious stability problems for the matrix considered here and return incorrect results, as can be seen for the case of $q = 1/2$.

Example 3.4.2 (Matrix inverse)**.** To illustrate the application of Theorem 3.3.2 we compute the inverse of

$$\mathsf{M} = \begin{pmatrix} -1 & 0 & 0 & 0 & -1/2 \\ 0 & 2 & 5/2 & 2 & -1 \\ -4 & 0 & 0 & 0 & -1 \\ 0 & -1 & 0 & -2 & 7/4 \\ 0 & 1 & 2 & 0 & 1 \end{pmatrix}. \tag{3.25}$$

The characteristic polynomial of M is $\chi(x) = x^5 - x - 1$, whose Galois group is the symmetric group S_5 and is thus non-solvable. The spectral radius of M is $\rho(\mathsf{M}) \simeq 1.16$. We partition M onto vector spaces $V_1 = \mathrm{span}\big(v_1\big)$, $V_2 = \mathrm{span}\big(v_3, v_5\big)$ and $V_3 = \mathrm{span}\big(v_2, v_4\big)$, giving

$$\mathsf{M}_1 = \begin{pmatrix} -1 \end{pmatrix}, \quad \mathsf{M}_2 = \begin{pmatrix} 0 & -1 \\ 2 & 1 \end{pmatrix}, \quad \mathsf{M}_3 = \begin{pmatrix} 2 & 2 \\ -1 & -2 \end{pmatrix}, \tag{3.26}$$

$$\mathsf{M}_{12} = \begin{pmatrix} 0 & -1/2 \end{pmatrix}, \ \mathsf{M}_{21} = \begin{pmatrix} -4 \\ 0 \end{pmatrix}, \ \mathsf{M}_{23} = \begin{pmatrix} 0 & 0 \\ 1 & 0 \end{pmatrix}, \ \mathsf{M}_{32} = \begin{pmatrix} 5/2 & -1 \\ 0 & 7/4 \end{pmatrix}, \tag{3.27}$$

and $\mathsf{M}_{13} = \mathsf{M}_{31} = 0$. The corresponding graph is thus the path-graph on three vertices, denoted by $\mathcal{P}_3$. By Theorem 3.3.2, the diagonal elements of M^{-1} are given

by

$$\big(\mathsf{M}^{-1}\big)_{11} = \mathsf{F}_{\mathcal{L}_3}[1], \qquad \big(\mathsf{M}^{-1}\big)_{22} = \mathsf{F}_{\mathcal{L}_3}[2], \qquad \big(\mathsf{M}^{-1}\big)_{33} = \mathsf{F}_{\mathcal{L}_3}[3], \tag{3.28a}$$

while the off-diagonal elements are

$$\big(\mathsf{M}^{-1}\big)_{21} = -\mathsf{F}_{\mathcal{L}_3\setminus\{1\}}[2]\,\mathsf{M}_{21}\,\mathsf{F}_{\mathcal{L}_3}[1], \qquad \big(\mathsf{M}^{-1}\big)_{12} = -\mathsf{F}_{\mathcal{L}_3\setminus\{2\}}[1]\,\mathsf{M}_{12}\,\mathsf{F}_{\mathcal{L}_3}[2], \tag{3.28b}$$

$$\big(\mathsf{M}^{-1}\big)_{32} = -\mathsf{F}_{\mathcal{L}_3\setminus\{2\}}[3]\,\mathsf{M}_{32}\,\mathsf{F}_{\mathcal{L}_3}[2], \qquad \big(\mathsf{M}^{-1}\big)_{23} = -\mathsf{F}_{\mathcal{L}_3\setminus\{3\}}[2]\,\mathsf{M}_{23}\,\mathsf{F}_{\mathcal{L}_3}[3], \tag{3.28c}$$

$$\big(\mathsf{M}^{-1}\big)_{31} = \mathsf{F}_{\mathcal{L}_3\setminus\{1,2\}}[3]\,\mathsf{M}_{32}\,\mathsf{F}_{\mathcal{L}_3\setminus\{1\}}[2]\,\mathsf{M}_{21}\,\mathsf{F}_{\mathcal{L}_3}[1], \tag{3.28d}$$

$$\big(\mathsf{M}^{-1}\big)_{13} = \mathsf{F}_{\mathcal{L}_3\setminus\{3,2\}}[1]\,\mathsf{M}_{12}\,\mathsf{F}_{\mathcal{L}_3\setminus\{3\}}[2]\,\mathsf{M}_{23}\,\mathsf{F}_{\mathcal{L}_3}[3]. \tag{3.28e}$$

The matrices $\mathsf{F}_{\mathcal{G}}[\alpha]$ are evaluated according to the recursive definition in Eq. (3.10b); for example

$$\begin{aligned}\mathsf{F}_{\mathcal{L}_3}[1] = \big[\mathsf{M}_1 - \mathsf{M}_{12}\mathsf{F}_{\mathcal{L}_3\setminus\{1\}}[2]\mathsf{M}_{21}\big]^{-1} &= \big[\mathsf{M}_1 - \mathsf{M}_{12}[\mathsf{M}_2 - \mathsf{M}_{23}\mathsf{F}_{\mathcal{L}_3\setminus\{1,2\}}[3]\mathsf{M}_{32}]^{-1}\mathsf{M}_{21}\big]^{-1},\\ &= \big[\mathsf{M}_1 - \mathsf{M}_{12}[\mathsf{M}_2 - \mathsf{M}_{23}\mathsf{M}_3^{-1}\mathsf{M}_{32}]^{-1}\mathsf{M}_{21}\big]^{-1}.\end{aligned} \tag{3.29}$$

Evaluating the flips and statics and reassembling them into matrix form gives

$$\mathsf{M}^{-1} = \frac{1}{8}\begin{pmatrix} 8 & 0 & -4 & 0 & 0\\ 64 & -32 & -16 & -32 & 40\\ -16 & 16 & 4 & 16 & -16\\ -60 & 16 & 15 & 12 & -20\\ -32 & 0 & 8 & 0 & 0\end{pmatrix}, \tag{3.30}$$

which is readily verified to be the inverse of M.

Example 3.4.3 (Matrix exponential)**.** As an example of the application of Theorem 3.3.3 and Lemma 3.3.1 we consider the matrix exponential of

$$\mathsf{M} = \begin{pmatrix} 1-\mathrm{i} & 0 & -\mathrm{i} & 0\\ 0 & 2-\mathrm{i} & -1/3 & 0\\ \mathrm{i} & 0 & -\mathrm{i} & 0\\ 3 & -7/2 & 1 & -1\end{pmatrix}. \tag{3.31}$$

We use a tensor product partition

$$\mathsf{M}_1 = \begin{pmatrix} 1-\mathrm{i} & 0\\ 0 & 2-\mathrm{i}\end{pmatrix}, \quad \mathsf{M}_2 = \begin{pmatrix} -\mathrm{i} & 0\\ 1 & -1\end{pmatrix}, \quad \mathsf{M}_{12} = \begin{pmatrix} -\mathrm{i} & 0\\ -1/3 & 0\end{pmatrix}, \quad \mathsf{M}_{21} = \begin{pmatrix} \mathrm{i} & 0\\ 3 & -7/2\end{pmatrix}.$$

Since every element of this matrix partition is non-zero, the corresponding graph is $\mathcal{K}_2$. Let us focus on the element $\exp(\mathsf{M})_{11}$, which forms the top-left corner of the

full matrix $\exp(\mathsf{M})$. By Theorem 3.3.3 the exact result for $\exp(t\mathsf{M})_{11}$ is given by

$$\mathcal{L}\big[\big(\mathrm{e}^{t\mathsf{M}}\big)_{11}\big] = \mathsf{F}_{\mathcal{K}_2}[1] = \big[s\mathsf{I} - \mathsf{M}_1 - \mathsf{M}_{12}[s\mathsf{I} - \mathsf{M}_2]^{-1}\mathsf{M}_{21}\big]^{-1}, \tag{3.32a}$$

$$= \begin{pmatrix} \dfrac{s+\mathrm{i}}{s^2-(1-2\mathrm{i})s-(2+\mathrm{i})} & 0 \\ \dfrac{-\mathrm{i}}{3s^3-(9-9\mathrm{i})s^2-(6+18\mathrm{i})s+15} & \dfrac{1}{s-(2-\mathrm{i})} \end{pmatrix}. \tag{3.32b}$$

The inverse Laplace transform can be carried out analytically; setting $t = 1$ in the result gives

$$\big(\mathrm{e}^{\mathsf{M}}\big)_{11} = \frac{\mathrm{e}^{(1-2\mathrm{i})/2}}{15}\begin{pmatrix} 3\left(5\cosh\frac{\sqrt{5}}{2} + \sqrt{5}\sinh\frac{\sqrt{5}}{2}\right) & 0 \\ -\mathrm{i}\left(5\mathrm{e}^{3/2} - 5\cosh\frac{\sqrt{5}}{2} - 3\sqrt{5}\sinh\frac{\sqrt{5}}{2}\right) & 15\,\mathrm{e}^{3/2} \end{pmatrix}, \tag{3.33a}$$

$$\approx \begin{pmatrix} 2.05220 - 3.19611\,\mathrm{i} & 0 \\ -0.442190 - 0.283927\,\mathrm{i} & 3.99232 - 6.21768\,\mathrm{i} \end{pmatrix}. \tag{3.33b}$$

Alternatively, we can evaluate this element by using a walk-sum, as presented in Lemma 3.3.1:

$$\big(\mathrm{e}^{\mathsf{M}}\big)_{11} = \mathrm{e}^{\mathsf{M}_1} + \int_0^1\int_0^{t_2} \mathrm{e}^{(1-t_2)\mathsf{M}_1}\,\mathsf{M}_{12}\,\mathrm{e}^{(t_2-t_1)\mathsf{M}_2}\,\mathsf{M}_{21}\,\mathrm{e}^{t_1\mathsf{M}_1}\,\mathrm{d}t_1\,\mathrm{d}t_2 \tag{3.34}$$

$$+\int_0^1\cdots\int_0^{t_2}\mathrm{e}^{(1-t_4)\mathsf{M}_1}\mathsf{M}_{12}\,\mathrm{e}^{(t_4-t_3)\mathsf{M}_2}\,\mathsf{M}_{21}\,\mathrm{e}^{(t_3-t_2)\mathsf{M}_1}\,\mathsf{M}_{12}\,\mathrm{e}^{(t_2-t_1)\mathsf{M}_2}\,\mathsf{M}_{21}\,\mathrm{e}^{t_1\mathsf{M}_1}\,\mathrm{d}t_1\cdots\mathrm{d}t_4+\cdots$$

Evaluating the first three terms yields

$$\big(\mathrm{e}^{\mathsf{M}}\big)_{11} \simeq \begin{pmatrix} 2.05083 - 3.19398\,\mathrm{i} & 0 \\ -0.441354 - 0.283390\,\mathrm{i} & 3.99232 - 6.21768\,\mathrm{i} \end{pmatrix}. \tag{3.35}$$

Although this result has been obtained by evaluating only the first three terms of an infinite series, it is already an excellent approximation to the exact answer: the maximum absolute elementwise error is $\sim 2.5 \times 10^{-3}$. This rapid convergence results from the exact resummation of the terms in the original Taylor series that correspond to walks on the graph $\mathcal{K}_2$ that contain loops.

Example 3.4.4 (Matrix logarithm of a defective matrix)**.** We compute the principal logarithm of the matrix

$$\mathsf{M} = \begin{pmatrix} -1+2\mathrm{i} & -1+2\mathrm{i} & 1 & 2-2\mathrm{i} & -2+2\mathrm{i} \\ -1 & -1+2\mathrm{i} & 1-2\mathrm{i} & 1 & -2+2\mathrm{i} \\ 0 & 1 & 2\mathrm{i} & 0 & 1 \\ -1 & -1+2\mathrm{i} & 1 & 2 & -2+2\mathrm{i} \\ 0 & 1 & -1+2\mathrm{i} & 0 & 2 \end{pmatrix}. \tag{3.36}$$

This matrix has only two eigenvectors associated respectively to the three-fold degenerate eigenvalue 2i and to the two-fold degenerate eigenvalue 1. We choose to partition M onto vector spaces $V_1 = \mathrm{span}\big(v_1, v_4\big)$, $V_2 = \mathrm{span}\big(v_2, v_3\big)$ and $V_3 = \mathrm{span}\big(v_5\big)$. The corresponding graph $\mathcal{G}$ is the complete directed graph on three vertices with the edge (13) missing since $\mathsf{M}_{31} = \big(0\ 0\big)$. Following Theorem 3.3.4 we have

$$\mathsf{F}_{\mathcal{G}}[1] = \big[\mathsf{I}_1 - x(\mathsf{I}_1 - \mathsf{M}_1) - x^2\mathsf{M}_{12}\mathsf{F}_{\mathcal{G}\setminus 1}[2]\mathsf{M}_{21} + x^3\mathsf{M}_{13}\mathsf{F}_{\mathcal{G}\setminus 1,2}[3]\mathsf{M}_{32}\mathsf{F}_{\mathcal{G}\setminus 1}[2]\mathsf{M}_{21}\big]^{-1}, \tag{3.37a}$$

$$\mathsf{F}_{\mathcal{G}}[3] = \big[\mathsf{I}_3 - x(\mathsf{I}_3 - \mathsf{M}_3) - x^2\mathsf{M}_{32}\mathsf{F}_{\mathcal{G}\setminus 3}[2]\mathsf{M}_{23} + x^3\mathsf{M}_{32}\mathsf{F}_{\mathcal{G}\setminus 1,3}[2]\mathsf{M}_{21}\mathsf{F}_{\mathcal{G}\setminus 3}[1]\mathsf{M}_{13}\big]^{-1}, \tag{3.37b}$$

$$\mathsf{F}_{\mathcal{G}}[2] = \big[\mathsf{I}_2 - x(\mathsf{I}_2 - \mathsf{M}_2) - x^2\,\mathsf{M}_{21}\mathsf{F}_{\mathcal{G}\setminus 2}[1]\mathsf{M}_{12} - x^2\,\mathsf{M}_{23}\mathsf{F}_{\mathcal{G}\setminus 2}[3]\mathsf{M}_{32} + x^3\,\mathsf{M}_{21}\mathsf{F}_{\mathcal{G}\setminus 2,3}[1]\mathsf{M}_{13}\mathsf{F}_{\mathcal{G}\setminus 2}[3]\mathsf{M}_{32}\big]^{-1}, \tag{3.37c}$$

with I_i the identity matrix of appropriate dimension and

$$\mathsf{F}_{\mathcal{G}\setminus i}[j] = \big[\mathsf{I} - x(\mathsf{I} - \mathsf{M}_j) - x^2\,\mathsf{M}_{jk}\mathsf{F}_{\mathcal{G}\setminus i,j}[k]\mathsf{M}_{kj}\big]^{-1}, \quad i \neq 2, \tag{3.38a}$$

$$\mathsf{F}_{\mathcal{G}\setminus 2}[j] = \mathsf{F}_{\mathcal{G}\setminus i,k}[j] = \big[\mathsf{I} - x(\mathsf{I} - \mathsf{M}_j)\big]^{-1}. \tag{3.38b}$$

with $i, j, k = (1, 2, 3)$, $i \neq j \neq k$. Then the matrix elements of the principal logarithm of M are given by

$$\big(\log \mathsf{M}\big)_{ii} = \int_0^1 x^{-1}(\mathsf{I} - \mathsf{F}_{\mathcal{G}}[i])\,\mathrm{d}x, \tag{3.39a}$$

$$\big(\log \mathsf{M}\big)_{31} = \int_0^1 -x\,\mathsf{F}_{\mathcal{G}\setminus 1,2}[3]\mathsf{M}_{32}\mathsf{F}_{\mathcal{G}\setminus 1}[2]\mathsf{M}_{21}\mathsf{F}_{\mathcal{G}}[1]\,\mathrm{d}x, \tag{3.39b}$$

$$\big(\log \mathsf{M}\big)_{ji} = \int_0^1 \mathsf{F}_{\mathcal{G}\setminus i}[j]\mathsf{M}_{ji}\mathsf{F}_{\mathcal{G}}[i]\,\mathrm{d}x, \quad i, j = (1,2) \text{ or } (2,3) \tag{3.39c}$$

and for $i, j = (2,1)$, $(3,1)$ or $(3,2)$:

$$\big(\log \mathsf{M}\big)_{ji} = \int_0^1 \mathsf{F}_{\mathcal{G}\setminus i}[j]\mathsf{M}_{ji}\mathsf{F}_{\mathcal{G}}[i] - x\,\mathsf{F}_{\mathcal{G}\setminus i,k}[j]\mathsf{M}_{jk}\mathsf{F}_{\mathcal{G}\setminus i}[k]\mathsf{M}_{ki}\mathsf{F}_{\mathcal{G}}[i]\,\mathrm{d}x. \tag{3.39d}$$

Reassembling them in a matrix, we obtain

$$\log \mathsf{M} = \frac{1}{2}\begin{pmatrix} \lambda + \mathrm{i} & \lambda & 2 & -\lambda - \mathrm{i} & \lambda - 2 \\ \frac{1}{4} + \mathrm{i} & \lambda + \mathrm{i} & -\lambda & -\frac{1}{4} - \mathrm{i} & \lambda + \mathrm{i} \\ -\frac{1}{4} & -\mathrm{i} & \lambda & \frac{1}{4} & -\mathrm{i} \\ \mathrm{i} & \lambda & 2 & -\mathrm{i} & \lambda - 2 \\ -\frac{1}{4} & -\mathrm{i} & \lambda & \frac{1}{4} & -\mathrm{i} \end{pmatrix}, \tag{3.40}$$

where $\lambda = 2\log 2 + \mathrm{i}\pi$.

Example 3.4.5 (Matrix exponential of a quaternionic matrix)**.** Consider any function $f(z) = \sum_n a_n z^n$ with $a_n \in \mathbb{R}$ for all $n \in \mathbb{N}$. Then the graph-theoretic nature of Theorem 2.3.4 allows the method of path-sums to be extended to matrices over non-commutative division rings $\mathbb{D}$. In particular, Theorems 3.3.1-3.3.4 hold for quaternionic matrices $\mathsf{M} \in \mathbb{H}^{D\times D}$ as well. For example, consider calculating $\exp(\pi\mathsf{M})$ with

M the quaternionic matrix

$$\mathsf{M} = \begin{pmatrix} \mathrm{i} & \mathrm{j} \\ \mathrm{k} & 1 \end{pmatrix}, \tag{3.41}$$

where i, j, and k are the quaternions, which satisfy $\mathrm{i}^2 = \mathrm{j}^2 = \mathrm{k}^2 = \mathrm{i}\,\mathrm{j}\,\mathrm{k} = -1$. Following Theorem 3.3.3, we find for example the matrix element M_{11} to be in the Laplace domain

$$\mathcal{L}\big[\exp(t\mathsf{M})_{11}\big] = (s - \mathrm{i} - \mathrm{j}(s-1)^{-1}\mathrm{k})^{-1}. \tag{3.42}$$

Calculating the other matrix elements, inverting the Laplace transforms and setting $t = \pi$, we obtain

$$\exp(\pi\mathsf{M}) = -\frac{1+e^{\pi}}{2}\begin{pmatrix} \mathrm{i} + \tanh\left(\frac{\pi}{2}\right) & \mathrm{j} - \mathrm{k} \\ \mathrm{k} - \mathrm{j} & \mathrm{i} + \tanh\left(\frac{\pi}{2}\right) \end{pmatrix}. \tag{3.43}$$

3.4.2 Generalised matrix powers

The matrix roots are among the most studied matrix functions [51] with numerous applications from finance to healthcare [61]. It is well known that a matrix may fail to have a p^{th} -root [51]. For example, a matrix M has a square root, defined by the relation $\left(\sqrt{\mathsf{M}}\right)^2 = \mathsf{M}$, if and only if the ascent sequence $d_1, d_2 \cdots$ defined by

$$d_i = \dim\left(\ker(\mathsf{M}^i)\right) - \dim\left(\ker(\mathsf{M}^{i-1})\right), \tag{3.44}$$

does not comprise the same odd integer twice or more [62]. Just as a matrix may fail to have a square root, it can fail to have an inverse, yet it always has generalised inverses. Similarly, we show in this section that a matrix always has generalised powers, which we obtain with the method of path-sums.

Definition 3.4.1 (Generalised matrix powers)**.** Let $\mathsf{M} \in \mathbb{C}^{D\times D}$ and let $\mathsf{M}|_{\ker(\mathsf{M})}$ and $\mathsf{M}|_{\mathrm{im}(\mathsf{M})}$ be the restrictions of M to its kernel and image, respectively. Then the generalised powers of M are defined as

$$\mathsf{M}^q_{gen} = \left(\mathsf{M}|_{\mathrm{im}(\mathsf{M})}\right)^q. \tag{3.45}$$

We will see that the Drazin inverse of M is recovered as the generalised power M^{-1}_{gen} and thus also call M^q_{gen} the Drazin powers of M. We obtain the generalised matrix powers using the method of path-sums as follows:

Proposition 3.4.1. *Let $\tilde{\mathsf{M}}(z)$ be the matrix defined by the path-sums on the right hand side of Eqs. (3.9a, 3.9b). Then the ordinary powers $\mathsf{M}^q_{ord} = \left(\mathsf{M}|_{\ker(\mathsf{M})}\right)^q + \left(\mathsf{M}|_{\mathrm{im}(\mathsf{M})}\right)^q$ and generalised powers $\mathsf{M}^q_{gen} = \left(\mathsf{M}|_{\mathrm{im}(\mathsf{M})}\right)^q$ of M are given by*

$$\mathsf{M}^q_{ord} = -\mathcal{Z}_b^{-1}\big\{\tilde{\mathsf{M}}(z)\big\}[n]\Big|_{n=-q-1}, \quad \mathsf{M}^q_{gen} = -\mathcal{Z}_u^{-1}\big\{\tilde{\mathsf{M}}(z)\big\}[n]\Big|_{n=-q-1}. \tag{3.46}$$

Here $\mathcal{Z}_b^{-1}\{.\}[n]$ and $\mathcal{Z}_u^{-1}[.]$ denote respectively the bilateral and unilateral inverse Z-transforms.

Proof. Let $\mathsf{M} \in \mathbb{C}^{D\times D}$ with $\dim(\ker(\mathsf{M})) = k_0$ and non-zero eigenvalues $\{\lambda_l\}_{1\leq l\leq D-k_0}$. Consider the matrix $\tilde{\mathsf{M}}(z)$ obtained in the Z-domain by the path-sum formula, Theorem 3.3.1. Let $\mathsf{M} = \mathsf{P}\mathsf{J}\mathsf{P}^{-1}$ be the Jordan decomposition of M. Observe that since $\mathsf{M}^q = \mathsf{P}\mathsf{J}^q\mathsf{P}^{-1}$, $\tilde{\mathsf{M}}(z) = \mathsf{P}[z^{-1} - \mathsf{J}]^{-1}\mathsf{P}^{-1}$ and the entries of $\tilde{\mathsf{M}}(z)$ are of the form

$$\big(\tilde{\mathsf{M}}(z)\big)_{ij} = \frac{Q_{ij}(z)\, z^{k_0}}{\prod_{l=1}^{D-k_0}(\lambda_l - z^{-1})}, \tag{3.47}$$

with $Q_{ij}(z)$ a polynomial in z. A partial fraction decomposition of the matrix entries separate terms with exclusively positive powers of z from those involving fractions of z. Thus, we can write

$$\big(\tilde{\mathsf{M}}(z)\big)_{ij} = \sum_{p=1}^{D-1} \alpha_p z^p + \frac{P_{ij}(z)}{\prod_{l=1}^{D-k_0}(\lambda_l z - 1)}, \tag{3.48}$$

where $P_{ij}(z)$ is a polynomial in z and $\alpha_p \in \mathbb{C}$ are the coefficients of the decomposition. Terms with strictly positive powers of z arise because of the z^{k_0} factor in Eq. (3.47) and thus correspond to the kernel of the matrix. These terms are discarded by the unilateral inverse Z-transform, and

$$\big(\mathsf{M}^q_{gen}\big)_{ij} = -\mathcal{Z}_u^{-1}\Big\{\frac{P_{ij}(z)}{\prod_{l=1}^{D-k_0}(\lambda_l z - 1)})\Big\}[n]\Big|_{n=-q-1}, \tag{3.49}$$

represents $\big(\mathsf{M}|_{\mathrm{im}(\mathsf{M})}\big)^q$, the powers of M restricted to its image. On the contrary, a bilateral inverse Z-transform conserves the terms associated with the kernel and yields ordinary powers

$$\big(\mathsf{M}^q_{ord}\big)_{ij} = -\mathcal{Z}_b^{-1}\Big\{\frac{Q_{ij}(z)\, z^{k_0}}{\prod_{l=1}^{D-k_0}(\lambda_l - z^{-1})}\Big\}[n]\Big|_{n=-q-1}. \tag{3.50}$$

The two agree when M is not singular. Finally, remark that since $\mathsf{M}^{-1}_{gen} = \big(\mathsf{M}|_{\mathrm{im}(\mathsf{M})}\big)^{-1}$ we have $\mathsf{M}^{-1}_{gen} = \mathsf{M}^\sharp$ as claimed. □

The method of path-sums, in conjunction with the appropriate inverse Z-transform, gives generalised as well as ordinary powers of a matrix. The generalised matrix powers always exist. We call them Drazin powers because they share the properties of the Drazin inverse: they coincide with the ordinary powers for non-singular matrices and $[\mathsf{M}^q, \mathsf{M}] = 0$, $\mathsf{M}^q\mathsf{M}^{q'} = \mathsf{M}^{q+q'}$, $\mathsf{M}^{-1} = \mathsf{M}^\sharp$, $\mathsf{M}^0 = \mathsf{M}^\flat = \mathsf{M}^\sharp\mathsf{M}$, $\mathsf{M}^{1/2}\mathsf{M}^{1/2} = \mathsf{M}^\flat$ etc. All of these properties are straightforward consequences of $\mathsf{M}^q_{gen} = \big(\mathsf{M}|_{\mathrm{im}(\mathsf{M})}\big)^q$.

Example 3.4.6 (Generalised and ordinary powers of a singular defective matrix)**.**

To illustrate the generalised and ordinary powers, consider

$$\mathsf{M} = \begin{pmatrix} -1 & 1 & -1 & -\frac{1}{3} \\ -1 & -2 & 2 & 0 \\ -1 & -2 & 2 & \frac{1}{3} \\ 2 & -2 & 2 & 1 \end{pmatrix}. \tag{3.51}$$

This matrix has a 2×2 Jordan block with eigenvalue 0 and has consequently no primary square-root[3]. Nonetheless, M has a Drazin square-root, which we obtain with the method of path-sums. In the Z-domain, Theorem 3.3.1 gives

$$\tilde{\mathsf{M}}(z) = \begin{pmatrix} \frac{2z^3+3z^2-3z}{3z^2-3} & \frac{z^3-3z^2}{3z^2-3} & \frac{-z^3+3z^2}{3z^2-3} & \frac{z^2}{3z-3} \\ \frac{z^2-2z^3}{z-1} & \frac{-z^3+3z^2-z}{z-1} & \frac{z^3-2z^2}{z-1} & \frac{-z^3}{z-1} \\ \frac{-6z^4-5z^3+3z^2}{3z^2-3} & \frac{-3z^4+5z^3+6z^2}{3z^2-3} & \frac{3z^4-2z^3-6z^2-3z}{3z^2-3} & \frac{-3z^3-z^2}{3z-3} \\ \frac{-2z^2}{z^2-1} & \frac{2z^2}{z^2-1} & \frac{-2z^2}{z^2-1} & \frac{-z}{z-1} \end{pmatrix}, \tag{3.52}$$

and the Drazin and ordinary powers of M are given by

$$\mathsf{M}^q_{gen} = \frac{1}{3}\begin{pmatrix} -1+2(-1)^{-q} & 1-2(-1)^{-q} & -1+2(-1)^{-q} & -1 \\ 3 & -3 & 3 & 3 \\ 4+(-1)^{-q} & -4-(-1)^{-q} & 4+(-1)^{-q} & 4 \\ 3-3(-1)^{-q} & -3+3(-1)^{-q} & 3-3(-1)^{-q} & 3 \end{pmatrix}, \tag{3.53a}$$

$$\mathsf{M}^q_{ord} = \mathsf{M}^q_{gen} + \frac{1}{3}\begin{pmatrix} 2\delta_{0,q} & \delta_{0,q} & -\delta_{0,q} & \delta_{0,q} \\ -3(\delta_{0,q}+2\delta_{1,q}) & 6\delta_{0,q}-3\delta_{1,q} & 3(\delta_{1,q}-\delta_{0,q}) & -3(\delta_{0,q}+\delta_{1,q}) \\ -5\delta_{0,q}-6\delta_{1,q} & 5\delta_{0,q}-3\delta_{1,q} & 3\delta_{1,q}-2\delta_{0,q} & -4\delta_{0,q}-3\delta_{1,q} \\ 0 & 0 & 0 & 0 \end{pmatrix}, \tag{3.53b}$$

where $\delta_{a,b}$ is the Kronecker delta. We observe that $\mathsf{M}^0_{ord} = \mathsf{I}$ and $\mathsf{M}^1_{ord} = \mathsf{M}$ while $\mathsf{M}^0_{gen} = \mathsf{M}^\flat$ and $\mathsf{M}^1_{gen} = \mathsf{M}|_{\mathrm{im}(\mathsf{M})}$, as expected. The Drazin square-root $\mathsf{M}^{1/2}_{gen}$ is obtain upon setting $q = 1/2$ in Eq. (3.53a), it fulfills $\mathsf{M}^{1/2}_{gen}\mathsf{M}^{1/2}_{gen} = \mathsf{M}|_{\mathrm{im}(\mathsf{M})}$.

3.4.3 Matrix exponential of block tridiagonal matrices

Let $\{\mathsf{M}_{k',k}\}$ be a partition of a matrix M such that $\mathsf{M}_{k'\neq k\pm1,k} = 0$. If this partition consists of N^2 pieces, the corresponding graph is the finite path-graph on N vertices $\mathcal{P}_N$, and M can therefore be said to be a $\mathcal{P}_N$-structured matrix. As mentioned in remarks 3.2.1 and 3.3.2, such a matrix is essentially a block tridiagonal matrix since there exists a permutation matrix P such that PMP^{-1} is block tridiagonal. For these matrices, the path-sum expression for the matrix exponential and inverse can be written in a particularly compact form. For $k = 1, \ldots, N$, we set $\tilde{\mathsf{M}}_k = s\mathsf{I} - \mathsf{M}_k$,

[3]Its ascent sequence is $1, 1, 0, 0, \ldots$

and define the finite continued fractions

$$\tilde{\mathsf{X}}_k = \left[\tilde{\mathsf{M}}_k - \mathsf{M}_{k,k+1}\tilde{\mathsf{X}}_{k+1}\mathsf{M}_{k+1,k}\right]^{-1}, \quad \tilde{\mathsf{Y}}_k = \left[\tilde{\mathsf{M}}_k - \mathsf{M}_{k,k-1}\tilde{\mathsf{Y}}_{k-1}\mathsf{M}_{k-1,k}\right]^{-1}, \qquad (3.54)$$

with $\tilde{\mathsf{X}}_N \equiv \tilde{\mathsf{M}}_N^{-1}$ and $\tilde{\mathsf{Y}}_1 \equiv \tilde{\mathsf{M}}_1^{-1}$. Note that the inversion height of $\tilde{\mathsf{X}}_k$ ($\tilde{\mathsf{Y}}_k$) is $N+1-k$ (k). Let $\tilde{\mathsf{U}} = \mathfrak{L}[\exp(t\,\mathsf{M})]$ be the Laplace transform of the matrix exponential of M; then the partition of $\tilde{\mathsf{U}}$ is given by

$$\tilde{\mathsf{U}}_{kk} = \left[\tilde{\mathsf{X}}_k^{-1} + \tilde{\mathsf{Y}}_k^{-1} - \tilde{\mathsf{M}}_k\right]^{-1}, \qquad (3.55a)$$

$$\tilde{\mathsf{U}}_{k,k'<k} = \prod_{j=k'+1}^{k} \left(\tilde{\mathsf{X}}_j \mathsf{M}_{j,j-1}\right) \tilde{\mathsf{U}}_{k'k'}, \qquad \tilde{\mathsf{U}}_{k,k'>k} = \prod_{j=k'-1}^{k} \left(\tilde{\mathsf{Y}}_j \mathsf{M}_{j,j+1}\right) \tilde{\mathsf{U}}_{k'k'}, \qquad (3.55b)$$

where $\prod_{j=1}^{n} a_j = a_n a_{n-1} \cdots a_2 a_1$ is a left product. Provided the required inverse Laplace-transforms are analytically available, Eq.(3.54-3.55b) yields the exact matrix exponential of M. Similar formulae for the inverse of arbitrary $\mathcal{P}_N$-structured matrices are obtained upon replacing $s\mathsf{I}$ by I in each of the $\tilde{\mathsf{M}}_k$.

3.4.4 Computational cost on tree-structured matrices

The number of simple paths in any finite graph is finite. Thus, as soon as a matrix M has a finite size, the path-sum expressions of Theorems 3.3.1-3.3.4 evaluate any function $f(\mathsf{M})$ exactly in a finite number ρ of operations, up to the integral transforms. In this final example we calculate ρ in the case of matrices M whose partition is an arbitrary tree, denoted by $\mathcal{T}_N$.

First, we consider the computational cost of evaluating a static $f(\mathsf{M})_{\alpha\alpha}$. Since a tree contains no simple cycles of length greater than 2, the vertex α requires dressing only by loops and edge cycles on $\mathcal{T}_N$. Consequently, the sequence of operations involved in dressing α fall into two categories: nesting (adding an edge cycle which dresses the internal vertex of a previous edge cycle) or branching (including an extra edge cycle at constant dressing depth). These two operations have the same computational cost, as each requires one inversion, two multiplications and one subtraction of $d \times d$ matrices. Due to this symmetry between branching and nesting, the computational costs of dressing a vertex on the path-graph on N vertices $\mathcal{P}_N$ (which involves nesting only) and the star graph on N vertices $\mathcal{S}_N$ (which involves branching only) are identical: each requires N inversions, $2(N-1)$ multiplications and $N-1$ additions to fully dress any vertex. Since any tree can be decomposed as a set of path-graphs (the branches) and star graphs (the nodes), the computational cost of evaluating $f(\mathsf{M})_{\alpha\alpha}$ when M is tree-structured depends only on the number of vertices of the tree: the cost is independent of the detailed structure of $\mathcal{T}_N$. The number of floating point operations required to evaluate the diagonal element $f(\mathsf{M})_{\alpha\alpha}$, denoted by $\rho_{\mathcal{T}_N;\alpha}$, scales as $3Nd^3$, while the computational density (the number of operations per usual matrix-element evaluated) is $\sim 3Nd$.

We now consider the cost of calculating an off-diagonal element $f(\mathsf{M})_{\omega\alpha}$. Let

$(\alpha\nu_2\cdots\nu_\ell\omega)$ be the unique simple path leading from α to ω on $\mathcal{T}_N$, and $\rho_{\mathcal{T}_N;\alpha}$ be the cost of fully dressing the vertex α on $\mathcal{T}_N$. Then the total cost of evaluating $f(\mathsf{M})_{\omega\alpha}$ is

$$2\ell d^3 + \sum_{i=1}^{\ell+1} \rho_{\mathcal{T}_N\backslash\{\alpha,\ldots,\nu_{i-1}\};\nu_i}, \tag{3.56}$$

where the first term accounts for the cost of evaluating the matrix multiplications along the simple path. Note that this cost depends on the structure of $\mathcal{T}_N$, since the number of vertices in each tree in the sequence $\mathcal{T}_N\backslash\{\alpha,\ldots,\nu_{i-1}\}$ depends on whether any of the previously-visited vertices are nodes of $\mathcal{T}_N$. Nevertheless, we can place an upper bound on the cost by considering the case where the tree $\mathcal{T}_N$ is the path-graph $\mathcal{P}_N$. Then $\mathcal{P}_N\backslash\{\alpha,\ldots,\nu_{i-1}\}$ contains $N+1-i$ vertices, and the total cost of evaluating the contribution of a simple path of length ℓ is $\sim \ell d^3(3N+2)$. Finally, we note that in the course of evaluating the contribution of a certain simple path p, we simultaneously evaluate the contributions of all subpaths of p. The operations counted by Eq. (3.56) therefore generate $(\ell+1)d^2$ elements of the partition of $f\big(\mathsf{M}\big)$. This improves the computational density of the path-sum method for tree-structured matrices to $\sim 3Nd$. Therefore, we conclude that evaluating any element of a partition of a matrix function of a tree-structured matrix using path-sums is efficient: i.e. the cost is linear in the number of vertices in the tree.

3.4.5 Quasideterminants

The determinant is a concept of central importance in commutative linear algebra. Initially, interest in the determinant lay in its equation-solving properties. Similarly, noncommutative analogues to the determinants were investigated in the context of systems of equations involving quaternions from the end of 19$^{\text{th}}$ century onwards[63, 64]. The concept of quasideterminant first arose in the late 1920s [65, 66, 67]. More recently, research on quasideterminants was revived by a series of papers by Gel'fand and coworkers [68, 69, 70] who discovered that they share some equation solving properties of the usual determinant, see [36]. Consequently, quasideterminants found many applications in mathematics [71, 72, 73, 74] and mathematical-physics [75, 76, 77, 78]. We begin by defining the quasideterminants following [36].

Definition 3.4.2 (Quasideterminants [36])**.** Let X be a $D\times D$ matrix with formal entries x_{ij}. Then X is invertible over the free division ring $\mathbb{D}(\mathcal{X})$ generated by $\mathcal{X}=\{x_{ij}\}_{1\le i\le D,1\le j\le D}$ and let $\mathsf{Y}=\mathsf{X}^{-1}=(y_{ij})$. The (i,j)th quasideterminant of X is the element of $\mathbb{D}(\mathcal{X})$ defined by

$$|\mathsf{X}|_{ij} = (y_{ji})^{-1}. \tag{3.57}$$

The quasideterminants are therefore inverses of the elements of the transpose of the matrix inverse of a matrix over a division ring. The reason for this seemingly complicated definition is that quasideterminants obey a simple heredity principle.

Proposition 3.4.2 (Heredity principle [36])**.** *Let* $\mathsf{X} \in \mathbb{D}^{D\times D}$*. If* $D = 1$*, then* $|\mathsf{X}|_{11} = x_{11}$*. Otherwise, for* $D \geq 2$*, let* X^{ij} *be the* $(D-1)\times(D-1)$ *matrix obtained from* X *upon deleting row the* i*th row and* j*th column. Then*

$$|\mathsf{X}|_{ij} = x_{ij} - r_i^j\, |\mathsf{X}^{ij}|^{-1\bullet}\, c_j^i, \tag{3.58}$$

where $\mathsf{M}^{-1\bullet}$ *designates the entry-wise (Hadamard) inverse of* M*,* $r_i^j \in \mathbb{D}^{1\times(D-1)}$ *and* $c_j^i \in \mathbb{D}^{(D-1)\times 1}$ *are respectively the* i*th row and the* j*th column of* X *with* x_{ij} *removed.*

As we shall see, the heredity principle above is recovered by the path-sum result in the case of the $\mathcal{K}_2$ graph[4]. We begin with a definition necessary to state the path-sum result on quasideterminants in full generality.

Definition 3.4.3 (Quasideterminantal matrices)**.** Let $\mathsf{X} \in \mathbb{D}^{D\times D}$ and $\{|\mathsf{X}|_{\omega\alpha}\}$ be a partition of X. The elements $|\mathsf{X}|_{\omega\alpha}$ of this partition are called quasideterminantal matrices.

Theorem 3.4.1 (**Generalised heredity principle for quasideterminantal matrices**)**.** *Consider* $\mathsf{X} \in \mathbb{D}^{D\times D}$*, let* $\mathsf{X}_{\alpha\omega}$ *be a general partition of* X *and let* $\mathcal{G}$ *be the graph of* $\{\mathsf{I} - \mathsf{X}\}_{\alpha\omega}$*. Then, as long as all of the required inverses exist, the quasideterminantal matrices* $\big|\mathsf{X}\big|_{\omega\alpha}$ *are given by the path-sum*

$$\big|\mathsf{X}\big|_{\omega\alpha}^{-1\bullet} = \sum_{\Pi_{\mathcal{G};\,\alpha\omega}} (-1)^{\ell_p} \big(\mathsf{X}^{(\alpha,\,\ldots\,,\,\nu_{\ell_p})}\big)^{-1}_{\omega\omega}\, \mathsf{X}_{\omega\nu_{\ell_p}} \cdots \big(\mathsf{X}^{(\alpha)}\big)^{-1}_{\nu_2}\, \mathsf{X}_{\nu_2\alpha}\, \mathsf{X}_{\alpha}^{-1}, \tag{3.59a}$$

where ℓ_p *is the length of the simple path and*

$$\big|\mathsf{X}\big|_{\alpha}^{-1\bullet} = \Big[\mathsf{X}_\alpha - \sum_{\Gamma_{\mathcal{G}_0;\,\alpha}} (-1)^{\ell_c} \mathsf{X}_{\alpha\mu_{\ell_c}} \big(\mathsf{X}^{(\alpha,\,\ldots\,,\,\mu_{\ell_c-1})}\big)^{-1}_{\mu_{\ell_c}\mu_{\ell_c}} \cdots \big(\mathsf{X}^{(\alpha)}\big)^{-1}_{\mu_2\mu_2} \mathsf{X}_{\mu_2\alpha}\Big]^{-1}, \tag{3.59b}$$

with ℓ_c *the length of the bare cycle. In these expressions* $\mathsf{M}^{-1\bullet}$ *designates the entry-wise inverse of* M*.*

Proof. We start with Proposition 1.2.8 of [36], where the authors remark that quasideterminants can be written as a sum of weighted walks on a weighted digraph[5]. With our notation, their result reads

$$|\mathsf{I} - \mathsf{X}|_{ii} = 1 - \sum_{w\in W_{\mathcal{G};\,ii}} \mathrm{W}[w], \quad |\mathsf{I} - \mathsf{X}|^{-1}_{ij} = \sum_{w\in W_{\mathcal{G};\,ji}} \mathrm{W}[w]. \tag{3.60}$$

This is just the representation of the power-series for the matrix inverse as a walk series (see more generally Eq. (3.5) of §3.2.2) in the case where the matrix is partitioned into its usual matrix elements. This extends straightforwardly to general

[4]Complete graph on 2 vertices.

[5]The authors use the term *path* for our *walk*, *simple path from i to i* for our *cycle off vertex i*, and *word* to designate the weight of a walk.

partitions

$$|\mathsf{I}-\mathsf{X}|_{\alpha\alpha} = 1 - \sum_{w\in W_{\mathcal{G};\,\alpha\alpha}} \mathrm{W}[w], \quad |\mathsf{I}-\mathsf{X}|^{-1}_{\alpha\omega} = \sum_{w\in W_{\mathcal{G};\,\omega\alpha}} \mathrm{W}[w], \tag{3.61}$$

and the generalised heredity principle for quasideterminantal matrices follows directly from the weighted path-sum Theorem 2.3.4. □

Remark 3.4.1 (Standard heredity principle)**.** The standard heredity principle for the quasideterminants of a matrix with formal entries follows directly from Theorem 3.4.1 in the case where X is partitioned onto $\mathcal{K}_2$, the complete undirected graph on two vertices. To see this, let P be a permutation matrix such that x_{ij} is a diagonal element of $(\mathsf{PXP}^{\mathrm{T}})$. The partition of $\mathsf{PXP}^{\mathrm{T}}$ into four blocks $\big(\mathsf{PXP}^{\mathrm{T}}\big)_{\alpha} \equiv x_{ij}$, $\big(\mathsf{PXP}^{\mathrm{T}}\big)_{\omega} \equiv \mathsf{X}^{ij}$ and thus $\mathsf{X}_{\omega\alpha} \equiv c^i_j$, $\mathsf{X}_{\alpha\omega} \equiv r^j_i$ is a valid general partition of $\mathsf{PXP}^{\mathrm{T}}$ and hence of X. Then Eq. (3.59b) reads

$$|\mathsf{X}|^{-1\bullet}_{\alpha} = \big[\mathsf{X}_{\alpha} - \mathsf{X}_{\alpha\omega}\,\mathsf{X}^{-1}_{\omega}\,\mathsf{X}_{\omega\alpha}\big]^{-1} \Longrightarrow |\mathsf{X}|_{ij} = x_{ij} - r^j_i\,|\mathsf{X}^{ij}|^{-1\bullet}\,c^i_j\,, \tag{3.62}$$

which is the standard heredity principle.

3.5 Proofs of Path-Sum Expressions for Common Matrix Functions

In this section we prove the path-sum results presented earlier without proof. We begin by proving the results of §3.2.2 relating the partitions of M^k and $f(\mathsf{M})$ to the partition of M. We then prove the path-sum results for a matrix raised to a complex power (§3.5.2), the matrix inverse (§3.5.3), the matrix exponential (§3.5.4), and the matrix logarithm (§3.5.5).

3.5.1 Partitions of matrix powers and functions

Consider an element $\mathsf{R}_{\omega}\mathsf{M}^k\mathsf{R}^{\mathrm{T}}_{\alpha}$ of a general partition of M^k. On inserting the identity in the form of the closure relation over projector-lattices between each appearance of M in the product and using $\varepsilon_{\mu} = \mathsf{R}^{\mathrm{T}}_{\mu}\mathsf{R}_{\mu}$, we obtain [20, 19]

$$\big(\mathsf{M}^k\big)_{\omega\alpha} = \sum_{\eta_k,\ldots,\eta_2} \mathsf{R}_{\omega}\mathsf{M}\,\mathsf{R}^{\mathrm{T}}_{\eta_k}\mathsf{R}_{\eta_k}\cdots\mathsf{M}\,\mathsf{R}^{\mathrm{T}}_{\eta_2}\mathsf{R}_{\eta_2}\mathsf{M}\,\mathsf{R}^{\mathrm{T}}_{\alpha} = \sum_{\eta_k,\ldots,\eta_2} \mathsf{M}_{\omega\eta_k}\cdots\mathsf{M}_{\eta_3\eta_2}\mathsf{M}_{\eta_2\alpha}, \tag{3.63}$$

with $\alpha \equiv \eta_1$ and $\omega \equiv \eta_{k+1}$. This expression describes matrix multiplication in terms of the partition of M and provides an explicit description of which pieces of M contribute to a given piece of M^k. It follows that the partition of a matrix function

$f(\mathsf{M})$ with power series $f\big(\mathsf{M}\big) = \sum_{k=0}^{\infty} f_k\, \mathsf{M}^k$ is given by

$$f\big(\mathsf{M}\big)_{\omega\alpha} = \sum_{k=0}^{\infty} f_k \sum_{\eta_k,\ldots,\eta_2} \mathsf{M}_{\omega\eta_k} \cdots \mathsf{M}_{\eta_3\eta_2} \mathsf{M}_{\eta_2\alpha}. \tag{3.64}$$

This equation relates the partition of $f\big(\mathsf{M}\big)$ to that of M.

3.5.2 A matrix raised to a complex power

Proof. We consider a matrix $\mathsf{M} \in \mathbb{C}^{D\times D}$. To prove Theorem 3.3.1 we start from the power series

$$\mathsf{M}^q = \sum_{k=0}^{\infty} \binom{q}{k} (\mathsf{M} - \mathsf{I})^k, \tag{3.65}$$

where $q \in \mathbb{C}$ and $\binom{q}{k} = q^{\underline{k}}/k!$ is a binomial coefficient, with $q^{\underline{k}}$ the falling factorial. Note that although the sum only converges when the spectral radius $\rho(\mathsf{M}-\mathsf{I}) < 1$, the result of Theorem 3.3.1 is valid for matrices of arbitrary spectral radius by analytic continuation, as will be shown at the end of this section. For the moment, we require that $\rho(\mathsf{M}-\mathsf{I}) \leq \|\mathsf{M}-\mathsf{I}\| < 1$, where $\|.\|$ is any induced norm. By applying the result of Eq. (3.5) to Eq. (3.65) we find that an element of a partition of M^q is given by

$$\big(\mathsf{M}^q\big)_{\omega\alpha} = \sum_{k=0}^{\infty} \binom{q}{k} \sum_{W_{\mathcal{G};\alpha\omega;k}} \bar{\mathsf{M}}_{\omega\eta_k} \cdots \bar{\mathsf{M}}_{\eta_3\eta_2} \bar{\mathsf{M}}_{\eta_2\alpha}, \tag{3.66}$$

where we have introduced the auxiliary matrix $\bar{\mathsf{M}} = \mathsf{M} - \mathsf{I}$ and $\mathcal{G}$ is the graph of the partition of $\bar{\mathsf{M}}$. We shall now recast this expression so as to make the loops of the walk $(\alpha)(\alpha\eta_2)\cdots(\eta_k\omega)(\omega)$ appear explicitly. To this end, we remark that when a loop off a vertex μ occurs $p \in \mathbb{N}$ consecutive times in a walk, the contribution of the walk comprises a factor of $(\bar{\mathsf{M}}_\mu)^p$. Thus

$$\big(\mathsf{M}^q\big)_{\omega\alpha} = \sum_{k=0}^{\infty} \binom{q}{k} \sum_{m=0}^{k} \sum_{W_{\mathcal{G}_0;\alpha\omega;m}} \sum_{\{p_i\}\vdash k-m} (\bar{\mathsf{M}}_\omega)^{p_{m+1}} \mathsf{M}_{\omega\mu_m} \cdots (\bar{\mathsf{M}}_{\mu_2})^{p_2} \mathsf{M}_{\mu_2\alpha} (\bar{\mathsf{M}}_\alpha)^{p_1}. \tag{3.67}$$

In this expression any two consecutive vertices μ_ℓ and $\mu_{\ell+1}$ are now distinct and the sum $\sum_{W_{\mathcal{G}_0;\alpha\omega;m}}$ runs thus over the walks of the loopless graph $\mathcal{G}_0$. Each integer $p_i \in \mathbb{N}$, called a loop number, represents the number of consecutive times a loop is undergone off a certain vertex. The notation $\{p_i\} \vdash k-m$ on the final sum therefore indicates that the final sum runs over all possible configurations of the p_i numbers, that is all configurations of $k-m$ loops on $m+1$ vertices, subject to the restriction that the loop number p_i on any loopless vertex is fixed to zero. This implies that $\sum_{i=1}^{m+1} p_i = k-m$ and the p_i are thus said to form a weak composition of $k-m$. We now remark that for any such weak composition and $q \in \mathbb{C}$, the following relation

holds:

$$\binom{q}{k} = \sum_{k_m} \sum_{k_{m-1}=0}^{k_m} \cdots \sum_{k_1=0}^{k_2} \frac{(-1)^m}{\prod_{r=1}^{m+1} p_r!} (-1)^{p_{m+1}} \big((-q-1) - k_m + p_{m+1}\big)^{\underline{p_{m+1}}} \cdots \\ \cdots (-1)^{p_2} (k_2 - k_1 + p_2)^{\underline{p_2}} \, (-1)^{p_1} (k_1 + p_1)^{\underline{p_1}}, \quad (3.68)$$

where the first sum is an *indefinite* sum to be evaluated at $k_m = -q-1$. From now on we will denote this by $\sum_{k_m=0}^{-q-1}$. Equation (3.68), which is independent of the value of each individual p_i, is proved by induction on m. Upon substituting this relation into Eq. (3.65) and rearranging the order of the summations we obtain

$$\big(\mathsf{M}^q\big)_{\omega\alpha} = \sum_{m=0}^{\infty} (-1)^m \sum_{W_{\mathcal{G}_0;\alpha\omega;m}} \sum_{\{p_i\}=0}^{\infty} \sum_{k_m=0}^{-q-1} \sum_{k_{m-1}=0}^{k_m} \cdots \sum_{k_1=0}^{k_2} (-\bar{\mathsf{M}}_\omega)^{p_{m+1}} \big((-q-1) - k_m + p_{m+1}\big)^{\underline{p_{m+1}}} \mathsf{M}_{\omega\mu_m} \cdots \\ \cdots (-\bar{\mathsf{M}}_{\mu_2})^{p_2} (k_2 - k_1 + p_2)^{\underline{p_2}} \mathsf{M}_{\mu_2\alpha} (\bar{\mathsf{M}}_\alpha)^{p_1} (k_1 + p_1)^{\underline{p_1}}, \quad (3.69)$$

where the sum $\sum_{\{p_i\}=0}^{\infty} = \sum_{p_1=0}^{\infty} \cdots \sum_{p_{m+1}=0}^{\infty}$ runs over all the loop numbers, subject to the restriction that the loop number p_i on any loopless vertex is fixed to zero. We now evaluate the contributions from the infinite loop sums in closed form by noting that

$$\sum_{p_i=0}^{\infty} (-\bar{\mathsf{M}}_\mu)^{p_i} \frac{(k_i - k_{i-1} + p_i)^{\underline{p_i}}}{p_i!} = (\mathsf{M}_\mu)^{-(k_i - k_{i-1})-1}, \quad (3.70)$$

where we have used the fact that $\rho(\bar{\mathsf{M}}_\mu) \leq \|\bar{\mathsf{M}}_\mu\| = \|\mathsf{M}_\mu - \mathsf{I}\| \leq \|\mathsf{M} - \mathsf{I}\| < 1$. Introducing Eq. (3.70) into Eq. (3.69) and setting $k_0 = 0$ by definition yields the expression

$$\big(\mathsf{M}^q\big)_{\omega\alpha} = \sum_{m=0}^{\infty} (-1)^m \sum_{W_{\mathcal{G}_0;\alpha\omega;m}} \sum_{k_m=0}^{-q-1} \sum_{k_{m-1}=0}^{k_m} \cdots \sum_{k_1=0}^{k_2} (\mathsf{M}_\omega)^{-((-q-1)-k_m)-1} \mathsf{M}_{\omega\mu_m} \cdots \\ \cdots (\mathsf{M}_{\mu_2})^{-(k_2-k_1)-1} \mathsf{M}_{\mu_2\alpha} (\mathsf{M}_\alpha)^{-k_1-1}. \quad (3.71)$$

This expression is an m-fold nested discrete convolution. In order to convert the discrete convolution to a product, we take the unilateral Z-transform of the above expression with respect to $n \equiv -q-1$. We obtain

$$\big(\mathsf{M}^q\big)_{\omega\alpha} = -\mathcal{Z}_u^{-1} \left\{ \sum_{m=0}^{\infty} \sum_{W_{\mathcal{G}_0;\alpha\omega;m}} \big[\mathsf{I}z^{-1} - \mathsf{M}_\omega\big]^{-1} \mathsf{M}_{\omega\mu_m} \cdots \right. \\ \left. \cdots \big[\mathsf{I}z^{-1} - \mathsf{M}_{\mu_2}\big]^{-1} \mathsf{M}_{\mu_2\alpha} \big[\mathsf{I}z^{-1} - \mathsf{M}_\alpha\big]^{-1} \right\} [n]\Big|_{n=-q-1}, \quad (3.72)$$

where $z \in \mathbb{C}$ is the Z-domain variable. Now the content of the inverse Z-transform is a sum of walk contributions. Indeed we can see $\mathrm{W}_\alpha^{\mathrm{eff}} = \big[\mathsf{I}z^{-1} - \mathsf{M}_\alpha\big]^{-1}$ as an effective

weight associated to vertex α. This effective weight results from the dressing of α by all the loops off α which is performed by Eq. (3.70). Then upon remarking that e.g. $\mathsf{M}_{\mu_2\alpha} = \mathsf{w}_{\mu_2\alpha}$ is the weight associated to edge $(\alpha\mu_2)$ from α to μ_2, Eq. (3.72) is

$$\big(\mathsf{M}^q\big)_{\omega\alpha} = -\mathcal{Z}_u^{-1}\Big\{ \sum_{W_{\mathcal{G}_0;\alpha\omega}} \mathrm{W}_{\omega}^{\mathrm{eff}}\, \mathsf{w}_{\omega\mu_m} \cdots \mathrm{W}_{\mu_2}^{\mathrm{eff}}\, \mathsf{w}_{\mu_2\alpha}\, \mathrm{W}_{\alpha}^{\mathrm{eff}} \Big\}[n]\Big|_{n=-q-1}. \tag{3.73}$$

This is now in a form suitable to the use of Theorem 2.3.4. We obtain

$$(\mathsf{M}^q)_{\omega\alpha} = -\mathcal{Z}_u^{-1}\left\{ \sum_{\Pi_{\mathcal{G}_0;\alpha\omega}} \mathsf{F}_{\mathcal{G}\setminus\{\alpha,\ldots,\nu_\ell\}}[\omega]\, \mathsf{M}_{\omega\nu_\ell} \cdots \mathsf{F}_{\mathcal{G}\setminus\{\alpha\}}[\nu_2]\, \mathsf{M}_{\nu_2\alpha}\, \mathsf{F}_{\mathcal{G}}[\alpha] \right\}[n]\Big|_{n=-q-1}, \tag{3.74}$$

where $\mathcal{G}$ is the graph of $\{(\mathsf{M}-\mathsf{I})_{\mu\nu}\}$, ℓ is the length of the simple path, and

$$\mathsf{F}_{\mathcal{G}}[\alpha] = \Big[\mathsf{I} - \sum_{\Gamma_{\mathcal{G};\alpha}} \mathsf{M}_{\alpha\mu_m} \mathsf{F}_{\mathcal{G}\setminus\{\alpha,\ldots,\mu_{m-1}\}}[\mu_m] \cdots \mathsf{F}_{\mathcal{G}\setminus\{\alpha\}}[\mu_2] \mathsf{M}_{\mu_2\alpha} \Big]^{-1}, \tag{3.75}$$

with m the length of the simple cycle. The quantity $\mathsf{F}_{\mathcal{G}}[\alpha]$ can itself be seen as an effective weight associated to vertex α resulting from the dressing of α by all the closed walks off α in $\mathcal{G}$. Since a loop is a simple cycle, the dressing of the vertices by their loops is included in $\mathsf{F}_{\mathcal{G}}[\alpha]$ as well. This is obvious if one considers a graph $\mathcal{G}$ that is reduced to a unique vertex α presenting a loop. In that case Eq. (3.75) yields $\mathsf{F}_{\alpha}[\alpha] = [\mathsf{I}z^{-1} - \mathsf{M}_{\alpha}]^{-1} \equiv \mathrm{W}_{\alpha}^{\mathrm{eff}}$. For convenience we can make the loop dressing completely explicit in Eq. (3.75) by separating the loops from the other simple cycles

$$\mathsf{F}_{\mathcal{G}}[\alpha] = \Big[\mathsf{I}z^{-1} - \mathsf{M}_{\alpha} - \sum_{\Gamma_{\mathcal{G}_0;\alpha}} \mathsf{M}_{\alpha\mu_m} \mathsf{F}_{\mathcal{G}\setminus\{\alpha,\ldots,\mu_{m-1}\}}[\mu_m] \cdots \mathsf{F}_{\mathcal{G}\setminus\{\alpha\}}[\mu_2] \mathsf{M}_{\mu_2\alpha} \Big]^{-1}, \tag{3.76}$$

and note that now the sum runs over the simple cycles of the loopless graph $\mathcal{G}_0$. Together with Eq. (3.74) the above Eq. (3.76) constitute the expressions presented in Theorem 3.3.1.

Now we prove that Eqs. (3.74, 3.76) yield M^q for any matrix by analytic continuation. First, for any finite-size matrix Eqs. (3.74, 3.76) present only a finite number of terms and must therefore converge, regardless of $\rho(\mathsf{M}-\mathsf{I})$. Second, Eqs. (3.74, 3.76) agree with the power-series Eq. (3.65) when it exists, i.e. when $\rho(\mathsf{M}-\mathsf{I}) < 1$. Third, the function M^q and the expressions Eqs. (3.74, 3.76) are analytic. It follows that Eqs. (3.74, 3.76) constitute the unique analytic continuation of the power-series of M^q. This proves Theorem 3.3.1. □

3.5.3 The matrix inverse

Proof. We consider an invertible matrix $\mathsf{M} \in \mathbb{C}^{D\times D}$. To prove Theorem 3.3.2 we write the matrix inverse as $\mathsf{M}^{-1} = \sum_{n=0}^{\infty} (\mathsf{I}-\mathsf{M})^n$. Note that the sum only converges

when the spectral radius $\rho(\mathsf{M}-\mathsf{I})<1$; nevertheless, the result of Theorem 3.3.2 is valid for matrices of arbitrary spectral radius by analytic continuation, see §3.5.2 above, we omit the details. Introducing an auxiliary matrix $\bar{\mathsf{M}}\equiv\mathsf{I}-\mathsf{M}$, we apply the result of Eq. (3.5) to the power series to obtain

$$\left(\mathsf{M}^{-1}\right)_{\omega\alpha}=\sum_{n=0}^{\infty}\sum_{W_{\mathcal{G};\alpha\omega;n}}\bar{\mathsf{M}}_{\omega\eta_n}\cdots\bar{\mathsf{M}}_{\eta_3\eta_2}\bar{\mathsf{M}}_{\eta_2\alpha}. \tag{3.77}$$

where $\mathcal{G}$ is the graph of the partition of $\bar{\mathsf{M}}$. We follow the same procedure as in §3.5.2 above and we omit the details; the result is

$$\left(\mathsf{M}^{-1}\right)_{\omega\alpha}=\sum_{n=0}^{\infty}\sum_{W_{\mathcal{G}_0;\alpha\omega;n}}\left[\mathsf{I}-\bar{\mathsf{M}}_{\omega}\right]^{-1}\bar{\mathsf{M}}_{\omega\nu_n}\cdots\left[\mathsf{I}-\bar{\mathsf{M}}_{\nu_2}\right]^{-1}\bar{\mathsf{M}}_{\nu_2\alpha}\left[\mathsf{I}-\bar{\mathsf{M}}_{\alpha}\right]^{-1}, \tag{3.78a}$$

$$=\sum_{n=0}^{\infty}\sum_{W_{\mathcal{G}_0;\alpha\omega;n}}(-1)^n\,\mathsf{M}_{\omega}^{-1}\,\mathsf{M}_{\omega\nu_n}\cdots\mathsf{M}_{\nu_2}^{-1}\,\mathsf{M}_{\nu_2\alpha}\,\mathsf{M}_{\alpha}^{-1}, \tag{3.78b}$$

where we have used $\bar{\mathsf{M}}_{\mu}=\mathsf{I}-\mathsf{M}_{\mu}$ and $\bar{\mathsf{M}}_{\mu\nu}=-\mathsf{M}_{\mu\nu}$. Eq. (3.78b) is a sum of walk contributions with effective vertex weights $\mathrm{W}_{\mu}^{\mathrm{eff}}=\mathsf{M}_{\mu}^{-1}$ resulting from the loop dressing of μ which occurs when $\mathsf{M}_{\mu}\neq 0$. We now use Theorem 2.3.4 and obtain

$$\left(\mathsf{M}^{-1}\right)_{\omega\alpha}=\sum_{\Pi_{\mathcal{G}_0;\alpha\omega}}(-1)^{\ell}\,\mathsf{F}_{\mathcal{G}\setminus\{\alpha,\ldots,\nu_\ell\}}[\omega]\mathsf{M}_{\omega\nu_\ell}\cdots\mathsf{F}_{\mathcal{G}\setminus\{\alpha\}}[\nu_2]\,\mathsf{M}_{\nu_2\alpha}\,\mathsf{F}_{\mathcal{G}}[\alpha], \tag{3.79a}$$

where $\mathcal{G}$ is the graph of $\{(\mathsf{M}-\mathsf{I})_{\mu\nu}\}$, ℓ is the length of the simple path, and

$$\mathsf{F}_{\mathcal{G}}[\alpha]=\Big[\mathsf{M}_{\alpha}-\sum_{\Gamma_{\mathcal{G}_0;\alpha}}(-1)^m\,\mathsf{M}_{\alpha\mu_m}\mathsf{F}_{\mathcal{G}\setminus\{\alpha,\ldots,\mu_{m-1}\}}[\mu_m]\cdots\mathsf{F}_{\mathcal{G}\setminus\{\alpha\}}[\mu_2]\mathsf{M}_{\mu_2\alpha}\Big]^{-1}, \tag{3.79b}$$

with m the length of the simple cycle. Similarly to §3.5.2, we have separated the contribution of the loops from that of the other simple cycles. This proves Theorem 3.3.2. □

3.5.4 The matrix exponential

Proof. We consider a matrix $\mathsf{M}\in\mathbb{C}^{D\times D}$. To prove Theorem 3.3.3 and Lemma 3.3.1, we start from the power series expression $\exp(t\,\mathsf{M})=\sum_{n=0}^{\infty}t^n\mathsf{M}^n/n!$. By applying the result of Eq. (3.5) to this series we find that the partition of $\exp(t\,\mathsf{M})$ is given by

$$\exp(t\,\mathsf{M})_{\omega\alpha}=\sum_{n=0}^{\infty}\frac{t^n}{n!}\sum_{W_{\mathcal{G};\alpha\omega;n}}\mathsf{M}_{\omega\eta_n}\cdots\mathsf{M}_{\eta_3\eta_2}\mathsf{M}_{\eta_2\alpha}. \tag{3.80}$$

with $\mathcal{G}$ the graph of the partition of M. Following the same procedure as in §3.5.2, we make the loop of the walks appear explicitly

$$\exp(t\,\mathsf{M})_{\omega\alpha} = \sum_{n=0}^{\infty} \frac{t^n}{n!} \sum_{m=0}^{n} \sum_{W_{\mathcal{G}_0;\alpha\omega;m}} \sum_{\{p_i\}\vdash n-m} (\mathsf{M}_\omega)^{p_{m+1}} \mathsf{M}_{\omega\mu_m} \cdots (\mathsf{M}_{\mu_2})^{p_2} \mathsf{M}_{\mu_2\alpha} (\mathsf{M}_\alpha)^{p_1}, \quad (3.81)$$

where the again loop numbers satisfy $\sum_{i=1}^{m+1} p_i = n - m$, with the restriction that the loop numbers on any loopless vertices are fixed to zero. Such a sequence is said to form a weak composition of $n - m$. We now note that for any weak composition of $n - m$, the following identity holds:

$$\frac{1}{p_1!\,p_2!\cdots p_{m+1}!} \int_0^t \mathrm{d}t_m \cdots \int_0^{t_2} \mathrm{d}t_1\, (t - t_m)^{p_{m+1}} \cdots (t_2 - t_1)^{p_2}\, t_1^{p_1} = \frac{t^n}{n!}. \quad (3.82)$$

This result – which does not depend on the value of each individual p_i – is straightforwardly proved by induction on m. By substituting this identity into Eq. (3.81) and rearranging the order of summations we obtain

$$\exp\big(t\,\mathsf{M}\big)_{\omega\alpha} = \quad (3.83a)$$

$$\sum_{m=0}^{\infty} \sum_{W_{\mathcal{G}_0;\alpha\omega;m}} \sum_{\{p_i\}=0}^{\infty} \int_0^t \mathrm{d}t_m \cdots \int_0^{t_2} \mathrm{d}t_1 \frac{\big[(t - t_m)\mathsf{M}_\omega\big]^{p_{m+1}}}{p_{m+1}!}\, \mathsf{M}_{\omega\mu_m} \cdots \frac{\big[(t_2 - t_1)\mathsf{M}_{\mu_2}\big]^{p_2}}{p_2!}\, \mathsf{M}_{\mu_2\alpha} \frac{\big[t_1\mathsf{M}_\alpha\big]^{p_1}}{p_1!},$$

$$= \sum_{m=0}^{\infty} \sum_{W_{\mathcal{G}_0;\alpha\omega;m}} \int_0^t \mathrm{d}t_m \cdots \int_0^{t_2} \mathrm{d}t_1\, \mathrm{e}^{(t-t_m)\mathsf{M}_\omega} \mathsf{M}_{\omega\mu_m} \cdots \mathrm{e}^{(t_2-t_1)\mathsf{M}_{\mu_2}}\, \mathsf{M}_{\mu_2\alpha}\, \mathrm{e}^{t_1\mathsf{M}_\alpha}. \quad (3.83b)$$

This intermediate result proves Lemma 3.3.1. In order to continue, we note that this expression is an m-fold nested convolution. To convert the convolution to a product we take the Laplace transform of both sides:

$$\mathcal{L}\big[\exp(t\,\mathsf{M})_{\omega\alpha}\big] = \sum_{m=0}^{\infty} \sum_{W_{\mathcal{G}_0;\alpha\omega;m}} \mathcal{L}\big[f_\omega(t)\big]\, \mathsf{M}_{\omega\mu_m} \cdots \mathcal{L}\big[f_{\mu_2}(t)\big]\, \mathsf{M}_{\mu_2\alpha}\, \mathcal{L}\big[f_\alpha(t)\big], \quad (3.84)$$

$$= \sum_{m=0}^{\infty} \sum_{W_{\mathcal{G}_0;\alpha\omega;m}} [s\mathsf{I} - \mathsf{M}_\omega]^{-1}\, \mathsf{M}_{\omega\mu_m} \cdots [s\mathsf{I} - \mathsf{M}_{\mu_2}]^{-1}\, \mathsf{M}_{\mu_2\alpha}\, [s\mathsf{I} - \mathsf{M}_\alpha]^{-1}, \quad (3.85)$$

where the second line follows on noting the result $\mathcal{L}\big[\exp(t\mathsf{M}_\mu)\big] = \big[s\mathsf{I} - \mathsf{M}_\mu\big]^{-1}$. As in the previous sections, we remark that Eq. (3.85) is a sum of walk contributions with an effective vertex weight of $\mathrm{W}_\mu^{\mathrm{eff}} = [s\mathsf{I} - \mathsf{M}_\mu]^{-1}$. On using Theorem 2.3.4 to

turn Eq. (3.85) into a path-sum, we obtain

$$\mathcal{L}\big[\exp\big(t\,\mathsf{M}\big)_{\omega\alpha}\big] = \sum_{\ell=0}^{\ell_{\max}} \sum_{\Pi_{\mathcal{G}_0;\alpha\omega;\ell}} \mathsf{F}_{\mathcal{G}\setminus\{\alpha,\ldots,\nu_\ell\}}[\omega]\,\mathsf{M}_{\omega\nu_\ell}\cdots\mathsf{F}_{\mathcal{G}\setminus\{\alpha\}}[\nu_2]\,\mathsf{M}_{\nu_2\alpha}\,\mathsf{F}_{\mathcal{G}}[\alpha]\,, \tag{3.86a}$$

$$\mathsf{F}_{\mathcal{G}}[\alpha] = \Big[s\mathsf{I} - \mathsf{M}_\alpha - \sum_{\Gamma_{\mathcal{G}_0;\alpha}} \mathsf{M}_{\alpha\mu_m}\mathsf{F}_{\mathcal{G}\setminus\{\alpha,\ldots,\mu_{m-1}\}}[\mu_m]\cdots\mathsf{F}_{\mathcal{G}\setminus\{\alpha\}}[\mu_2]\mathsf{M}_{\mu_2\alpha}\Big]^{-1}, \tag{3.86b}$$

where ℓ and m are the length of the simple path and of the simple cycle, respectively. In this expression, the contribution from the loops is explicitly separated from that of the other simple cycles. □

3.5.5 The matrix logarithm

Proof. In this section, we consider a matrix $\mathsf{M} \in \mathbb{C}^{D\times D}$ with no eigenvalue on the negative real axis. To prove Theorem 3.3.4 we write the matrix logarithm as $\log\mathsf{M} = -\sum_{n=1}^{\infty}(\mathsf{I}-\mathsf{M})^n/n$. This series only converges when the spectral radius $\rho(\mathsf{M}-\mathsf{I}) < 1$; nevertheless, the result of Theorem 3.3.4 is valid for matrices of arbitrary spectral radius by analytic continuation. We introduce the auxiliary matrix $\bar{\mathsf{M}} \equiv \mathsf{I} - \mathsf{M}$ and rewrite the power series as

$$\big(\log\mathsf{M}\big)_{\omega\alpha} = -\sum_{n=1}^{\infty}\frac{1}{n}\sum_{W_{\mathcal{G}_0;\alpha\omega;n}} \bar{\mathsf{M}}_{\omega\nu_n}\cdots\bar{\mathsf{M}}_{\nu_3\nu_2}\bar{\mathsf{M}}_{\nu_2\alpha}, \tag{3.87a}$$

$$= -\sum_{n=1}^{\infty}\frac{1}{n}\sum_{m=0}^{n}\sum_{W_{\mathcal{G}_0;\alpha\omega;m}}\sum_{\{p_i\}\vdash n-m}\big(\bar{\mathsf{M}}_\omega\big)^{p_{m+1}}\bar{\mathsf{M}}_{\omega\mu_m}\cdots\big(\bar{\mathsf{M}}_{\mu_2}\big)^{p_2}\bar{\mathsf{M}}_{\mu_2\alpha}\big(\bar{\mathsf{M}}_\alpha\big)^{p_1}, \tag{3.87b}$$

with $\mathcal{G}$ the graph of the partition of $\bar{\mathsf{M}}$. The second equality is obtained by making the loops explicit through the same procedure as in §3.5.2. Just as in the previous sections, the loop numbers form a weak composition of $n-m$. For any such composition, the following identity holds:

$$\frac{1}{n} = \int_0^1 x^{m-1}\,x^{p_1}x^{p_2}\,\cdots\,x^{p_{m+1}}\,\mathrm{d}x. \tag{3.88}$$

This identity allows the contributions from the infinite loop sums in Eq. (3.87b) to be evaluated in closed form. By restructuring the double summation we obtain

$$\big(\log\mathsf{M}\big)_{\omega\alpha} = -\delta_{\omega\alpha}\int_0^1 \bar{\mathsf{M}}_\alpha\left[\mathsf{I}-x\bar{\mathsf{M}}_\alpha\right]^{-1}\mathrm{d}x \tag{3.89}$$

$$-\sum_{m=1}^{\infty}\sum_{W_{\mathcal{G}_0;\alpha\omega;m}}\int_0^1 x^{m-1}\left[\mathsf{I}-x\bar{\mathsf{M}}_\omega\right]^{-1}\bar{\mathsf{M}}_{\omega\mu_m}\cdots\left[\mathsf{I}-x\bar{\mathsf{M}}_{\mu_2}\right]^{-1}\bar{\mathsf{M}}_{\mu_2\alpha}\left[\mathsf{I}-x\bar{\mathsf{M}}_\alpha\right]^{-1}\mathrm{d}x,$$

where we have written $\big[\mathsf{I} - x\bar{\mathsf{M}}_\mu\big]^{-1}$ for $\sum_{p=0}^{\infty}(x\bar{\mathsf{M}}_\mu)^p$ and $\delta_{\omega\alpha}$ is a Kronecker delta. Note that the first part of this expression – which represents contributions from walks consisting entirely of loops – has a slightly different structure than the second part, owing to the absence of the term with zero loops when $\omega = \alpha$. Just as for the previously obtained matrix functions, the integrand of Eq. (3.89) is a sum of walk contributions with effective vertex weights $\mathrm{W}_\mu^{\mathrm{eff}} = \big[\mathsf{I} - x\bar{\mathsf{M}}_\mu\big]^{-1}$. On using the path-sum formula, Theorem 2.3.4, Eq. (3.89) transforms to

$$\big(\log \mathsf{M}\big)_{\omega\alpha} = \tag{3.90a}$$
$$\begin{cases} \displaystyle\int_0^1 \mathrm{d}x\; x^{-1}\,\big(\mathsf{I} - \mathsf{F}_{\mathcal{G}}[\alpha]\big)\,, & \omega = \alpha, \\ \displaystyle -\sum_{\Pi_{\mathcal{G}_0;\alpha\omega}} \int_0^1 \mathrm{d}x\; x^{\ell-1}\,\mathsf{F}_{\mathcal{G}\setminus\{\alpha,\ldots,\nu_\ell\}}[\omega]\bar{\mathsf{M}}_{\omega\nu_\ell}\cdots\mathsf{F}_{\mathcal{G}\setminus\{\alpha\}}[\nu_2]\,\bar{\mathsf{M}}_{\nu_2\alpha}\,\mathsf{F}_{\mathcal{G}}[\alpha], & \omega \neq \alpha, \end{cases}$$

where ℓ the length of the simple path and

$$\mathsf{F}_{\mathcal{G}}[\alpha] = \Big[\mathsf{I} - x\bar{\mathsf{M}}_\alpha - \sum_{\Gamma_{\mathcal{G}_0;\alpha}} x^m\,\bar{\mathsf{M}}_{\alpha\mu_m}\mathsf{F}_{\mathcal{G}\setminus\{\alpha,\ldots,\mu_{m-1}\}}[\mu_m]\;\cdots\;\bar{\mathsf{M}}_{\mu_3\mu_2}\mathsf{F}_{\mathcal{G}\setminus\{\alpha\}}[\mu_2]\bar{\mathsf{M}}_{\mu_2\alpha}\Big]^{-1}, \tag{3.90b}$$

with m the length of the simple cycle. Note that we have again explicitly separated the contribution of the loops from that of the other simple cycles. Theorem 3.3.4 is now directly obtained upon replacing $\bar{\mathsf{M}}$ by $\mathsf{I} - \mathsf{M}$. □

3.6 Summary and Outlook

The method of path-sums is based on three main concepts: firstly, the partitioning of a discrete matrix M into an ensemble of submatrices whose dimensionalities can be freely chosen; secondly, the mapping between multiplication of M and walks on a graph $\mathcal{G}$ whose edge pattern encodes the structure of M; and thirdly, the exact closed-form resummation of certain classes of walks on $\mathcal{G}$ through the dressing of vertices by cycles. By combining these concepts, any partition of a function of a finite matrix $f\big(\mathsf{M}\big)$ – whose entries do not necessarily have to commute with one another – can be exactly evaluated in a finite number of steps, provided the required inverse transforms are analytically available.

Using a directed graph to encode the structure of a matrix allows any structure and symmetries that the matrix possesses to be easily recognized and exploited. We thus expect the method of path-sums to have widespread applications in, for example, the study of Markov chains and quantum many-body physics, where the relevant matrix – the many-body Hamiltonian – is both sparse and highly structured. In Chapters 4 and 5 we present applications of the method to the study of quantum dynamics.

A major issue which we have not addressed so far is that of the truncation of a path-sum. On highly connected graphs the number of simple paths and simple

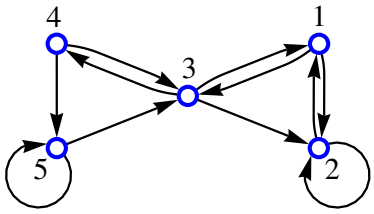

Figure 3.3: Graph used to illustrate path-sum truncations.

cycles can be very large, so that an exact evaluation of the flips and statics of $f(\mathsf{M})$ may have a prohibitive computational cost. Additionally, for most applications requiring the computation of a function of a matrix, an inexact but accurate result is sufficient, in particular if the matrix M itself is known only with a finite precision. In such cases, it is desirable to truncate the exact expressions given in the Theorems of §3.3, e.g. by dressing vertices to a depth smaller than their exact dressing depth or by neglecting certain simple paths. This may also be motivated by considerations external to the method: in quantum mechanics, simple paths and cycles on the graph of the Hamiltonian represent physical processes (similarly to Feynman diagrams, see Chapter 4) some of which might be negligible. The accuracy of truncated numerical approximations to the path-sum will thus be of paramount importance in many applications. Consequently, we discuss below a few preliminary results we have established on this subject.

The first step in understanding truncated path-sums is to clarify what we mean by *truncation*. Indeed, as indicated above, there are many ways one can truncate a path-sum. We begin by showing that there exists 3 non-equivalent types of truncations.

Truncation types

Consider a path-sum expression for a common matrix function, e.g. the walk-generating function off vertex 1 on the graph depicted on Fig. (3.3),

$$g_{\mathcal{G};11}(z) = \frac{1}{1-\frac{z^2}{1-z}-\frac{z^2}{1-z^2-\frac{z^3}{1-z}}-\frac{z^3}{(1-z)\left(1-z^2-\frac{z^3}{1-z}\right)}}. \tag{3.91}$$

Truncating this expression by removing one or more terms can be done in a large number of ways, each of which yields a different approximation to $g_{\mathcal{G};11}(z)$. Let $g^{\mathfrak{T}}_{\mathcal{G};11}(z)$ be one such truncation of $g_{\mathcal{G};11}(z)$. We define $\mathcal{E}$ and $\mathcal{E}_{\mathfrak{T}}$ the sets of all edges traversed by the simple paths and simple cycles contributing to $g_{\mathcal{G};11}(z)$ and $g^{\mathfrak{T}}_{\mathcal{G};11}(z)$, respectively. Finally we define the symmetric difference $\bar{\mathcal{E}}_{\mathfrak{T}} = \mathcal{E} \ominus \mathcal{E}_{\mathfrak{T}}$ which is the set of edges that have been removed from $\mathcal{E}$ by the truncation. Then the truncation $g^{\mathfrak{T}}_{\mathcal{G};11}(z)$ falls into one of three categories:

i) $\bar{\mathcal{E}}_{\mathfrak{T}} \cap \mathcal{E}_{\mathfrak{T}} = \emptyset$, that is the simple paths/cycles neglected from $g_{11}(z)$ in the truncation traverse edges that are not traversed by any of the simple paths/cycles

retained in the truncation. This is for example the case of the truncation

$$g^{\mathfrak{T}}_{\mathcal{G};11}(z) = \frac{1}{1-\frac{z^2}{1-z^2-\frac{z^3}{1-z}}}, \tag{3.92}$$

which is the exact walk generating function of the graph:

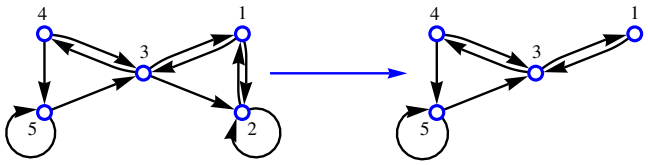

Truncation of type i.

Truncations of this type simply correspond to removing edges from the graph. This can cause the graph to become disconnected, in which case the truncated walk generating functions correspond to a graph with less vertices than are present in the initial graph. Consequently $g^{\mathfrak{T}}_{\mathcal{G}}(z)$ will be a ratio of polynomials of smaller degree than those entering $g_{\mathcal{G}}(z)$.

ii) $\bar{\mathcal{E}}_{\mathfrak{T}} \cap \mathcal{E}_{\mathfrak{T}} = \bar{\mathcal{E}}_{\mathfrak{T}}$, that is all the edges traversed by the simple paths/cycles neglected in the truncation are also traversed by simple paths/cycles that have been retained in the truncation. To clarify this, consider the following example:

$$g^{\mathfrak{T}}_{\mathcal{G};11}(z) = \frac{1}{1-\frac{z^2}{1-\mathbf{z}}-\frac{z^2}{1-z^2-\frac{z^3}{1-z}}-\frac{z^3}{(1-\mathbf{0}\times\mathbf{z})\left(1-z^2-\frac{z^3}{1-z}\right)}}. \tag{3.93}$$

which corresponds to neglecting the loop off vertex 2 when dressing vertex 2 in the triangle (1321) while taking it into account when dressing vertex 2 in the back-track (121). The truncated $g^{\mathfrak{T}}_{\mathcal{G};11}(z)$ is the exact walk-generating function of the graph:

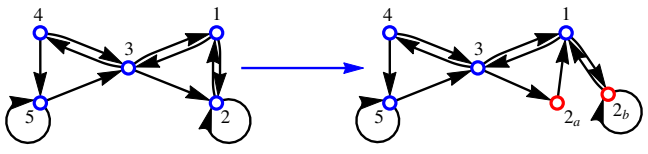

Truncation of type ii.

On this graph the loop off vertex 2 is indeed only present when going through the back-track (12_b1) and not the triangle (132_a1). In the general case such truncations correspond to graphs with more vertices than are present in the initial graph. This has a surprising consequence: the approximation $g^{\mathfrak{T}}_{\mathcal{G}}(z)$ will be of higher degree than the rational function $g_{\mathcal{G}}(z)$ it approximates.

iii) $\bar{\mathcal{E}}_{\mathfrak{T}} \cap \mathcal{E}_{\mathfrak{T}} \neq \emptyset$ and $\bar{\mathcal{E}}_{\mathfrak{T}} \cap \mathcal{E}_{\mathfrak{T}} \neq \bar{\mathcal{E}}_{\mathfrak{T}}$, i.e. the truncation is a mixture of the above two types of truncations. The degree $g^{\mathfrak{T}}_{\mathcal{G}}(z)$ can be higher or lower than that of $g_{\mathcal{G}}(z)$.

This brief analysis applies generally to any truncation of a path-sum and thus shows that truncating path-sums is not simple: in particular it does not necessarily corresponds to zeroing out elements of the matrix M whose function $f(\mathsf{M})$ is being calculated.

Remark 3.6.1 (Simulating non-Markovian dynamics)**.** Truncations of type ii) could perhaps be used to simulate non-Markovian behaviors in physical systems. Indeed, such truncations correspond to neglecting edges depending on their context (i.e. inside of which simple path/cycle is a vertex being dressed). In Chapter 4 we show that in the context of quantum dynamics, each edge of the graph representing the configurations available to a physical system correspond to a physical process provoking a change in the state of the system. Then walks, simple paths and simple cycles represent succession of physical processes occurring in the system, i.e. its histories. In this picture, truncations of type ii) are equivalent to certain physical processes taking place or not depending on the previous history of the system, something characteristically non-Markovian.

Behavior of truncated path-sums

The question of the quality of the approximation obtained by truncating a path-sum remains largely open. A naive approach to this question based on evaluating the number of walks taken into account in a truncated path-sum encounters a variety of problems: i) the number of walks taken into account and neglected are both typically infinite; and ii) the weights of the walks might play a dominant role.

A more promising alternative consists of constraining the weight of fully dressed simple paths and simple cycles based on their length. In the region of convergence of the power-series representation of $f(\mathsf{M})$ this is straightforward. To see this, consider the power-series expansion $f(z) = \sum_n f_n z^n$ with convergence radius ρ_f. Let $\mathsf{M} \in \mathbb{C}^{D\times D}$, $\{\mathsf{M}_{\alpha\omega}\}$ a partition of M with graph $\mathcal{G}$ and define $m = \max_{\alpha,\omega} \|\mathsf{M}_{\alpha\omega}\|$. Clearly the weight $\mathrm{W}[p]$ of a fully dressed prime $p \in \Pi_{\mathcal{G}} \cup \Gamma_{\mathcal{G}}$ of length $\ell(p)$ and with end points μ, ν in the path-sum expression of $f(\mathsf{M})$ is upper bounded by the total weight carried by all the walks with end points μ, ν and of length greater than or equal to $\ell(p)$, i.e.

$$\mathrm{W}[p] \leq \sum_{n\geq \ell(p)} |W_{\mathcal{G};\mu\nu}|(n) f_n m^n, \tag{3.94}$$

where we assumed existence of the power-series. This holds as long as $m \times b < \rho_f$ with b the maximum eigenvalue of the largest connected component of $\mathcal{G}$ containing vertices μ and ν.

The result of Eq. (3.94) works well for entire functions, predicting for example a super exponential decay of $\mathrm{W}[p]$ as a function of $\ell(p)$ for $f(z) = e^z$ on path-graphs

[6]. This approach fails however for many functions of interest, e.g. $\log(z)$, z^q etc., for which the region of convergence of the power-series representation of $f(\mathsf{M})$ is finite. In such situations it may be possible to establish the decay of fully dressed primes from more general arguments. Recent research [80, 81, 82, 83] showed that the entries $f\big(\mathsf{M}\big)_{ij}$ of certain matrix functions decay exponentially with the length of the shortest simple path between the vertices that correspond to entries M_{ii} and M_{jj}. Furthermore, Prof. Benzi and coworkers have recently extended these results to the norm of the statics and flips of any tensor-partition of $f\big(\mathsf{M}\big)$ [84]. We are convinced that these results are related with the weight of individual prime walks, such as is the case for entire functions. For matrices which are deterministically known, the demonstration of such a link has resisted our attempts so far. For random matrices however, the results of Chapter 5 establish that on average the weight of a fully dressed simple path decays exponentially with its length. In turn this implies that on average, matrix functions are exponentially localised.

[6]This result is closely related to the decay away from the diagonal of $\exp(\mathsf{M})$ with M tridiagonal, established by [79].

Chapter 4
Quantum Dynamics

With application to quantum mechanics, path integrals suffer most grievously from a serious defect. They do not permit a discussion of spin operators or other such operators in a simple and lucid way.

R. P. Feynman

In this chapter we study the real-time dynamics of quantum systems using the method of walk-sums, a weaker form of path-sum and which is equivalent to the walk-sum Lemma 3.3.1 for the matrix exponential. In this chapter however, we derive the method of walk-sums relying solely on physical arguments. As we shall see, these draw a picture of quantum dynamics that is very similar to that underpinning Feynman's path integral approach.

This chapter is organised as follows. In section 4.1 we present two physically motivated derivations of Lemma 3.3.1. In particular we demonstrate that the Lemma describes the dynamic of quantum systems via a sum over histories, a discrete analogue to Feynman path-integrals. We give explicit formulas to calculate physical quantities of interest in the walk-sum formalism, such as expectation values and conditional expectation values. In section 4.2, we illustrate walk-sum by determining analytically the dynamics of continuous time quantum random walks. Our results remain valid for non-Abelian walks, where the internal and external dynamics of the 'walking' particle are coupled. Finally, in section 4.3 we investigate the dynamics of systems of strongly interacting Rydberg-excited Mott insulators using the method of walk-sums. The work in this chapter forms the basis of two articles that are currently under revision.

4.1 Walk-sum: a physical derivation

We consider a quantum many-body system $\mathbb{S}$ to be comprised of two parts S and S'. The physical approach to the walk-sum Lemma is based on the following observation: If S' is a large set of constituents whose dynamics is frozen, then all interactions between S and S' can be evaluated exactly and the evolution of S is described by a small effective Hamiltonian. Walk-sum expresses the true many-body dynamics in terms of such simple situations with a frozen S' and a few evolving constituents S. This approach might seem similar in essence to mean field theory where an atom of interest interacts with a field resulting from the mean behaviour of all other particles. The difference is that here we make the mapping from many-body to few-body dynamics exact, that is we make S interact with all possible fields it could be subjected to depending on the configuration of S'.

In practice, the walk-sum method divides the matrix representing the time evolution operator of a finite-dimensional quantum system into small pieces. These pieces are called conditional evolution operators and are introduced in section 4.1.1, where we describe the general approach of the method. In section 4.1.2 we derive an equation that allows one to calculate any conditional evolution operator and therefore any desired piece of the full evolution operator. We then show in section 4.1.3 that the generation of conditional evolution operators can be represented by walks on a graph. This facilitates the evaluation of the walk-sum expression. In section 4.1.4 we give the expression of the conditional evolution operators in the Laplace domain. Finally, we demonstrate how the method allows one to evaluate expectation values and conditional expectation values in §4.1.5.

4.1.1 Model system and general approach

We consider a quantum many-body system $\mathbb{S}$ that is described by a time-independent Hamiltonian H and comprised of N physical constituents. The state space of the kth constituent is spanned by d_k internal levels, where d_k can be different for every k. Let $\{|i_k\rangle\}$ be an orthonormal basis of length d_k associated with constituent k, and $\mathsf{P}_{k,i} = |i_k\rangle\langle i_k|$ be the projector onto state $|i_k\rangle$. Next we split the system $\mathbb{S}$ into two parts S and S'. Here constituent s is taken to be S, and all remaining constituents are grouped in S'. Note that constituent s can be comprised of one or several physical particles. We define so-called projector-lattices

$$\varepsilon_\mu = \otimes_{k\in S'}\mathsf{P}_{k,i_k} \otimes \mathsf{I}_s = \overbrace{|\mu\rangle\langle\mu|}^{\text{Acts on } S'} \otimes \overbrace{\mathsf{I}_s}^{\text{Acts on } S} \tag{4.1}$$

that are projection operators in the state space of the full system $\mathbb{S}$. The index μ is a short-hand notation for the configuration onto which S' is projected and I_s is the identity operator on S. There is a total of $\prod_{k\neq s}^{N} d_k$ different projector-lattices corresponding to all possible combinations of projectors P_{k,i_k}. Projector-lattices are themselves orthogonal projectors and the ensemble of all possible projector-lattices is closed,

$$\varepsilon_\nu\varepsilon_\mu = \delta_{\nu,\mu}\,\varepsilon_\nu, \quad \sum_\nu \varepsilon_\nu = \mathsf{I}, \tag{4.2}$$

where I is the identity operator on the state-space of the whole many-body system $\mathbb{S}$. Next we partition the time evolution operator $\mathsf{U} = \exp[-\mathrm{i}\mathsf{H}t]$ (from now on we set $\hbar = 1$) into submatrices with projector lattices,

$$\varepsilon_\nu\mathsf{U}(t)\varepsilon_\mu = \otimes_{k\in S'}\mathsf{T}_{k,i_k\leftarrow j_k} \otimes \mathsf{U}_{\nu\leftarrow\mu}(t) = \underbrace{|\nu\rangle\langle\mu|}_{\text{Acts on } S'} \otimes \underbrace{\mathsf{U}_{\nu\leftarrow\mu}(t)}_{\text{Acts on } S}. \tag{4.3}$$

Here $\mathsf{T}_{k,i\leftarrow j} = |i_k\rangle\langle j_k|$ denotes a transition operator in subsystem k, and $\mathsf{U}_{\nu\leftarrow\mu}(t)$ is a so-called conditional evolution operator that is represented by a (small) $d_s \times d_s$

matrix. $\mathsf{U}_{\nu\leftarrow\mu}(t)$ generates the time evolution of subsystem S provided that (i) the remaining many-body system S' was initially in configuration $|\mu\rangle$, and (ii) the state of S' at time t is given by $|\nu\rangle$. The closure relation in Eq. (4.2) implies that the full time evolution operator $\mathsf{U}(t)$ can be represented in terms of conditional evolution operators,

$$\mathsf{U}(t) = \sum_{\nu,\,\mu} \Big\{ \underbrace{|\nu\rangle\langle\mu|}_{\text{Acts on } S'} \otimes \underbrace{\mathsf{U}_{\nu\leftarrow\mu}(t)}_{\text{Acts on } S} \Big\}. \tag{4.4}$$

In the language of Chapter 3, the ensemble $\{\mathsf{U}_{\nu\leftarrow\mu}(t)\}$ forms a tensor product partition of $\mathsf{U}(t)$. The method of walk-sums allows one to compute conditional evolution operators efficiently, i.e. in a number of operations scaling polynomially in the number of involved particles, and independently of one another. If in a particular physical problem only a small subset of all possible configurations of S' is relevant, then our approach allows one to approximate the full time evolution with a moderate computational effort.

4.1.2 Derivation of the conditional evolution operators

In this section we derive an explicit expression for conditional evolution operators using two different approaches: the first emphasises their interpretations in terms of histories of the system and the second, simpler, relies on existing results from perturbation theory.

Conditional evolution operators as superpositions of histories

We begin with writing the time evolution operator $\mathsf{U}(t)$ of the complete system $\mathbb{S}$ as a succession of infinitesimal time evolutions

$$\mathsf{U}(t) = \exp[-\mathrm{i}\mathsf{H}t] = \lim_{\delta t\to 0} \prod_{n=1}^{M} \delta\mathsf{U} = \lim_{\delta t\to 0} \prod_{n=1}^{M} \Big\{ \sum_{\alpha} \varepsilon_\alpha\, \delta\mathsf{U} \Big\}, \tag{4.5}$$

where $\delta\mathsf{U} = \mathsf{I} - \mathrm{i}\mathsf{H}\delta t$ is the infinitesimal evolution operator from $(n-1)\delta t$ to $n\delta t$ and $M = t/\delta t$. In the last step in Eq. (4.5) we inserted the closure relation for projector lattices [see Eq. (4.2)]. In the following, we derive explicit expressions for the conditional time evolution operators $\mathsf{U}_{\nu\leftarrow\mu}(t)$ by a re-summation of terms arising in $\varepsilon_\nu \mathsf{U}(t)\varepsilon_\mu$. Let us first focus on $\varepsilon_\nu\mathsf{U}(t)\varepsilon_\nu$, and in particular the term where all intermediate projector lattices ε_α in Eq. (4.5) are all equal to ε_ν,

$$\mathcal{U}_\nu^{(0)} = \varepsilon_\nu \prod_{n=1}^{M} \{\varepsilon_\nu\, \delta\mathsf{U}\}\varepsilon_\nu = \varepsilon_\nu\, \delta\mathsf{U}\, \varepsilon_\nu\, \delta\mathsf{U} \ldots \varepsilon_\nu\, \delta\mathsf{U}\varepsilon_\nu. \tag{4.6}$$

The physical meaning of this term is the following. First S' is projected into configuration ν, then $\delta\mathsf{U}$ evolves the full system $\mathbb{S}$ from 0 to δt. Then ε_ν projects S' onto configuration ν, followed by a time evolution of $\mathbb{S}$ for δt, and so on. In the limit

$\delta t \to 0$, S' is frozen by continuous (Zeno) measurements of $|\nu\rangle\langle\nu|$ and S evolves freely under the influence of S' in configuration ν. We find

$$\lim_{\delta t\to 0} \mathcal{U}_\nu^{(0)} = \lim_{\delta t\to 0} \prod_{n=1}^{M} (\varepsilon_\nu - \mathrm{i}\,\varepsilon_\nu \mathsf{H} \varepsilon_\nu \delta t) = u_\nu(t,0), \tag{4.7}$$

where

$$\mathsf{u}_\nu(t,t') = \varepsilon_\nu\, e^{-\mathrm{i}\,\varepsilon_\nu \mathsf{H} \varepsilon_\nu (t-t')} \tag{4.8}$$

is a so-called Zeno evolution operator that evolves S between times t and t' while S' is frozen in configuration $|\nu\rangle$. Zeno-evolution operators obey the following relations

$$\mathsf{u}_\nu \mathsf{u}_\mu = 0 \quad \text{if } \nu \neq \mu, \quad \varepsilon_\nu \mathsf{u}_\nu = \mathsf{u}_\nu \varepsilon_\nu = \mathsf{u}_\nu, \quad \text{and} \quad \mathsf{u}_\nu^\dagger \mathsf{u}_\nu = \mathsf{u}_\nu \mathsf{u}_\nu^\dagger = \varepsilon_\nu. \tag{4.9}$$

Next we discuss the projection $\varepsilon_\nu \mathsf{U}(t) \varepsilon_\mu$ for $\mu \neq \nu$ and focus on those terms that are of the form

$$\mathcal{U}_{\nu\mu}^{(1)} = \quad \varepsilon_\nu\, \delta\mathsf{U}\, \varepsilon_\nu\, \delta\mathsf{U} \ldots \varepsilon_\nu\, \delta\mathsf{U}\, \varepsilon_\nu \quad \delta\mathsf{U} \quad \varepsilon_\mu\, \delta\mathsf{U}\, \varepsilon_\mu\, \delta\mathsf{U} \ldots \varepsilon_\mu\, \delta\mathsf{U}\, \varepsilon_\mu \tag{4.10a}$$

$$= -\mathrm{i}\delta t \underbrace{\varepsilon_\nu\, \delta\mathsf{U}\, \varepsilon_\nu\, \delta\mathsf{U} \ldots \varepsilon_\nu\, \delta\mathsf{U}\, \varepsilon_\nu}_{=\mathcal{X}\ (M-M'\ \text{times}\ \delta U)} \varepsilon_\nu \mathsf{H} \varepsilon_\mu \underbrace{\varepsilon_\mu\, \delta\mathsf{U}\, \varepsilon_\mu\, \delta\mathsf{U} \ldots \varepsilon_\mu\, \delta\mathsf{U}\, \varepsilon_\mu}_{=\mathcal{Y}\ (M'-1\ \text{times}\ \delta U)}, \tag{4.10b}$$

where we employed $\varepsilon_\nu\, \delta\mathsf{U}\, \varepsilon_\mu = -\mathrm{i}\delta t\, \varepsilon_\nu \mathsf{H} \varepsilon_\mu$. Now let $t = M\delta t$ and $t' = M'\delta t$. The term $\mathcal{U}_{\nu\mu}^{(1)}$ can be interpreted as follows. Initially S' is projected into state $|\mu\rangle$ and we observe that $\lim_{\delta t\to 0} \mathcal{Y} = u_\mu(t',0)$. This is the Zeno evolution operator for S that keeps S' static in state $|\mu\rangle$ between 0 and t'. Then the subsystem S' makes a jump from configuration $|\mu\rangle$ to configuration $|\nu\rangle$ [term $\varepsilon_\nu \mathsf{H} \varepsilon_\mu$], followed by the evolution of S between t' and t with S' frozen in state $|\nu\rangle$ [term $\mathcal{X}$ in Eq. (4.10a) fulfils $\lim_{\delta t\to 0} \mathcal{X} = u_\mu(t,t')$]. Note that the limit $t \to 0$ cannot be taken directly in $\mathcal{U}_{\nu\mu}^{(1)}$, since there are $M \to \infty$ ($\delta t \to 0$) similar terms appearing in $\varepsilon_\nu \mathsf{U}(t) \varepsilon_\mu$ that differ from $\mathcal{U}_{\nu\mu}^{(1)}$ only in the position of the jump operator $\varepsilon_\nu \mathsf{H} \varepsilon_\mu$, i.e. the time t' at which S' makes the transition $\mu \to \nu$. Summing over all these terms and taking the limit $t \to 0$ yields

$$\lim_{\delta t\to 0} \sum_{q=1}^{M} -\mathrm{i}\delta t\, \mathcal{X}(t, q\delta t)\, \mathsf{H}\, \mathcal{Y}(q\delta t - \delta t, 0) = -\mathrm{i} \int_0^t \mathsf{u}_\nu(t,t')\, \mathsf{H}\, \mathsf{u}_\mu(t',0) dt', \tag{4.11}$$

and the integral is thus a continuous sum over the time for the jump $\mu \to \nu$ to occur. The full expansion of $\varepsilon_\nu \mathsf{U}(t) \varepsilon_\mu$ also contains terms with an arbitrary number of intermediary configurations η_q between the initial and final configurations μ and ν, respectively. For each of these configurations, the jump $\eta_q \to \eta_{q+1}$ can occur at

any time t_q between 0 and the next jump at time t_{q+1}. Thus

$$\varepsilon_\nu \mathsf{U}(t)\varepsilon_\mu = \mathsf{u}_\nu(t,0)\delta_{\mu,\nu} + \tag{4.12}$$
$$\sum_{n=1}^{\infty} \mathrm{i}^{-n} \sum_{\eta_1,\ldots,\eta_n} \int_0^t \int_0^{t_n} \ldots \int_0^{t_2} \mathsf{u}_\nu(t,t_n)\mathsf{H}\mathsf{u}_{\eta_n}(t_n,t_{n-1})\mathsf{H}\ldots\mathsf{u}_{\eta_1}(t_2,t_1)\mathsf{H}\mathsf{u}_\mu(t_1,0)dt_1\ldots dt_n,$$

where the sum over n counts the number of jumps between different intermediate configurations η_q. While S evolves smoothly in time, Eq. (4.12) describes S' as evolving stroboscopically in its state-space: e.g. S' is static in configuration μ from 0 to time t_1, then jumps instantaneously to another configuration ν where its stays static until t_2, and so on. Each succession of configurations adopted by S' from 0 to time t is a possible history of S'. The dynamics of S as obtained by Eq. (4.12) then appears as the superposition of the effects on S of all the possible histories of S'.

The expression for $\varepsilon_\nu \mathsf{U}(t)\varepsilon_\mu$ in Eq. (4.12) simplifies greatly on using the mixed-product property of the tensor product $(A\otimes B)(C\otimes D) = AC\otimes BD$. Indeed, this implies that for any two projector-lattices ε_ν and ε_μ there exist small $d_s \times d_s$ matrices H_ν, $\mathsf{H}_{\nu\leftarrow\mu}$ and $\mathsf{U}_{\nu\leftarrow\mu}(t)$ such that

$$\varepsilon_\nu \mathsf{H}\varepsilon_\nu = \otimes_{k\in S'}\mathsf{P}_{k,i_k}\otimes \mathsf{H}_\nu = \overbrace{|\nu\rangle\langle\nu|}^{\text{Acts on } S'} \otimes \overbrace{\mathsf{H}_\nu}^{\text{Acts on } S}, \tag{4.13a}$$
$$\mathsf{u}_\nu(t) = \otimes_{k\in S'}\mathsf{P}_{k,i_k}\otimes e^{-\mathrm{i}\mathsf{H}_\nu t} = |\nu\rangle\langle\nu| \otimes e^{-\mathrm{i}\mathsf{H}_\nu t}, \tag{4.13b}$$
$$\varepsilon_\nu \mathsf{H}\varepsilon_\mu = \otimes_{k\in S'}\mathsf{T}_{k,i_k\leftarrow j_k}\otimes \mathsf{H}_{\nu\leftarrow\mu} = |\nu\rangle\langle\mu| \otimes \mathsf{H}_{\nu\leftarrow\mu}. \tag{4.13c}$$

The H_ν matrices are called statics because they physically correspond to small effective Hamiltonians driving S when S' is static in $|\nu\rangle$, i.e. frozen in configuration ν. Similarly, the $\mathsf{H}_{\nu\leftarrow\mu}$ matrices are called flips and represent how a jump of S' from μ to ν affects the dynamics of S. Together they form a tensor-product partition of the Hamiltonian. The H_ν are Hermitian and $(\mathsf{H}_{\nu\leftarrow\mu})^\dagger = \mathsf{H}_{\mu\leftarrow\nu}$. Using these matrices and the mixed-product property we can completely separate the evolution of S from the evolution of S'. It follows that Eq. (4.12) is equivalent to

$$\mathsf{U}_{\nu\leftarrow\mu}(t) = e^{-\mathrm{i}\mathsf{H}_\nu t}\delta_{\mu,\nu} + \sum_{n=1}^{\infty} \mathrm{i}^{-n} \tag{4.14}$$
$$\times \sum_{\eta_1,\ldots,\eta_n} \int_0^t \int_0^{t_n} \ldots \int_0^{t_2} e^{-\mathrm{i}\mathsf{H}_\nu(t-t_n)}\mathsf{H}_{\nu\leftarrow\eta_n} e^{-\mathrm{i}\mathsf{H}_{\eta_n}(t_n-t_{n-1})}\mathsf{H}_{\eta_n\leftarrow\eta_{n-1}}\ldots e^{-\mathrm{i}\mathsf{H}_\mu t_1} dt_1\ldots dt_n.$$

Note that this expression for $\mathsf{U}_{\nu\leftarrow\mu}(t)$ only comprises $d_s\times d_s$ matrices. With Eq. (4.14) we achieved to transform the complications associated with the real-time dynamics of a quantum many-body system into the sum over the intermediary configurations $\eta_1,\ldots\eta_n$ of S'. In the following section 4.1.3, we will show that each contribution to the sum in Eq. (4.14) can be represented as a walk on a graph. This visualisation not only clearly brings out all the physical processes contributing to $\mathsf{U}_{\nu\leftarrow\mu}$ and facilitates the evaluation of Eq. (4.14), but most importantly it gives the physical meaning of

walks, simple paths and simple cycles as system histories.

Perturbation theory

We now provide a simpler and shorter alternative derivation of the conditional evolution operators from a perturbative expansion of the time evolution operator in the transitions undergone by S'. We start with the well-known expression (see, e.g., Complement AI.2 in [85]), called Dyson series for the evolution operator. In time-dependent perturbation theory, it is used to describe the dynamics of a system with Hamiltonian H_0 in the presence of a perturbation V

$$\mathsf{U}(t,0) = \exp[-\mathrm{i}(\mathsf{H}_0+\mathsf{V})t] = \exp[-\mathrm{i}\mathsf{H}_0 t] + \sum_{n=1}^{\infty} \mathrm{i}^{-n} \int_0^t \int_0^{t_n} \dots \int_0^{t_2} e^{-\mathrm{i}\mathsf{H}_0(t-t_n)}\, \mathsf{V}\, e^{-\mathrm{i}\mathsf{H}_0(t_n-t_{n-1})}\, \mathsf{V}\, \dots e^{-\mathrm{i}\mathsf{H}_0 t_1} dt_1 \dots dt_n. \tag{4.15}$$

In order to establish Eq. (4.12) via Eq. (4.15), we expand the Hamiltonian H in terms of the complete set of projector-lattices in Eq. (4.2) and obtain $\mathsf{H} = \mathsf{H}_0 + \mathsf{V}$, where

$$\mathsf{H}_0 = \sum_{\nu} \varepsilon_\nu \mathsf{H} \varepsilon_\nu, \quad \mathsf{V} = \sum_{\nu \neq \mu} \varepsilon_\nu \mathsf{H} \varepsilon_\mu. \tag{4.16}$$

If these expressions are introduced in Eq. (4.15), the orthogonality of the projector lattices directly yields the result in Eq. (4.12). From this, the mixed product property of the tensor-product gives Eq. (4.14). This indicates another interpretation for the result of Eq. (4.14): the transitions undergone by S' can be seen as perturbations affecting the evolution of S.

4.1.3 Representing the time evolution on a graph

The sum over the intermediary configurations η_q in Eq. (4.14) can be interpreted as a sum over the histories of S', a history being a succession of configurations adopted by S' from 0 to time t. To visualise the histories, we construct a graph $\mathcal{G}$ as follows:
i) For each configuration ν available to S', draw a vertex v_ν.
ii) For each non-zero flip, i.e. when S' is allowed to make a transition between two specific configurations μ and ν, draw an edge between v_μ and v_ν.
Because of i), we call $\mathcal{G}$ the configuration graph of the system. Now we can see that a multiplication by $e^{-\mathrm{i}\mathsf{H}_\nu \tau}$ in Eq. (4.14) represents the evolution of S while S' is stationary at vertex v_ν during time τ. A multiplication by $\mathsf{H}_{\nu\leftarrow\mu}$ in Eq. (4.14) corresponds to an instantaneous move of S' along the edge $v_\mu \to v_\nu$. Consequently, the histories of S' appear as walks on $\mathcal{G}$ and their superposition is obtained as the sum over all the walks, in complete analogy with the Feynman path-integrals. If the system had continuous degrees of freedom, the sum over histories, that is the sum over the walks, would become an integral over histories which corresponds to an integral over the walks, i.e. a Feynman path-integral. An equivalent to the

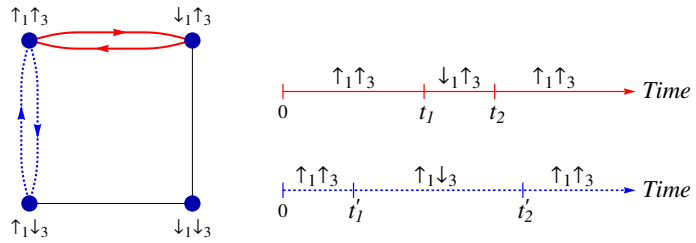

(a) (b)

Figure 4.1: (a) A square, the graph $\mathcal{G}$ of all configurations available to S', here an ensemble of two spin-1/2 particles labelled 1 and 3. Each edge represents a transition allowed by the Hamiltonian in Eq. (4.17). Highlighted in solid-red and dashed-blue are two walks of S' on $\mathcal{G}$, i.e. two possible histories of S' between time 0 and time t. (b) The histories of S' represented by the solid-red and dashed-blue walks in (a) where t_1, t_2, t'_1 and t'_2 are the jumping times. This representation of the histories can also be thought of as the discrete equivalent of Feynman diagrams, the physical processes being the spin flips caused by the Hamiltonian.

Feynman diagrams also exists in our situation: this is the succession of physical processes underwent by S' during a history. Finally, from a practical point of view, the graph itself facilitates the visualisation of the histories of S' contributing to a given conditional evolution operator. To clarify these notions, we now construct the configuration graph of a small physical system.

Example 4.1.1. Consider a 1D chain of three spin-1/2 particles, and choose S to be the central spin, labelled 2. S' is thus comprised of the other two spins 1 and 3. Suppose that the Hamiltonian of the system is

$$\mathsf{H} = \sum_{i=1}^{3} \Delta\, \sigma_x^i + \sum_{i=1}^{2} J\, \sigma_z^i \sigma_z^{i+1}, \tag{4.17}$$

where $\sigma_{x,z}$ are Pauli matrices and Δ and J are two real parameters. There are $2^2 = 4$ orthogonal configurations available to S' and $\mathcal{G}$ has 4 vertices. Indeed, choosing the configurations to be those specifying the direction of the spins along the z-axis[1], the projector-lattices are $\varepsilon_{\uparrow_1\uparrow_3} = |\uparrow_1\uparrow_3\rangle\langle\uparrow_1\uparrow_3|$, $\varepsilon_{\uparrow_1\downarrow_3} = |\uparrow_1\downarrow_3\rangle\langle\uparrow_1\downarrow_3|$, $\varepsilon_{\downarrow_1\uparrow_3} = |\downarrow_1\uparrow_3\rangle\langle\downarrow_1\uparrow_3|$ and $\varepsilon_{\downarrow_1\downarrow_3} = |\downarrow_1\downarrow_3\rangle\langle\downarrow_1\downarrow_3|$. We find that the flips and statics are given by

$$\mathsf{H}_{\uparrow_1\uparrow_3} = 2J\sigma_z^s + \Delta\sigma_x^s, \quad \mathsf{H}_{\downarrow_1\downarrow_3} = -2J\sigma_z^s + \Delta\sigma_x^s, \tag{4.18a}$$

$$\mathsf{H}_{\downarrow_1\uparrow_3} = \mathsf{H}_{\uparrow_1\downarrow_3} = \Delta\sigma_x^s, \quad \mathsf{H}_{\nu\leftarrow\mu} = \Delta\, \mathsf{I}_s, \tag{4.18b}$$

where ν and μ are two configurations of S' that differ by exactly *one* spin flip. The graph $\mathcal{G}$ has therefore 4 edges and is the square. The graph $\mathcal{G}$ as well as two

[1]One could equally well choose to specify the spins along another axis.

examples for histories of S', two walks and the equivalents of Feynman diagrams are all represented in Fig. 4.1.

In order to make the superposition of histories manifest in the expression for $\mathsf{U}_{\nu\leftarrow\mu}(t)$, we relabel the sum over intermediary configurations into a sum over all the walks on $\mathcal{G}$. If the initial and final configurations of S' appearing in Eq. (4.14) are respectively μ and ν, then the relevant walks all start on vertex v_μ and terminate on the vertex v_ν. The conditional evolution operator $\mathsf{U}_{\nu\leftarrow\mu}$ is therefore

$$\mathsf{U}_{\nu\leftarrow\mu}(t) = e^{-\mathrm{i}\mathsf{H}_\nu t}\delta_{\mu,\nu} + \sum_{n=1}^{\infty} \mathrm{i}^{-n} \sum_{W_{\mathcal{G};\nu\mu;n}} \tag{4.19}$$
$$\times \int_0^t \int_0^{t_n} \dots \int_0^{t_2} e^{-\mathrm{i}\mathsf{H}_\nu(t-t_n)} \mathsf{H}_{\nu\leftarrow\eta_n} e^{-\mathrm{i}\mathsf{H}_{\eta_n}(t_n-t_{n-1})} \mathsf{H}_{\eta_n\leftarrow\eta_{n-1}} \dots e^{-\mathrm{i}\mathsf{H}_\mu t_1} dt_1 \dots dt_n,$$

where $W_{\mathcal{G};\nu\mu;n}$ is the ensemble of walks of length n on $\mathcal{G}$ from v_μ to v_ν. Eq. (4.19) is the walk-sum Lemma 3.3.1 applied to the matrix exponential $\exp[-\mathrm{i}\mathsf{H}t]$.

4.1.4 Evaluation of conditional evolution operators

Conditional evolution operators are most conveniently evaluated in the Laplace domain, because this transformation turns the nested convolutions in Eq. (4.19) into a product of matrices. Let $\tilde{\mathsf{M}}_\mu(s) = \mathcal{L}\big(\exp[-\mathrm{i}\mathsf{H}_\mu t]\big) = (s\mathsf{I}_s + \mathrm{i}\mathsf{H}_\mu)^{-1}$ be the element-wise Laplace transform of $\exp[-\mathrm{i}\mathsf{H}_\mu t]$ with s the Laplace domain variable. It follows that the Laplace transform of a conditional evolution operator is given by

$$\tilde{\mathsf{U}}_{\nu\leftarrow\mu}(s) = \tilde{\mathsf{M}}_\nu(s)\delta_{\mu,\nu} + \sum_{n=1}^{\infty} \sum_{W_{\mathcal{G};\nu\mu;n}} \mathrm{i}^{-n}\, \tilde{\mathsf{M}}_\nu(s)\, \mathsf{H}_{\nu\leftarrow\eta_n} \dots \mathsf{H}_{\eta_1\leftarrow\mu}\, \tilde{\mathsf{M}}_\mu(s). \tag{4.20}$$

This is the expression we use in computations. It only involves multiplications and additions of $d_s \times d_s$ matrices. Considering the case where all the $\tilde{\mathsf{M}}_\mu(s)$ can be obtained analytically, we remark that the matrix elements of the $\tilde{\mathsf{M}}_\mu(s)$ are ratios of polynomials in s. The roots of the denominator polynomial are $-\mathrm{i}\lambda_\mu$ with λ_μ an eigenvalue of H_μ. This is therefore also true for any element of the sum in Eq. (4.20) and performing the inverse transform into the time-domain can be done according to the formula

$$\mathsf{U}_{\nu\leftarrow\mu}(t) = \sum_\mu \mathrm{Res}[e^{st}\tilde{\mathsf{U}}_{\nu\leftarrow\mu}(s), -\mathrm{i}\lambda_\mu], \tag{4.21}$$

where $\mathrm{Res}[f(s), \lambda]$ denotes the residue of $f(s)$ at λ. In all practical situations the infinite sum in Eq. (4.19) is truncated at some order K. With this approximation only walks of length $n \leq K$ are taken into account. It is important to establish the convergence properties of such truncated walk-sums.

Convergence

Consider the contribution to $\mathsf{U}_{\nu\leftarrow\mu}(t)$ of the walks of length exactly K, denoted $\mathsf{U}^{[K]}_{\nu\leftarrow\mu}(t)$. A naive bound for the norm of this quantity is

$$\left\|\mathsf{U}^{[K]}_{\nu\leftarrow\mu}(t)\right\| \leq |W_{\mathcal{G};\nu\mu;K}|\frac{(\Omega\, t)^K}{K!}, \tag{4.22}$$

with $\Omega = \max_n\{\mathsf{H}_{\eta_{n+1}\leftarrow\eta_n}\}$ and $|W_{\mathcal{G};\nu\mu;K}|$ is the number of walks of length K on $\mathcal{G}$ between vertices v_ν and v_μ. It is noteworthy that $|W_{\mathcal{G};\nu\mu;K}|$ is bounded by a polynomial in the number N of particles of the system, see below. The bound demonstrates that provided $\mathbb{S}$ comprises a finite number of particles, the series of Eq. (4.19) is absolutely and uniformly convergent for any finite time.

Computational cost: polynomial scaling in N

In this section we show that the number of floating point operations required to approximate a conditional evolution operator to order K scales polynomially in the number of particles N of the system. For simplicity and without loss of generality, we assume that all particles have d internal levels and that S contains p particles, and thus $d_s = d^p$. The evaluation of a single walk of length K to a conditional evolution operator requires $2K+1$ multiplications of $d_s \times d_s$ matrices (K statics and $K+1$ flips), i.e. $\sim 2Kd_s^3$ operations. Then all the walk contributions must be added together. This represents an additional $|W_{\mathcal{G};\nu\mu;K}|d_s^2$ operations. The total number $\mathcal{N}_K$ of operations required to obtain $U_{\mu\leftarrow\nu}$ at order K is therefore

$$\mathcal{N}_K = (2Kd_s^3 + d_s^2)|W_{\mathcal{G};\nu\mu;K}|. \tag{4.23}$$

The remaining task is to derive an upper bound for $|W_{\mathcal{G};\nu\mu;K}|$.

Suppose that the flips of the Hamiltonian H of $\mathbb{S}$ [see Eq. (4.13)] are only non-zero for those configurations μ and ν of S' where at most q particles change their state in a transition from μ to ν. For example, the expressions for the flips in Eqs. (4.18) and (4.78) demonstrate that the Hamiltonians in Eqs. (4.17) and (4.75) have $q = 1$. In fact, most of the common Hamiltonians have $q = 1,\ 2$. With p particles in S there are $N-p$ particles in S', and thus there are $\binom{N-p}{q}$ ways to choose which q particles among $N-p$ undergo a transition. Furthermore, for each particle that changes a state there are at most $d-1$ possible basis states available for the transition. In total, there are thus at most $V < \binom{N-p}{q}(d-1)^q$ configurations directly accessible to S' from any given one. By construction of $\mathcal{G}$, this is also an upper-bound on the number of vertices that share an edge with any given vertex on $\mathcal{G}$. It follows that there are at most V^K walks of length K attached to any vertex of $\mathcal{G}$, and thus we find

$$|W_{\mathcal{G};\nu\mu;K}| < \tbinom{N-p}{q}^K (d-1)^{qK}, \tag{4.24}$$

which scales polynomially in $N-p$ for small q.

Remark 4.1.1 (Spin-1/2 systems)**.** The upper-bound Eq. (4.24) is very loose and

we only use it to demonstrate that $|W_{\mathcal{G};\nu\mu;K}|$ is always bounded by a polynomial in N. For example, for a system with $N+1$ spin-1/2 particles, one particle in S ($p=1$) and a Hamiltonian with $q=1$, the graph $\mathcal{G}$ is the N-hypercube, denoted $\mathcal{H}_N$. In this case, we have found that the number of walks of length $\ell = d+2k > 0$, $k \in \mathbb{N}$, $0 \leq d \leq N$, between two vertices μ and ν separated by a distance d is[2]

$$|W_{\mathcal{H}_N;\,\mu\nu;\,d+2k}| = \frac{2}{2^N} \sum_{i=0}^{\lfloor N/2 \rfloor} (2i+p_N)^{d+2k} \sum_{j=0}^{\lfloor N/2 \rfloor} \binom{N-d}{\lfloor \frac{N}{2} \rfloor - i - j} \binom{d}{j} (-1)^j, \tag{4.25}$$

where $p_N = N \bmod 2$ and $\lfloor \cdot \rfloor$ is the floor function. This is substantially smaller than the N^{d+2k} of the bound Eq. (4.24), indeed for $N \gg 1$, $N \gg \ell$, we have $|W_{\mathcal{H}_N;\,\mu\nu;\,d+2k}| \sim 2^{-k}(N-d/2-1)^k (d+2k)!/k! \ll N^{d+2k}$ and for $\ell \gg N$, $|W_{\mathcal{H}_N;\,\mu\nu;\,d+2k}| \sim 2^{-N+1}\, N^{d+2k} \ll N^{d+2k}$.

The observation that the number of walks of length K on $\mathcal{G}$ is always bounded by a polynomial in N is a direct consequence of the sparsity of quantum Hamiltonians: there are not so many configurations accessible to S' through K jumps. Together with Eq. (4.23), Eq. (4.24) yields the following upper bound for the number of operations required to obtain $\mathsf{U}_{\mu\leftarrow\nu}$ at order K

$$\mathcal{N}_K < (2K d_s^3 + d_s^2) \binom{N-p}{q}^K (d-1)^{qK}. \tag{4.26}$$

It follows that when $q \ll N$, the computational cost for the evaluation up to order K of a single conditional evolution operator scales polynomially with the number of particles N.

At the opposite, the progression of the accuracy with K as well as it scaling with N at fixed K are open questions. In any case, to approximate well the *entire* wave-function of the system $|\psi\rangle$, it is necessary that the number of conditional evolution operators responsible for most of the norm of $|\psi\rangle$ scales polynomially with N. This means the system is well confined to a part of its Hilbert-space whose size also grows polynomially with N. We note that an increase in time requires to include higher order terms in Eq. (4.19). Finally, we remark that conditional expectation values converge much faster than ordinary expectation values because the former quantities are insensitive to the norm of the overall state vector. In the next section we discuss how expectation values and conditional expectation values can be calculated via conditional evolution operators.

4.1.5 Expectation values and conditional expectation values

Here we demonstrate how conditional evolution operators can be employed for the evaluation of expectation values and conditional expectation values. For simplicity we assume that the initial state of the full system is given by $|\psi(0)\rangle = |\mu\rangle \otimes |\psi_s(0)\rangle$,

[2] We prove this by induction on N.

where $|\psi_s(0)\rangle$ is the initial state of S. Note, all the relations of this sections are easily extended to more general initial pure states $\sum_\mu c_\mu|\mu\rangle \otimes |\psi_s(0)\rangle$ upon introducing a sum over μ as appropriate. The state vector of the full system can then be obtained via Eq. (4.4) and is given by

$$|\psi(t)\rangle = \mathsf{U}(t)|\psi(0)\rangle = \sum_\nu \Big\{ |\nu\rangle \otimes |\psi_s(t)\rangle_{\nu\leftarrow\mu} \Big\}, \tag{4.27}$$

where $|\psi_s(t)\rangle_{\nu\leftarrow\mu} = \mathsf{U}_{\nu\leftarrow\mu}(t)|\psi_s(0)\rangle$ is a piece of the wavefunction of the full system. Any mean value of an observable O can be calculated via Eq. (4.27). With the definition $\varepsilon_{\nu'}\mathsf{O}\varepsilon_\nu = |\nu'\rangle\langle\nu| \otimes \mathsf{O}_{\nu'\nu}$, we find

$$\langle O\rangle = \langle\psi_s(0)| \sum_{\nu',\nu} \mathsf{U}^\dagger_{\mu\to\nu'}\, \mathsf{O}_{\nu'\nu}\, \mathsf{U}_{\nu\leftarrow\mu}\, |\psi_s(0)\rangle. \tag{4.28}$$

In this expression $\mathsf{U}^\dagger_{\mu\to\nu'} = \big(\mathsf{U}_{\nu'\leftarrow\mu}\big)^\dagger$. It follows that any expectation value of an observable O can be computed directly from conditional evolution operators if O is expanded in the projector lattice basis ε_ν.

Next we investigate in more detail the meaning of the piece $|\psi_s(t)\rangle_{\nu\leftarrow\mu} = \mathsf{U}_{\nu\leftarrow\mu}(t)|\psi_s(0)\rangle$ of the full state vector. To this end, we write the projection of $|\psi(t)\rangle$ onto the range of ε_ν as

$$\varepsilon_\nu\, |\psi(t)\rangle = |\nu\rangle \otimes |\psi_s(t)\rangle_{\nu\leftarrow\mu} = \sum_{\ell=1}^{d_s} \alpha_\ell\, |\nu\ell_s\rangle, \tag{4.29}$$

where the probability amplitudes α_ℓ of state $|\nu\ell_s\rangle$ (S' in configuration ν, S in state $|\ell_s\rangle$) are determined by $\mathsf{U}_{\nu\leftarrow\mu}(t)$. This shows that $\mathsf{U}_{\nu\leftarrow\mu}(t)$ directly evolves the projection of the full state vector $|\psi(t)\rangle$ onto a d_s-dimensional subspace corresponding to S' in configuration ν, as shown in Fig. 4.2. We emphasise that conditional evolution operators are submatrices of U [see Eq. (4.4)] and therefore not necessarily unitary. It follows that $\mathsf{U}_{\nu\leftarrow\mu}(t)$ does not generally conserve the norm of $|\psi_s(0)\rangle$. Indeed, Eq. (4.29) implies that the norm of $|\psi_s(t)\rangle_{\nu\leftarrow\mu}$ is given by the probability of finding S' in configuration ν at time t, knowing that it was initially in configuration μ,

$$\langle\psi_s(0)|\, \mathsf{U}^\dagger_{\mu\to\nu}(t)\, \mathsf{U}_{\nu\leftarrow\mu}(t)\, |\psi_s(0)\rangle = \langle\varepsilon_\nu\rangle_t. \tag{4.30}$$

We now turn to conditional expectation values and show that some of them can be computed directly via a single conditional evolution operator. To this end, we note that the expectation value of an arbitrary operator O_s acting on S with respect to $|\psi_s(t)\rangle_{\nu\leftarrow\mu}$ is given by

$$\langle\psi_s(0)|\, \mathsf{U}^\dagger_{\mu\to\nu}(t)\, \mathsf{O}_s\, \mathsf{U}_{\nu\leftarrow\mu}(t)\, |\psi_s(0)\rangle = \langle O_s\varepsilon_\nu\rangle_t, \tag{4.31}$$

where $\langle O_s\varepsilon_\nu\rangle_t$ is the expectation value of $\mathsf{O}_s\varepsilon_\nu$ at time t. Eqs. (4.30, 4.31) directly yield the conditional expectation value $\langle O_s/\nu\rangle$ of O_s, knowing that S', initially in

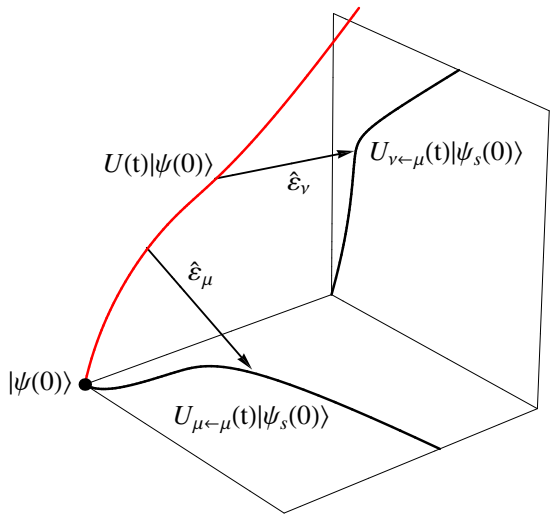

Figure 4.2: The conditional evolution operator $\mathsf{U}_{\nu\leftarrow\mu}(t)$ evolves only the projection of the full evolution $\mathsf{U}(t)|\psi(0)\rangle$ onto the subspace of the full state-space that corresponds to S' being in configuration ν. Note that in this picture, S' is initially in configuration μ.

configuration μ, is in configuration ν at time t, [3]

$$\langle O_s/\nu\rangle = \frac{\langle O_s\varepsilon_\nu\rangle}{\langle\varepsilon_\nu\rangle} = \frac{\langle\psi_s(0)|\,\mathsf{U}^\dagger_{\mu\to\nu}(t)\,\mathsf{O}_s\,\mathsf{U}_{\nu\leftarrow\mu}(t)\,|\psi_s(0)\rangle}{\langle\psi_s(0)|\,\mathsf{U}^\dagger_{\mu\to\nu}(t)\,\mathsf{U}_{\nu\leftarrow\mu}(t)|\psi_s(0)\rangle}. \tag{4.32}$$

Finally, Eqs. (4.2) and (4.32) imply that the full set of conditional probabilities allows one to compute the mean value of an operator acting on S, $\sum_\nu\langle O_s/\nu\rangle\langle\varepsilon_\nu\rangle = \langle O_s\rangle$. We use the preceding results in sections §4.2 and §4.3, where we apply the walk-sum method to study continuous-time coined quantum random walks and the dynamics of strongly interacting Rydberg-excited Mott insulators. But first, we give a very simple example to illustrate the method.

Example 4.1.2 (Dynamics of 3 spins)**.** Consider a small 1D chain with 3 spin-1/2 particles evolving according to the Hamiltonian in Eq. (4.17). Suppose that initially all three spins are up along z, i.e. $|\psi(0)\rangle = |\uparrow_1\uparrow_2\uparrow_3\rangle$ and suppose that we are interested in the time evolution of the conditional expectation value $\langle\uparrow_2\ /\ \uparrow_1\uparrow_3\rangle$. This is the probability for spin 2 to be up along z knowing the other 2 spins are up along z. To implement walk-sum, we take S to be the spin 2 and S' comprises spins 1 and 3. Similarly to the example of section 4.1.3, we choose the configurations of S' to specify the direction of these spins along the z-axis and obtain the flips and statics of Eq. (4.18). The graph $\mathcal{G}$ is the square represented in Fig. 4.1. According

[3] The fact that $\langle O_s\varepsilon_\nu\rangle/\langle\varepsilon_\nu\rangle$ is indeed the conditional expectation value follows from $[\mathsf{O}_s,\varepsilon_\nu]=0$ and $\varepsilon_\nu^2=\varepsilon_\nu$ [86].

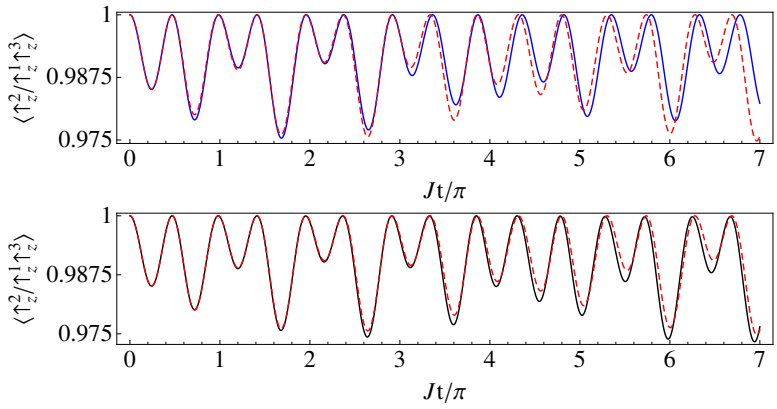

Figure 4.3: Top figure: evolution of $\langle\uparrow_2 / \uparrow_1\uparrow_3\rangle$ evaluated by walk-sum at order 2 (solid blue line) compared to the exact solution (dashed red line). Bottom figure: evolution of $\langle\uparrow_2 / \uparrow_1\uparrow_3\rangle$ evaluated by walk-sum at order 4 (solid black line) compared to the exact solution (dashed red line). Note that order 4 is the next non-zero order after order 2. Parameters: $J/\Delta = 4$.

to Eq. (4.32), the quantity $\langle\uparrow_2 / \uparrow_1\uparrow_3\rangle$ is given by

$$\langle\uparrow_2 / \uparrow_1\uparrow_3\rangle = \frac{\langle\psi_s(0)|\mathsf{U}^\dagger_{\uparrow_1\uparrow_3\to\uparrow_1\uparrow_3}\mathsf{P}_{\uparrow_2}\mathsf{U}_{\uparrow_1\uparrow_3\leftarrow\uparrow_1\uparrow_3}|\psi_s(0)\rangle}{\langle\psi_s(0)|\mathsf{U}^\dagger_{\uparrow_1\uparrow_3\to\uparrow_1\uparrow_3}\mathsf{U}_{\uparrow_1\uparrow_3\leftarrow\uparrow_1\uparrow_3}|\psi_s(0)\rangle}, \tag{4.33}$$

where $\mathsf{P}_{\uparrow_2} = |\uparrow_2\rangle\langle\uparrow_2|$ and $|\psi_s(0)\rangle = |\uparrow_2\rangle$ is the initial state of subsystem S. Considering the closed walks off vertex $v_{\uparrow_1\uparrow_3}$ on $\mathcal{G}$ and keeping only walks of length 2 or less, the conditional evolution operator in the Laplace domain $\tilde{\mathsf{U}}_{\uparrow_1\uparrow_3\leftarrow\uparrow_1\uparrow_3}$ is given by

$$\tilde{\mathsf{U}}_{\uparrow_1\uparrow_3\leftarrow\uparrow_1\uparrow_3}(s) \simeq \overbrace{\tilde{\mathsf{M}}_{\uparrow_1\uparrow_3}}^{\text{Walk of length 0}} + (-\mathrm{i}\Delta)^2 \overbrace{\tilde{\mathsf{M}}_{\uparrow_1\uparrow_3}(\tilde{\mathsf{M}}_{\downarrow_1\uparrow_3} + \tilde{\mathsf{M}}_{\uparrow_1\downarrow_3})\tilde{\mathsf{M}}_{\uparrow_1\uparrow_3}}^{\text{Two walks of length 2}}, \tag{4.34}$$

where the factor $(-i\Delta)^2$ comes from the flips. The two walks of length two taken into account here are those highlighted by solid-red and dashed-blue lines in Fig. 4.1. In Fig. 4.3 we compare the walk-sum result for the time evolution of $\langle\uparrow_2 / \uparrow_1\uparrow_3\rangle$ to the exact result. For short times $Jt \lesssim 3\pi$, the agreement between the walk-sum estimation of $\langle\uparrow_2 / \uparrow_1\uparrow_3\rangle$ at order 2 and the exact result is excellent. Differences appear for $Jt \gtrsim 3\pi$ and grow larger with time. At order 4, which is the next non-zero order, the difference between the walk-sum estimation and the exact result does not exceed 5×10^{-3} for t up to $Jt \sim 7\pi$, which represents a relative error of less than 0.5%. As a comparison, the method of path-sums yields $\tilde{\mathsf{U}}_{\uparrow_1\uparrow_3\leftarrow\uparrow_1\uparrow_3}(s)$ exactly as

$$\begin{aligned}\tilde{\mathsf{U}}_{\uparrow_1\uparrow_3\leftarrow\uparrow_1\uparrow_3}(s) = \Big[&s\mathsf{I} - \Delta\sigma_x - 2J\sigma_z \\ &- 2\Delta^2[s\mathsf{I} - \Delta\sigma_x - \Delta^2\mathsf{B}]^{-1} - 2\Delta^4\mathsf{AB}[s\mathsf{I} - \Delta\sigma_x - \Delta^2\mathsf{B}]^{-1}\Big]^{-1},\end{aligned} \tag{4.35}$$

where $\mathsf{A} = [s\mathsf{I} - \Delta\sigma_x]^{-1}$ and $\mathsf{B} = [s\mathsf{I} - \Delta\sigma_x + 2J\sigma_z - \Delta^2\mathsf{A}]^{-1}$.

4.1.6 Two state vector formalism

To conclude the discussion devoted to the physical interpretation of the conditional evolution operators, we demonstrate that the Aharonov-Bergmann-Lebowitz rule of the Two State Vector Formalism [87, 88] can be naturally expressed with conditional evolution operators. This formalism was developed by Aharonov and coworkers to answer the following question. A quantum system initially in state $|\psi_0\rangle$ at t_0 is measured at a later time t_f in state $|\psi_f\rangle$. What is the probability to find this system in state $|\psi_q\rangle$ at any time $t \in [t_0, t_f]$? The conditional probability of finding $|\psi_q\rangle$ at t knowing the system starts in $|\psi_0\rangle$ and ends up in $|\psi_f\rangle$ noted $\Pr(0; q; f \,/\, 0; f)$ was shown by the authors to be [87]

$$\Pr(0; q; f \,/\, 0; f) = \frac{|\langle\Phi|\mathsf{P}_q|\Psi\rangle|^2}{|\langle\Phi|\Psi\rangle|^2} = \frac{|\langle\Phi|\mathsf{P}_q|\Psi\rangle|^2}{|\langle\Phi|\sum_i \mathsf{P}_{q_i}|\Psi\rangle|^2}, \tag{4.36}$$

where $\mathsf{P}_q = |\psi_q\rangle\langle\psi_q|$ and $\{\mathsf{P}_{q_i}\}$ is an ensemble of orthonormal projectors with $\sum_i \mathsf{P}_{q_i} = \mathsf{I}$, $\mathsf{P}_q \in \{\mathsf{P}_{q_i}\}$. This result is known as the Aharonov-Bergmann-Lebowitz (ABL) rule and $|\Psi\rangle = \mathsf{U}|\psi_0\rangle$ and $\langle\Phi| = \langle\psi_f|\mathsf{U}^\dagger$ are known as the forward and backward evolving states, respectively.

Now we derive the ABL rule using the conditional evolution operators. For simplicity we assume that $|\psi_0\rangle$, $|\psi_f\rangle$ and $|\psi_q\rangle$ are either identical or orthogonal. When considering quantum evolutions as sums of walks, i.e. superpositions of histories, the information about the initial, intermediary and final states is encoded in the vertices of the graph $\mathcal{G}$ through which S' must pass. More precisely, the probability $\Pr(0; q; f)$ that S' evolves along any of the of walks from v_0 to v_f passing through v_q at t is

$$\Pr(0; q; f) = |\langle\psi_f|\mathsf{U}^\dagger_{f\to q}(t_f, t)\mathsf{U}_{q\leftarrow 0}(t, 0)|\psi_0\rangle|^2. \tag{4.37}$$

This follows from Eq. (4.31). Additionally, the probability that S' be found on v_f at t_f knowing that it started on v_0 at $t = 0$ is, according again to Eq. (4.31),

$$\Pr(0; f) = |\langle\psi_f|\mathsf{U}_{f\leftarrow 0}(t_f, 0)|\psi_0\rangle|^2. \tag{4.38}$$

Thus the probability of finding the system in state $|\psi_q\rangle$ at t *knowing* that it was initially in $|\psi_0\rangle$ and is to be found in $|\psi_f\rangle$ at t_f is, as dictated by Eq. (4.32),

$$\Pr(0; q; f \,/\, 0; f) = \frac{|\langle\psi_f|\mathsf{U}^\dagger_{f\to q}\mathsf{U}_{q\leftarrow 0}|\psi_0\rangle|^2}{|\langle\psi_f|\mathsf{U}_{f\leftarrow 0}|\psi_0\rangle|^2}. \tag{4.39}$$

This is the the expression derived by Aharonov and coworkers. Indeed, upon introduction of the closure relation on projector-lattices at t in the denominator of

Eq. (4.39), $|\langle\psi_f|\mathsf{U}_{f\leftarrow 0}|\psi_0\rangle|^2 = \sum_{q_i} |\langle\psi_f|\mathsf{U}_{f\leftarrow q_i}(t_f,t)\mathsf{U}_{q_i\leftarrow 0}(t,0)|\psi_0\rangle|^2$ and thus

$$\Pr(0;q;f\,/\,0;f) = \frac{|\langle\psi_f|\mathsf{U}^{\dagger}_{f\rightarrow q}\mathsf{U}_{q\leftarrow 0}|\psi_0\rangle|^2}{\sum_{q_i}|\langle\psi_f|\mathsf{U}_{f\leftarrow q_i}(t_f,t)\mathsf{U}_{q_i\leftarrow 0}(t,0)|\psi_0\rangle|^2}. \tag{4.40}$$

Several remarks are now in order. First, if S has more than one internal level $d_s \geq 1$ then Eq. (4.39) is really a generalised form of the ABL rule. Indeed in our derivation of Eq. (4.39), we took the measurements at t, t_q and t_f to concern only S' and to be thus generalised measurements. The usual form of the ABL rule is recovered through additional constrains on the internal state of S, i.e. by introducing projectors $\mathsf{P}_{s,i}$. Second, in the derivation of Eq. (4.39), we conveniently supposed that $|\psi_0\rangle$, $|\psi_q\rangle$ and $|\psi_f\rangle$ directly correspond to vertices v_0, v_q and v_f on a graph $\mathcal{G}$. This is possible only if the states are either orthogonal or identical, i.e. that they form part of an orthonormal basis of the configuration space of S'. If this is not possible, the state(s) that are not part of the chosen basis whose states are in correspondence with the vertices of $\mathcal{G}$, must be decomposed onto that basis. Formally they then correspond to several vertices that the walks must visit.

The equivalence between Eq. (4.39) and the ABL rule Eq. (4.36) demonstrates the idea that post-selection can indeed be seen as a constraint on the walks or, in Feynman's terminology, the paths, accessible to a quantum system. The walk-sum and path-sum methods are thus naturally suited to study post-selection in quantum systems.

4.2 Quantum random walks

For the things we have to learn before we can do, we learn by doing.

Aristotle

Since quantum mechanics was first devised, the superposition and uncertainty principles have proven to be permanent sources of rich and counterintuitive behaviors in physical systems. Perhaps the most striking consequence of these principles is the fundamental capacity of quantum systems to perform some computations with an efficiency simply beyond that of the classical realm. Among the numerous schemes proposed to implement quantum computations, one of the most surprising is the one based on quantum random walks (QW). These were introduced by Aharonov and coworkers [89] as the quantum equivalent of a classical random walk. Surprisingly, the authors showed that a quantum particle moving freely on a lattice could undergo very long distance jumps, thus behaving very differently from its classical counterpart. Subsequent studies on QW uncovered a large array of unexpected properties, such as much faster mixing and hitting times on certain lattices than their classical equivalents [90, 91]. In the mean time, it was shown that QW could be used to solve decision problems [92], perform quantum computations [93] and as a tool in quantum algorithm design [94]. As a consequence QW are now a very active field of research

[95, 96, 97]. One of the latest development of the field concerns the experimental simulation of bosonic to fermionic through exotic statistics using 1D QW of photons on arrays of waveguides [98, 99, 100, 101, 102]. Future experiments in this domain will undoubtedly implement similar schemes on different 2D and 3D lattices and might include polarisation dependent jumping amplitudes. These would enable an exploration of dynamical behaviors and correlations in non-Abelian lattices, which are paramount to simulations of lattice field theories [103, 104, 105] and topological insulators [106, 107]. It is thus important to dispose of a single efficient and easy to implement theoretical method to compute the dynamics of non-interacting particles in any QW. In this context, we solve exactly all continuous-time quantum random-walks performed by non-interacting particles on any lattice, including finite sized and faulty lattices and including the non-Abelian case with coupling between internal and external dynamics. We achieve this using the method of walk-sums.

We consider an ensemble of non-interacting particles each with m internal levels living on a D-dimensional lattice $\mathcal{L}$ with N sites, possibly infinite. Since the particles are non-interacting, the Hilbert space is factorable as a tensor product of the state-spaces associated to each particle and we shall thus consider only one particle without loss of generality. Initially located on a single site denoted 0, the particle can jump to other sites along each direction d with a probability amplitude B_d. This quantity can be a matrix describing any possible dependencies of the jumping amplitude on internal degrees of freedom. In the general case, the jumping amplitudes along different directions may not commute: $[\mathsf{B}_d, \mathsf{B}_{d'}] \neq 0$. In this situation we say that the walk is non-Abelian. When located on a single site α, the energy of the particle is described by another matrix A which does not necessarily commute with any of the B_d. The Hamiltonian governing the evolution of the particle is

$$\mathsf{H} = \mathsf{A} \otimes \mathsf{I}_{\mathcal{L}} + \sum_d \mathsf{B}_d \otimes \Delta_d, \tag{4.41}$$

where $\mathsf{I}_{\mathcal{L}} = \sum_\alpha |\alpha\rangle\langle\alpha|$ is the identity on the spatial degree of freedom, $|\alpha\rangle\langle\alpha|$ being the projector onto site α. For latter convenience we also introduce I_σ, the identity on the internal degree of freedom of the particle. The Δ_d operators act on the spatial degree of freedom and are responsible for the particle jumps. For example, on a 1D lattice where jumps are allowed only between neighbouring sites, $\Delta_x = \sum_x \{|x+1\rangle\langle x| + |x\rangle\langle x+1|\}$. In lattice field theories, the Δ_d operators are commonly the discretised momentum operators p_d and are therefore tridiagonal for 1D lattices.

We compute the dynamics of the particle driven by the Hamiltonian of Eq.(4.41) using walk-sum and path-sum. In particular, we will see that the walk-sums involved in a conditional evolution operator $\mathsf{U}_{\alpha \leftarrow 0}(t)$, which transfers the particle from site 0 to site α, can be evaluated exactly as soon as the *number* of walks of a given length on the lattice is known, even when $[\mathsf{A}, \mathsf{B}_d] \neq 0$. Firstly, we consider the isotropic case where $\mathsf{B} = \mathsf{B}_d$ is identical along all dimensions. Secondly, we tackle the general non-isotropic case with arbitrary jump operators. We give examples of isotropic and non-isotropic quantum random walks.

4.2.1 Isotropic case

In the isotropic case we consider a particle with m internal levels which evolves according to the Hamiltonian

$$\mathsf{H} = \mathsf{A} \otimes \mathcal{I}_{\mathcal{L}} + \mathsf{B} \otimes \sum_d \Delta_d, \tag{4.42}$$

where Δ_d are the jump operators on the lattice along dimension d. Jumps between non-nearest neighbours are accounted for by adding edges to the lattice, linking pairs of sites between which jumps are allowed. The lattice so obtained is denoted $\mathcal{L}$ and its adjacency matrix is simply $\sum_d \Delta_d$. The matrices A and B are arbitrary possibly non-commuting $k \times k$ matrices that act on the internal degree of freedom of the particle.

Following the terminology of §4.1.1, the statics represent the action of the Hamiltonian on the particle when it is static on a lattice site α. When calculating $\mathsf{U} = \exp[-i\mathsf{H}t]$, the static is thus $-i\mathsf{A}$. Similarly, the flips represent the action of the Hamiltonian on the particle when it jumps from a site to another, here this is $-i\mathsf{B}$. Let α be a site of the lattice and 0 the site on which the particle is initially located. Then the conditional evolution operator $\mathsf{U}_{\alpha\leftarrow 0}(t)$ is a $k \times k$ matrix acting on the internal degree of freedom of the particle and which specifies only the initial and final sites of the particle. We evaluate $\mathsf{U}_{\alpha\leftarrow 0}(t)$ in the Laplace domain, see §4.1.4. Noting that the Hamiltonian is isotropic, we find the contribution $\mathrm{W}[w_\ell] = (s\mathsf{I}_\sigma + \mathrm{i}\mathsf{A})^{-1}\big[-\mathrm{i}\mathsf{B}(s\mathsf{I}_\sigma + \mathrm{i}\mathsf{A})^{-1}\big]^\ell$ of any walk of length ℓ to be identical. Therefore the walk-sum expression for $\tilde{\mathsf{U}}_{\alpha\leftarrow 0}(s)$, Eq (4.20), simplifies to

$$\tilde{\mathsf{U}}_{\alpha\leftarrow 0}(s) = (s\mathsf{I}_\sigma + \mathrm{i}\mathsf{A})^{-1} \sum_\ell |W_{\mathcal{L};\alpha 0;\ell}| \big[-\mathrm{i}\mathsf{B}(s\mathsf{I}_\sigma + \mathrm{i}\mathsf{A})^{-1}\big]^\ell, \tag{4.43}$$

where $|W_{\mathcal{L};\alpha 0;\ell}| \equiv \#W_{\mathcal{L};\alpha 0;\ell}$ is the *number* of walks of length ℓ from site 0 to site α on $\mathcal{L}$. This quantity is analytically known for various lattices among which, the infinite path-, square and cubic lattices, the infinite triangular, honeycomb and dice lattices and finite path-, circular-, complete and hypercubic lattices. Therefore, when the number of walks is known, the sum of Eq.(4.43) is analytically available. Otherwise, the number of walks can be found numerically in $O(N^3)$ operations by computing powers of the adjacency matrix of the lattice [20]. The result of Eq.(4.43) solves continuous time isotropic quantum random walk over any lattice with arbitrary coupling between internal and external dynamics, and remains valid when $[\mathsf{A}, \mathsf{B}] \neq 0$.

Remark 4.2.1 (Isotropic commuting case)**.** In the case A and B commute, we can evaluate the conditional evolution operator directly in the time domain

$$\mathsf{U}_{\alpha\leftarrow 0}(t) = e^{-\mathrm{i}\mathsf{A}t} \sum_\ell |W_{\mathcal{L};\alpha 0;\ell}| \frac{t^\ell}{\ell!} (-\mathrm{i}\mathsf{B})^\ell. \tag{4.44}$$

In this situation, the conditional evolution operator is the exponential generating function of $\{W_{\mathcal{L};\alpha 0;\ell}\}_{0\leq\ell}$ evaluated at $-\mathrm{i}\mathsf{B}t$.

Example 4.2.1 (Isotropic commuting quantum random walk on square lattices)**.** As a simple example of isotropic quantum random-walk, consider a spin one particle living on a square lattice $\mathcal{L}$. The Hamiltonian we consider is

$$\mathsf{H} = \delta\, \mathsf{I}_\sigma \otimes \mathsf{I}_{\mathcal{L}} + J\, \mathsf{J}_x \otimes \Delta_{\mathcal{L}}, \tag{4.45}$$

with δ and J real parameters, I_σ and $\mathsf{I}_{\mathcal{L}}$ respectively the identity operator on the internal and external degrees of freedom. The operator $\Delta_{\mathcal{L}}$ is responsible for the particle jumps on the lattice, its matrix representation is provided by the adjacency matrix of $\mathcal{L}$. Finally, J_x is the spin-1 matrix along x. The term $\mathsf{J}_x \otimes \Delta_{\mathcal{L}}$ therefore connects the internal and external dynamics of the particle. The walk is nonetheless isotropic and, since $[\mathsf{I}_\sigma, \mathsf{J}_x] = 0$, we can use Eq. (4.44) to evaluate $\mathsf{U}(t)$.

First, we consider the case where the lattice is infinite, i.e. $\mathcal{L} \equiv \mathbb{Z}^2$. On this lattice, the number of walks of length $2\ell + |x| + |y|$ between the initial site 0 and a site with lattice coordinates (x, y) is $|W_{\mathcal{L};\,(x,y)0;\,2\ell+|x|+|y|}| = \binom{2\ell+|x|+|y|}{\ell}\binom{2\ell+|x|+|y|}{\ell+|x|}$. Supposing $J > 0$ without loss of generality we easily evaluate Eq.(4.44) and find the evolution operator to be

$$\begin{aligned}\langle x, y|\mathsf{U}(t)|0\rangle = e^{-\mathrm{i}\delta t}\delta_{x,0}\delta_{y,0}(\mathsf{I} - \mathsf{J}_x^2) + \\ e^{-\mathrm{i}\delta t}(-\mathrm{i})^{|x|+|y|}\mathfrak{J}_{|x|}(2Jt)\,\mathfrak{J}_{|y|}(2Jt)\big(\delta_{|x|+|y|,\mathrm{Odd}}\,\mathsf{J}_x + \delta_{|x|+|y|,\mathrm{Even}}\,\mathsf{J}_x^2\big),\end{aligned} \tag{4.46}$$

where $\mathfrak{J}_a(x)$ is the Bessel-J function with parameter a and δ is the Kronecker delta function. The Bessel-J function is a signature of the ballistic spread of the wave packet throughout the lattice [98]. Finally, we observe that if the particle is initially in the internal state $|\psi(0)\rangle$ with $\langle\psi(0)|\mathsf{J}_x|\psi(0)\rangle = 0$, then the evolution operator creates a kind of antiferromagnet: the spin configuration of sites located at an odd Manhattan distance from the initial site is orthogonal to that of the sites located at an even distance.

We now turn to the finite lattice case. Let N_x be the number of sites in the x direction and N_y the number of sites in the y direction. We label the sites of the lattice with their coordinates, the initial site being (x_0, y_0). The number of walks of any length from the initial site to any site $(x_0, y_0) \to (x, y)$ is found either via direct diagonalisation of the adjacency matrix $\Delta_{\mathcal{L}}$ or via the inverse Z-transform of the lattice walk-generating functions. Both approaches yield

$$\begin{aligned}|W_{\mathcal{L};\,(x,y)\leftarrow(x_0,y_0);\,\ell}| = \frac{2^{\ell+2}}{(N_x+1)(N_y+1)}\sum_{j=1}^{N_x}\sum_{j'=1}^{N_y}\sum_{k=0}^{\ell}\binom{\ell}{k}\cos\big(\frac{\pi j}{N_x+1}\big)^{\ell-k}\cos\big(\frac{\pi j'}{N_y+1}\big)^{k} \\ \times\sin\big(\frac{x\,\pi j}{N_x+1}\big)\sin\big(\frac{x_0\,\pi j}{N_x+1}\big)\sin\big(\frac{y\,\pi j'}{N_y+1}\big)\sin\big(\frac{y_0\,\pi j'}{N_y+1}\big).\end{aligned} \tag{4.47}$$

The evolution operator then follows from Eq. (4.44):

$$\langle x,y|\mathsf{U}(t)|x_0,y_0\rangle = e^{-\mathrm{i}\delta t}\sum_{j=1}^{N_x}\sum_{j'=1}^{N_y} S_{x,x_0}(j)S_{y,y_0}(j')\times \tag{4.48}$$
$$\Big[\mathsf{I}-\mathrm{i}\mathsf{J}_x\sin\big(2\,C_x t+2\,C_y t\big)-2\,\mathsf{J}_x^2\sin^2\big(C_x t+C_y t\big)\Big],$$

with $C_x=\cos(\frac{\pi j}{N_x+1})$, $C_y=\cos(\frac{\pi j'}{N_y+1})$, $S_{x,x_0}(j)=\sin\big(\frac{x\,\pi j}{N_x+1}\big)\sin\big(\frac{x_0\,\pi j}{N_x+1}\big)$ and $S_{y,y_0}(j')=\sin\big(\frac{y\,\pi j'}{N_y+1}\big)\sin\big(\frac{y_0\,\pi j'}{N_y+1}\big)$.

Example 4.2.2 (Isotropic non-commuting quantum random walk on the triangular lattice)**.** Consider a spin-1/2 particle living on an infinite triangular lattice, located initially on site $(0,0)$. The particle is subjected to the following Hamiltonian

$$H = J\sigma_z\otimes\mathsf{I}_{\mathcal{L}}+\sigma_x\otimes\mathsf{T} \tag{4.49}$$

where J is a real number, $\sigma_{x,z}$ are Pauli matrices, T is the matrix representation of the nearest neighbour jump operator on the triangular lattice, i.e. the adjacency matrix of the lattice. The interest of the walk considered here lies in that the contribution of odd and even length walks is proportional to σ_x and I_σ, respectively. Therefore, we expect that the propagation of a particle initially localised on a single site will depend strongly on its spin state. We shall see that this is indeed the case.

The Hamiltonian of Eq. (4.49) describes an isotropic quantum random walk, but since $[\sigma_z,\sigma_x]\neq 0$, we must use Eq. (4.43) rather than Eq. (4.44). We find

$$\mathsf{U}(t) = \mathcal{L}^{-1}\Big[\sum_n [s\mathsf{I}_\sigma+\mathrm{i}\sigma_z]^{-1}\Big(-\mathrm{i}\sigma_x[s\mathsf{I}_\sigma+\mathrm{i}\sigma_z]^{-1}\Big)^n\otimes\mathsf{T}^n\Big]_t, \tag{4.50a}$$
$$= \mathcal{L}^{-1}\Big[(s\mathsf{I}_\sigma-\mathrm{i}\sigma_z)\otimes\big((1+s^2)\mathsf{I}_{\mathcal{L}}+\mathsf{T}^2\big)^{-1}-\mathrm{i}\sigma_x\otimes\mathsf{T}\big((1+s^2)\mathsf{I}_{\mathcal{L}}+\mathsf{T}^2\big)^{-1}\Big]_t, \tag{4.50b}$$
$$= \mathsf{I}_\sigma\otimes\cos(\mathsf{E}t)-\mathrm{i}J\sigma_z\otimes\sin(\mathsf{E}t)\mathsf{E}^{-1}-\mathrm{i}\,\sigma_x\otimes\mathsf{T}\sin(\mathsf{E}t)\mathsf{E}^{-1}, \tag{4.50c}$$

with $\mathsf{E}^2=J^2\mathsf{I}_{\mathcal{L}}+\mathsf{T}^2$. It will not be necessary to determine whether $J^2\mathsf{I}_{\mathcal{L}}+\mathsf{T}^2$ has a square root and, if so, which square root one should use for E. Indeed power series expansions of $\cos(\mathsf{E}t)$ and $\sin(\mathsf{E}t)\mathsf{E}^{-1}$ only involves even powers of E and the square-root really never appears in the calculations. The operators on the spatial degree of freedom are given by

$$\langle x,y|\cos(\mathsf{E}t)|0,0\rangle = \sum_{n=0}^{\infty}\frac{(\mathrm{i}t)^{2n}}{2n!}c_n(x,y), \tag{4.51a}$$
$$\langle x,y|\mathrm{i}\sin(\mathsf{E}t)\mathsf{E}^{-1}|0,0\rangle = \sum_{n=0}^{\infty}\frac{(\mathrm{i}t)^{2n+1}}{(2n+1)!}c_n(x,y), \tag{4.51b}$$
$$\langle x,y|\mathrm{i}\mathsf{T}\sin(\mathsf{E}t)\mathsf{E}^{-1}|0,0\rangle = \sum_{n=0}^{\infty}\frac{(\mathrm{i}t)^{2n+1}}{(2n+1)!}C_n(x,y), \tag{4.51c}$$

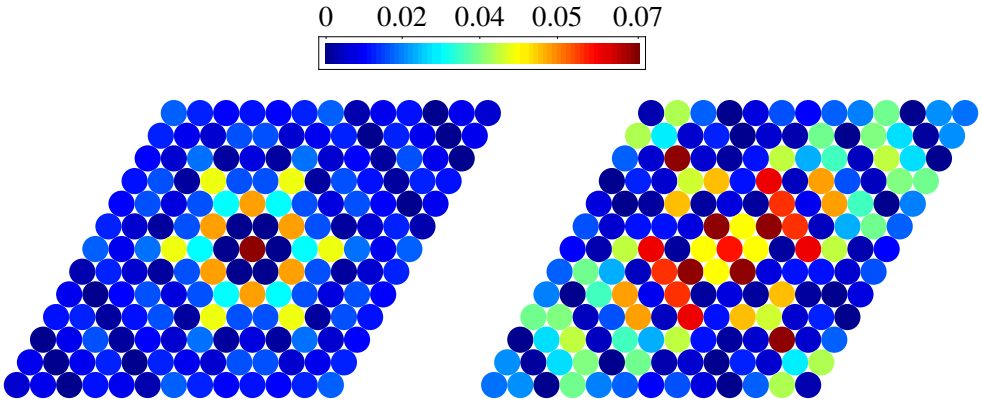

Figure 4.4: Probabilities $\Pr[\uparrow_z]$ (left) and $\Pr[\downarrow_z]$ (right) after a time $t/J = 3\pi/2$. The lattice is infinite, but only those sites with $(x, y) \in [-6, 6]$ are represented. The initial site $(0, 0)$ is the central site of the figures. For clarity we have truncated the colorscheme at 0.07 and $\Pr[\uparrow_z]$ goes up to 0.12 on the central site 0, and $\Pr[\downarrow_z]$ goes up to 0.3 on the neighbours of 0.

with $c_n(x, y)$ the number of walks of length n from vertex $(0, 0)$ to vertex (x, y) on a lattice whose weighted adjacency matrix is $J^2\mathsf{I}_\sigma + \mathsf{T}^2$ and $C_n(x, y) = c_n(x + 1, y) + c_n(x - 1, y) + c_n(x, y + 1) + c_n(x, y - 1) + c_n(x - 1, y - 1) + c_n(x + 1, y + 1)$. These quantities are known analytically, e.g.

$$c_n(x, y) = \sum_{q=0}^{n} \binom{n}{q} J^{2n-2q} \sum_{k=0}^{2n} (-2)^{2n-k} \binom{2n}{k} \sum_{j=0}^{k} \binom{k}{j} \binom{k}{j - x - y} \binom{k}{j - x}. \quad (4.52)$$

In spite of this, the power series of Eqs. (4.51) have no known closed form. They can nonetheless be computed to very high accuracy.

On Fig. (4.4) we show the probabilities $\Pr[\uparrow_z]$ and $\Pr[\downarrow_z]$ that a particle, initially located on site 0 with its spin up along z, be found to have spin up along z and down along z, respectively. We observe that the particle propagation through the lattice strongly depends on its spin state. For example, the probability that the particle be found up along z on the neighbours of the initial site 0 is $\sim 1.5 \times 10^{-5}$ after $t/J = 3\pi/2$. This is because most of the walks from 0 to its neighbours have an odd length, forcing the particle to flip its spin. Consequently, an up spin particle cannot propagate from site to site, rather it must tunnel to the second nearest neighbours of a site. For this reason, $\Pr[\uparrow_z]$ on site 0 decays slowly, while $\Pr[\downarrow_z]$ is found to be sizable far from the initial site. If the particle spin is initially up along x, then both odd and even length walks leave the spin unchanged and one could expect a ballistic propagation of the unimpeded spin. However, the statics of the Hamiltonian are $J\sigma_z$ and the particle evolves rapidly into a superposition of up and down spin along x, see Fig. (4.5).

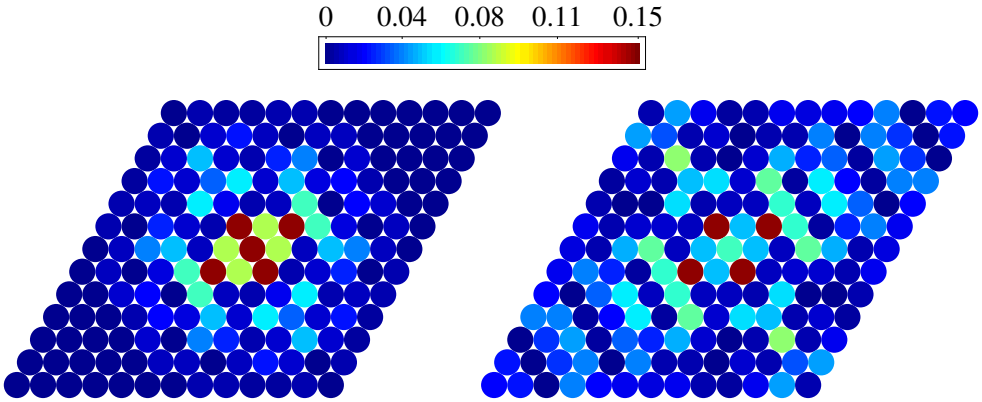

Figure 4.5: Probability $\Pr[\uparrow_x]$ that a particle, initially located on the central site 0 with spin up along x, be found to have its spin up along x after times $t/J = \pi/2$ (left) and $t/J = 3\pi/2$ (right).

4.2.2 Non-isotropic case

We now turn to non-isotropic quantum random walks. In this situation the contributions of all walks of a given length ℓ are not identical anymore. Rather, they depend on the length of the walk along each dimension since $\mathsf{B}_d \neq \mathsf{B}_{d'}$. Additionally, when $[\mathsf{B}_d, \mathsf{B}_{d'}] \neq 0$, the contribution of a walk also depends on the particular order with which jumps along each direction occur. For these reasons, the procedure we used in the isotropic case does not extend to the non-isotropic one. Instead we partition the Hamiltonian as a matrix of operators acting only on the external degree of freedom of the particle

$$\mathsf{H}_{ij} = a_{ij}\,\mathsf{I}_{\mathcal{L}} + \sum_d b_{d;ij}\,\Delta_d, \tag{4.53}$$

where $\mathsf{A} = (a_{ij})$ and $\mathsf{B}_d = (b_{d;ij})$ are the matrix representation of the operators A and B_d, respectively. Since the above representation of the Hamiltonian separates the internal (i.e. spin) degree of freedom from the external one, we call it a spin-partition of the Hamiltonian. If the flips and statics of the spin-partition are pairwise commuting, i.e. if all $[\Delta_d, \Delta_{d'}] = 0$, then the evolution operator is directly obtained as $\mathsf{U}(t) = \exp[-\mathrm{i}\mathsf{H}t]$ and will depend on functions $f\big(\Delta_d\big)$ of the Δ_d operators. In the situation where $[\Delta_d, \Delta_{d'}] \neq 0$ the matrix-exponential of the Hamiltonian is evaluated using path-sum, see §3.3.3. The functions $f(\Delta_d)$ are available analytically, at least as power-series, thanks to the highly structured nature of the jump operators Δ_d. In many cases, these series do not have known elegant closed forms but can be evaluated to high accuracy with little computational effort. Taken together these three steps yield the $k \times k$ conditional evolution operators $\mathsf{U}_{\alpha\leftarrow 0}(t)$ analytically. In the following, we give examples of non-isotropic quantum random walks.

4.2.3 Double jump quantum walk

For our first example, we consider a spin-1/2 particle living on an infinite 1D lattice. The particle, initially located on site 0 is subjected to the following Hamiltonian:

$$\mathsf{H}_{i,j,k} = J_0\,\sigma_i \otimes \mathsf{I}_x + J_1\,\sigma_j \otimes \Delta_x + J_2\,\sigma_k \otimes \Delta_{\langle\langle x\rangle\rangle}, \tag{4.54}$$

with $(i,j,k) \in [x,y,z]$ arbitrary, I_x the identity operator on the spatial degree of freedom, Δ_x the nearest neighbour jump operator and $\Delta_{\langle\langle x\rangle\rangle} = \sum_x |x+2\rangle\langle x| + |x\rangle\langle x+2|$ the second nearest neighbour jump operator. We shall consider here only the 24 interesting non-trivial cases where at least two of i,j,k are different. We obtain the solution via two different partitions of the Hamiltonian.

Spin-partition

We first use a spin-partition of the Hamiltonian to solve for the dynamics of the particle. This partition is obtained from the projector-lattices

$$\varepsilon_{\uparrow_z} = |\uparrow_z\rangle\langle\uparrow_z| \otimes \mathsf{I}_x, \quad \text{and} \quad \varepsilon_{\downarrow_z} = |\downarrow_z\rangle\langle\downarrow_z| \otimes \mathsf{I}_x, \tag{4.55}$$

where $\mathsf{I}_x = \sum_x |x\rangle\langle x|$ is identity operator on the spatial degree of freedom along direction x. These projector-lattices correspond to a tensor-product partition of the Hamiltonian. Choosing the spin quantisation axis to be z, we find the following flips and statics of the partition to be

$$\mathsf{H}_{\uparrow,\downarrow} = J_0\langle\uparrow_z|\sigma_i|\downarrow_z\rangle + J_1\langle\uparrow_z|\sigma_j|\downarrow_z\rangle\Delta_x + J_0\langle\uparrow_z|\sigma_k|\downarrow_z\rangle\Delta_{\langle\langle x\rangle\rangle}, \tag{4.56}$$

and similarly for $\mathsf{H}_{\downarrow,\uparrow}$, $\mathsf{H}_{\downarrow,\downarrow}$ and $\mathsf{H}_{\uparrow,\uparrow}$. Once again, the flips and statics are all pairwise commuting and we can exponentiate $\mathsf{H}_{i,j,k}$ directly in the time domain. The exact evolution operator is therefore

$$\mathsf{U}_{i,j,k}(t) = \cos(\mathsf{E}_{i,j,k}t)\mathsf{I}_\sigma - \mathrm{i}\big[J_0\sigma_i + J_1\sigma_j\Delta_x + J_2\sigma_k\Delta_{\langle\langle x\rangle\rangle}\big]\,\sin(\mathsf{E}_{i,j,k}t)\mathsf{E}^{-1}_{i,j,k}, \tag{4.57}$$

with $\mathsf{E}_{i,j,k}$ an operator acting on the spatial degree of freedom and which depends on (i,j,k):

$$\mathsf{E}^2_{i,j,k} = J_0^2\mathsf{I}_\mathcal{L} + J_1^2\Delta_x^2 + J_2^2\Delta^2_{\langle\langle x\rangle\rangle}\,, \qquad i\neq j\neq k \tag{4.58a}$$

$$\mathsf{E}^2_{i,j,j} = J_0^2\mathsf{I}_\mathcal{L} + \big(J_1\Delta_x + J_2\Delta_{\langle\langle x\rangle\rangle}\big)^2, \qquad i\neq j \tag{4.58b}$$

$$\mathsf{E}^2_{j,i,j} = J_1^2\Delta_x^2 + \big(J_0\mathsf{I}_\mathcal{L} + J_2\Delta_{\langle\langle x\rangle\rangle}\big)^2, \qquad i\neq j \tag{4.58c}$$

$$\mathsf{E}^2_{j,j,i} = J_2^2\Delta^2_{\langle\langle x\rangle\rangle} + \big(J_0\mathsf{I}_\mathcal{L} + J_1\Delta_x\big)^2, \qquad i\neq j. \tag{4.58d}$$

Functions of the above operators are known analytically through power series, even though these do not have elegant closed forms. For example,

$$\langle x|\cos(\mathsf{E}_{i,j,k}t)|0\rangle = \sum_{n=0}^{\infty}\frac{(\mathrm{i}t)^{2n}}{2n!}c_x^{i,j,k}(n), \tag{4.59a}$$

$$\langle x|\mathrm{i}\sin(\mathsf{E}_{i,j,k}t)\mathsf{E}_{i,j,k}^{-1}|0\rangle = \sum_{n=0}^{\infty}\frac{(\mathrm{i}t)^{2n+1}}{(2n+1)!}c_x^{i,j,k}(n), \tag{4.59b}$$

$$\langle x|\mathrm{i}\Delta_x\sin(\mathsf{E}_{i,j,k}t)\mathsf{E}_{i,j,k}^{-1}|0\rangle = \sum_{n=0}^{\infty}\frac{(\mathrm{i}t)^{2n+1}}{(2n+1)!}\Big(c_{x-1}^{i,j,k}(n)+c_{x+1}^{i,j,k}(n)\Big), \tag{4.59c}$$

$$\langle x|\mathrm{i}\Delta_{\langle\langle x\rangle\rangle}\sin(\mathsf{E}_{i,j,k}t)\mathsf{E}_{i,j,k}^{-1}|0\rangle = \sum_{n=0}^{\infty}\frac{(\mathrm{i}t)^{2n+1}}{(2n+1)!}\Big(c_{x-2}^{i,j,k}(n)+c_{x+2}^{i,j,k}(n)\Big), \tag{4.59d}$$

where $c_x^{i,j,k}(n) = \langle x|(J_0^2\mathsf{I}_{\mathcal{L}} + J_1^2\Delta_x^2 + J_2^2\Delta_{\langle\langle x\rangle\rangle}^2)^n|0\rangle$. Functions of $\mathsf{E}_{i,j,j}$, $\mathsf{E}_{j,i,j}$ and $\mathsf{E}_{j,j,i}$ are obtained similarly, we omit the details. Noting that $[\Delta_x, \Delta_{\langle\langle x\rangle\rangle}] = 0$ and that Δ_x and $\Delta_{\langle\langle x\rangle\rangle}$ are both $\mathcal{P}_\infty$-structured matrices, we find the following analytical closed forms for the quantities $c_x^{i,j,k}(n)$, $c_x^{i,j,j}(n)$ etc.

$$c_x^{i,j,k}(n) = \sum_{p_1,p_2=0}^{n}\binom{n}{p_1,p_2}J_0^{2(n-p_1-p_2)}J_1^{2p_1}J_2^{2p_2}\sum_{\substack{q=0\\ q/2\text{ even}\\ |x|-q\text{ even}}}^{2p_1+|x|}\binom{2p_1}{p_1-\frac{|x|-q}{2}}\binom{2p_2}{p_2-\frac{q}{4}}, \tag{4.60a}$$

$$c_x^{i,j,j}(n) = \sum_{p=0}^{n}J_0^{2(n-p)}\sum_{q=0}^{p}\binom{2p}{q}J_1^{2p-q}J_2^{q}\sum_{\substack{q'=-2q\\ q-q'/2\text{ even}\\ q-|x|+q'\text{ even}}}^{2q}\binom{2p-q}{p-\frac{q}{2}-\frac{|x|-q'}{2}}\binom{q}{\frac{q}{2}-\frac{q'}{4}}, \tag{4.60b}$$

$$c_x^{j,i,j}(n) = \sum_{p=0}^{n}\binom{n}{p}J_1^{2(n-p)}\sum_{q=0}^{2p}J_0^{2p-q}J_2^{q}\sum_{\substack{q'=0\\ q-q'/2\text{ even}\\ |x|-q'\text{ even}}}^{2q}\binom{2n-2p}{n-p-\frac{|x|-q'}{2}}\binom{q}{\frac{q}{2}-\frac{q'}{4}}, \tag{4.60c}$$

$$c_x^{j,j,i}(n) = \sum_{p=0}^{n}\binom{n}{p}J_2^{2(n-p)}\sum_{q=0}^{2p}\binom{2p}{q}J_0^{2p-q}J_1^{q}\sum_{\substack{q'=0\\ q-q'\text{ even}\\ |x|/2-q'/2\text{ even}}}^{2q}\binom{2n-2p}{n-p-\frac{|x|-q'}{4}}\binom{q}{\frac{q}{2}-\frac{q'}{2}}, \tag{4.60d}$$

where $\binom{n}{p_1,p_2}$ is a multinomial coefficient.

The diffusion of the particle through the lattice is here again strongly spin-dependent. Consider for example the j,i,j case, where the onsite and second nearest-neighbour jump amplitude matrices σ_j are the same while the first nearest neighbour jump amplitude matrix σ_i is different. In this situation, the contribution of odd and even length walks to $\mathsf{U}_{j,i,j}(t)$ is respectively proportional to σ_i and σ_j. Since sites located at odd distances from the initial site 0 can be reached only via odd length walks, a particle whose spin is initially up along i on 0 will be found to have its spin down along i on all odd-distance sites, see Fig. (4.6). A system comprising

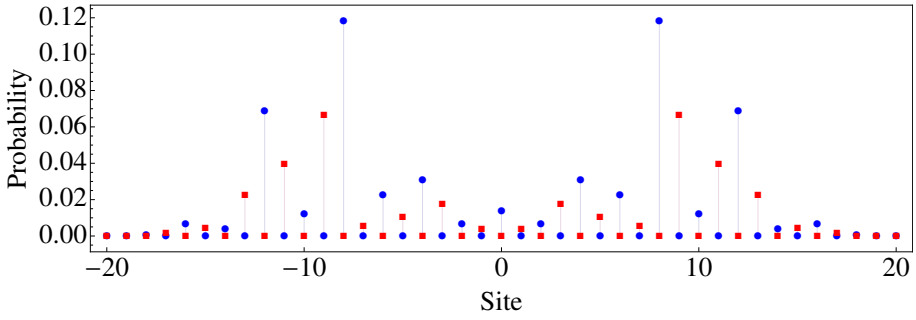

Figure 4.6: Probabilities that a particle, initially located on site 0 with its spin up along j and undergoing the double jump quantum walk, be found up along j (blue circles) or down along j (red squares). The up and down spin components of the wavepackets are completely separated over the lattice. Parameters $J_0 = J_2 \equiv J$, $J_1 = 2J$, $t/J = \pi$.

N particles undergoing the j, i, j double-jump dynamically evolves into a kind of antiferromagnet, in the absence of interactions !

Neighbour-partition

Alternatively, we may solve this quantum random walk with path-sum, partitioning the Hamiltonian into blocks grouping two neighbouring sites. In this case the statics are all

$$\mathsf{H}_S = \begin{pmatrix} J_0\sigma_i & J_1\sigma_j \\ J_1\sigma_j & J_0\sigma_i \end{pmatrix}, \tag{4.61a}$$

and the flips are

$$\mathsf{H}_F = \begin{pmatrix} J_2\sigma_k & 0 \\ J_1\sigma_j & J_2\sigma_k \end{pmatrix}. \tag{4.61b}$$

The Hamiltonian is therefore a tridiagonal block matrix and the graph of the partition is a weighted infinite path-graph with loops on all vertices. These have weights H_S while edges from left to right and from right to left have weight H_F and $\mathsf{H}_F^\dagger$, respectively. Let 0 be any vertex of the graph. We label vertices of the graph from 0 onwards with $\alpha \in \mathbb{Z}$, $\alpha < 0$ being on the left of 0. Since the graph has the structure of the infinite path-graph, the Green's functions are given by

$$\mathsf{G}(s;0,0) = \left[s\mathsf{I} - \mathsf{H}_S - \mathsf{H}_F\mathsf{Q}^\dagger\mathsf{H}_F^\dagger - \mathsf{H}_F^\dagger\mathsf{Q}\mathsf{H}_F\right]^{-1}, \tag{4.62a}$$

$$\mathsf{G}(s;0,|\alpha|) = (\mathsf{Q}\mathsf{H}_F)^{|\alpha|}\,\mathsf{G}(s;0,0), \tag{4.62b}$$

$$\mathsf{G}(s;0,-|\alpha|) = (\mathsf{Q}^\dagger\mathsf{H}_F^\dagger)^{|\alpha|}\,\mathsf{G}(s;0,0), \tag{4.62c}$$

where Q is a solution of the quadratic matrix equation $(s\mathsf{I} - \mathsf{H}_S)\mathsf{Q} - \mathsf{H}_F^\dagger\mathsf{Q}\mathsf{H}_F\mathsf{Q} = \mathsf{I}$ [108]. Noting that the Hamiltonian is an infinite block circulant matrix, we obtain

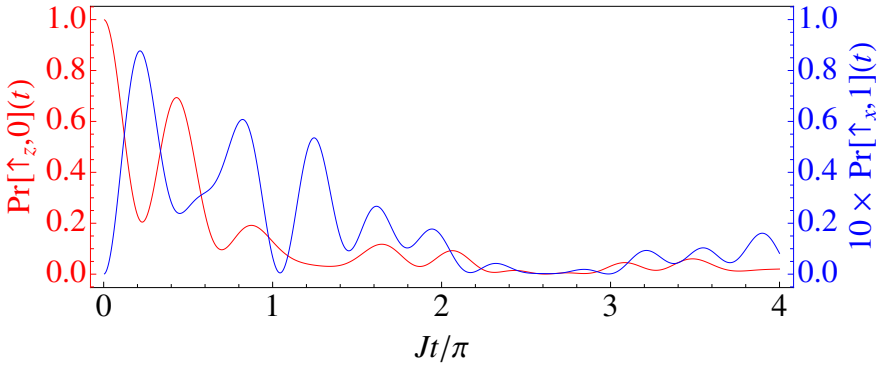

Figure 4.7: Probabilities $\Pr[\uparrow_z, 0](t)$ and $\Pr[\uparrow_x, 1](t)$ as a function of time, parameters in the text.

$\mathsf{G}(s;0,\alpha)$ from the results of [109] as

$$\mathsf{G}(s;0,\alpha) = \frac{(-1)^\alpha}{2\pi \mathrm{i}} \oint z^{\alpha-1}\big(s\mathsf{I} - \mathsf{H}_S + z^{-1}\mathsf{H}_F e^{-2\mathrm{i}\pi\theta} + z\mathsf{H}_F^\dagger\big)^{-1} dz, \tag{4.63}$$

where the contour is the unit circle $|z| = 1$. Computing the Green's functions $\mathsf{G}(s;0,\alpha)$ for specified i, j and k is easily performed with Eq. (4.63). The conditional evolution operators then follow according to §3.3.3: $\mathsf{U}_{\alpha\leftarrow 0}(t) = \mathcal{L}^{-1}\big(\mathsf{G}(s;0,\alpha)\big)_{-\mathrm{i}t}$. When working out examples we found that performing the inverse Laplace transform before the contour integration leads to faster and more stable computations than evaluating the contour integral first.

As an example, consider the case where $J_0 = J_1 = J_2 \equiv J$ and $i = z$, $j = x$, $k = y$. A spin-1/2 particle is initially localised on a lattice site 0 and with spin up along z. Suppose that we are interested in the time-evolution of the probabilities that the spin be found up along z on the same site, denoted $\Pr[\uparrow_z, 0](t)$, and that it be found up along x on a neighbouring site, denoted $\Pr[\uparrow_x, 1](t)$. We calculate these quantities from $\mathsf{U}_{0\leftarrow 0}(t)$ and $\mathsf{U}_{1\leftarrow 0}(t)$. The full solution is obtained analytically, but is cumbersome and will not be reproduced here. The dynamics of $\Pr[\uparrow_z, 0](t)$ and $\Pr[\uparrow_x, 1](t)$ is shown on Fig. 4.7.

Remark 4.2.2 (Finite lattice)**.** The finite lattice case can also be tackled with a neighbour-partition and using path-sums. In this case however, $\mathsf{G}(s;0,\alpha)$ is obtained as a matrix-valued continued fraction of finite depth, for which we do not know any elegant form. Imposing periodic boundary conditions however, the Hamiltonian is seen to be a finite block circulant matrix and $\mathsf{G}(s;0,\alpha)$ is obtained again from the results of [109].

4.2.4 Dirac dynamics on a lattice

In this last example, we apply the techniques developed so far to solve the 1D lattice Dirac equation. The relativistic electron obeying this equation lives on a quantised

space and cannot be localised to within less than a non-zero length δx. As we shall see, this leads to interesting connections between the maximum speed of quantum evolution and the speed of light, and Zitterbewegung and spin.

Solution to the 1D Dirac equation

The 1D lattice Dirac equation with no potential reads in Hamiltonian form[4]

$$\mathsf{H}\psi = \left\{ -\mathrm{i}\hbar c \begin{pmatrix} 0 & \sigma_x \mathsf{d}_x \\ \sigma_x \mathsf{d}_x & 0 \end{pmatrix} + \begin{pmatrix} \mathsf{I}_\sigma m_0 c^2 & 0 \\ 0 & -\mathsf{I}_\sigma m_0 c^2 \end{pmatrix} \right\} \psi = \mathrm{i}\hbar\, \partial_t \psi. \tag{4.64}$$

where $\mathsf{d}_x = \delta_x^{-1}(|x\rangle\langle x+1| - |x\rangle\langle x-1|)$ is the discretised derivative and δ_x the minimum localisation length. We recognize that the Dirac Hamiltonian is a quantum random walk Hamiltonian, the walk being performed by a physical entity with 4 internal levels: the electron-positron pair. Since $[\mathsf{I}_\sigma, \sigma_x] = 0$, the evolution operator is obtained directly from a spin-partition as $\mathsf{U}_{\mathrm{Dirac}}(t) = e^{-\mathrm{i}\mathsf{H}t/\hbar}$. This is

$$\mathsf{U}_{\mathrm{Dirac}}(t) = \\ \begin{pmatrix} \cos(\frac{t}{\hbar}\mathsf{E}_{1\mathrm{D}})\,\mathsf{I}_\sigma - \mathrm{i}\, m_0 c\, \sin(\frac{t}{\hbar}\mathsf{E}_{1\mathrm{D}})\mathsf{E}_{1\mathrm{D}}^{-1}\,\mathsf{I}_\sigma & -\mathrm{i}\,\mathsf{p}_x \sin(\frac{t}{\hbar}\mathsf{E}_{1\mathrm{D}})\mathsf{E}_{1\mathrm{D}}^{-1}\,\sigma_x \\ -\mathrm{i}\,\mathsf{p}_x \sin(\frac{t}{\hbar}\mathsf{E}_{1\mathrm{D}})\mathsf{E}_{1\mathrm{D}}^{-1}\,\sigma_x & \cos(\frac{t}{\hbar}\mathsf{E}_{1\mathrm{D}})\,\mathsf{I}_\sigma + \mathrm{i}\, m_0 c\, \sin(\frac{t}{\hbar}\mathsf{E}_{1\mathrm{D}})\mathsf{E}_{1\mathrm{D}}^{-1}\,\mathsf{I}_\sigma \end{pmatrix}, \tag{4.65}$$

where $\mathsf{E}_{1\mathrm{D}} = c\sqrt{(m_0 c)^2 \mathsf{I}_{1\mathrm{D}} + \mathsf{p}_x^2}$ is the 1D relativistic kinetic energy operator and $\mathsf{p}_x = -\mathrm{i}\hbar\,\mathsf{d}_x$ is the discretised momentum operator along x.

Remark 4.2.3 (Relativistic kinetic energy operator)**.** As in example 4.2.3, only even powers of the relativistic kinetic energy operator are required to obtain $\mathsf{U}_{\mathrm{Dirac}}(t)$. However, this operator is of intrinsic interest and simple to obtain using path-sum or walk-sum. Thus we now derive its matrix elements. Using the path-sum result for the matrix powers §3.3.1, and noting that $(m_0 c)^2 \mathsf{I}_{1\mathrm{D}} + \mathsf{p}_x^2$ is an infinite block tridiagonal matrix we find

$$\langle 2\alpha|\mathsf{E}_{1\mathrm{D}}|0\rangle = m_0 c^2 A^{2\alpha} \frac{-(\alpha - \frac{3}{2})!}{2\sqrt{\pi}\,\alpha!}\; {}_2F_1(-\frac{1}{2}+\alpha, \frac{1}{2}+\alpha; 1+2\alpha; -4A^2), \tag{4.66}$$

with $\alpha = x/\delta_x$ the distance in units of δ_x, $A = \hbar/(2\delta x m_0 c)$ and ${}_2F_1$ is the Gauss hypergeometric function. Alternatively, we may obtain this operator as a walk-series. Indeed

$$\mathsf{E}_{1\mathrm{D}} = m_0 c^2 \sqrt{1 + \left(\frac{\mathsf{p}_x}{m_0 c}\right)^2} = m_0 c^2 \sum_{n=0}^{\infty} \frac{(-1)^n}{(1-2n)4^n} \binom{2n}{n} \left(\frac{\mathsf{p}_x}{m_0 c}\right)^{2n}. \tag{4.67}$$

The elements of $(\mathsf{p}_x/m_0 c)^{2n}$ are simply the number of walks between any two ver-

[4] In this section we let $\hbar$ appear explicitly to facilitate dimensional analyses and physical interpretations.

tices of the infinite path-graph with loops and edges weighting $2\mathrm{i}\hbar/(m_0 c\,\delta_x)$ and $-\mathrm{i}\hbar/(m_0 c\,\delta_x)$, respectively. Thus,

$$\langle 2\alpha|\left(\frac{\mathsf{p}_x}{m_0 c}\right)^{2n}|0\rangle = \left(\frac{-\mathrm{i}\hbar}{2\delta x m_0 c}\right)^{2n}(-1)^{n-\alpha}\binom{2n}{n-\alpha}. \tag{4.68}$$

Inserting this result in Eq. (4.67) yields Eq. (4.66). Interestingly, the series of Eq. (4.67) converges only when $|A| \leq 1/2$, that is $\delta x \geq \hbar/m_0 c = \lambda_e$, the electron Compton wavelength. We remark that the maximum speed of quantum evolution, derived from purely geometrical considerations on the structure of the Hilbert space [110, 111], imposes that a particle which cannot be localised to within less than δ_x cannot propagate faster than $|-\mathrm{i}\hbar/\delta x m_0|$. This is precisely the speed of light c if $\delta_x = \lambda_e$ is the Compton wavelength. In other terms, if massive particles cannot be localised to within less than their Compton wavelength, then the structure of the quantum Hilbert space bars them from propagating faster than light.

Eq.(4.66) is the exact analytical expression of the matrix elements of the fully relativistic kinetic energy operator. The formula fits perfectly numerical calculation for $\mathsf{E}_{1\mathrm{D}}$ on a quantised space. We also check that it fulfills the basic properties expected of $\mathsf{E}_{1\mathrm{D}}$. First, consider a particle at rest, that is $|\psi\rangle = \sum_\alpha \psi|\alpha\rangle$ is a constant throughout space. Then, using Eq.(4.68), we observe that $\mathsf{p}_x^{2n}|\psi\rangle = 0$ as expected. Thus it follows that $\mathsf{E}_{1\mathrm{D}}|\psi\rangle = m_0 c^2|\psi\rangle$, a result which we also obtain directly from Eq.(4.66). For a particle with non-zero momentum, it is also easy to verify that Eq.(4.66) yields the correct kinetic energy in the non-relativistic limit

$$\mathsf{E}_{1\mathrm{D}}|\psi\rangle = m_0 c^2\left(|\psi\rangle - \frac{\hbar^2}{2m_0}\mathsf{d}_x^2|\psi\rangle + ...\right). \tag{4.69}$$

Finally, the calculations presented here extend straightforwardly to finite lattices on using the results of 2.4.2.

We now return to the calculation of the Dirac evolution operator. We expand the sine and cosine functions appearing in Eq. (4.65) in terms of powers of p_x. Using Eq. (4.68), we find

$$\langle 2\alpha|\cos(\frac{t}{\hbar}\mathsf{E}_{1\mathrm{D}})|0\rangle = \frac{\Omega^\alpha}{S^\alpha}\sum_{n=0}^{\infty}(-S)^n\frac{(ct/\hbar)^{2n}}{(2n)!}\binom{n}{\alpha}Q_\alpha(n), \tag{4.70a}$$

$$\langle 2\alpha|\sin(\frac{t}{\hbar}\mathsf{E}_{1\mathrm{D}})\mathsf{E}_{1\mathrm{D}}^{-1}|0\rangle = \frac{\Omega^\alpha}{S^\alpha}\sum_{n=0}^{\infty}(-S)^n\frac{(ct/\hbar)^{2n+1}}{(2n+1)!}\binom{n}{\alpha}Q_\alpha(n), \tag{4.70b}$$

with $Q_\alpha(n) = {}_2F_1\big(\frac{1}{2}(\alpha-n), \frac{1}{2}(1+\alpha-n); 1+\alpha; 4\frac{\Omega^2}{S^2}\big)$, $\Omega = -\hbar^2/(2\delta x^2)$ and $S = m_0^2 c^2 + \hbar^2/\delta x^2$. The series of Eqs. (4.70) are very badly behaved, difficult to evaluate for large enough n and bear little resemblance to anything physical. For these reasons we recast these series into series of Bessel functions of the first kind $\mathfrak{J}_a(x)$, which

demonstrate the ballistic spread of the wavepacket

$$\langle 2\alpha|\cos(\frac{t}{\hbar}\mathsf{E}_{1\mathrm{D}})|0\rangle = S^{1/4}\sqrt{\frac{\pi ct}{2\hbar}}\sum_{k=0}^{\infty}\frac{(ct|\Omega|/2\hbar\sqrt{S})^{2k+\alpha}}{k!(k+\alpha)!}\mathfrak{J}_{2k+\alpha-\frac{1}{2}}(\sqrt{S}\frac{t}{\hbar}), \tag{4.71a}$$

$$\langle 2\alpha|\sin(\frac{t}{\hbar}\mathsf{E}_{1\mathrm{D}})\mathsf{E}_{1\mathrm{D}}^{-1}|0\rangle = -S^{-1/4}\sqrt{\frac{\pi ct}{2\hbar}}\sum_{k=0}^{\infty}\frac{(ct|\Omega|/2\hbar\sqrt{S})^{2k+\alpha}}{k!(k+\alpha)!}\mathfrak{J}_{2k+\alpha+\frac{1}{2}}(\sqrt{S}\frac{t}{\hbar}). \tag{4.71b}$$

The derivation of the above results, starting from Eqs. (4.70), is *extremely* involved and *very difficult* so it is not reproduced here[5]. The same derivation shows that the Dirac propagator matrix elements accept the following approximations when $\sqrt{S}(ct/\hbar) \gg 1$, i.e. the particle has spread over a region much larger than δx,

$$\langle 2\alpha|\cos(\frac{t}{\hbar}\mathsf{E}_{1\mathrm{D}})|0\rangle \simeq \mathfrak{J}_{\alpha}\left(\frac{|\Omega|}{\sqrt{S}}\frac{t}{\hbar}\right)\cos(\sqrt{S}\frac{t}{\hbar}-\alpha\frac{\pi}{2}), \tag{4.72a}$$

$$\langle 2\alpha|\sin(\frac{t}{\hbar}\mathsf{E}_{1\mathrm{D}})\mathsf{E}_{1\mathrm{D}}^{-1}|0\rangle \simeq \frac{1}{\sqrt{S}}\mathfrak{J}_{\alpha}\left(\frac{|\Omega|}{\sqrt{S}}\frac{t}{\hbar}\right)\sin(\sqrt{S}\frac{t}{\hbar}-\alpha\frac{\pi}{2}), \tag{4.72b}$$

$$\begin{aligned}\langle 2\alpha+1|\mathsf{p}_x\sin(\frac{t}{\hbar}\mathsf{E}_{1\mathrm{D}})\mathsf{E}_{1\mathrm{D}}^{-1}|0\rangle \simeq \mathrm{i}\sqrt{\frac{|\Omega|}{S}}\Bigg\{&\mathfrak{J}_{|\alpha|}\left(\frac{|\Omega|}{\sqrt{S}}\frac{t}{\hbar}\right)\sin(|\alpha|\frac{\pi}{2}-\sqrt{S}\frac{t}{\hbar})\\ &-\mathfrak{J}_{|\alpha+1|}\left(\frac{|\Omega|}{\sqrt{S}}\frac{t}{\hbar}\right)\sin(|\alpha+1|\frac{\pi}{2}-\sqrt{S}\frac{t}{\hbar})\Bigg\}.\end{aligned} \tag{4.72c}$$

These results demonstrate not only the ballistic spread of the wavepacket, but also the existence of Zitterbewegung even in the absence of interference between electron and positron degrees of freedom. Indeed the Bessel-J function represents the ballistically spreading envelop while the sine and cosine functions correspond to fast oscillations of the particle with frequency $\omega = c\sqrt{S}/\hbar$. To understand what this frequency is, remember that $S = m_0^2c^2 + \hbar^2/\delta x^2$: $\sqrt{S}$ is therefore the relativistic momentum of an electron-positron pair localised to within δx. In particular, if the pair cannot be localised to within less than an electron Compton-wavelength, i.e. if $\delta_x = \lambda_e$, we obtain $\omega = \sqrt{2}m_0c^2/\hbar$. This is just a factor of $\sqrt{2}$ under the known frequency for Zitterbewegung obtained from the usual Dirac equation on a continuous space $\delta_x = 0$. This discrepancy disappears in the presence of interferences between the negative and positive energy components in the same wavepacket, interferences required for the appearance of Zitterbewegung in the usual Dirac equation. In other terms, we found the interferences to beat at $2m_0c^2/\hbar$. Furthermore, in the limit $\delta x \to 0$, we found that only the oscillations present in the interfering terms survive, which explains why interference is required for Zitterbewegung in the absence of minimum localisation length, and why the frequency associated to Zitterbewegung is usually $2m_0c^2/\hbar$.

Originally, the existence of Zitterbewegung led Schrödinger to remark that an electron moving at the speed of light in a circular motion of radius $\lambda_e/2$ has exactly

[5]I would be more than happy to provide it if required.

the Zitterbewegung frequency and an angular momentum of $m_0c^2/\omega = \hbar/2$, which he interpreted as the electron spin. The problem with this argument was that, in the absence of minimum localisation length, Zitterbewegung exists only when both positive and negative energy components are present in the same wavepacket. Thus Schrödinger's idea fails to explain why spin, if originating from Zitterbewegung, exists and is important in non-relativistic quantum theory where positron components are negligible in electron wavepackets. For this reason the idea was abandoned. However, we demonstrated here that as soon as electrons cannot be localised to within less than a non-zero minimum length δx, then Zitterbewegung always exists, in particular in the non-relativistic limit, and Schrödinger's heuristic argument meets no contradiction.

Solutions to the 2D and 3D Dirac equations with non-zero minimum localisation length

Proceeding exactly as for the 1D Dirac equation, we find the dynamics of the relativistic particle on a 2D space to be

$$U^{\mathrm{2D}}_{\mathrm{Dirac}}(t) = \begin{pmatrix} \cos(\frac{t}{\hbar}\mathsf{E}_{\mathrm{2D}})\mathsf{I}_\sigma - \mathrm{i}\, m_0c\, \sin(\frac{t}{\hbar}\mathsf{E}_{\mathrm{2D}})\mathsf{E}^{-1}_{\mathrm{2D}}\mathsf{I}_\sigma & -\mathrm{i}\, \sin(\frac{t}{\hbar}\mathsf{E}_{\mathrm{2D}})\mathsf{E}^{-1}_{\mathrm{2D}}\,(\mathsf{p}_x\sigma_x + \mathsf{p}_y\sigma_y) \\ -\mathrm{i}\, \sin(\frac{t}{\hbar}\mathsf{E}_{\mathrm{2D}})\mathsf{E}^{-1}_{\mathrm{2D}}\,(\mathsf{p}_x\sigma_x + \mathsf{p}_y\sigma_y) & \cos(\frac{t}{\hbar}\mathsf{E}_{\mathrm{2D}})\mathsf{I}_\sigma + \mathrm{i}\, m_0c\, \sin(\frac{t}{\hbar}\mathsf{E}_{\mathrm{2D}})\mathsf{E}^{-1}_{\mathrm{2D}}\mathsf{I}_\sigma \end{pmatrix},$$

with $\mathsf{E}_{\mathrm{2D}} = c\sqrt{(m_0c)^2\mathsf{I}_{\mathrm{2D}} + \mathsf{p}_x^2 + \mathsf{p}_y^2}$, and the solution to the 3D Dirac equation reads

$$U^{\mathrm{3D}}_{\mathrm{Dirac}}(t) = \begin{pmatrix} \cos(\frac{t}{\hbar}\mathsf{E}_{\mathrm{3D}})\mathsf{I}_\sigma - \mathrm{i}\, m_0c\, \sin(\frac{t}{\hbar}\mathsf{E}_{\mathrm{3D}})\mathsf{E}^{-1}_{\mathrm{3D}}\mathsf{I}_\sigma & -\mathrm{i}\, \sin(\frac{t}{\hbar}\mathsf{E}_{\mathrm{3D}})\mathsf{E}^{-1}_{\mathrm{3D}}\,(\mathsf{p}_x\sigma_x + \mathsf{p}_y\sigma_y + \mathsf{p}_z\sigma_z) \\ -\mathrm{i}\, \sin(\frac{t}{\hbar}\mathsf{E}_{\mathrm{3D}})\mathsf{E}^{-1}_{\mathrm{3D}}\,(\mathsf{p}_x\sigma_x + \mathsf{p}_y\sigma_y + \mathsf{p}_z\sigma_z) & \cos(\frac{t}{\hbar}\mathsf{E}_{\mathrm{3D}})\mathsf{I}_\sigma + \mathrm{i}\, m_0c\, \sin(\frac{t}{\hbar}\mathsf{E}_{\mathrm{3D}})\mathsf{E}^{-1}_{\mathrm{3D}}\mathsf{I}_\sigma \end{pmatrix},$$

with $\mathsf{E}_{\mathrm{3D}} = c\sqrt{(m_0c)^2\mathsf{I}_{\mathrm{3D}} + \mathsf{p}_x^2 + \mathsf{p}_y^2 + \mathsf{p}_z^2}$. These propagators present no further difficulty than the 1D Dirac equation since functions of E_{2D} and E_{3D} are given by power series similar to that of Eqs. (4.71). Note, the values for the parameters Ω and S change to

$$S_{\mathrm{2D}} = m_0^2c^2 + \frac{\hbar^2}{\delta q^2},\ \Omega_{2D} = \frac{-\hbar^2}{2\delta q^2}, \tag{4.73a}$$

$$S_{\mathrm{3D}} = m_0^2c^2 + \frac{3\hbar^2}{2\delta q^2},\ \Omega_{3D} = \frac{-3\hbar^2}{4\delta q^2}, \tag{4.73b}$$

with $\delta q = \delta x = \delta y = \delta z$, is the minimum localisation length along each dimensions of our quantised space.

4.3 Dynamics of Rydberg-excited Mott-insulators

Physicists like to think that all you have to do is say, these are the conditions, now what happens next?

R. P. Feynman

In this final section we investigate the dynamics of systems of strongly interacting Rydberg-excited Mott insulators using the method of walk-sums. We are interested in determining the existence of crystalline dispositions of the Rydberg excitations as well as coherent crystalline dispositions of the excitations, known as supersolids. This new phase of matter, characterised by the simultaneous existence of both diagonal and off-diagonal long-range order, was first suggested to exist in Helium [112, 113, 114, 115]. Recent studies have shown that supersolid phases might be obtainable in optical-lattices [116, 117, 118]. In contrast to these results, the possible dynamical creation of supersolids remains largely unexplored [119]. A system ideally suited to study this question is that of Rydberg-excited atoms from a Mott insulator in an optical lattice. These are formed by laser driving in the presence of strong long-range dipole-dipole interaction. The interaction causes the excitation probability of an atom to either be inhibited (blockade) or be enhanced (antiblockade) depending on the presence of a nearby Rydberg-excited atom. Previously quantum computation and simulation schemes using similar effects have been proposed [120, 121, 122, 123, 124]. Subsequent studies have shown that crystalline dispositions of the Rydberg excitations could form the ground states of certain 1D and 2D lattices [125, 126, 127, 128] and could also be created dynamically [129, 130, 131]. Yet these studies have not found supersolidity and have been confined to specific parameter regimes.

In this section we explore both non coherent transient crystal phases in 1D and 3D and highly correlated supersolids in 2D lattices. In particular we show that the lowest order of walk-sums provides simple analytical insights into small time dynamics while higher orders allow us to simulate the system in strongly interacting, highly correlated situations. In the first sub-section below, we detail the physical model employed for the description of Rydberg excitation in Mott-insulators. We then implement the method of walk-sums to calculate the mean number of Rydberg-excited atoms throughout the lattice and their correlations. Second, we derive simple low-order walk-sum results for these quantities and demonstrate that Rydberg-excited 1D and 3D Mott insulators evolve over short times into crystalline dispositions of the Rydberg excitations. The third sub-section confirms these results using a walk-sum based mean-field like approximation of the dynamics. In particular, we show that some of the crystals can be selectively favored through the laser detuning. Finally, relying exclusively on walk-sums, we show that a 2D Mott insulator with 6600 atoms evolves over longer times into far from equilibrium transient supersolid states. We characterise these states by calculating their pressure, and first, second and fourth order correlation-functions.

4.3.1 Model system and implementation of walk-sum

We consider an ensemble of atoms that are prepared in the Mott-insulating phase with unit filling via a strong optical lattice comprising N sites. For simplicity, we consider the lattice to be isotropic with lattice spacing L. A laser, illuminating this lattice from the direction $\mathbf{d} = (\cos\phi\,\sin\theta)\mathbf{x} + (\sin\phi\,\sin\theta)\mathbf{y} + (\cos\theta)\mathbf{z}$ where e.g. $\mathbf{x}$ is the unit length vector in the x direction, drives the atoms from their ground state $|g\rangle$ to a highly-excited Rydberg state $|r\rangle$ with principal quantum number n. We assume that atomic transitions to other internal levels are negligible such that the atoms are well described by two-level systems. Two Rydberg atoms at lattice sites i and j interact via the long-range dipole-dipole interaction that is of the form [120]

$$A_{ij} = (4\pi\epsilon_0 R_{ij}^3)^{-1}\big[\boldsymbol{\mu_i}.\boldsymbol{\mu_j} - 3R_{ij}^{-2}(\boldsymbol{\mu_i}.\boldsymbol{R_{ij}})(\boldsymbol{\mu_j}.\boldsymbol{R_{ij}})\big], \tag{4.74}$$

with $\boldsymbol{R_{ij}}$ the relative distance between atoms i and j and $\boldsymbol{\mu_i}$ the dipole moment of atom i. We take all the dipoles to be parallel to the laser beam orientation $\mathbf{d}$, i.e. $\boldsymbol{\mu_i} = \mu_i\,\mathbf{d}$ with $\mu_i = \|\boldsymbol{\mu}_i\|$. Furthermore, the dipole moments of all atoms are identical $\mu_i = \mu_j \equiv \mu$ and equal to $\mu = (3/2)\mathsf{n}(\mathsf{n}-1)ea_0$ [132], with e the electron charge and a_0 the Bohr radius. The laser and dipole-dipole interactions we consider are in the MHz-GHz range and induce dynamics fast compared to incoherent processes and the motion of the atoms. These will limit the lifetime of Rydberg-excited quantum states created by fast laser pulses to several μs but can safely be neglected on the much shorter time scales considered here [133]. In this limit and with the rotating-wave approximation the atoms are described by the Hamiltonian [120]

$$\mathsf{H} = \sum_i \Big\{\Delta\mathsf{P}^i - \frac{1}{2}\Omega\,\sigma_x^i + \frac{1}{2}\sum_{j\neq i} A_{ij}\mathsf{P}^i\mathsf{P}^j\Big\}, \tag{4.75}$$

with Δ the laser detuning, Ω the Rabi-frequency, σ_x the Pauli matrix, $\mathsf{P}^i = |r_i\rangle\langle r_i|$ and, for later convenience $\mathsf{G}^i = \mathsf{I}^i - \mathsf{P}^i = |g_i\rangle\langle g_i|$, the projectors onto the Rydberg and ground states of atom i, respectively. For later convenience we also introduce the Rydberg-radius a_R as the distance between two excited atoms along direction $\mathbf{d}$ such that $|A(a_R)| = \Omega$. For linear, square and cubic lattices with a lattice spacing L, the ratio a_R/L characterises the strongly and weakly interacting regimes with $a_R/L \gtrsim 1$ and $a_R/L \lesssim 1$, respectively.

We are interested in the real time dynamics of the system governed by the Hamiltonian of Eq. (4.75) and in particular in the number of and correlations between Rydberg excitations throughout the lattice. Thus we will concentrate our computational efforts on calculating the Rydberg-fraction $f_R = \sum_j\langle\mathsf{P}_j\rangle/N$ and two-excitation correlation function $g_2(i,j) = \langle\mathsf{P}^i\mathsf{P}^j\rangle/\langle\mathsf{P}^i\rangle\langle\mathsf{P}^j\rangle$, also known as density-density correlation function. On an infinite lattice these quantities can be expressed simply in terms of two conditional expectation values: $\langle r_i/r_j\rangle$ and $\langle r_i/g_j\rangle$, the probabilities that atom i be excited knowing atom j is excited and knowing that it is in its ground-state, respectively. Indeed, translational symmetry implies that any atom has the same probability to be excited $\langle\mathsf{P}^i\rangle = \langle\mathsf{P}^j\rangle$, and therefore $f_R = \langle\mathsf{P}^i\rangle = \langle r_i/r_j\rangle\langle\mathsf{P}^j\rangle + \langle r_i/g_j\rangle\langle\mathsf{G}^j\rangle$.

Since all atoms are equivalent, in particular $i \equiv j$, the Rydberg-fraction becomes

$$f_R = \frac{\langle r_i/g_j\rangle}{1 - \langle r_i/r_j\rangle + \langle r_i/g_j\rangle}. \tag{4.76a}$$

Given that the two-excitation correlation function is $g_2(i,j) = \langle r_i/r_j\rangle f_R^{-1}$, it follows that

$$g_2(i,j) = \frac{\langle r_i/r_j\rangle}{\langle r_i/g_j\rangle}\big(1 - \langle r_i/r_j\rangle + \langle r_i/g_j\rangle\big). \tag{4.76b}$$

The conditional expectation values $\langle r_i/r_j\rangle$ and $\langle r_i/g_j\rangle$ are now obtained directly using walk-sum.

For the implementation of walk-sum, we choose S to be any one atom of an infinite lattice and assume that all atoms are initially in their ground state $|g\rangle$. We choose the projector-lattices to be tensor products of projectors P^i and G^i on S',

$$\varepsilon_{i_1\ldots i_n} = \otimes_{i_k\in S'\setminus\{i_1\ldots i_n\}}\mathsf{G}^{i_k}\ \otimes_{i_l\in\{i_1\ldots i_n\}\subseteq S'}\mathsf{P}^{i_l}\ \otimes \mathsf{I}_s. \tag{4.77}$$

The projector lattice $\varepsilon_{i_1\ldots i_n}$ projects S' in a state where all atoms at positions $i_1\ldots i_n$ are excited, and all other atoms of S' are in their ground state. With this definition, we find that the flips are given by

$$\mathsf{H}_{i_1\ldots i_{n\pm1}\leftarrow i_1\ldots i_n} = -\frac{1}{2}\,\Omega\,\mathsf{I}_s, \quad \text{and 0 otherwise,} \tag{4.78}$$

that is $\mathsf{H}_{\nu\leftarrow\mu} \neq 0$ if and only if ν differs from μ by exactly one spin flip. The evaluation of the statics yields

$$\mathsf{H}_{i_1\ldots i_n} = \Big(n\Delta + \frac{1}{2}\sum_{\substack{i_p\neq i_l\\(i_p,i_l)\in\{i_1\ldots i_n\}}} A_{i_p i_l}\Big)\,\mathsf{I}_s + \Big(\Delta + \sum_{i_l\in\{i_1\ldots i_n\}} A_{s i_l}\Big)\mathsf{P}^s - \frac{1}{2}\Omega\,\sigma_x^s. \tag{4.79}$$

The conditional expectation values $\langle r_s/r_j\rangle$ and $\langle r_s/g_j\rangle$ are calculated according to Eqs. (4.28) and (4.32),

$$\langle r_s r_j\rangle = \langle g_s|\sum_{\eta(j)}\mathsf{U}^\dagger_{g_s\to\eta(j)}\,\mathsf{P}^s\,\mathsf{U}_{\eta(j)\leftarrow g_s}|g_s\rangle, \tag{4.80a}$$

$$\langle r_j\rangle = \langle g_s|\sum_{\eta(j)}\mathsf{U}^\dagger_{g_s\to\eta(j)}\,\mathsf{U}_{\eta(j)\leftarrow g_s}|g_s\rangle, \tag{4.80b}$$

where the sums run over all configurations $\eta(j)$ of S' where atom j is excited. We compute the conditional evolution operators $\mathsf{U}_{\eta(j)\leftarrow g_s}$ in the Laplace domain via Eq. (4.20). For example, the conditional evolution operator $\tilde{\mathsf{U}}_{j\leftarrow g_s}$ with only atom j excited in the final configuration $\eta(j)$ of S' and for walks of length $\ell \leq 3$ is given

by

$$\tilde{\mathsf{U}}_{j\leftarrow 0}(s) \simeq \frac{\mathrm{i}\Omega}{2}\tilde{\mathsf{M}}_j\tilde{\mathsf{M}}_0 + \left(\frac{\mathrm{i}\Omega}{2}\right)^3 \sum_{\substack{p=1 \\ p\neq j,\, p\neq s}} \tilde{\mathsf{M}}_j(\tilde{\mathsf{M}}_0 + \tilde{\mathsf{M}}_{j,p})(\tilde{\mathsf{M}}_p + \tilde{\mathsf{M}}_j)\tilde{\mathsf{M}}_0, \tag{4.81}$$

where subscript 0 denotes the configuration with no excited atom. In this expression, the factors $\mathrm{i}\Omega/2$ and $(\mathrm{i}\Omega/2)^3$ come from the flips and $\tilde{\mathsf{M}}_{i_1\ldots i_n}(s) = \mathcal{L}\big[\exp[-\mathrm{i}\mathsf{H}_{i_1\ldots i_n}t]\big]$. The sum over p in Eq. (4.81) accounts for an up-spin in an intermediate configuration of S' that is not present in the initial and final configurations. Note that intermediate atomic-excitations are similar to virtual particles appearing in the Feynman diagrams of QED. In the following section we discuss the results we obtain for f_R and $g_2(s,j)$.

4.3.2 Lowest order results

The procedure presented in the preceding section allows us to simulate the dynamics of the system resulting from the full Hamiltonian. In order to study the dynamics over long times $t \gtrsim \pi/\Omega$ and deeply in the strongly interacting regime $L \ll a_R$, we find it necessary to take into account all walks up to length 6. Such evolution times are required to study the development of long-range correlations in 2D lattices and the apparition of transient supersolid states which we discuss in §4.3.4. Nevertheless, it is also useful to dispose of low order approximations of the dynamics that are valid over short times $t \lesssim \pi/\Omega$ and which can be obtained at little computational cost. Therefore in this section we explore the lowest order walk-sum approximations for the Rydberg fraction and density-density correlation function.

At the lowest order of walk-sum only those histories of S' that have the minimum possible number of jumps between the initial and final configurations are considered. First, for $\langle r_s/g_j\rangle$ we find according to Eqs. (4.80)

$$\langle r_s/g_j\rangle \;=\; \frac{\Omega^2}{\chi^2}\sin\left(\frac{\chi}{2}t\right)^2, \tag{4.82}$$

with $\chi^2 = \Delta^2 + \Omega^2$ the generalised Rabi frequency. This result can be understood using one-body physics. Indeed, in the case of $\langle r_s/g_j\rangle$, the history of S' with the smallest number of jump starts and ends on $|gg\ldots g\rangle$ and has no jumps at all, i.e. S' is frozen from 0 to t in $|gg\ldots g\rangle$. During this history, atom S evolves as an isolated 2-level atom whose transition is driven by a laser with detuning Δ and Rabi frequency Ω, hence Eq. (4.82). Second, in the case of $\langle r_s/r_j\rangle$ one must consider those final configurations of S' where j is excited. Since all the atoms of S' are initially in their ground state, at least j needs to undergo the transition $|g\rangle \to |r\rangle$ for the final configuration of S' to comprise j in its Rydberg state. Thus the lowest non-zero order is the first order, i.e. the shortest history of S' connecting the initial and final configurations has one jump $|gg\ldots g_j\ldots g\rangle \to |gg\ldots r_j\ldots g\rangle$ and the lowest order approximation of $\langle r_s/r_j\rangle$ is

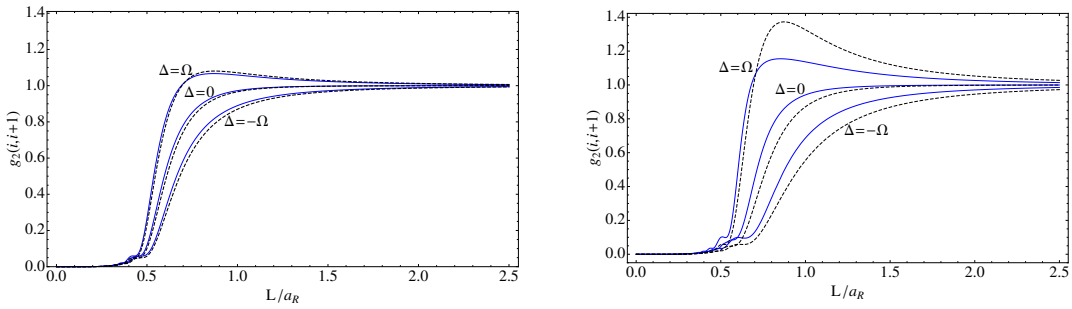

Figure 4.8: Density-density correlation function between nearest neighbours $g_2(i, i+1)$ on an infinite 1D lattice as a function of the lattice spacing in units of the Rydberg radius L/a_R, evaluated at the 1st order of walk-sum Eqs. (4.76b, 4.80,4.83b) (solid blue lines), and using the Ω-expansion (dashed black lines). The time is $t = \pi/4\Omega$ (left figure) and $t = \pi/2\Omega$ (right figure). The transition between the strongly and weakly interacting regimes clearly occurs around $L \simeq a_R$ as expected. Parameters $\boldsymbol{d} = \boldsymbol{z}$, $\mathsf{n} = 40$ and $\Omega = 30$MHz, which yields $a_R \simeq 13\mu$m.

$$\langle r_s/r_j\rangle = \frac{\langle g_s|\mathsf{U}_{0\to j}^\dagger \mathsf{P}_s \mathsf{U}_{j\leftarrow 0}|g_s\rangle}{\langle g_s|\mathsf{U}_{0\to j}^\dagger \mathsf{U}_{j\leftarrow 0}|g_s\rangle}, \tag{4.83a}$$

$$\mathsf{U}_{1\leftarrow 0}(t) = -\mathrm{i}\int_0^t e^{-\mathrm{i}\mathsf{H}_1(t-t_1)}\mathsf{H}_{1\leftarrow 0}e^{-\mathrm{i}\mathsf{H}_0 t_1}dt_1. \tag{4.83b}$$

Evaluating these expressions present no difficulty and yields the first order result for $\langle r_s/r_j\rangle$. This result is cumbersome and will not be reproduced here. Together with Eqs. (4.76) and (4.82), this provides the first order approximation to f_R and $g_2(s, j)$. We will discuss the result for f_R in the following section and for now we concentrate on the density-density correlation function $g_2(s, j)$. We show this quantity on Fig. 4.8 where we compare it to the prediction of the Ω-expansion [134], denoted $g_2(s, j)_\Omega$, which is a perturbative expansion of the density-density correlation function in Ω. The differences between the two grow with time and with the laser detuning. Indeed, for $t \gtrsim \pi/\Omega$ and/or $|\Delta| \gtrsim \Omega$, the Ω-expansion yields unrealistically large values for the density-density correlation function, typically in the $10^3 - 10^4$ range. This behavior is due to the Ω-expansion being valid only in the weakly interacting regime $L \gtrsim a_R$. Indeed we find that when $t \lesssim \pi/\Omega$, the Ω-expansion follows very closely

$$g_2(s, j)_\Omega \simeq \frac{\langle r_s/r_j\rangle}{\langle r_s/g_j\rangle}. \tag{4.84}$$

From Eq.(4.76b), we see that this estimation is correct only in the weakly interacting regime where $1 - \langle r_s/r_j\rangle + \langle r_s/g_j\rangle \simeq 1$, that is $\langle r_s/r_j\rangle - \langle r_s/g_j\rangle \simeq 0$. In particular this fails for $L \lesssim a_R$ and large laser detunings $|\Delta| \gtrsim \Omega$ because of strong blockade or antiblockade effects [135, 136, 130].

The interest of the density-density correlation function lies in that it qualifies

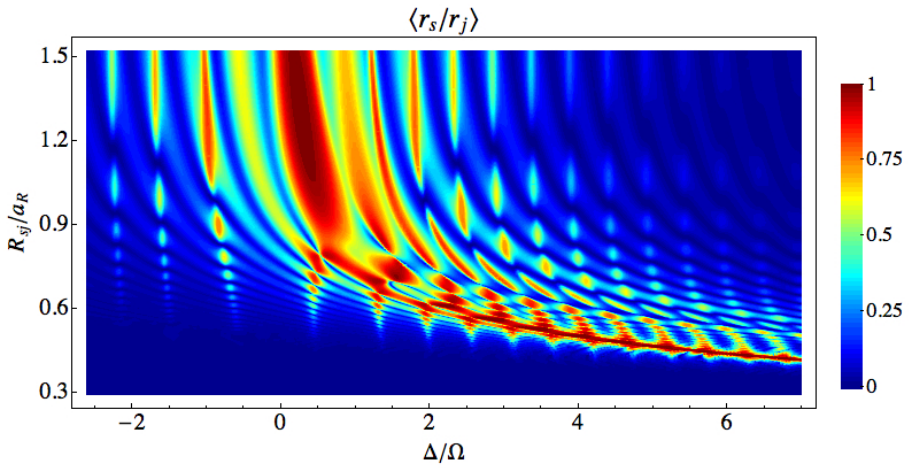

Figure 4.9: Conditional expectation value $\langle r_s/r_j\rangle$ after a laser pulse of duration $t = \pi/\Omega$ as a function of the laser detuning Δ and of the distance R_{sj} between atoms s and j in units of the Rydberg radius a_R. The oscillating behavior of $\langle r_s/r_j\rangle$ with R_{sj} is a signature of crystalline dispositions of Rydberg excitations in which both atoms s and j participate. Parameters: laser orientation $\boldsymbol{d} = \boldsymbol{z}$, $n = 40$ and $\Omega = 10$MHz.

the nature (liquid, crystal) of the disposition of Rydberg-excitations throughout the lattice. Indeed in the presence of a crystalline disposition of the excitations, the probability $\langle r_s/r_j\rangle$ for atom S to be excited knowing atom j is excited should be enhanced for sites j that participate in the crystal with S and depressed otherwise. Consequently, $\langle r_s/r_j\rangle$ should present peaks and valleys whose periodicity matches that of the crystalline dispositions of the excitations. We show on Fig.4.9 the first order result for $\langle r_s/r_j\rangle$ as a function of the detuning Δ and of the distance R_{sj} between atoms s and j. To verify the existence of transient crystalline dispositions of the Rydberg excitations as well as further explore their properties, we use a walk-sum based mean-field-like approach to the system dynamics. Before we do so however, we show that simple closed form expressions for f_R and $g_2(s,j)$ are available from pseudo 0^{th} order walk-sum results.

Remark 4.3.1 (Pseudo 0^{th} order results)**.** Consider the result for $\langle r_s/r_j\rangle$ in the limit where one approximates the integral of Eq.(4.83b) by the sole point $t_1 = 0$. In that case Eq.(4.83b) goes to the definite limit

$$\langle r_s/r_j\rangle = \frac{\Omega^2}{\chi_{sj}^2}\sin\left(\frac{\chi_{sj}}{2}t\right)^2, \tag{4.85}$$

where $\chi_{sj}^2 = (\Delta + A_{sj})^2 + \Omega^2$ is an effective generalised Rabi frequency with effective detuning $\Delta + A_{sj}$. Eq. (4.85) describes $\langle r_s/r_j\rangle$ as if S' had been static from 0 to t in the configuration $|gg\ldots r_j\ldots g\rangle$ and atom S had evolved accordingly, i.e. as an isolated atom whose transition is driven by a laser with effective detuning $\Delta + A_{sj}$ and Rabi frequency Ω. Eq.(4.85) is thus indeed a kind of 0^{th} order approximation of

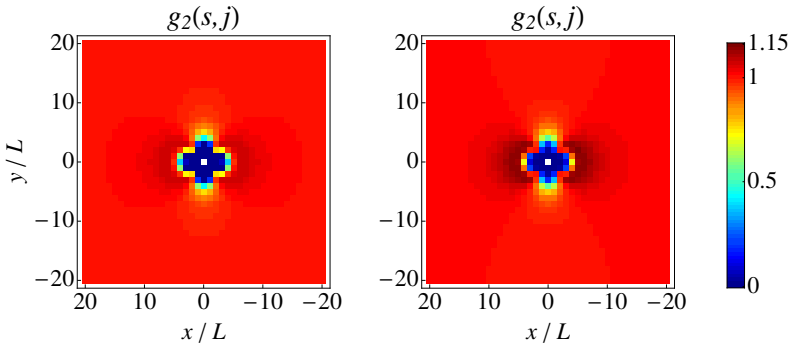

Figure 4.10: Two-body correlation-function $g_2(s,j)$ between the central atom S (white) and any other atom j in a $N \simeq 1700$ atoms square lattice, one atom / pixel. Left figure : lowest order Eq. (4.86b), right figure : converged 3rd order result, the two results are in good agreement. Parameters $\theta = \pi/2$, $\phi = 0$, $L = 2\mu$m, $\Delta = \Omega = 30$MHz and $t = \pi/2\Omega$.

$\langle r_s/r_j \rangle$. Eqs. (4.76) then give very simple expressions for the Rydberg fraction and two-excitations correlation function

$$f_R = \frac{(\Omega^2/\chi^2)\sin\left(\frac{\chi}{2}t\right)^2}{1 - \frac{\Omega^2}{\chi_{sj}^2}\sin\left(\frac{\chi_{sj}}{2}t\right)^2 + \frac{\Omega^2}{\chi^2}\sin\left(\frac{\chi}{2}t\right)^2}, \tag{4.86a}$$

$$g_2(s,j) = \frac{\chi^2 \sin\left(\frac{\chi_{sj}}{2}t\right)^2}{\chi_{sj}^2 \sin\left(\frac{\chi}{2}t\right)^2}\left[1 - \frac{\Omega^2}{\chi_{sj}^2}\sin\left(\frac{\chi_{sj}}{2}t\right)^2 + \frac{\Omega^2}{\chi^2}\sin\left(\frac{\chi}{2}t\right)^2\right]. \tag{4.86b}$$

We find Eq.(4.86b) to work well for small times $t \lesssim \pi/\Omega$ and in the weakly interacting regime or in strongly blockaded situations, where the probability of finding more than one excitation in the vicinity of S and j is small. This condition is easily fulfilled in 1D systems where we find indeed Eq. (4.86b) to yield similar results to the Ω-expansion [134] provided $|\Delta| \lesssim \Omega$ with $\Delta \leq 0$. Positive detunings in the strongly interacting regime $L \lesssim a_R$ lead to antiblockade effects which are largely missed by the zeroth order. The zeroth order result can be a good approximation for short times in higher dimensions as well, as shown on Fig. 4.10 where we compare Eq. (4.86b) to a converged 3rd order result over a 2D square lattice. We find however that the time spans over which zeroth order results are valid vary widely depending on the geometry and regime considered, e.g. in 3D antiblockade effects are inevitable and very important deep in the strongly interacting regime $L \ll a_R$, where the 0^{th} order result fails even for very short times. Finally, we remark that in spite of its simplicity, Eq. (4.86b) predicts a 2^{nd} order quantum phase transition with critical point $\Delta = \Omega = 0$, where g_2 is non-analytic. Additionally, the minimum distance separating two uncorrelated atoms, i.e. the correlation length, diverges as one approaches the critical point, another signature of phase transition. This transition was predicted in random clouds of atoms in [125] and corresponds to a

change of ground state, from a crystal of excitations in the positive detuning region to state $|gg\dots g\rangle$ for negative detunings. At the opposite of Eq.(4.86b), we consistently find Eq. (4.86a) to be a poor approximation of f_R as given by higher orders or by the mean-field-like approach of §4.3.3. This is because the pseudo 0^{th} order result Eq. (4.86a) depends explicitly on R_{sj} although, by translational symmetry of the infinite lattice, it should not. That is, Eq. (4.86a) breaks an important symmetry of the exact Eq.(4.76a).

4.3.3 Crystals of Rydberg excitations

We have seen the signature of crystals of Rydberg excitations through $g_2(s,j)$ at order 1. To confirm the apparition of these crystals, we perform a mean-field-like approximation of the exact Hamiltonian. This consists of simplifying the form of the interaction with [125]

$$A_{sj}\mathsf{P}^s\mathsf{P}^j \simeq A_{sj}\big(\mathsf{P}^s f_R + \mathsf{P}^j f_R - f_R^2\big)\, g_2(s,j). \tag{4.87}$$

Introducing this in the Hamiltonian of Eq. (4.75), we obtain a block diagonal mean-field Hamiltonian, each block being

$$\mathsf{H}_s(t) = \Delta\mathsf{P}_s - \frac{1}{2}\Omega\,\sigma_x^s + \sum_{j>s}\langle r_s/r_j\rangle A_{sj}\mathsf{P}_s, \tag{4.88}$$

where we used $f_R\, g_2(s,j) = \langle r_s/r_j\rangle$. Using walk-sum results for $\langle r_s/r_j\rangle$ the mean-field-like Hamiltonian above is completely determined. We solve the resulting time-dependent Schrödinger equation numerically and, by translational symmetry of the infinite lattice, we obtain the Rydberg fraction as $f_R = \langle\mathsf{P}^s\rangle$. We observe that for $t \lesssim \pi/\Omega$ and $L \gtrsim a_R$, the mean-field-like Rydberg fraction is nearly indistinguishable from the first-order walk-sum result for f_R. The two differ however in the strongly interacting regime where higher orders are required to obtain similar f_R from walk-sum.

We investigate the existence of crystalline disposition of Rydberg excitations from the mean-field-like approach by calculating f_R as a function of the laser detuning in the strongly interacting regime $L < a_R$. Indeed, due to the inter-atomic interactions, we expect atoms participating in a crystal $\mathcal{L}_\kappa$ where Rydberg excitations are located every κ sites to perceive this crystal with an effective detuning of $\Delta_{\text{eff}} = \Delta + \sum_{(j,k)\in\mathcal{L}_\kappa} A_{jk}$. When the laser detuning is such that $\Delta_{\text{eff}} = 0$, the crystal is antiblockaded and the excitation probability of any atom participating in the crystal is enhanced. Therefore if the crystal $\mathcal{L}_\kappa$ is populated, $f_R(\Delta)$ should peak at $\Delta = -\sum_{j\in\mathcal{L}_\kappa} A_{sj}$. We show such a behavior of $f_R(\Delta)$ on Fig. (4.11) in the case of an infinite cubic lattice.

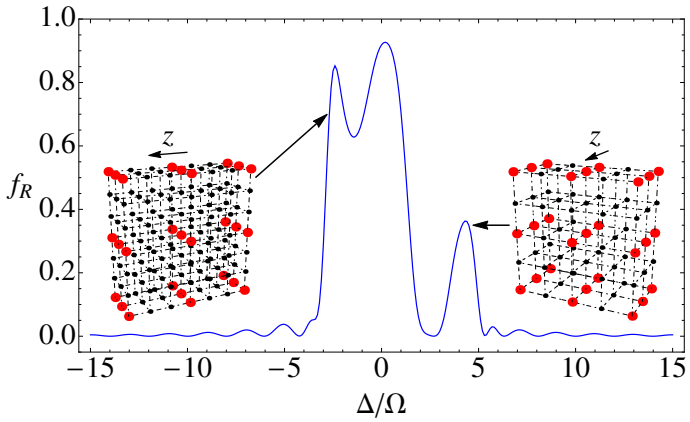

Figure 4.11: Rydberg fraction f_R as a function of the laser detuning Δ after a $t = \pi/\Omega$ on an infinite cubic lattice. The left and central peaks correspond to multiple excitations of competing crystals, one of which is illustrated. At the opposite, the right peak represents the excitation of a unique crystal. Note the different z-axes in the two illustrations. Ground state and Rydberg excited atoms are represented as black dots and large red disks, respectively. Parameters: $\mathsf{n} = 40$, $\theta = 0$, $\phi = 0$, $\Omega = 30$MHz, $L = 8\mu$m, $L/a_R \simeq 0.62$.

4.3.4 Dynamical supersolids?

We now turn to the study of the long time dynamics $t \gtrsim \pi/\Omega$ in the strongly interacting regime $L \ll a_R$ and demonstrate the apparition of transient supersolids over large 2D square lattices. Because we need to look at long times over a large square lattice, we calculate the system evolution operator $\mathsf{U}(t)$ using backtrack-less walk-sum, an intermediary method between walk-sum and path-sum.

We have seen in §3.2.2 that ordinary matrix power-series are equivalent to sums of walks. Furthermore, we have shown in §3.5.4 that walk-sum stems from the exact resummation of all self-loops on the graph of a matrix partition. Consequently walk-sum is a power-series on the loop-less graph $\mathcal{G}_0$ with effective vertex weights representing loop sums. Similarly, path-sum stems from the exact resummation of all cycles on the graph and can be seen as a cycle-less power-series with effective vertex-weights representing cycle-sums. In this picture, walk-sum is an intermediary method between power-series and path-sum. Clearly, other intermediary methods exist, for example that obtained by resumming exactly self-loops and backtracks. We call this method backtrack-less walk-sum. This method differs from walk-sum in two aspects: i) walks contributing to conditional evolution operators are backtrack-less; and ii) the loop sums vertex-weights $\tilde{\mathsf{M}}_\mu$ appearing in walk-sum are replaced by effective vertex-weights representing the sum of all loops and backtracks over an edge adjacent to μ. For example, consider again the conditional evolution operator

$\tilde{\mathsf{U}}_{j\leftarrow g_s}$ of Eq. (4.81). Its backtrack-less walk-sum expression at order 3 is

$$\tilde{\mathsf{U}}_{j\leftarrow 0}(s) \simeq \frac{\mathrm{i}\Omega}{2}\tilde{\mathsf{M}}_j\tilde{\mathsf{M}}_0\Big[\mathsf{I}+\frac{\Omega^2}{4}\tilde{\mathsf{M}}_j\tilde{\mathsf{M}}_0\Big]^{-1}+ \tag{4.89}$$
$$\left(\frac{\mathrm{i}\Omega}{2}\right)^3\sum_{\substack{p=1\\ p\neq j,\,p\neq s}}\left\{\tilde{\mathsf{M}}_j\tilde{\mathsf{M}}_0\Big[\mathsf{I}+\frac{\Omega^2}{4}\tilde{\mathsf{M}}_j\tilde{\mathsf{M}}_0\Big]^{-1}\tilde{\mathsf{M}}_p\tilde{\mathsf{M}}_0\Big[\mathsf{I}+\frac{\Omega^2}{4}\tilde{\mathsf{M}}_p\tilde{\mathsf{M}}_0\Big]^{-1}+\right.$$
$$\left.\tilde{\mathsf{M}}_j\tilde{\mathsf{M}}_{j,p}\Big[\mathsf{I}+\frac{\Omega^2}{4}\tilde{\mathsf{M}}_j\tilde{\mathsf{M}}_{j,p}\Big]^{-1}\left(\tilde{\mathsf{M}}_j\tilde{\mathsf{M}}_0\Big[\mathsf{I}+\frac{\Omega^2}{4}\tilde{\mathsf{M}}_j\tilde{\mathsf{M}}_0\Big]^{-1}+\tilde{\mathsf{M}}_p\tilde{\mathsf{M}}_0\Big[\mathsf{I}+\frac{\Omega^2}{4}\tilde{\mathsf{M}}_p\tilde{\mathsf{M}}_0\Big]^{-1}\right)\right\},$$

where the inverses result from summations over the backtracks, e.g.

$$\frac{\mathrm{i}\Omega}{2}\tilde{\mathsf{M}}_j\tilde{\mathsf{M}}_0\Big[\mathsf{I}+\frac{\Omega^2}{4}\tilde{\mathsf{M}}_j\tilde{\mathsf{M}}_0\Big]^{-1}=(\mathrm{i}\Omega/2)^{-1}\sum_{n\geq 1}\Big(\frac{\mathrm{i}\Omega}{2}\tilde{\mathsf{M}}_j\frac{\mathrm{i}\Omega}{2}\tilde{\mathsf{M}}_0\Big)^n. \tag{4.90}$$

The advantage of backtrack-less walk-sum and other intermediary methods is that they converge faster than walk-sum. The drawback is that they are not monotonously convergent: a calculation may seem to have converged e.g. at order 6 of backtrack-less walk-sum so that orders 7, 8 and 9 yield indistinguishable results when order 10 provokes a large jump of the solution. This problem is also known in path-integral approaches to many-body physics, where the resummation of families of diagrams can suddenly jump to another solution as a new family is included in the calculation. This difficulty may be circumvented by sampling randomly over families of diagrams, a method known as diagrammatic Monte-Carlo. We suspect that a similar procedure would work for backtrack-less walk-sum and other intermediary methods but we have not implemented such an approach. Thus, in this section we use pure backtrack-less walk-sum and assume that the convergence we observe is genuine. We must signal that recent simulations of strongly interacting 1D lattices have cast serious doubts on this assumption.

Using backtrack-less walk-sum, we obtained all conditional evolution operators whose final configuration of S' presents up to 6 simultaneous Rydberg excitations. This is justified here by the strong dipole-dipole interaction which creates large gaps between configurations with different excitation numbers when $L \ll a_R$. In other words, deep in the strongly interacting regime, Rydberg excitations are dilute and typically less than six of them are expected to live simultaneously on the lattice due to strong blockade effects. There is a total of $\binom{N-1}{6} \sim N^6$ such conditional evolution operators. Consequently, when $N \gtrsim 100$ we limit our calculations to three simultaneous excitations plus randomly chosen subsets of configurations with $4 \leq \ell \leq 6$ excitations. There is also an approximation on each of the conditional evolution operators we calculate due to us keeping only those histories of S' that present strictly less than 7 jumps in backtrack-less walk-sum. We verify the validity of our approximations through convergence of the correlation functions with increasing number of simultaneous excitations and by varying the randomly chosen samples of configurations with $4 \leq \ell \leq 6$. We typically obtain convergence for 2D

lattices with $N \approx 6600$ for arbitrary sets of parameters in the Hamiltonian with moderate computational effort: calculations require 18Gbytes of memory but only take up to 5 hours on 4 CPU cores at 2.2GHz.

We found that the system dynamically evolves into a supersolid of Rydberg excitations when there exists couples of atoms which do not interact directly, i.e. when

$$1 - 3\,(\mathbf{r_{ij}}.\mathbf{d})^2 = 0, \tag{4.91}$$

with $\mathbf{r_{ij}} = \boldsymbol{R_{ij}}/R_{ij}$. This condition is independent of the lattice spacing L in the case of a 2D square lattice considered here. Because the lattice arranges the atoms in a discrete fashion, only certain couples of atoms fall exactly onto the line that fulfills Eq. (4.91) where their dipole-dipole interaction is zero. From now on a pair of Rydberg excitations at sites i and j which fulfills Eq. (4.91) will be called a free pair. When $\Delta = 0$, all the configurations of the system where Rydberg excitations populate exclusively free pairs have the same mean energy $\langle \mathsf{H} \rangle = 0$, which is also the case of the initial state $|gg\ldots g\rangle$. In the same time the dipole-dipole interaction creates an energy gap between configurations were the excitations occur exclusively in free pairs and those were they do not. In the strongly interacting regime, this gap is typically larger than the Rabi frequency Ω. We therefore expect the system to evolve mostly into a superposition of configurations with Rydberg atoms forming free pairs and thus exhibiting long-range correlations. Indeed, in the presence of free pairs we observe states with non-zero order-parameter $\langle \mathsf{T}_j \rangle$ and, as shown in Fig. 4.12, they also display a density-density correlation $g_2(s,j)$ which substantially differs from 1 throughout the lattice. This indicates the presence of long-range diagonal order. In Fig. 4.12 we also represent $g_1(s,j) = \langle \mathsf{T}_s\mathsf{T}_j^\dagger + \mathsf{T}_s^\dagger\mathsf{T}_j\rangle - \langle \mathsf{T}_s + \mathsf{T}_s^\dagger\rangle\langle \mathsf{T}_j + \mathsf{T}_j^\dagger\rangle$ and $g_1'(s,j) = \langle \mathsf{T}_s^\dagger\mathsf{T}_j^\dagger + \mathsf{T}_s\mathsf{T}_j\rangle - \langle \mathsf{T}_s + \mathsf{T}_s^\dagger\rangle\langle \mathsf{T}_j + \mathsf{T}_j^\dagger\rangle$, where $\mathsf{T}_j = |g_j\rangle\langle r_j|$. These correlation-functions characterise quantum coherence, i.e. off diagonal order, in blockaded and antiblockaded situations, respectively. We observe that $g_1(s,j)$ and $g_1'(s,j)$ are markedly different from 0 throughout the lattice. This indicates the presence off-diagonal long-range order. Additionally we remark that $g_2(s,j)$ and $g_1'(s,j)$ are correlated while both of them are anticorrelated to $g_1(s,j)$. Furthermore, all three correlation-functions peak precisely where S and j form a free pair and we find $\langle \mathsf{P}_s\rangle = \sum_j \langle \mathsf{P}_s\mathsf{P}_j\rangle$, within our numerical accuracy. This indicates that excitations occur at least in pairs. Furthermore, we find the sum $\sum_j \langle \mathsf{P}_s\mathsf{P}_j\rangle$ to be dominated by a 99% contribution from free pairs, which shows that excitations occur almost exclusively in free pairs. Finally, we remark that by tuning the laser beam orientation $\mathbf{d}$ one can choose which pairs of atoms are free through Eq. (4.91) and hence the structure of the correlations.

To further determine the nature of the observed states we compute their pressure $p_{2\mathrm{D}} = -(\partial E/\partial \mathcal{A})_{T,Nf_R}$ where E and $\mathcal{A} = NL^2$ are the energy and area of the system, respectively. The derivative is taken at constant temperature $T = 0$ and number of excitations Nf_R. To obtain p_{2D} we turn off the laser at time t_0 and calculate the

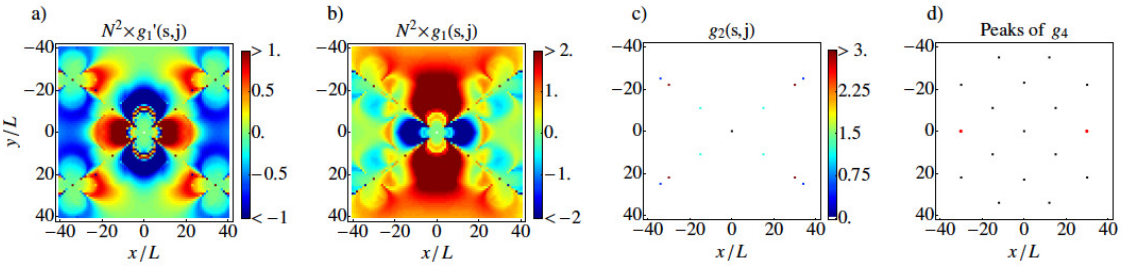

Figure 4.12: Backtrack-less walk-sum obtained correlation-functions multiplied by the number of pairs **a)** $g_1'(s,j)$, **b)** $g_1(s,j)$ and **c)** $g_2(s,j)$ over a square lattice with $N \approx 6600$ atoms. There is one atom/pixel, S is the central one. In **c)**, $g_2(s,j) \simeq 0$ except at the few sites where S and j form a free pair. **d)** Locations of the dominant peaks of $g_4 = \langle \mathsf{P}_s\mathsf{P}_j\mathsf{P}_k\mathsf{P}_l\rangle / \langle \mathsf{P}_s\rangle\langle \mathsf{P}_j\rangle\langle \mathsf{P}_k\rangle\langle \mathsf{P}_l\rangle$ (black squares) and $g_4' = \langle \mathsf{G}_s\mathsf{P}_j\mathsf{P}_k\mathsf{P}_l\rangle / \langle \mathsf{G}_s\rangle\langle \mathsf{P}_j\rangle\langle \mathsf{P}_k\rangle\langle \mathsf{P}_l\rangle$ (red disks) for all j, k forming free pairs with S. Convergence indicates a precision $\sim 10^{-4}$. Parameters : square lattice in the xy-plane, lattice spacing $L = 1.5\mu$m, Rydberg state principal number $n = 40$, $\Omega = 30$MHz, $\Delta = 0$, $t = 8\pi/\Omega$, laser angles $\theta \sim 0.43\pi$ and $\phi = \pi/2$. The system is deeply in the strongly interacting regime $a_R/L \simeq 9$.

effect of a time-dependent contraction of the lattice spacing $L(t)$ on the system. The resulting Hamiltonian $\mathsf{H}'(t)$ commutes with itself at any time as well as with any of the $\mathsf{P}_i\mathsf{P}_j$ thus leaving f_R unchanged while $E(t) = \sum_{i,j} A_{ij}(t)\langle\psi(t_0)|\mathsf{P}_i\mathsf{P}_j|\psi(t_0)\rangle$ changes only through $L(t)$. This yields $p_{2\mathrm{D}} = (3/2)E/\mathcal{A}$. As discussed above the sum over $\langle \mathsf{P}_i\mathsf{P}_j\rangle$ in $E(t)$ is dominated by free pairs for which $A_{ij} = 0$. We thus find these states to have a very small pressure. Physically this is because Eq. (4.91) is independent of the lattice spacing L. Consequently, during a contraction, atoms forming free pairs never interact directly and the system keeps a nearly vanishing potential energy E. We expect the small pressure to increase the lifetime of the observed states $\tau \propto p_{2\mathrm{D}}^{-1/2}$ compared to states containing interacting excitations. Indeed, in the latter case, interactions between the excitations induce center of mass motions of the Rydberg atoms that destroy the states.

The presence of both diagonal and off-diagonal long-range order together with a nearly vanishing quantum pressure qualifies the observed states as supersolids [137, 138]. Their translational symmetry become apparent from 4-body correlation-functions as shown in Fig. (4.12-d). It is important to note that these supersolid states are far from equilibrium and do not appear in the phase diagram of the Hamiltonian, rather they are dynamically created by the laser. The behavior of the supersolids over very long evolution times $t \gg \pi/\Omega$ remains an open question. During the evolution times we can simulate with walk-sum, i.e. $t \lesssim 10\,\pi/\Omega$, we observe a gradual increase in the long-range correlations. This could indicate an absence of thermalisation but the question cannot be immediately settled. Additionally, a realistic simulation of the very long time dynamics of large 2D Rydberg-excited Mott insulators will have to take into account decoherence effects, which are beyond the scope of this work.

4.4 Summary

In this chapter, we derived the walk-sum Lemma for the matrix-exponential using physical arguments. We have shown how this Lemma gives rise to a description of the dynamics of quantum system with discrete degrees of freedom as a sum of histories. The resulting method, termed the method of walk-sums, can approximate any desired piece of an evolution operator independently of any other. Furthermore, the number of operations involved in approximating any such piece at order K scales polynomially with the system size. This result holds independently of the system geometry and the nature of its interactions. However, the computation of the *entire* evolution operator remains intractable in the general case, as it involves an exponentially large number of conditional evolution operators. There are nonetheless many situations for which only a few conditional evolution operators are relevant to the dynamic of the whole system. For example, this is true in the case of strongly interacting Rydberg-excited Mott insulators, where blockade effects limit the number of final excitations in the lattice.

Finally, it is worth noting that the deep origin of the computational speed-up achieved by the method of walk-sums resides in exact summations of infinite families of terms performed at the graph-theoretic level by Eq. (4.19, 4.20). These resummations make walk-sums fundamentally different from power series and are explicitly apparent in the full graph theoretic treatment provided in Chapters 2 and 3.

Chapter 5
Dynamical Localisation in a Many-Body System

Physics is mathematical not because we know so much about the physical world, but because we know so little; it is only its mathematical properties that we can discover.

B. Russell

In this chapter, we characterise and study dynamical localisation of a finite interacting quantum many-body system. We present explicit bounds on the disorder strength required for the onset of localisation of the dynamics of arbitrary ensemble of sites of the XYZ spin-1/2 model. We obtain these results using a novel form of the fractional moment criterion, which we establish, together with the path-sum representation of the system resolvent. These techniques are not specific to the XYZ model and hold in a much more general setting. We further present detailed bounds constraining two observable quantities in the localised regime: the magnetisation of any sublattice of the system as well as the linear magnetic response function of the system. We confirm our results through numerical simulations.

The work of this chapter forms the basis of an article that is currently under review for publication in *Communications in Mathematical Physics* and was carried out in collaboration with Mark Mitchison and Juan Jose Mendoza-Arenas for the TEBD simulations and with Zheng Choo for Lemma 5.6.1.

5.1 Introduction

The mathematical and physical understanding of Anderson localisation for a single particle in a lattice with random on-site potentials has greatly progressed since it was first recognised in 1958 [139, 140, 141]. In contrast, the theory of many-body localisation is still in its infancy, despite the large amount of recent research focusing on localisation in disordered many-particle systems (for example Refs. [142, 143, 144, 145, 146, 147, 148, 149, 150, 151, 152, 153]). In particular, there is still no clear consensus on the precise definition of the many-body localised phase, with a number of different definitions having been proposed in the recent literature (e.g. Refs. [143, 145, 154, 149, 153, 155]). Consequently, a global picture of many-body localisation is still lacking.

An important advance towards the conceptual understanding of the problem was the introduction of the notion of localisation in the quantum configuration or Fock space [156], which has emerged as a powerful framework for understanding

many-body localisation [142, 143, 149, 155]. Configuration-space localisation has also proved useful in understanding the absence of thermalisation in integrable systems [157] and glassy dynamics in strongly interacting systems [158]. Following these developments, we treat the evolution of the many-body quantum state as that of a single fictitious particle moving in an exponentially large configuration space. This viewpoint leads us quite naturally to define many-body dynamical localisation as Anderson localisation of this effective one-particle problem. Furthermore, it facilitates a non-perturbative, mathematically rigorous treatment.

Rigorous mathematical results concerning localisation in interacting many-body systems have been established in [154] and [159]. However, the critical disorder inducing a many-body localisation transition as predicted by these studies is difficult to ascertain and the physical consequences of the localisation remain, in part, unexplored.The contribution of the present work to the study of many-body localisation is thus three-fold. First we provide an explicit bound for the critical amount of disorder necessary for localisation to occur. Second, we make concrete predictions of experimental signatures of the localisation by providing bounds for two physically observable quantities in the localised regime: the magnetisation of any finite ensemble of sites immersed in the system as well as the linear magnetic response function. We confirm our predictions with Time Evolving Block Decimation (TEBD) simulations of a 1D system. Third, our approach to many-body localisation differs from existing approaches [154] and [159]. While we do use a form of fractional moment criterion as a mathematical signature of localisation, we rely on the path-sums representation of the Green's functions associated to any sublattice of the full system to prove that this criterion is met for a finite amount of disorder. The path-sums approach employed here facilitates the manipulation and systematic representation of matrix resolvents and Green's functions. Thus, we hope that it will ultimately contribute to the proof of localisation in *infinite* interacting many-body systems, which remains elusive.

The chapter is organised as follows. In §5.2 we present the model system and general mathematical strategy we employ. For the sake of concreteness we focus on the particular case of a finite, interacting spin-$\frac{1}{2}$ system described by the XYZ-Hamiltonian. This section culminates in a criterion characterising the localised regime. In §5.3 we begin with bounds for the onset of dynamical localisation in one-body systems as well as bounds for the onset of localisation of functions of random matrices. In §5.3.2 we give similar results in the many-body setting. We then provide precise constraints for the magnetisation of arbitrary sublattices of the system as well as the correlations between spins at sites of the sublattice in the localised regime. The bound on the latter quantity is shown to imply a bound on the linear magnetic response function to magnetic perturbations, which we find to be vanishingly small deep in the localised regime. The proofs of all technical results are given in section §5.4-§5.8. Section §5.5 contains the proof of the main result concerning the onset of localisation and a brief presentation of the path-sums approach. In §5.6 we gather the proofs of technical lemmas necessary to the proof presented in §5.5. Finally, in §5.7 and §5.8 we derive the results concerning the

magnetisation and correlations in the localised regime.

5.2 Model system and approach

5.2.1 Model system

The XYZ-Hamiltonian

We consider a lattice $\mathcal{L}$ of N spin-1/2 particles governed by the XYZ-Hamiltonian, which represents one of the simplest models of strongly-interacting many-body systems. The Hamiltonian reads

$$\mathsf{H} = \sum_i B_i \sigma_i^z + \sum_{\langle ij \rangle} \left\{ J_x \sigma_i^x \sigma_j^x + J_y \sigma_i^y \sigma_j^y + \Delta \sigma_i^z \sigma_j^z \right\}, \tag{5.1}$$

where J_x, J_y and Δ are real and parametrise the spin-spin interactions, and $\sum_{\langle ij \rangle}$ denotes a sum over nearest neighbours. The $\{B_i\}_{i \in [1,N]}$ variables are local magnetic fields which we assume to be independent and identically distributed (iid) random variables taken from a Gaussian distribution with standard deviation σ_B. For convenience, we choose the basis states of the Hilbert space to be configurations of spins along the direction of the magnetic fields, e.g. for a two spin-1/2 system this is $\{|\uparrow\uparrow\rangle, |\uparrow\downarrow\rangle, |\downarrow\uparrow\rangle, |\downarrow\downarrow\rangle\}$, where $\uparrow$ and $\downarrow$ designate the situations where the spin is aligned and antialigned with the magnetic fields, respectively.

For $J_x \neq J_y$, the XYZ-Hamiltonian does not conserve the total number of up and down spins present at any time in the system. Since we can add the sum of all the random magnetic fields $\sum_i B_i$ to the Hamiltonian without affecting the dynamics, an up spin is effectively equivalent to a particle seeing a random onsite potential $2B_i$ at site i, while a down spin always sees 0 onsite potential, being effectively equivalent to the absence of a particle. In this sense, the XYZ Hamiltonian *does not conserve the number of particles* present in the system. At the opposite, when $J_x = J_y$, the number of up- and down-spins present in the system is conserved by H. We call this specific situation the XXZ regime.

Mathematical description

We consider the total system described by the XYZ Hamiltonian (5.1), denoted by $\mathbb{S}$, as comprising two parts S and S'. We shall use a partial basis of the configuration space of $\mathbb{S}$ that specifies only the state of S'. From hereon we designate the configurations available to S and S' by Roman and Greek letters, respectively.

Mathematically this procedure corresponds to working with a tensor product partition of the Hamiltonian into smaller matrices, see Chapter 3. Recall that these small matrices, denoted $\mathsf{H}_{\omega \leftarrow \alpha}$, are submatrices of H of size $2^{|S|} \times 2^{|S|}$ with $|S|$ the number of sites in S and fulfill the characteristic relation of tensor product partitions

$$|\omega\rangle\langle\alpha| \otimes \mathsf{H}_{\omega \leftarrow \alpha} = \left(\mathsf{P}_\omega \otimes \mathsf{I}_S\right) . \mathsf{H} . \left(\mathsf{P}_\alpha \otimes \mathsf{I}_S\right), \tag{5.2a}$$

or equivalently

$$\mathsf{H}_{\omega\leftarrow\alpha} = \big(\langle\omega| \otimes \mathsf{I}_S\big) \,.\, \mathsf{H} \,.\, \big(|\alpha\rangle \otimes \mathsf{I}_S\big), \tag{5.2b}$$

with I_S the identity matrix on the spins of S and $\mathsf{P}_\alpha = |\alpha\rangle\langle\alpha|$ the projector onto configuration α of S'. The matrix $\mathsf{H}_\alpha \equiv \mathsf{H}_{\alpha\leftarrow\alpha}$ is a small effective Hamiltonian governing the evolution of S when S' is static in configuration α. For this reason the H_α matrices are called statics. Similarly, the matrix $\mathsf{H}_{\omega\leftarrow\alpha}$ represents the impact on S of a transition of S' from configuration α to ω and for this reason is called a flip. For the choice $S = \emptyset$, $S' = \mathbb{S}$ the statics and flips of the Hamiltonian identify with its matrix elements $\mathsf{H}_{\omega\leftarrow\alpha} = (\mathsf{H})_{\omega\alpha}$. For the opposite choice $S = \mathbb{S}$, $S' = \emptyset$, there is no flip and only one static, which is the Hamiltonian itself $\mathsf{H}_\alpha = \mathsf{H}$. In general, the statics and flips can be thought of as generalised matrix elements, which interpolate between the entries of H and H itself. Thanks to Eq. (5.2b), we find the statics of a tensor product partition of the XYZ Hamiltonian, Eq. (5.1), to be

$$\begin{aligned}\mathsf{H}_\alpha = &\sum_{i\in S} B_i\sigma_i^z + \sum_{i\in S}\sum_{\substack{j\in\langle i\rangle\\ j\in S}}(J_x\sigma_i^x\sigma_j^x + J_y\sigma_i^y\sigma_j^y + \Delta\sigma_i^z\sigma_j^z)\\ &+ \sum_{i\in S}\sum_{\substack{j\in\langle i\rangle\\ j\in S'}}\Delta\sigma_i^z(1-2\delta_{\downarrow_j,\alpha}) + \sum_{i\in S'} B_i(1-2\delta_{\downarrow_i,\alpha})\mathsf{I}_S\\ &+ \Delta\sum_{i\in S'}\sum_{\substack{j\in\langle i\rangle\\ j\in S'}}(1-2\delta_{\downarrow_i\uparrow_j,\alpha} - 2\delta_{\uparrow_i\downarrow_j,\alpha})\mathsf{I}_S,\end{aligned} \tag{5.3}$$

where, $|\alpha|$ is the number of up-spins at sites of S' when it is in configuration α, and, for example, $\delta_{\downarrow_j,\alpha}$ is 1 if the spin at site j is down in configuration α and 0 otherwise. For latter convenience, we define $Y_\alpha = \sum_{i\in S'} B_i(1-2\delta_{\downarrow_i,\alpha})$ a random variable representing the disorder due solely to S' in the static H_α. The static is thus conveniently separated into two pieces as

$$\mathsf{H}_\alpha = Y_\alpha\,\mathsf{I}_S + \tilde{\mathsf{H}}_\alpha, \tag{5.4}$$

where $\tilde{\mathsf{H}}_\alpha$ depends deterministically on α and comprises the random B-fields at sites of S but does not depend on any of the random B-fields at sites of S'. The flips of the Hamiltonian are

$$\mathsf{H}_{\omega\leftarrow\alpha} = \begin{cases}(\mathsf{H}_{\omega\leftarrow\alpha})_{ji} = J_x + J_y, & \text{if } (\alpha i) \text{ and } (\omega j) \text{ differ by the flips of two}\\ & \text{neighbouring spins as follows } \uparrow\downarrow\longleftrightarrow\downarrow\uparrow,\\ (\mathsf{H}_{\omega\leftarrow\alpha})_{ji} = J_x - J_y, & \text{if } (\alpha i) \text{ and } (\omega j) \text{ differ by the flips of two}\\ & \text{neighbouring spins as follows } \uparrow\uparrow\longleftrightarrow\downarrow\downarrow\\ 0, & \text{otherwise,}\end{cases} \tag{5.5}$$

with for example (αi) the configuration of $\mathbb{S}$ where S' and S are in configuration α and i, respectively. In the following we will only need the two-norm of the flips,

which is bounded as follows $\|\mathsf{H}_{\omega\leftarrow\alpha}\| \leq n_{\mathcal{L}}(J_x^2+J_y^2)^{1/2} := n_{\mathcal{L}}\mathcal{J}$, with $n_{\mathcal{L}}$ the maximum number of neighbours that any site of S' has on the lattice $\mathcal{L}$. On Euclidean lattices $\mathcal{L} \equiv \mathbb{Z}^d$, this is 2^d.

5.2.2 Dynamics of the system equivalent particle

Our goal is to establish dynamical localisation of S' regardless of the state of S. In many-body situations, it is useful to consider localisation of the system directly in its configuration space rather than on the physical lattice [143, 149, 154]. As long as the system is finite, the configuration space associated to any partition $\mathbb{S} = S \cup S'$ of the system is a discrete graph $\mathcal{G}_{S,S'}$, which we construct as follows:

i) For each configuration α available to S', we draw a vertex v_α.

ii) If $\mathsf{H}_{\omega\leftarrow\alpha} \neq 0$, we draw an edge $(\alpha\omega)$ from vertex v_α to vertex v_ω.

iii) To each edge $(\alpha\omega)$, we associate the weight $\mathsf{H}_{\omega\leftarrow\alpha}$.

Finally, we define $d(\alpha,\omega)$ the distance between two configurations of the system as the length of the shortest walk on $\mathcal{G}_{S,S'}$ from vertex v_α to vertex v_ω.

The configuration graph gives an alternative picture of the system dynamics. For the choice $S = \emptyset$, $S' = \mathbb{S}$ the statics and flips are the matrix entries of the Hamiltonian $\mathsf{H}_{\omega\leftarrow\alpha} = (\mathsf{H})_{\omega\alpha}$ and the dynamics in real space is equivalent to that of a single particle in the configuration space, which we call the System Equivalent Particle (SEP), undergoing a continuous time quantum random walk on $\mathcal{G}_{\emptyset,\mathbb{S}}$. Furthermore, in the XXZ regime where $J_x = J_y$, if there is initially single up-spin in a sea of down-spins (or the opposite), the configuration graph $\mathcal{G}_{\emptyset,\mathbb{S}}$ is simply the real-space lattice and the SEP represents this single up-spin.

For general partitions $\mathbb{S} = S \cup S'$, S can be interpreted as the internal degree of freedom of the SEP, while its trajectory on the graph $\mathcal{G}_{S,S'}$ represents the evolution of S'. When S' is in configuration α, the SEP is on site v_α and feels the random potential Y_α, which we then call the configuration potential at α. Depending on the amount of disorder present in the various configuration potentials, the SEP may be dynamically localised, which corresponds to many-body localisation of S', regardless of the state of S.

5.2.3 Criterion for many-body localisation

In analogy with the case of a single particle on a lattice [141], the natural signature of SEP dynamical localisation is simply the absence of diffusion of the SEP on $\mathcal{G}_{S,S'}$. This is expressed rigorously using the same tensor product partition that we used for the Hamiltonian but this time for the evolution operator $\mathsf{P}_I(\mathsf{H})e^{-i\mathsf{H}t}$, where P_I is the projector onto the eigensubspace of H with energy in bounded interval I. The elements of this partition fulfill the characteristic relation

$$|\omega\rangle\langle\alpha| \otimes \Big(\mathsf{P}_I(\mathsf{H})e^{-i\mathsf{H}t}\Big)_{\omega\leftarrow\alpha} = \big(\mathsf{P}_\omega \otimes \mathsf{I}_S\big)\,.\,\mathsf{P}_I(\mathsf{H})e^{-i\mathsf{H}t}\,.\,\big(\mathsf{P}_\alpha \otimes \mathsf{I}_S\big), \tag{5.6a}$$

or equivalently

$$\Big(\mathsf{P}_I(\mathsf{H})e^{-i\mathsf{H}t}\Big)_{\omega\leftarrow\alpha} = \big(\langle\omega|\otimes\mathsf{I}_S\big)\,.\,\mathsf{P}_I(\mathsf{H})e^{-i\mathsf{H}t}\,.\,\big(|\alpha\rangle\otimes\mathsf{I}_S\big). \tag{5.6b}$$

For convenience, we say that $(\mathsf{P}_I(\mathsf{H})e^{-i\mathsf{H}t})_{\omega\leftarrow\alpha}$ is a flip of the evolution operator when $\omega\neq\alpha$ and, otherwise, a static of the evolution operator. In this formalism, localisation of the SEP on the configuration graph $\mathcal{G}_{S,S'}$ is characterised by an exponential bound on the norm of the flips of the evolution operator ($\hbar=1$)

$$\mathbb{E}\bigg[\sup_{t\in\mathbb{R}}\Big\|\Big(\mathsf{P}_I(\mathsf{H})e^{-i\mathsf{H}t}\Big)_{\omega\leftarrow\alpha}\Big\|\bigg]\leq Ce^{-d(\alpha,\omega)/\zeta}, \tag{5.7a}$$

or equivalently

$$\mathbb{E}\bigg[\sup_{t\in\mathbb{R}}\Big\|\big(\langle\omega|\otimes\mathsf{I}_S\big)\mathsf{P}_I(\mathsf{H})e^{-i\mathsf{H}t}\big(|\alpha\rangle\otimes\mathsf{I}_S\big)\Big\|\bigg]\leq Ce^{-d(\alpha,\omega)/\zeta}. \tag{5.7b}$$

In these expressions $\mathbb{E}[.]$ is the expectation with respect to all the random variables, $\sup_{t\in\mathbb{R}}$ is the supremum over time, $C<\infty$, $\zeta>0$ and $\|.\|$ is the 2-norm. Note, for the choice $S=\emptyset$, $S'=\mathbb{S}$, Eq. (5.7) reduces to an exponential bound on off-diagonal matrix elements of the evolution operator.

By construction, the criterion of Eqs. (5.7) is a natural extension of the criterion for dynamical localisation of isolated particles. Furthermore, we show below that the criterion is met for a finite amount of disorder in a finite interacting many-body system described by the XYZ-Hamiltonian of Eq. (5.1) and that once verified, Eqs. (5.7) lead to constraints on the magnetisation of S', the correlations between its sites and the linear magnetic response function.

Before we progress, three remarks are in order. First, for technical reasons, we only consider finite energy intervals I. We note however that for any realistic finite system this is not constraining since there must be a finite energy interval containing all possible spectra of the random XYZ model[1]. Second, from now on we restrict ourselves to sublattices S' comprising only non-adjacent sites. This is not a fundamental requirement of our approach, but it facilitates the mathematical proofs. The case of adjacent sites is discussed in Remark 5.3.9, p. 127 below. Third, since we consider a finite system with exclusively discrete degrees of freedom, the spectrum of H is discrete.

By construction, the criterion of Eq. (5.7b) is a natural extension of the criterion for dynamical localisation of isolated particles. Furthermore, we show below that the criterion is met for a finite amount of disorder in a finite interacting many-body system described by the XXZ-Hamiltonian of Eq. (5.1) and that once verified, Eq. (5.7b) leads to strong constraints on the magnetisation of S' and on the correlations between its sites.

[1] We do not assume nor use this in the mathematical proofs.

5.3 Dynamical localisation

In this section we present the main results of the present chapter. For the sake of clarity, we only sketch here the outline of the proofs and defer all the proofs to §5.4 and §5.5. In §5.3.1, we begin with bounds for the onset of dynamical localisation in one-body systems as well as bounds for the onset of localisation of functions of random matrices. In §5.3.2 we give bounds for the onset of dynamical localisation in a many-body system and in §5.3.3-5.3.4 we describe observable signatures of this localisation.

5.3.1 One-body localisation and localisation of matrix functions

We begin by studying the simplest situation: that of single up-spin in a sea of down-spins (or the opposite), in the XXZ regime. In this case, the problem is effectively one-body since in the XXZ regime, the Hamiltonian conserves the total number of up- and down-spins present in the system at any time. One-body dynamical localisation is now a well understood phenomenon and Theorem 5.3.1 presented in this section is already known [160, 161, 141]. For the sake of completeness and since its derivation uses a simple form of path-sum, we include it in this chapter.

Theorem 5.3.1 (One-body dynamical localisation)**.** *Consider a single particle evolving on $\mathbb{Z}^\delta$ according to the Hamiltonian of Eq. (5.1). Let I be an interval of energy with finite Lebesgue measure $|I|$. Let a and b be two points of $\mathbb{Z}^\delta$ and d the distance between them. Then for all $0 < s < 1$,*

$$\mathbb{E}\Big[\sup_{t\in\mathbb{R}}\big|\langle a|\mathsf{P}_I e^{-\mathrm{i}\mathsf{H}t}|b\rangle\big|\Big] \leq C\, e^{-\frac{d}{(2-s)\zeta}}, \tag{5.8a}$$

where

$$\zeta^{-1} = \ln\Big[\frac{1-s}{2\delta-1}\Big(\frac{\sigma_B\sqrt{2\pi}}{2|J|}\Big)^s\Big] > 0 \quad \textit{for} \quad \sigma_B > \Big(\frac{2\delta-1}{1-s}\Big)^{1/s}\frac{2|J|}{\sqrt{2\pi}}\,, \tag{5.8b}$$

$$C = \frac{1}{2\pi}\big(2|I|\big)^{\frac{1}{2-s}}\frac{\|\rho\|_\infty^s}{1-s}\frac{2\delta}{2\delta-1}\frac{1}{1-e^{-1/\zeta}}, \tag{5.8c}$$

with $\|\rho\|_\infty = 1/(\sigma_B\sqrt{2\pi})$.

The path-sum based proof of this proposition is presented in §5.4. We also obtain a more general mathematical result concerning the average exponential decay of uniformly bounded functions of certain finite random matrices:

Theorem 5.3.2 (Localisation of matrix functions)**.** *. Let $\{Y_\alpha\}$ be an ensemble of independent random variables with probability distributions ρ_α Hölder continuous of order 1 and define $\|\rho\|_\infty = \max_\alpha \|\rho_\alpha\|$. Let $\mathsf{M} \in \mathbb{C}^{n\times n}$ be a normal matrix, R its spectral radius and $\mathsf{R}_\mathsf{M}(z) = (z\mathsf{I}-\mathsf{M})^{-1}$ its resolvent. If there exists a partition $\{\mathsf{M}_{\alpha\omega}\}$ of M such that all statics are of the form $\mathsf{M}_{\alpha\alpha} = Y_\alpha\mathsf{I} + \tilde{\mathsf{M}}_{\alpha\alpha}$ with $\tilde{\mathsf{M}}_{\alpha\alpha}$ a deterministic*

matrix, then for all $0 < s < 1$ *and any bounded function* $f(z)$ *analytic on a region containing all the possible spectra* $\mathrm{Sp}(\mathsf{M})$*, we have*

$$\mathbb{E}\Big[\big\|\big(\mathsf{R}_{\mathsf{M}}(z)\big)_{\alpha\omega}\big\|^s\Big] \leq \sum_{\ell \geq d(\alpha,\omega)} |\Pi_{\mathcal{G};\alpha\omega}|(\ell) \frac{\Omega_{\alpha\omega}^{\ell s}}{(1-s)^{\ell+1}} (2\|\rho\|_\infty)^{s\ell+s}, \tag{5.9a}$$

where $\mathcal{G}$ *is the graph of the partition,* $\Omega_{\alpha\omega} = \max_{\alpha,\omega} \|\mathsf{M}_{\alpha\omega}\|$ *and* $\mathbb{E}[.]$ *represents the expectation with respect to all random variables. Furthermore, if* $\Omega_{\alpha\omega}^s < (1-s)(2\|\rho\|_\infty)^{-1}$*, then the expected weight of a fully dressed prime walk decays exponentially with its length. In this situation,*

$$\mathbb{E}\Big[\big\|\big(\mathsf{R}_{\mathsf{M}}(z)\big)_{\alpha\omega}\big\|^s\Big] \leq \frac{\|\rho\|_\infty^s}{1-s} \frac{2}{1-e^{-1/\zeta}} e^{-\frac{d(\alpha,\omega)}{\zeta}}, \tag{5.9b}$$

$$\mathbb{E}\Big[\sup_{t\in\mathbb{R}} \big\|f(\mathsf{M})_{\alpha\omega}\big\|\Big] \leq \frac{1}{2\pi}\|f\|_\infty (2R)^{\frac{1}{2-s}} \frac{\|\rho\|_\infty^s}{1-s} \frac{2}{1-e^{-1/\zeta}} e^{-\frac{d(\alpha,\omega)}{(2-s)\zeta}}, \tag{5.9c}$$

where

$$\zeta^{-1} = \ln\Big[\frac{1-s}{\lambda_{\mathcal{G}}\,\|\rho\|_\infty^s \Omega_{\alpha\omega}^s}\Big] > 0, \tag{5.9d}$$

with $\lambda_{\mathcal{G}}$ *the largest eigenvalue of* $\mathcal{G}$*.*

Remark 5.3.1 (Structure of the random matrices)**.** The theorem is to be understood as a statement regarding random matrices with *fixed structure*. In other words, the emplacement of the zero entries of M does not vary and only the non-zero entries are allowed to be random. This fixes the graph $\mathcal{G}$ and the distance $d(\alpha,\omega)$ between any two vertices is well defined.

Remark 5.3.2 (Sparsity of M)**.** Although the theorem holds even when M is full, in this situation the theorem becomes trivial since $\max_{\alpha,\omega}\{d(\alpha,\omega)\} = 1$.

Remark 5.3.3 (Off-diagonal disorder)**.** The theorem still holds if each flip is also a function of a random variable. In this situation, let $Y_{\alpha\omega}$ be the random variable upon which $\mathsf{M}_{\alpha\omega}$ depends. Then, if for all flips the expectation $\mathbb{E}_{Y_{\alpha\omega}}\big[\|\mathsf{M}_{\alpha\omega}\|\big]$ exists, the theorem remains valid upon replacing $\Omega_{\alpha\omega}$ by $\max_{\alpha,\omega}\mathbb{E}_{Y_{\alpha\omega}}\big[\|\mathsf{M}_{\alpha\omega}\|\big]$.

Remark 5.3.4 (Correlated random variables)**.** Let $(\alpha_1\eta_2\cdots\alpha_j\cdots\alpha_\ell)$ be a prime walk on $\mathcal{G}$. Then the Theorem holds in the situation where the Y_α are correlated upon replacing $\|\rho\|_\infty^\ell$ by $\prod_{j=1}^\ell \|\rho_{\alpha_j|}\|_\infty$, where $\|\rho_{\alpha_j|}\|_\infty$ is the infinity norm of the conditional probability distribution of Y_{α_j} knowing $Y_{\alpha_{j+1}}, \cdots, Y_{\alpha_\ell}$.

5.3.2 Many-body localisation

A major difficulty in the study of many-body localisation as compared to one-body localisation lies in that the effective amount of disorder present in the system grows only *logarithmically* with the size of the relevant space $\mathcal{G}_{S,S'}$. Indeed, since there are only $|S'|$ random B-fields affecting the sites of S', there are only $|S'|$ linearly

independent configuration potentials. In the same time S' can adopt up to $2^{|S'|}$ configurations. Thus, the total amount of disorder affecting the SEP is very small as compared to the size of the space on which it evolves. Furthermore, this disorder is also highly correlated, as the configuration potentials are linearly dependent. These observations explain why the proof of localisation for many-body systems is much more involved than its one-body counterpart and leads to much larger bounds on the minimum amount of disorder required for localisation to happen.

Outline of our approach:
We obtain a bound on the disorder strength required for the many-body localisation criterion Eq. (5.7a) to be met as follows:

1) We relate Eq. (5.7a) to a novel form of fractional moment criterion. More precisely, we consider generalised Green's functions which evolve the SEP on its configuration space. These are matrices dictating the evolution of S' regardless of that of S. They arise from a tensor product partition of the system resolvent $(z\mathsf{I}-\mathsf{H})^{-1}$. We show that if fractional powers of the 2-norm of these generalised Green's functions are exponentially bounded, then Eq. (5.7a) is satisfied.

2) We express generalised Green's functions non-perturbatively using the method of path-sums, which represents the generalised Green's functions as a superposition of simple paths undergone by the SEP on its configuration space. Simple paths are walks forbidden from visiting any vertex more than once. On Euclidean lattices they are known as self-avoiding walks.

3) Using path-sums representations, we directly obtain an upper-bound on the required fractional norms. No induction on the number of particles is required, in contrast to Refs. [154] and [159].

These steps finally yield the main theorem of the present chapter (see §5.5 for details):

Theorem 5.3.3 (Many-body dynamical localisation in an interacting system)**.** *Consider an ensemble of particles evolving on a finite lattice $\mathcal{L}$ comprising N sites according to the XYZ-Hamiltonian of Eq. (5.1). Let S' an ensemble of non-adjacent lattice sites and I be an interval of energy with finite Lebesgue measure $|I|$. Then for any $0 < s < 1$ and any $2^{-|S'|} < s_1 < 1$,*

$$\mathbb{E}\left[\sup_{t\in\mathbb{R}}\left\|\left(\mathsf{P}_I(\mathsf{H})e^{-i\mathsf{H}t}\right)_{\omega\leftarrow\alpha}\right\|\right] \leq C(\omega,\alpha)\, e^{-\frac{(s_1-s)}{s_1(2-s)}\frac{d(\alpha,\omega)}{\zeta}}, \tag{5.10a}$$

where

$$C(\omega,\alpha) = \frac{1}{2\pi}\big(2|I|\big)^{\frac{1}{2-s}} c[s_1]^{\frac{s}{s_1}} \frac{2^{-|S'|s} D^s}{(\sigma_B\sqrt{2\pi})^s} \times \left(\frac{1}{s|S'|}\Phi\big(e^{-1/\zeta}, 1, d(\alpha,\omega)+1-s^{-1}\big)\right)^{\frac{s_1-s}{s_1}}, \tag{5.10b}$$

$$\zeta^{-1} = s\log\Big(\frac{\sigma_B\sqrt{2\pi}}{Dn_{\mathcal{L}}\mathcal{J}\,|S'|^{1/s}}\Big), \tag{5.10c}$$

where ζ is the localisation length and

$$\zeta > 0 \quad \textit{if and only if} \quad \sigma_B > \sigma_B^{min} = Dn_{\mathcal{L}}\mathcal{J}\,|S'|^{1/s}/\sqrt{2\pi}. \tag{5.10d}$$

In these expressions, $\mathcal{J} = (J_x^2+J_y^2)^{1/2}$, $n_{\mathcal{L}}$ is the maximum number of neighbours that any site of S' has on $\mathcal{L}$, $D = 2^N$, $c[s_1] = 4^{1-s_1}k^{s_1}/(1-s_1)$ where k is a finite universal constant and Φ is the Hurwitz-Lerch zeta-function, which decays algebraically with $d(\alpha,\omega)$ when $d(\alpha,\omega) > s^{-1}-1$.

Remark 5.3.5 (Meaning of the bound)**.** Because we partition the system into two subsystems S and S', we emphasise that the meaning of the above bound is different from what is usually understood from such bounds. If Eq. (5.10a) holds for some disorder σ_B and sublattice S' comprising $|S'|$ non-adjacent sites, then the dynamic of *any* and hence *all* sublattices comprising $|S'|$ non-adjacent sites is localised, regardless of the dynamics of the rest of the system.

Remark 5.3.6 (Dependency on the system size)**.** The bound we obtain on the critical amount of disorder required for the onset of localisation scales exponentially with the system size N. This is unsurprising in view of the fact that the XYZ Hamiltonian does not conserve the number of particles in the system. For this reason, adding a single site to the lattice doubles the number of configurations available to the system.

Remark 5.3.7 (Dependency on the system partition)**.** In the situation where the Hamiltonian is partitioned into its matrix elements, i.e. the flips and statics are the entries of the Hamiltonian $\mathsf{H}_{\omega\leftarrow\alpha} = (\mathsf{H})_{\omega\alpha}$, we have $S = \emptyset$, $S' = \mathbb{S}$ and thus $|S'| = |\mathbb{S}| = N$. This degrades both the bound on the critical disorder $\sigma_B^{\min}$ and the localisation length ζ linearly with the system size. It is therefore beneficial to use partitions with small $|S'|$ values.

Remark 5.3.8 (Dependency on the interaction strength along z)**.** The bound obtained above for the critical amount of disorder does not depend on the interaction parameter Δ, but rather holds for any Δ. This is because of a crucial step of our proof, where we determine a bound for the norm of a generalised Green's functions independently of the details of the self-energy. By the same token, we lose information about any influence the interaction strength Δ might have on the onset of localisation. Thus, our approach does not permit us to study the influence of Δ.

We could partially circumvent this problem by treating the deterministic interaction term in configuration α as a realisation of a random variable $\tilde{\Delta}_\alpha$ whose probability distribution can be evaluated from the Hamiltonian. Then one would take expectations with respect to a new random configuration potential $\tilde{Y}_\alpha = Y_\alpha + \tilde{\Delta}_\alpha$ and the strength Δ of the interaction would play a role similar to the variance of the random B-fields.

Remark 5.3.9 (Dependency on the lattice)**.** The theorem holds regardless of the dimension and details of the physical lattice. This is because we require S' to comprise only non-adjacent sites. In this situation, the configuration graph $\mathcal{G}_{S,S'}$ must be an $|S'|$-hypercube $\mathcal{H}_{|S'|}$ or a subgraph of it, regardless of the physical lattice. Indeed, $\mathcal{H}_{|S'|}$ connects all configurations of S' differing by one spin flip. Thus if the configuration graph is not $\mathcal{H}_{|S'|}$ or a subgraph of it, then there is at least one transition allowed between two configurations of S' differing by two spin flips. This corresponds to two non-adjacent spins flipping at the same time, which is not allowed by the Hamiltonian. This approach leads to simpler results when deriving observable signatures of the localised regime, see §5.3.3, §5.3.4 and Appendices 5.7 and 5.8. Our results can nonetheless be extended so as to hold in situations where S' comprises adjacent sites. For example, if the physical lattice is $\mathbb{Z}^d$, $d \geq 1$, then the bound on the critical disorder becomes $\sigma_B^{\min} = D2^d\mathcal{J}\, d^{1/s}|S'|^{1/s}/(2\sqrt{2\pi})$.

Remark 5.3.10 (Extension to other Hamiltonians)**.** While we present Theorem 5.3.3 explicitly in the case of the XYZ-Hamiltonian, we do so for the sake of concreteness. The arguments developed in the proof of the theorem do not make use of the specifics of the XYZ-Hamiltonian, so that the theorem can easily be extended other Hamiltonians and other probability distributions ρ for the random magnetic fields[2], as considered in Ref. [154].

Remark 5.3.11 (Use of the 2-norm)**.** Theorem 5.3.3 is stated in terms of the 2-norm which might seem to obscure the physical meaning of the bound Eq. (5.10a). Indeed physical quantities of interest such as the system magnetisation and correlations functions are most naturally expressed in terms of the Frobenius norm. Nonetheless we show explicitly in the next section that Theorem 5.3.3 implies constraints on such physical quantities, as would be expected if the theorem involved the Frobenius norm.

5.3.3 Localisation of sublattice magnetisation

In this section and the next we discuss observable consequences of the criterion for many-body localisation Eq. (5.7a). Although the bound for the onset of many-body localisation presented in Theorem 5.3.3 holds for any finite ensemble of non-adjacent sites S', there is a particular choice of sites for S' that leads to a simple structured configuration graph, allowing for easier interpretations of the consequences of SEP dynamical localisation.

[2]So long as ρ remains Hölder continuous.

Suppose that S' consists of a set of sites that are well separated in real space. In this case, the surrounding sites belonging to S effectively act as a spin bath with which the sites of S' can freely exchange spin excitations. Clearly, S will act more effectively as a bath in higher dimensions, when each site of the lattice has more nearest neighbours. A key consequence of this choice is that the number of up-spins in S' can vary, even in the XXZ regime $J_x = J_y$ where the total number of up spins in the entire system is conserved. Thus, in this situation and regardless of the values of J_x and J_y, every one of the $2^{|S'|}$ configurations available to S' is accessible. Furthermore, each configuration of S' is connected to exactly $|S'|$ other configurations, because each spin within S' is free to flip its state when $J_x \neq J_y$, or, in the XXZ regime, by virtue of its contact with the spins of S. These considerations uniquely specify the configuration graph of S' as the $|S'|$-hypercube. Then the dynamics of the SEP is that of a particle undergoing a continuous-time quantum random walk on the hypercube, perceiving highly correlated random potentials at the various sites.

Now an important consequence of the structure of the hypercube is that the distance $d(\alpha, \omega)$ between any two configurations α and ω available to S' is at least equal to the difference between the number of up-spins in the two configurations $d(\alpha, \omega) \geq |n_\alpha - n_\omega|$, with n_α the number of up-spins in S' when it is in configuration α. Thus SEP dynamical localisation as per our criterion Eq. (5.7a) immediately implies localisation in the number of up-spins in the sublattice

$$\mathbb{E}\left[\sup_{t\in\mathbb{R}}\left\|\left(\mathsf{P}_I(\mathsf{H})e^{-i\mathsf{H}t}\right)_{n'\leftarrow n}\right\|\right] \leq Ce^{-|n-n'|/\zeta}, \tag{5.11a}$$

or equivalently

$$\mathbb{E}\Big[\sup_{t\in\mathbb{R}}\left\|\left(\langle n'|\otimes \mathsf{I}_S\right)\mathsf{P}_I(\mathsf{H})e^{-i\mathsf{H}t}\left(|n\rangle\otimes \mathsf{I}_S\right)\right\|\Big] \leq Ce^{-|n-n'|/\zeta}, \tag{5.11b}$$

where $|n\rangle$ and $|n'\rangle$ represent any superposition of configurations of S' with exactly n and n' up-spins, respectively.

This yields an observable signature of the many-body localisation of the system: the magnetisation of any sublattice is constrained within an interval centered on its value at time $t = 0$. More precisely, let $N^{\uparrow}_{S'}(t)$ and $N^{\downarrow}_{S'}(t)$ be the number of up- and down-spins in the sublattice S' at time t, respectively. We define the disorder-averaged normalised magnetisation as $M(t) = \mathbb{E}\big[N^{\uparrow}_{S'}(t) - N^{\downarrow}_{S'}(t)\big]/|S'|$, with $\mathbb{E}[.]$ the expectation with respect to all random magnetic fields. In Appendix 5.7 we show that this quantity is bounded at any time as follows

$$1 - n^{\downarrow}(\zeta) \leq M(t) \leq n^{\uparrow}(\zeta) - 1, \tag{5.12}$$

with $n^{\uparrow}(\zeta)$ and $n^{\downarrow}(\zeta)$ two time-independent quantities depending on the localisation

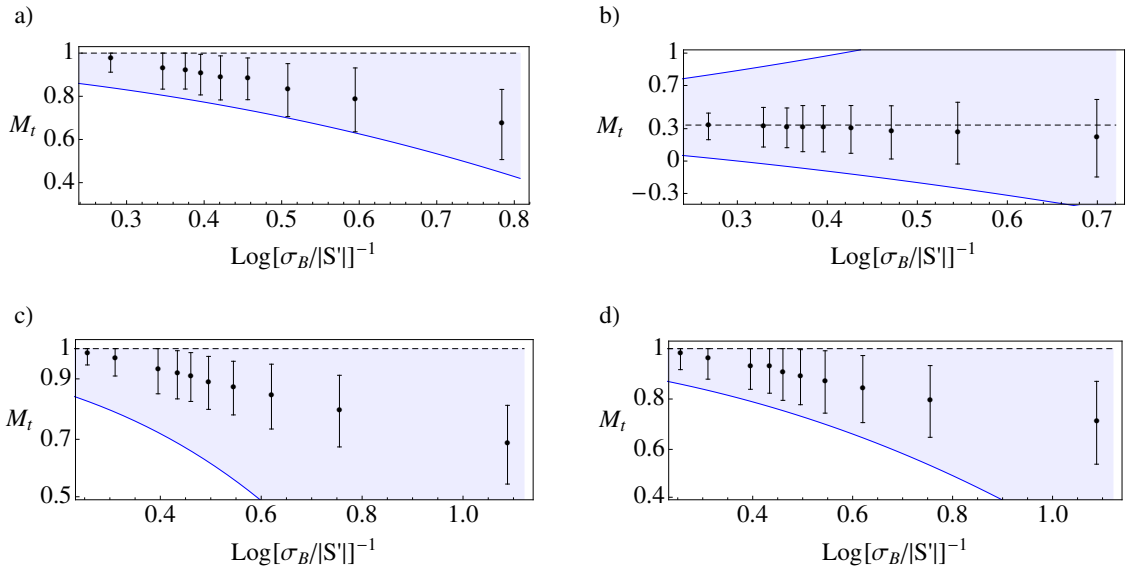

Figure 5.1: Data points: disorder-averaged normalised magnetisation $M(t)$ of various sublattices of a 1D lattice with $N = 60$ sites. Each error bar represents one standard deviation around the disorder average. Initially, spins located at even and odd sites are up and down, respectively. The sublattices S' shown here comprise: **a)** sites 5 - 13 - 21 - 29 - 37 - 45 - 53, initial magnetisation $M(0) = 1$; **b)** sites 13 - 21 - 28 - 40 - 45 - 57, initial magnetisation $M(0) = 1/3$; **c)** sites 5 - 11 - 17 - 23 - 29 - 35 - 41 - 47 - 53 - 59, initial magnetisation $M_0 = 1$; **d)** sites 9 - 19 - 29 - 39 - 49 - 59, initial magnetisation $M(0) = 1$. Each data point represents 300 TEBD simulations of $\mathbb{S}$ which is initially populated by 30 up-spins and 30 down-spins. Simulations parameters: XXZ regime $J_x = J_y = 1$, $\Delta = 1/2$, evolution time: $t = 5J_x^{-1}$, longer evolution times did not yield significantly different results. In shaded is the region of allowed magnetisation $M(t)$ as per Eq. (5.12) as a function of $\ln(\sigma_B/|S'|)^{-1} \propto \zeta$. Constants C and ζ where used as free parameters to fit all results.

length ζ and constant C of Eq. (5.7a):

$$n^{\uparrow}(\zeta) = C^2 \sum_{m=0}^{|S'|} \frac{2m}{|S'|} \sum_{d=0}^{|S'|} \mathcal{N}(|S'|, n_0, m, d) e^{-2d/\zeta}, \tag{5.13a}$$

$$n^{\downarrow}(\zeta) = C^2 \sum_{m=0}^{|S'|} \frac{2m}{|S'|} \sum_{d=0}^{|S'|} \mathcal{N}(|S'|, |S'| - n_0, m, d) e^{-2d/\zeta}, \tag{5.13b}$$

with $n_0 = N_{S'}^{\uparrow}(0)$ the initial number of up-spins in S' and

$$\mathcal{N}(|S'|, n_0, m, d) = \begin{cases} \binom{n_0}{d/2+(n_0-m)/2} \binom{|S'|-n_0}{d/2-(n_0-m)/2}, & d + n_0 - m \text{ even}, \\ 0, & \text{otherwise}. \end{cases} \tag{5.14}$$

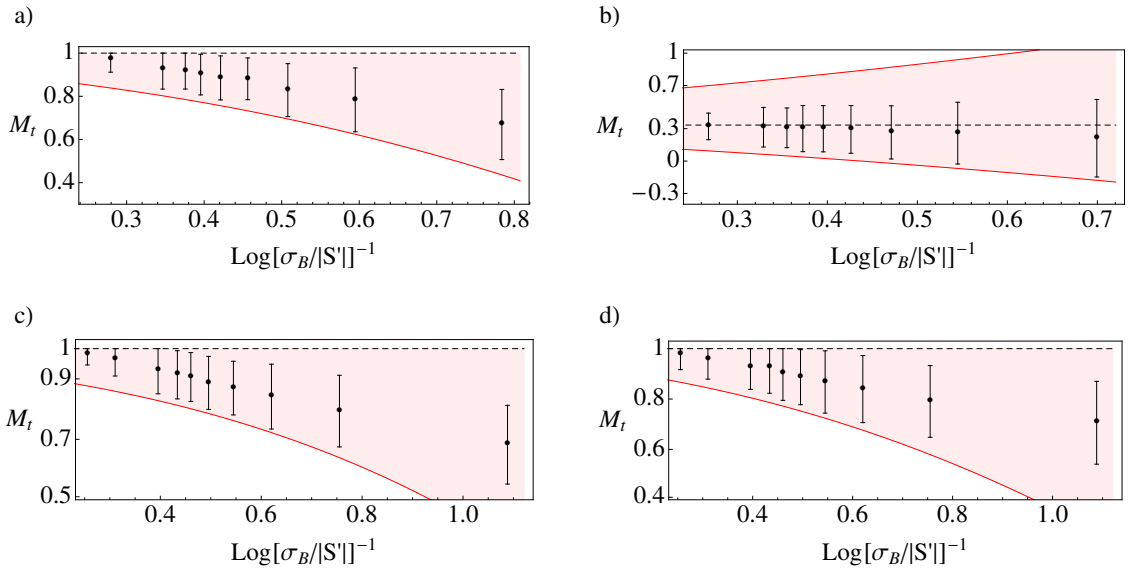

Figure 5.2: Same simulations as in Figure 5.1, but here fitting the values of C and ζ independently for each figure. The TEBD results are consistent with localisation of the system in its configuration space.

In the strongly localised regime, the bound Eq. (5.12) becomes

$$\lim_{\zeta\to 0} 1 - n^{\downarrow}(\zeta) = \lim_{\zeta\to 0} n^{\uparrow}(\zeta) - 1 = M(0), \tag{5.15}$$

that is the sublattice magnetisation is constrained around its initial value, as expected. On Figures (5.1) and (5.2) we compare the bounds of Eq. (5.12) with TEBD simulations of a half-filled 1D lattice of 60 sites in the XXZ regime. Our implementation of the TEBD algorithm is based on the open-source Tensor Network Theory (TNT) library [162]. We use C and ζ as free parameters to fit the simulation results with our theoretical predictions. This means that we do not use their values as predicted by Theorem 5.3.3. This is because we could only simulate disorder strengths σ_B which are below the bound σ_B^{min} obtained in the theorem. In Fig. (5.1) we determine the values of C and ζ so as to fit the magnetisations of all observed sublattices at once. Our result are in good agreement with the simulated magnetisations, which demonstrates that the behaviour of this physical quantity is well captured by our bound Eq. (5.12). In particular, the simulations show that the sublattice magnetisation is strongly constrained around its initial value deep in the localised regime, as predicted by our theoretical bounds. In Fig. 5.2, the values of C and ζ are fitted for each sublattice separately. The excellent agreement between theory and simulation here shows that the overall dependency of the simulated magnetisation with the disorder is very well captured by our bounds.

These results demonstrate the validity of our criterion, which quantitatively predicts a physically observable signature of many-body localisation.

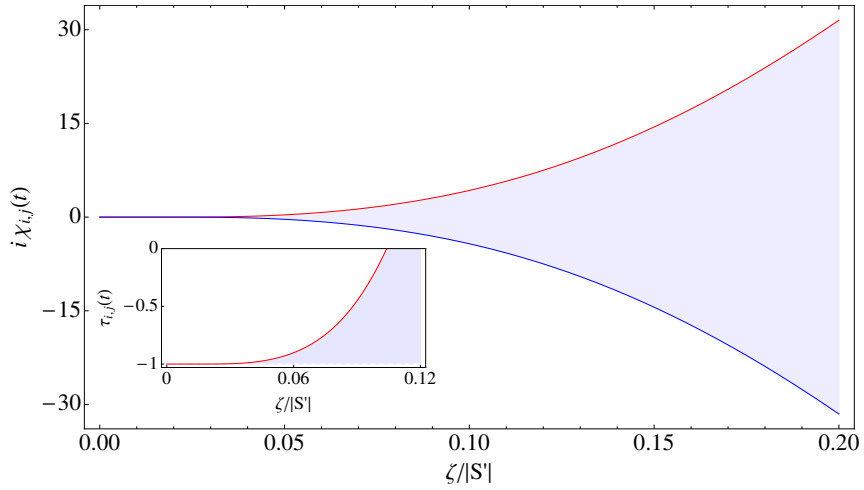

Figure 5.3: Bounds on the disorder-averaged magnetic linear response $i\chi_{i,j}(t)$ in the localised regime, as a function of the localisation length ζ. The shaded region is the region allowed by the bound Eq. (5.21) We consider here a sublattice S' comprising $|S'| = 10$ sites. Initially, the sublattice is in a configuration α with $|\alpha| = 3$ up spins and i and j are up and down in α, respectively. In inset: bound on the disorder averaged correlation function $\tau_{i,j}(t)$, initially $\tau_{i,j}(0) = -1$. The shaded region is the region allowed by the bounds Eqs. (5.18).

5.3.4 Localisation of sublattice correlations and magnetic susceptibility

Similarly to the sublattice magnetisation presented above, we prove in Appendix 5.8 that once the criterion for many-body dynamical localisation Eq. (5.7a) is fulfilled, then the correlations between any two sites of the sublattice S' will be localised around their initial value. The correlations at time t between two sites i and j of S' that we consider are given by

$$\tau_{i,j}(t) = \mathbb{E}\big[\mathrm{Tr}[\mathsf{P}_I(\mathsf{H})\,\sigma_z^i(t)\,\mathsf{P}_I(\mathsf{H})\,\sigma_z^j\,\rho_{\mathbb{S}}]\big], \tag{5.16}$$

where $\mathbb{E}[.]$ is the expectation with respect to all random magnetic fields, $\rho_{\mathbb{S}}$ is the initial density matrix of the entire system $\mathbb{S}$ and $\sigma_z^i(t) = e^{i\mathsf{H}t}\sigma_z^i e^{-i\mathsf{H}t}$. The quantity $\tau_t(i,j)$ is of interest because it relates to the disorder-averaged linear magnetic response function $\chi_{i,j}(t)$. More precisely we have

$$\chi_{i,j}(t) = -i\,\mathbb{E}\big[\langle[\sigma_z^i(t), \sigma_z^j(0)]\rangle\big] = -i\big(\tau_{i,j}(t) - \tau_{j,i}(-t)\big), \tag{5.17}$$

which determines the response of the magnetisation at site i to a time-dependent magnetic field applied at site j [163].

In the situation where S' is initially in a single configuration α and is dynamically localised as per our criterion Eq. (5.7a), we obtain the following bounds for the sublattice correlations

$$\begin{cases} \tau_{i,j}(t) \leq 2\mathcal{K}(|S'|,\,|\alpha|) - 1, & j \text{ is up in } \alpha, \\ \tau_{i,j}(t) \geq -2\mathcal{K}(|S'|,\,|\alpha|) + 1, & j \text{ is down in } \alpha, \end{cases} \tag{5.18a}$$

and simultaneously

$$\begin{cases} \tau_{i,j}(t) \geq -2\mathcal{Q}(|S'|,\,|\alpha|) + 1, & j \text{ is up in } \alpha, \\ \tau_{i,j}(t) \leq 2\mathcal{Q}(|S'|,\,|\alpha|) - 1, & j \text{ is down in } \alpha, \end{cases} \tag{5.18b}$$

where $|\alpha|$ is the number of up-spins in S' when it is in configuration α and $\mathcal{K}$ and $\mathcal{Q}$ are given by

$$\mathcal{K}(|S'|,\,|\alpha|) =$$
$$\begin{cases} C^2 \sum_{m=1}^{|S'|-1} \sum_{d=0}^{|S'|-1} \mathcal{N}(|S'|-1, |\alpha|-1, m-1, d)\, e^{-2d/\zeta}, & i \text{ is up in } \alpha, \\ C^2 \sum_{m=1}^{|S'|-1} \sum_{d=1}^{|S'|-1} \mathcal{N}(|S'|-1, |\alpha|, m-1, d-1)\, e^{-2d/\zeta}, & i \text{ is down in } \alpha, \end{cases} \tag{5.19a}$$

$$\mathcal{Q}(|S'|,\,|\alpha|) =$$
$$\begin{cases} C^2 \sum_{m=1}^{|S'|-1} \sum_{d=1}^{|S'|-1} \mathcal{N}(|S'|-1, |\alpha|, m-1, d-1)\, e^{-2d/\zeta}, & i \text{ is up in } \alpha, \\ C^2 \sum_{m=1}^{|S'|-1} \sum_{d=0}^{|S'|-1} \mathcal{N}(|S'|-1, |\alpha|-1, m-1, d)\, e^{-2d/\zeta}, & i \text{ is down in } \alpha. \end{cases} \tag{5.19b}$$

Now let $\tau^-_{i,j}(\zeta)$ and $\tau^+_{i,j}(\zeta)$ designate the bounds of Eqs. (5.18) obtained above for $\tau_{i,j}(t)$, that is

$$\tau^-_{i,j}(\zeta) \leq \tau_{i,j}(t) \leq \tau^+_{i,j}(\zeta). \tag{5.20}$$

Then a bound on the disorder-averaged magnetic response function follows straightforwardly,

$$\tau^+_{j,i}(\zeta) - \tau^-_{i,j}(\zeta) \leq i\chi_{i,j}(t) \leq \tau^+_{i,j}(\zeta) - \tau^-_{j,i}(\zeta). \tag{5.21}$$

In particular, in the strong disorder limit, we find analytically that

$$\lim_{\zeta\to 0} \tau^-_{i,j}(\zeta) = \lim_{\zeta\to 0} \tau^+_{i,j}(\zeta) = \lim_{\zeta\to 0} \tau_{i,j}(t) = \tau_{i,j}(0), \tag{5.22}$$

and similarly $\lim_{\zeta\to 0} \tau_{j,i}(-t) = \tau_{j,i}(0)$. In other terms, the correlations are constrained around their initial value, as expected. Since furthermore $\tau_{i,j}(0) = \tau_{j,i}(0)$, Eqs.(5.21, 5.22) prove that in the strongly localised regime the disorder-averaged magnetic response function vanishes

$$\lim_{\zeta\to 0} i\chi_{i,j}(t) = 0. \tag{5.23}$$

This implies that the disorder-averaged magnetic susceptibility $\tilde{\chi}_{i,j}(\omega)$, defined as the temporal Fourier transform of $\chi_{i,j}(t)$, decreases in magnitude as the disorder strength increases, and vanishes in the strongly localised regime. Therefore, in this regime the system displays a negligibly small induced magnetisation in response to a magnetic perturbation applied to a distant region of the lattice. Examples of the bounds Eqs. (5.18) and Eq. (5.21) as a function of ζ are shown in Fig. (5.3). Here

again, our criterion for many-body dynamical localisation implies strong constraints on an observable physical quantity.

5.4 Proofs of the one-body results

Consider the situation where a single up-spin lives in a sea of down-spins (or the opposite) in the XXZ regime. In this situation we choose the most natural (and only physically meaningful) partition $S = \emptyset$, $S' = \mathbb{S}$. Mathematically, this corresponds to partitioning the Hamiltonian into its usual matrix elements. Choosing this partition, the configuration graph is identifiable to the physical lattice and a configuration of S' simply specifies the position of the unique up-spin. Consequently, the configuration potentials Y_α are of the form $2B_\alpha - \mathcal{B}$ with B_α the random magnetic field felt by the up-spin at site α and $\mathcal{B}$ the total sum of all random magnetic fields. This quantity is an overall energy shift to the Hamiltonian and can be removed without affecting the results[3]. Finally, we note that the generalised Green's functions reduce to the usual Green's functions.

Consider two points a and b of $\mathbb{Z}^\delta$ and let d be their distance. The starting point of the proof of one-body localisation in δ-dimensions is the following criterion, discovered by Aizenman and Molchanov [164],

$$\begin{cases} \exists C < \infty,\ \zeta > 0,\ 0 < s < 1 \text{ with} \\ \mathbb{E}\Big[\big|G(a,b;z)\big|^s\Big] \leq Ce^{-d/\zeta}, \end{cases} \Longrightarrow \begin{cases} \exists C' < \infty,\ \zeta' > 0 \text{ with} \\ \mathbb{E}\Big[\sup_{t\in\mathbb{R}} \big|\langle a|\mathsf{P}_I e^{-i\mathsf{H}t}|b\rangle\big|\Big] \leq C'e^{-d/\zeta'}, \end{cases} \tag{5.24}$$

where we may use $C' = \frac{1}{2\pi}\big(2|I|\big)^{\frac{1}{2-s}} C$, as we prove in a more general setting in §5.6.1. Relying on this criterion, we prove in this section that the fractional moments of the system Green's functions $\big|G(a,b;z)\big|^s$ are, on average, exponentially bounded.

5.4.1 One-dimensional chain

We first consider a 1D chain of down-spins, denoted $\mathcal{L}$. Initially, a single up-spin is present on site a. Let b be another site of $\mathcal{L}$ located at a distance d from a. Since there is always only a single simple path between any two points of $\mathcal{L}$, the path-sum representation of the system Green's function $G(a,b;z)$ yields

$$\begin{aligned} \mathbb{E}\big[|G(a,b;\,z)|^s\big] &= |2J|^{ds}\,\mathbb{E}\left[\Big|\prod_{j=0}^{d} G_{\mathcal{L}^j}(a_j,a_j;\,z)\Big|^s\right], \\ &\leq |2J|^{ds}\,\mathbb{E}\left[\prod_{j=0}^{d}\big|G_{\mathcal{L}^j}(a_j,a_j;\,z)\big|^s\right], \end{aligned} \tag{5.25}$$

[3]Calculations with and without $\mathcal{B}$ yield the same bound for the onset of localisation.

with $a_0 \equiv a$, $a_d \equiv b$, $\mathcal{L}^j \equiv \mathcal{L}\backslash\{a_0, \cdots, a_{j-1}\}$, $\mathbb{E}[.]$ the expectation with respect to the random magnetic fields and we used $\mathsf{H}_{a_{j+1}\leftarrow a_j} = 2J$. We progress by transforming the expectation of Eq. (5.25) into nested conditional expectations:

$$\begin{aligned}\mathbb{E}\big[|G(a,b;\,z)|^s\big] &= |2J|^{ds} \\ &\mathbb{E}_{\{B\}\backslash[a,b]}\left[\mathbb{E}_{B_{a_d}|}\left[\cdots\mathbb{E}_{B_{a_1}|}\left[\mathbb{E}_{B_{a_0}|}\Big[\prod_{j=0}^{d}\big|G_{\mathcal{L}^j}(a_j,a_j;\,z)\big|^s\Big]\right]\cdots\right]\right].\end{aligned} \tag{5.26}$$

In this expression, $\mathbb{E}_{B_{a_j}|}[.]$ is a short hand notation for the conditional expectation with respect to the magnetic field B_{a_j} at site a_j knowing $B_{a_{j+1}}, \cdots, B_{a_d}$ and all magnetic fields affecting sites outside of the interval $[a,b]$. Finally, $\mathbb{E}_{\{B\}\backslash[a,b]}[.]$ is the expectation with respect to the magnetic fields affecting sites outside of the interval $[a,b]$.

At this point it is essential to recall that the product over Green's functions represents a simple path. Thus the magnetic field B_{a_k} appearing in $G_{\mathcal{L}^{j\leq k}}(a_{j\leq k}, a_{j\leq k};\,z)$ cannot appear in any of the subsequent Green's functions $G_{\mathcal{L}^{j>k}}(a_{j>k}, a_{j>k};\,z)$ since once traversed by the simple path, site a_k has been removed form the lattice $\mathcal{L}$. In particular, the only Green's function that can depend on B_{a_0} is $G_{\mathcal{L}}(a_0,a_0;\,z)$. Then,

$$\mathbb{E}_{B_{a_0}|}\Big[\prod_{j=0}^{d}\big|G_{\mathcal{L}^j}(a_j,a_j;\,z)\big|^s\Big] = \prod_{j=1}^{d}\big|G_{\mathcal{L}^j}(a_j,a_j;\,z)\big|^s\,\mathbb{E}_{B_{a_0}|}\Big[\big|G_{\mathcal{L}}(a_0,a_0;\,z)\big|^s\Big], \tag{5.27}$$

Furthermore, the dependency of $G_{\mathcal{L}}(a_0,a_0;\,z)$ on B_{a_0} is very simple: indeed by virtue of the path-sum representation of matrix inverses, we have

$$G_{\mathcal{L}}(a_0,a_0;\,z) = \big[z - 2B_{a_0} - \mathsf{H}_{a_0} - \Sigma_0\big]^{-1}, \tag{5.28}$$

with H_{a_0} is the deterministic part of the potential felt by the spin at site a_0 and Σ_0 the sum of all cycles off a_0 on $\mathcal{L}^0$. In this context however, it is known as the self-energy. It is noteworthy that the self-energy being a sum of cycles on $\mathcal{L}^0 \equiv \mathcal{L}\backslash\{a_0\}$, it does not depend on B_{a_0} and, by construction, neither does $z - \mathsf{H}_{a_0}$. Therefore, the dependency of $|G_{\mathcal{L}}(a_0,a_0;\,z)|^s$ on B_{a_0} is of the form $|2B_{a_0} + M|^{-s}$, with $M \in \mathbb{C}$. Thanks to these observations and using the result of Proposition 5.5.2 (see p. 141), the conditional expectation of Eq. (5.27) is upper bounded by

$$\mathbb{E}_{B_{a_0}|}\Big[\big|G_{\mathcal{L}}(a_0,a_0;\,z)\big|^s\Big] \leq \frac{\|\rho\|_\infty^s}{1-s}. \tag{5.29}$$

where $\|\rho\|_\infty = 1/(\sigma_B\sqrt{2\pi})$ is the infinity-norm of the probability distribution ρ of the random magnetic fields, with σ_B its variance.

We then repeat the above procedure for all the subsequent conditional expectations, always observing that $|G_{\mathcal{L}^j}(a_j,a_j;\,z)|^s$ is of the form $|B_{a_j} + M|^{-s}$ for some

$M \in \mathbb{C}$ which does not depend on B_{a_j}. Thus we obtain

$$\mathbb{E}\big[|G(a,b;\,z)|^s\big] \leq |2J|^{ds}\,\mathbb{E}_{\{B\}\setminus[a,b]}\left[\left(\frac{1}{(1-s)(\sigma_B\sqrt{2\pi})^s}\right)^{d+1}\right], \\ = \frac{\|\rho\|_\infty^s}{1-s} \times \frac{(2|J|)^{ds}}{(1-s)^d}\frac{1}{(\sigma_B\sqrt{2\pi})^{ds}}. \tag{5.30}$$

This exhibits exponential decay with d as soon as $\sigma_B > 2|J|/\big(\sqrt{2\pi}(1-s)^{1/s}\big)$ for some $0 < s < 1$.

5.4.2 $\delta > 1$ dimensional lattices

The only difference between the $\delta > 1$ and the $\delta = 1$ dimensional cases is that when the physical lattice is more than one dimensional, there exists more than one simple path of length $\ell \geq d$ between any two vertices of the lattice located at distance d from each other. The path-sum representation of the Green's function is then

$$\mathbb{E}\big[|G(a,b;\,z)|^s\big] = \mathbb{E}\left[\left|\sum_{\ell\geq d}\sum_{\Pi_{\mathcal{L}^\delta;\,ab;\,\ell}}(2J)^\ell\prod_{j=0}^{\ell}G_{\mathcal{L}^j}(a_j,a_j;\,z)\right|^s\right], \tag{5.31}$$

with $\Pi_{\mathcal{L}^\delta;\,ab;\,\ell}$ the ensemble of simple-paths of length ℓ from a to b on $\mathcal{L}^\delta$. Remarking that for any ensemble of complex numbers $\{c_j\}$ and $0 < s < 1$, $|\sum_j c_j|^s \leq \sum_j |c_j|^s$, the above becomes

$$\mathbb{E}\big[|G(a,b;\,z)|^s\big] \leq \sum_{\ell\geq d}\sum_{\Pi_{\mathcal{L}^\delta;\,ab;\,\ell}}|2J|^{\ell s}\,\mathbb{E}\left[\prod_{j=0}^{\ell}\big|G_{\mathcal{L}^j}(a_j,a_j;\,z)\big|^s\right]. \tag{5.32}$$

Each element of the sum can now be treated with the technique presented in the 1 dimensional case. Since furthermore on $\mathcal{L}(\delta) \equiv \mathbb{Z}^\delta$ the number of simple paths of length $\ell > 0$ is clearly upper bounded by $2\delta(2\delta-1)^{\ell-1}$, we obtain

$$\mathbb{E}\Big[|G_{\mathcal{L}(\delta)}(a,b;\,z)|^s\Big] \leq \frac{\|\rho\|_\infty^s}{1-s}\sum_{\ell=d}^{\infty}\frac{2\delta(2\delta-1)^{\ell-1}(2|J|)^{\ell s}}{(1-s)^\ell(\sigma_B\sqrt{2\pi})^{\ell s}}, \tag{5.33}$$

The above series converges when $\sigma_B > \big((2\delta-1)/(1-s)\big)^{1/s} \times 2|J|/\sqrt{2\pi}$, in which case

$$\mathbb{E}\Big[\sup_{t\in\mathbb{R}} \big|\langle a|\mathsf{P}_I e^{-\mathrm{i}\mathsf{H}t}|b\rangle\big|\Big] \leq C\, e^{-\frac{d}{(2-s)\zeta}}, \tag{5.34}$$

$$\zeta^{-1} = \ln\Big[\frac{1-s}{2\delta-1}\Big(\frac{\sigma_B\sqrt{2\pi}}{2|J|}\Big)^s\Big] > 0 \quad \text{for} \quad \sigma_B > \Big(\frac{2\delta-1}{1-s}\Big)^{1/s}\frac{2|J|}{\sqrt{2\pi}},$$

$$C = \frac{1}{2\pi}\big(2|I|\big)^{\frac{1}{2-s}}\frac{\|\rho\|_\infty^s}{1-s}\frac{2\delta}{2\delta-1}\frac{1}{1-e^{-1/\zeta}}. \tag{5.35}$$

This establishes Proposition 5.3.1.

▶ We prove Theorem 5.3.2.

Proof. The demonstration of the theorem is entirely identical to the proof of one-body localisation on $\delta \geq 1$ lattices, with the exception that the constant C' of Eq. (5.4) has an additional $\|f\|_\infty$ factor, i.e. $C' = \frac{1}{2\pi}\big(2|I|\big)^{\frac{1}{2-s}}\|f\|_\infty C$ as can be seen from the derivation of Proposition 5.5.1 below. We omit the details. □

5.5 Proofs of the many-body results

5.5.1 A generalised fractional moment criterion

As we have seen in §5.2.2 and §5.2.3, localisation of the many-body dynamics is equivalent to the dynamical localisation of the SEP on its configuration space. This observation led to the following signature of many-body localisation Eq. (5.7b)

$$\mathbb{E}\Big[\sup_{t\in\mathbb{R}} \big\|\big(\langle\omega|\otimes \mathsf{I}_S\big)\mathsf{P}_I(\mathsf{H})e^{-i\mathsf{H}t}\big(|\alpha\rangle\otimes\mathsf{I}_S\big)\big\|\Big] \leq Ce^{-d(\alpha,\omega)/\zeta}. \tag{5.36}$$

In order to demonstrate that there exists a finite value of the variance σ_B of the random magnetic fields such that Eq. (5.36) is satisfied, we use a generalisation of the fractional moment criterion originally developed by Aizenman and Molchanov in the one-body setting [164, 165]. This criterion can be summarised as follows. Let a and b be two points of a lattice, then

$$\begin{cases}\exists C<\infty,\ \zeta>0,\ 0<s<1 \text{ with}\\ \mathbb{E}\Big[\big|G(a,b;z)\big|^s\Big] \leq Ce^{-d/\zeta},\end{cases} \Longrightarrow \begin{cases}\exists C'<\infty,\ \zeta'>0 \text{ such that}\\ \mathbb{E}\Big[\sup_{t\in\mathbb{R}}\big|\langle a|\mathsf{P}_I e^{-i\mathsf{H}t}|b\rangle\big|\Big] \leq C'e^{-d/\zeta'}.\end{cases}$$

where $G(a,b;z)$ is the Green's function evaluated between points a and b. For our purpose it is necessary to extend this criterion to arbitrary system partitions $\mathbb{S} = S\cup S'$. In particular, one must extend the notion of Green's function between two points of a lattice to that of Green's functions between two configurations accessible to S'.

This is easily achieved using a tensor-product partition of the system resolvent $\mathsf{R}_\mathsf{H}(z) = \big(z\mathsf{I}-\mathsf{H}\big)^{-1}$. In continuity with existing conventions regarding the Green's

functions, we denote the elements of this partition

$$G_{\mathcal{G}_{S,S'}}(\omega,\alpha;z) := \big(\mathsf{R}_{\mathsf{H}}(z)\big)_{\omega\leftarrow\alpha}, \tag{5.37}$$

and call them *generalised Green's functions*. These are $2^{|S|}\times 2^{|S|}$ submatrices of the system resolvent $\mathsf{R}_{\mathsf{H}}(z)$. As required of a tensor-product partition of the resolvent, the generalised Green's functions fulfill the characteristic relation

$$|\omega\rangle\langle\alpha|\otimes G_{\mathcal{G}_{S,S'}}(\omega,\alpha;z) = \big(\mathsf{P}_\omega\otimes\mathsf{I}_S\big)\,.\,\mathsf{R}_{\mathsf{H}}(z)\,.\,\big(\mathsf{P}_\alpha\otimes\mathsf{I}_S\big), \tag{5.38a}$$

with $\mathsf{P}_\alpha = |\alpha\rangle\langle\alpha|$. Equivalently,

$$G_{\mathcal{G}_{S,S'}}(\omega,\alpha;z) = \big(\langle\omega|\otimes\mathsf{I}_S\big)\,.\,\mathsf{R}_{\mathsf{H}}(z)\,.\,\big(|\alpha\rangle\otimes\mathsf{I}_S\big). \tag{5.38b}$$

Using generalised Green's functions, Aizenman's fractional moment criterion can be extended to arbitrary system partitions:

Lemma 5.5.1 (Fractional moment criterion for arbitrary system partitions)**.** *Let $\mathbb{S} = S\cup S'$ be a system partition, $\mathcal{G}_{S,S'}$ the graph associated to it and $d(\alpha,\omega)$ the distance between vertices v_α and v_ω on $\mathcal{G}_{S,S'}$. If there exists $C<\infty$ and $\zeta<\infty$ such that, for $0<s<1$,*

$$\mathbb{E}\Big[\big\|G_{\mathcal{G}_{S,S'}}(\omega,\alpha;\,z)\big\|^s\Big] < Ce^{-d(\alpha,\omega)/\zeta}, \tag{5.39}$$

then

$$\mathbb{E}\bigg[\sup_{t\in\mathbb{R}}\Big\|\Big(\mathsf{P}_I(\mathsf{H})e^{-i\mathsf{H}t}\Big)_{\omega\leftarrow\alpha}\Big\|\bigg] \le \frac{1}{2\pi}\big(2|I|\big)^{\frac{1}{2-s}}\,Ce^{-\frac{d(\alpha,\omega)}{(2-s)\zeta}}, \tag{5.40}$$

where $|I|$ is the Lebesgue measure of I.

To preserve the flow of the argument, we defer the proof of this result to Appendix 5.6.1. Thanks to Lemma 5.5.1 above, we may focus our efforts on bounding fractional norms of the generalised Green's functions. We achieve this using their path-sums representation.

5.5.2 Bounding the norms of generalised Green's functions

Following the result of Lemma 5.5.1, we are left with the task of proving that there exists an amount of disorder σ_B such that the fractional norms of generalised Green's functions are exponentially bounded, i.e.

$$\mathbb{E}\left[\big\|G_{\mathcal{G}_{S,S'}}(\omega,\alpha;z)\big\|^s\right] \le Ce^{-d(\alpha,\omega)/\zeta}, \tag{5.41}$$

with $s\in(0,1)$, $C<\infty$ and most importantly $0<\zeta<\infty$.

In the spirit of the proof for the one-body situation [141], we bound the expectation of the fractional moments of the generalised Green's functions using their

path-sums representation

$$\begin{aligned}
&\mathbb{E}\Big[\big\|G_{\mathcal{G}_{S,S'}}(\omega,\alpha;\,z)\big\|^s\Big] \\
&\qquad\leq \mathbb{E}\Big[\sum_{\Pi_{\mathcal{G};\alpha\omega}} \|G_{\mathcal{G}^\ell_{S,S'}}(\alpha_\ell,\alpha_\ell;\,z)\|^s \prod_{j=0}^{\ell-1} \big\|\mathsf{H}_{\alpha_{j+1}\leftarrow\alpha_j} G_{\mathcal{G}^j_{S,S'}}(\alpha_j,\alpha_j;\,z)\big\|^s\Big], \\
&\qquad\leq \sum_{\ell\geq d(\alpha,\omega)}^{L_p} |\Pi_{\mathcal{G}_{S,S'};\alpha\omega}|(\ell)\,(n_{\mathcal{L}}\mathcal{J})^{\ell s}\,\mathbb{E}\Big[\prod_{j=0}^{\ell}\big\|G_{\mathcal{G}^j_{S,S'}}(\alpha_j,\alpha_j;\,z)\big\|^s\Big]. \qquad (5.42)
\end{aligned}$$

In these expressions we use $\|\mathsf{H}_{\alpha_{j+1}\leftarrow\alpha_j}\| \leq n_{\mathcal{L}}\mathcal{J}$ for all flips of the Hamiltonian. The quantity $|\Pi_{\mathcal{G}_{S,S'};\alpha\omega}|(\ell)$ is the number of simple paths of length ℓ on $\mathcal{G}_{S,S'}$ from α to ω and L_p is the length of the longest simple path on $\mathcal{G}_{S,S'}$. As long as $|S'|$ is finite, L_p is finite. In most cases, the number of simple paths is unknown and we may simply upper bound it by the total number of walks of length ℓ on $\mathcal{G}_{S,S'}$ from α to ω, denoted $|W_{\mathcal{G}_{S,S'};\alpha\omega}|(\ell)$, or if this is also unknown by powers of the largest eigenvalue $\lambda_{\mathcal{G}_{S,S'}}$ of $\mathcal{G}_{S,S'}$. In order to progress, it is necessary to identify explicitly the configuration graph $\mathcal{G}_{S,S'}$. In fact, if S' comprises only non-adjacent sites, then $\mathcal{G}_{S,S'}$ must be the $|S'|$-hypercube $\mathcal{H}_{|S'|}$. To understand why, remark that the $|S'|$-hypercube connects all configurations of S' differing by one spin flip. For example, the configuration graph $\mathcal{H}_2$ is shown on Fig. 5.4. Thus, if $\mathcal{G}_{S,S'}$ is neither the $|S'|$-hypercube nor a subgraph of it, then there is at least one transition allowed between two configurations of the S' differing by two spin flips, e.g. $\uparrow\uparrow\longrightarrow\downarrow\downarrow$. This corresponds to two *non-adjacent* spins flipping at the same time, which is not allowed by the XYZ Hamiltonian. Thus, from now on we shall consider that the configuration space is the $|S'|$-hypercube $\mathcal{G}_{S,S'} \equiv \mathcal{H}_{|S'|}$, this being the case least favorable to localisation[4]. The number of simple paths of length ℓ on $\mathcal{H}_{|S'|}$ is bounded by the number of walks of length ℓ on $\mathcal{H}_{|S'|}$. This is analytically known for any two vertices of any hypercube. For the sake of simplicity however, we use the larger bound $|\Pi_{\mathcal{G}_{S,S'};\alpha\omega}|(\ell) \leq |S'|^\ell$.

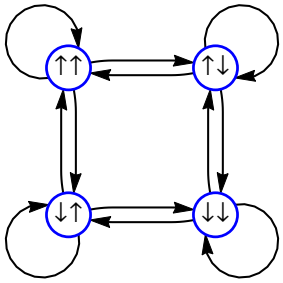

Figure 5.4: Graph $\mathcal{H}_2$

As noted in §5.3.2, a major difficulty in the study of many-body localisation as compared to one-body localisation lies in that even when walking along a simple path on $\mathcal{G}_{S,S'}$, the SEP encounters configuration potentials that are linearly dependent on the ones it previously encountered. Indeed, since there are only $|S'|$ random B-fields affecting the sites of S', there are only $|S'|$ linearly independent configuration potentials. By contrast, the configuration graph $\mathcal{G}_{S,S'}$ has $2^{|S'|}$ vertices. A negative consequence of this is that *all* the self-energies entering *all* the generalised Green's functions depend on *all* configurations potentials. Thus, contrary to the one-body

[4]The $|S'|$-hypercube being the largest and most connected configuration graph allowed by the Hamiltonian, it has the largest number of simple paths and simple cycles. By Eq. (5.42), this is the least favorable case for localisation .

case, the generalised Green's functions have a complicated dependency on the configuration potentials. This dependency is analytically accessible for sufficiently small S', e.g. $|S'| = 1 - 6$, yet analytical calculations of the required expectations remain very difficult as we shall see below.

Another consequence of the linear dependency between the configuration potentials is that we cannot distribute the conditional expectations in the product of generalised Green's functions as is possible in the one-body case. This further complicates the calculation of the required expectation along a simple path $\mathbb{E}\Big[\prod_{j=0}^{\ell} \big\|G_{\mathcal{G}^j_{S,S'}}(\alpha_j, \alpha_j; z)\big\|^s\Big]$. In order to recover simpler expressions, we note that the expectation above involves the product measure $d\varrho_{\{B_j\}_{j\notin S'}} \prod_{j=1}^{|S'|} d\varrho_{Y_{\alpha_j}}$, with $\varrho_{Y_{\alpha_j}}$ the cumulative distribution function of Y_{α_j} . Therefore, we can upper bound the expectation of a product of norms of generalised Green's functions by a product of expectations on using the generalised Hölder inequality [166]. This leads to

$$\mathbb{E}\Big[\prod_{j=0}^{\ell} \big\|G_{\mathcal{G}^j_{S,S'}}(\alpha_j, \alpha_j; z)\big\|^s\Big] \leq \prod_{j=0}^{\ell} \Big(\mathbb{E}\Big[\big\|G_{\mathcal{G}^j_{S,S'}}(\alpha_j, \alpha_j; z)\big\|^{q_j s}\Big]\Big)^{1/q_j}, \tag{5.43}$$

with $\sum_{j=0}^{\ell} q_j^{-1} = 1$. We will see below that the above can only be bounded if $q_j s < 1$ for all j. Using $q_j = \ell + 1$ for all j we thus need $s < 1/(\ell+1)$ to guarantee the existence of the above expectations. Since the graph $\mathcal{G}_{S,S'}$ is a subgraph of $\mathcal{H}_{|S'|}$, the longest simple path has length at most $\ell = L_p \leq 2^{|S'|}$ and $s < 1/(2^{|S'|}+1)$ is sufficient to guarantee existence of all expectations. We will see later that this requirement on s can be waived using a technical result from Ref. [154].

We now turn to bounding expectations of individual generalised Green's functions. Using conditional expectations we have

$$\mathbb{E}\Big[\big\|G_{\mathcal{G}^j_{S,S'}}(\alpha_j, \alpha_j; z)\big\|^{s_j}\Big] = \mathbb{E}_{\{B_j\}_{j\notin S'}, \{Y_{\alpha_i}\}_{i\neq j}}\Big[\mathbb{E}_{Y_{\alpha_j}|}\Big[\big\|G_{\mathcal{G}^j_{S,S'}}(\alpha_j, \alpha_j; z)\big\|^{s_j}\Big]\Big], \tag{5.44}$$

with $s_j = q_j s$ and $\mathbb{E}_{Y_{\alpha_j}|}[.]$ is the expectation with respect to Y_{α_j} knowing the value of $|S'| - 1$ linearly independent configuration potentials affecting S', here denoted $\{Y_{\alpha_i}\}_{i\neq j}$, as well as all magnetic fields affecting sites outside of the sublattice S'.

As noted earlier, thanks to path-sum, for sufficiently small $|S'|$ (typically less than 6) the exact dependency of a generalised Green's functions on a certain configuration potential is explicitly accessible. Yet, this dependency is still too complicated to be used to bound the expectation of the Green's function with respect to this configuration potential. To see this, let us consider again the simple example where S' comprises only two sites, denoted 1 and 2. In this situation the configuration graph of $|S'|$ is the square $\mathcal{H}_2$ and the configurations available to S' are $\uparrow\uparrow$, $\uparrow\downarrow$, $\downarrow\uparrow$ and $\downarrow\downarrow$, see Fig. (5.4). The corresponding configuration potentials are $Y_{\uparrow\uparrow} = B_1 + B_2$,

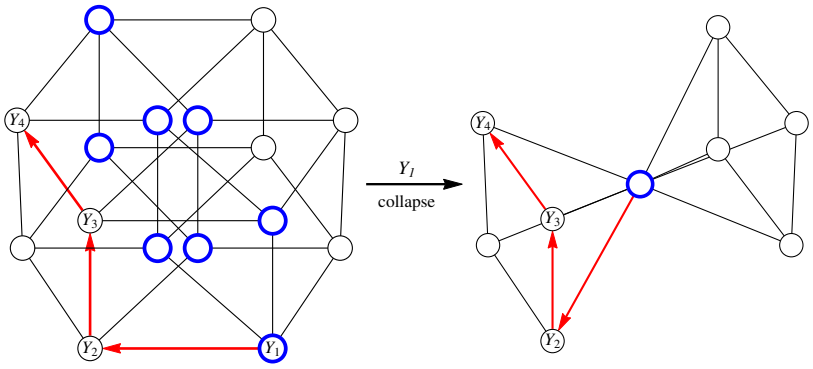

Figure 5.5: Left: configuration graph $\mathcal{H}_4$ of a sublattice S' comprising 4 sites. The red arrows represent a simple path along which S' successively encounters the random configuration potentials $Y_1 \to Y_2 \to Y_3 \to Y_4$. In thick blue are the configurations of S' whose random potential is linearly dependent on Y_1. Right: configuration graph of the sublattice after collapsing all configurations whose random potential is linearly dependent on Y_1 into a single vertex. Note: for clarity the self-loops are not represented on these graphs.

$Y_{\uparrow\downarrow} = B_1 - B_2$, $Y_{\downarrow\uparrow} = -Y_{\uparrow\downarrow} = -B_1 + B_2$ and $Y_{\downarrow\downarrow} = -Y_{\uparrow\uparrow} = -B_1 - B_2$. Then

$$\begin{aligned} G_{\mathcal{H}_2}(\uparrow\uparrow, \uparrow\uparrow; z) = \Big[z\mathsf{I} - Y_{\uparrow\uparrow}\mathsf{I} - \tilde{\mathsf{H}}_{\uparrow\uparrow} - 4J^2\,\Sigma_{\uparrow\downarrow}(Y_{\uparrow\uparrow}) - 4J^2\,\Sigma_{\downarrow\uparrow}(Y_{\uparrow\uparrow}) \\ - 16J^4\,\Sigma_{\downarrow\uparrow}^{\uparrow\downarrow}\,\Sigma_{\downarrow\downarrow}^{\uparrow\downarrow}(Y_{\uparrow\uparrow})\,\Sigma_{\uparrow\downarrow}(Y_{\uparrow\uparrow}) \\ -16J^4\,\Sigma_{\uparrow\downarrow}^{\downarrow\uparrow}\,\Sigma_{\downarrow\downarrow}^{\downarrow\uparrow}(Y_{\uparrow\uparrow})\,\Sigma_{\downarrow\uparrow}(Y_{\uparrow\uparrow}) \Big]^{-1}, \end{aligned} \tag{5.45}$$

where $\Sigma_{\uparrow\downarrow}(Y_{\uparrow\uparrow}) = \left[z\mathsf{I} - Y_{\uparrow\downarrow}\mathsf{I} - \tilde{\mathsf{H}}_{\uparrow\downarrow} - \Sigma_{\downarrow\downarrow}^{\uparrow\downarrow}(Y_{\uparrow\uparrow})\right]^{-1}$, $\Sigma_{\downarrow\downarrow}^{\uparrow\downarrow}(Y_{\uparrow\uparrow}) = \left[z\mathsf{I} + Y_{\uparrow\uparrow}\mathsf{I} - \tilde{\mathsf{H}}_{\downarrow\downarrow} - \Sigma_{\downarrow\uparrow}^{\uparrow\downarrow}\right]^{-1}$ and similarly for $\Sigma_{\downarrow\uparrow}(Y_{\uparrow\uparrow})$ and $\Sigma_{\downarrow\downarrow}^{\downarrow\uparrow}(Y_{\uparrow\uparrow})$. The quantities $\Sigma_{\downarrow\uparrow}^{\uparrow\downarrow}$ and $\Sigma_{\uparrow\downarrow}^{\downarrow\uparrow}$ are analytically available and do not depend on $Y_{\uparrow\uparrow}$. The generalised Green's function $G_{\mathcal{H}_2}(\uparrow\uparrow, \uparrow\uparrow; z)$ is therefore an exactly known matrix-valued rational function of $Y_{\uparrow\uparrow}$. For this later reason, it is very difficult to find an analytical upper bound for $\mathbb{E}_{Y_{\uparrow\uparrow}}\left[\|G_{\mathcal{H}_2}(\uparrow\uparrow, \uparrow\uparrow; z)\|^s\right]$, in particular a bound which is independent of largely unknown quantities such as the spectrum of the Hamiltonian.

Thus, instead of attempting to bound the expectation of a generalised Green's functions $G_{\mathcal{G}^j_{S,S'}}(\alpha_j, \alpha_j; z)$, we remark that it is a submatrix of a larger matrix whose dependency on Y_{α_j} is much simpler. To see this, consider merging all the vertices of $\mathcal{G}^j_{S,S'}$ whose configuration potentials are linearly dependent on Y_{α_j}. We call this operation an Y_{α_j}-collapse and the so created vertex, the collapsed vertex, which we denote $v_{Y_{\alpha_j}}$. An illustration of this procedure in shown on Fig. (5.5). The Y_{α_j}-collapse gives rise to a new graph, denoted $\mathcal{G}^j_{S,S'}(Y_{\alpha_j})$, from which we immediately

obtain the generalised Green's function of the collapsed vertex as

$$G_{\mathcal{G}^j_{S,S'}(Y_{\alpha_j})}(v_{Y_{\alpha_j}}, v_{Y_{\alpha_j}};\, z) = \Big[z\mathsf{I} - Y_{\alpha_j}\mathsf{I} - \Sigma_{Y_{v_{\alpha_j}}}\Big]^{-1}, \tag{5.46}$$

where $\Sigma_{v_{Y_{\alpha_j}}}$ is the self-energy associated to the ensemble of configurations which are linearly dependent on Y_{α_j}, i.e. it is the sum of all cycles off $v_{Y_{\alpha_j}}$ on $\mathcal{G}^j_{S,S'}(Y_{\alpha_j})\backslash\{v_{Y_{\alpha_j}}\}$. Since all vertices whose configuration potential is linearly dependent on Y_{α_j} have been merged to form $v_{Y_{\alpha_j}}$, none of the remaining vertices of $\mathcal{G}^j_{S,S'}(Y_{\alpha_j})\backslash\{v_{Y_{\alpha_j}}\}$ depend on Y_{α_j}. Consequently, $\Sigma_{v_{Y_{\alpha_j}}}$ is independent of Y_{α_j}. Furthermore, $G_{\mathcal{G}^j_{S,S'}}(\alpha_j, \alpha_j;\, z)$ is a submatrix of $G_{\mathcal{G}^j_{S,S'}(Y_{\alpha_j})}(v_{Y_{\alpha_j}}, v_{Y_{\alpha_j}};\, z)$: more precisely it is the submatrix corresponding to S' being in configuration α_j. From these observations we deduce

$$\|G_{\mathcal{G}^j_{S,S'}}(\alpha_j, \alpha_j;\, z)\|^{s_j} \leq \big\|G_{\mathcal{G}^j_{S,S'}(Y_{\alpha_j})}(v_{Y_{\alpha_j}}, v_{Y_{\alpha_j}};\, z)\big\|^{s_j}, \tag{5.47}$$

and therefore

$$\mathbb{E}_{Y_{\alpha_j|}}\Big[\|G^j_{\mathcal{G}_{S,S'}}(\alpha_j, \alpha_j;\, z)\|^{s_j}\Big] \leq \mathbb{E}_{Y_{\alpha_j|}}\Big[\big\|G_{\mathcal{G}^j_{S,S'}(Y_{\alpha_j})}(v_{Y_{\alpha_j}}, v_{Y_{\alpha_j}};\, z)\big\|^{s_j}\Big]. \tag{5.48}$$

The right hand side of the above is bounded thanks to the following lemma, whose proof we defer to Appendix 5.6.2:

Lemma 5.5.2. *Let Y be a normally distributed random variable with density function ρ. Let $\mathsf{A} \in \mathbb{C}^{n\times n}$ be a normal matrix. Then the following bound holds for any $0 < s < 1$,*

$$\mathbb{E}_Y\Big[\big\|[Y\mathsf{I} + \mathsf{A}]^{-1}\big\|^s\Big] \leq \frac{(2n)^s}{1-s}\|\rho\|^s_\infty, \tag{5.49}$$

where $\|.\|$ is the 2-norm and $\|.\|_\infty$ the infinity norm.

Using the lemma and on assuming that $s_j < 1$, we obtain

$$\mathbb{E}_{Y_{\alpha_j|}}\Big[\big\|G_{\mathcal{G}^j_{S,S'}(Y_{\alpha_j})}(v_{Y_{\alpha_j}}, v_{Y_{\alpha_j}};\, z)\big\|^{s_j}\Big] \leq \frac{(2D_j)^{s_j}}{1-s_j}\|\rho_{Y_{\alpha_j|}}\|^{s_j}_\infty. \tag{5.50}$$

The quantity D_j is the dimension of $G_{\mathcal{G}^j_{S,S'}(Y_{\alpha_j})}(v_{Y_{\alpha_j}}, v_{Y_{\alpha_j}};\, z)$ or, in other terms, D_j is the rank of the perturbation associated with modifications of Y_{α_j}. We bound D_j on noting that: i) each vertex of $\mathcal{G}_{S,S'}$ is associated with a vector space of dimension $2^{|S|}$; ii) at most half of the vertices of $\mathcal{G}_{S,S'}$ are linearly dependent on any given configuration potential. From these observations it follows that $D_j \leq 2^{|S|}\times 2^{|S'|}/2 := D/2$. Finally, $\rho_{Y_{\alpha_j|}}$ is the probability distribution of configuration potential Y_{α_j} knowing the value of $|S'|-1$ linearly independent configuration potentials affecting S' as well as all magnetic fields affecting sites outside of the sublattice S'. We show in §5.6.4 that this distribution is normal and its variance is at least σ_B. Taken together, Eqs. (5.48) and (5.50) thus yield the following bound concerning individual

Green's functions

$$\mathbb{E}_{Y_{\alpha_j|}}\Big[\|G^j_{\mathcal{G}_{S,S'}}(\alpha_j,\alpha_j;\,z)\|^{s_j}\Big] \leq \frac{(2D_j)^{s_j}}{1-s_j}\|\rho_{Y_{\alpha_j|}}\|^{s_j}_\infty. \tag{5.51}$$

Using the result of Eq. (5.51) in conjunction with Eqs. (5.42, 5.43, 5.44), we finally arrive at the desired bound for the disorder-averaged fractional norm of any generalized Green's function

$$\mathbb{E}\Big[\big\|G_{\mathcal{G}_{S,S'}}(\omega,\alpha;\,z)\big\|^s\Big] \leq \sum_{\ell\geq d(\alpha,\omega)}^{L_p} |\Pi_{\mathcal{G}_{S,S'};\alpha\omega}|(\ell)(n_{\mathcal{L}}\mathcal{J})^{\ell s}\prod_{j=0}^{\ell}\left(\frac{(2D_j)^{s_j}}{1-s_j}\|\rho_{Y_{\alpha_j|}}\|^{s_j}_\infty\right)^{1/q_j}. \tag{5.52}$$

We establish in Appendix 5.6.4 that $\|\rho_{Y_{\alpha_j|}}\|_\infty \leq \|\rho\|_\infty = (\sigma_B\sqrt{2\pi})^{-1}$. Furthermore $|\Pi_{\mathcal{G}_{S,S'};\alpha\omega}|(\ell) \leq |S'|^\ell$, $D_j \leq D/2$ and

$$\prod_{j=0}^{\ell}\Big(\frac{1}{1-s_j}\Big)^{1/q_j} = \prod_{j=0}^{\ell}\Big(\frac{1}{1-(\ell+1)s}\Big)^{1/(\ell+1)} = \frac{1}{1-(\ell+1)s}, \tag{5.53}$$

upon choosing $q_j = \ell+1$, which is allowed by the sole requirement on the q_j, $\sum_{j=0}^{\ell} q_j^{-1} = 1$. Now define $r := \big(Dn_{\mathcal{L}}\mathcal{J}\|\rho\|_\infty\big)^s|S'|$, then the above observations lead to

$$\begin{aligned}\mathbb{E}\Big[\big\|G_{\mathcal{G}_{S,S'}}(\omega,\alpha;\,z)\big\|^s\Big] &\leq |S'|^{-1}\sum_{\ell\geq d(\alpha,\omega)}^{L_p}\frac{r^{\ell+1}}{1-(\ell+1)s},\\ &\leq |S'|^{-1}\Big|\sum_{\ell\geq d(\alpha,\omega)}^{\infty}\frac{r^{\ell+1}}{1-(\ell+1)s}\Big|.\end{aligned} \tag{5.54}$$

When $r<1$, the series of Eq. (5.54) converges, and we obtain the bound

$$\mathbb{E}\Big[\big\|G_{\mathcal{G}_{S,S'}}(\omega,\alpha;\,z)\big\|^s\Big] \leq |S'|^{-1}\frac{r^{1/s}}{s}B_r\big(d(\alpha,\omega)+1-s^{-1},0\big), \tag{5.55}$$

with $B_z(a,b) = \int_0^z t^{a-1}(1-t)^{b-1}dt$ is the incomplete Euler Beta function. To make the bound of Eq. (5.55) easier to understand, we note that for $0<s<1$, $0<z<1$ and $a\in\mathbb{R}$,

$$z^{1/s}B_z(a,0) < z^{(a-1)+1/s}\Phi\left(z,1,a\right), \tag{5.56}$$

with Φ the Hurwitz-Lerch zeta-function and $\Phi\left(z,1,a\right)$ decays algebraically with a for $a>0$. Thus we find

$$\mathbb{E}\Big[\big\|G_{\mathcal{G}_{S,S'}}(\omega,\alpha;\,z)\big\|^s\Big] \leq \frac{1}{s|S'|}\Phi\left(e^{-\frac{1}{\zeta}},1,d(\alpha,\omega)+1-s^{-1}\right)e^{-\frac{d(\alpha,\omega)}{\zeta}}. \tag{5.57a}$$

In this expression, we have defined

$$\zeta^{-1} = s \log\Big(\frac{\sigma_B\sqrt{2\pi}}{Dn_{\mathcal{L}}\mathcal{J}\,|S'|^{1/s}}\Big), \tag{5.57b}$$

i.e. $r = e^{-1/\zeta}$. In particular we have,

$$r > 1 \iff \zeta > 0 \iff \sigma_B > Dn_{\mathcal{L}}\mathcal{J}\,|S'|^{1/s}/\sqrt{2\pi}. \tag{5.57c}$$

At this point, the requirement $s < 1/(2^{|S'|}+1) < 2^{-|S'|}$, which we used in the proof, clearly seems to heavily degrade the condition on σ_B for the onset of localisation: indeed $s < 2^{-|S'|} \Rightarrow \sigma_B \geq |S'|^{1/s} \geq |S'|^{2^{|S'|}}$ is extremely large, even for moderate $|S'|$. We circumvent this difficulty by adapting a result of Ref. [154] to our situation:

Lemma 5.5.3 (Based on Aizenman and Warzel [154])**.** *If there exists $s_{max} < 1$ such that for all s, $0 < s < s_{max}$,*

$$\mathbb{E}\Big[\big\|G_{\mathcal{G}_{S,S'}}(\omega,\alpha;\,z)\big\|^s\Big] < Ce^{-d(\alpha,\omega)/\zeta}, \tag{5.58}$$

then for all $s \in (0,1)$ we have

$$\mathbb{E}\Big[\|G_{\mathcal{G}_{S,S'}}(\omega,\alpha;\,z)\|^s\Big] \leq c[s_1]^{s/s_1}\frac{2^{|S|s}}{(\sigma_B\sqrt{2\pi})^s}C^{\frac{s_1-s}{s_1}}e^{-\frac{(s_1-s)}{s_1}\frac{d(\alpha,\omega)}{\zeta}}, \tag{5.59}$$

with $s_{max} < s_1 < 1$ and $c[s_1] = 4^{1-s_1}k^{s_1}/(1-s_1)$ with k a finite universal constant.

We call this result *the extension lemma*. For the sake of clarity we defer its proof to Appendix 5.6.3. Using the extension lemma, we may extend the exponential bound from $0 < s < 1/(2^{|S'|}+1)$ to $0 < s < 1$. We obtain, for all $0 < s < 1$,

$$\begin{aligned}\mathbb{E}\Big[\big\|G_{\mathcal{G}_{S,S'}}(\omega,\alpha;\,z)\big\|^s\Big] \leq c[s_1]^{\frac{s}{s_1}}\frac{2^{-|S'|s}D^s}{(\sigma_B\sqrt{2\pi})^s}\times \\ \left(\frac{1}{s|S'|}\Phi\big(e^{-1/\zeta},1,d(\alpha,\omega)+1-s^{-1}\big)\right)^{\frac{s_1-s}{s_1}}e^{-\frac{(s_1-s)}{s_1}\frac{d(\alpha,\omega)}{\zeta}},\end{aligned} \tag{5.60}$$

where we used $2^{|S|} = D \times 2^{-|S'|}$ and the Hurwitz-Lerch zeta-function decays algebraically with $d(\alpha,\omega)$ when $d(\alpha,\omega) > s^{-1} - 1$. The results of Eqs. (5.57, 5.60) together with Lemma 5.5.1 establish Theorem 5.3.3.

Remark 5.5.1 (Wegner estimate and dissipative operators)**.** Instead of using Lemma 5.5.2 to upper bound $\mathbb{E}_{Y_{\alpha_j|}}\Big[\big\|G_{\mathcal{G}^j_{S,S'}(Y_{\alpha_j})}(v_{Y_{\alpha_j}},v_{Y_{\alpha_j}};\,z)\big\|^{s_j}\Big]$ as we did in Eq. (5.50), we may use two alternative arguments:

1) First, we may use the celebrated Wegner estimate for multi-particle systems [167]. The Wegner estimate provides the spectral density of H which in turn relates to the spectral density of $\Sigma_{Y_{v_{\alpha_j}}}$. This permits an alternative calculation

of an upper bound for the expectation and the end result in only a factor of 2 larger than that obtained by Lemma 5.5.2.

2) The second approach consist in noting that for $z \in \mathbb{C}^+$, $\Sigma_{Y_{v_{\alpha_j}}}$ being Hermitian, $z\mathsf{I} - \Sigma_{Y_{v_{\alpha_j}}}$ is dissipative [168, 169]. This allows to bound the expectation using arguments from [154, 170]. The bound is then extended to the entire complex plane (using conjugation and analytic continuation) and leads to a result similar to that obtained from Lemma 5.5.2.

These observations indicate that there is not much room for improvement of the bound on $\mathbb{E}_{Y_{\alpha_j|}}\Big[\big\|G_{\mathcal{G}^j_{S,S'}(Y_{\alpha_j})}(v_{Y_{\alpha_j}}, v_{Y_{\alpha_j}};\, z)\big\|^{s_j}\Big]$. Rather, work aiming at improving the overall bound for the onset of localisation should focus on bounding the expectation of an individual generalised Green's function from its explicit form as in Eq. (5.45), without recurring to Y-collapses.

5.6 Technical results

In this section we regroup four technical results: 1) we prove Lemma 5.5.1 relating exponential bounds on fractional norms of generalised Green's functions to dynamical localisation; 2) we prove Lemma 5.5.2, which provides an upper bound on expectations of the form $\mathbb{E}_Y\big[\|Y\mathsf{I} + \mathsf{A}\|^s\big]$; 3) we prove the extension Lemma 5.5.3; and 4) we study the marginal and joint distributions of the configuration potentials.

5.6.1 Generalised fractional moment criterion

In this section we establish Lemma 5.5.1, which we restate here for convenience.

Lemma 5.5.1. *Let $\mathbb{S} = S \cup S'$ be a system partition, $\mathcal{G}_{S,S'}$ the graph associated to it and $d(\alpha, \omega)$ the distance between vertices v_α and v_ω on $\mathcal{G}_{S,S'}$. If there exists $C < \infty$ and $\zeta < \infty$ such that*

$$\mathbb{E}\Big[\big\|G_{\mathcal{G}_{S,S'}}(\omega, \alpha;\, z)\big\|^s\Big] < Ce^{-d(\alpha,\omega)/\zeta}, \tag{5.61}$$

then for $0 < s < 1$,

$$\mathbb{E}\Big[\sup_{t\in\mathbb{R}}\big\|\big(\langle\omega|\otimes\mathsf{I}_S\big)\mathsf{P}_I(\mathsf{H})e^{-i\mathsf{H}t}\big(|\alpha\rangle\otimes\mathsf{I}_S\big)\big\|\Big] \leq \frac{1}{2\pi}\big(2|I|\big)^{\frac{1}{2-s}}\, Ce^{-\frac{d(\alpha,\omega)}{(2-s)\zeta}}, \tag{5.62}$$

where $|I|$ is the Lebesgue measure of I.

Proof. To prove the lemma, we first use Cauchy's integral relation for the matrix

exponential [51] to relate the exponential of the Hamiltonian with its resolvent

$$\big(\langle\omega|\otimes \mathsf{I}_S\big)\mathsf{P}_I(\mathsf{H})e^{-i\mathsf{H}t}\big(|\alpha\rangle\otimes \mathsf{I}_S\big) = \big(\langle\omega|\otimes \mathsf{I}_S\big)\,\frac{1}{2\pi i}\oint_{\gamma_I} e^{-izt}\,\mathsf{R}_{\mathsf{H}}(z)dz\,\big(|\alpha\rangle\otimes \mathsf{I}_S\big), \quad (5.63)$$

with γ_I a contour enclosing all the eigenvalues $\lambda\in \mathrm{Sp}(\mathsf{H})\cap I$, with $\mathrm{Sp}(\mathsf{H})$ the *discrete* spectrum of H, and only these. Using a line integral along the contour γ_I yields the upper bound

$$\sup_{t\in\mathbb{R}}\big\|\big(\langle\omega|\otimes \mathsf{I}_S\big)\mathsf{P}_I(\mathsf{H})e^{-i\mathsf{H}t}\big(|\alpha\rangle\otimes \mathsf{I}_S\big)\big\| \leq \frac{1}{2\pi}\int_I \big\|G_{\mathcal{G}_{S,S'}}\big(\omega,\alpha;\gamma_I(x)\big)\big\|\,d\gamma_I, \quad (5.64)$$

where $d\gamma_I = \gamma_I'(x)dx$ and we used $\|e^{-izt}\|_\infty = 1$ for $z\in\mathbb{R}$ [5]. More generally, for uniformly bounded functions $f(z)$ we would have $\|f\|_\infty$. In order for the fractional moments to appear, we use Hölder's inequality with $1 = s\,a+2(1-a)$, $a = 1/(2-s)$ and $s\in(0,1)$ [161]. This gives

$$\int_I \big\|G_{\mathcal{G}_{S,S'}}\big(\omega,\alpha;\gamma_I(x)\big)\big\|\,d\gamma_I \leq \left(\int_I \big\|G_{\mathcal{G}_{S,S'}}\big(\omega,\alpha;\gamma_I(x)\big)\big\|^2\,d\gamma_I\right)^{1-a}\times \left(\int_I \big\|G_{\mathcal{G}_{S,S'}}\big(\omega,\alpha;\gamma_I(x)\big)\big\|^s\,d\gamma_I\right)^{a}. \quad (5.65)$$

Now we show that the first term of the right hand side is upper bounded by 1. To this end, we note that $\mathrm{Sp}(\mathsf{H})$ is discrete and the eigenvalues have almost surely multiplicity one [161, 171]. Furthermore, H is Hermitian and thus if the domain is finite, the spectral theorem indicates that for all $\lambda\in\mathrm{Sp}(\mathsf{H})$,

$$\lim_{\varepsilon\downarrow 0} -i\varepsilon\,\mathsf{R}_{\mathsf{H}}(\lambda+i\varepsilon) = \mathsf{P}_\lambda, \quad (5.66)$$

with $\mathsf{P}_\lambda = |\varphi_\lambda\rangle\langle\varphi_\lambda|$ the projector onto the eigenstate corresponding to eigenvalue λ. Therefore,

$$\begin{aligned}\int_I \big\|G_{\mathcal{G}_{S,S'}}\big(\omega,\alpha;\gamma_I(x)\big)\big\|^2\,d\gamma_I &= \sum_{\lambda\in\mathrm{Sp}(\mathsf{H})\cap I}\|\langle\omega|\mathsf{P}_\lambda\,|\alpha\rangle\|^2\\ &= \sum_{\lambda\in\mathrm{Sp}(\mathsf{H})\cap I}\|\langle\omega|\mathsf{P}_\lambda\,|\alpha\rangle\langle\alpha|\mathsf{P}_\lambda\,|\omega\rangle\|,\\ &= \sum_{\lambda\in\mathrm{Sp}(\mathsf{H})\cap I}\|\langle\omega|\varphi_\lambda\rangle\langle\varphi_\lambda|\alpha\rangle\langle\alpha|\varphi_\lambda\rangle\langle\varphi_\lambda|\omega\rangle\|, \quad (5.67)\end{aligned}$$

where we used $\|\mathsf{M}\|^2 = \|\mathsf{M}\mathsf{M}^\dagger\|$ and $|\alpha\rangle$ and $|\omega\rangle$ are short hand notations for $|\alpha\rangle\otimes\mathsf{I}_S$ and $|\omega\rangle\otimes\mathsf{I}_S$, respectively. Now we remark that $\langle\varphi_\lambda|\alpha\rangle\langle\alpha|\varphi_\lambda\rangle$ is a positive real number which we denote $|\langle\varphi_\lambda|\alpha\rangle|^2$, and similarly $\langle\omega|\varphi_\lambda\rangle\langle\varphi_\lambda|\omega\rangle \equiv |\langle\varphi_\lambda|\omega\rangle|^2\in\mathbb{R}^+$.

[5] We need only consider $z\in\mathbb{R}$ as all the poles of the resolvent are on the real line so that the contour can be brought arbitrarily close to it.

Thus

$$\sum_{\lambda\in\mathrm{Sp}(\mathsf{H})\cap I} \|\langle\omega|\varphi_\lambda\rangle\langle\varphi_\lambda|\alpha\rangle\langle\alpha|\varphi_\lambda\rangle\langle\varphi_\lambda|\omega\rangle\| \leq \sum_{\lambda\in\mathrm{Sp}(\mathsf{H})\cap I} |\langle\varphi_\lambda|\omega\rangle|^2 \sum_{\lambda'\in\mathrm{Sp}(\mathsf{H})\cap I} |\langle\varphi_{\lambda'}|\alpha\rangle|^2, \leq 1. \tag{5.68}$$

Inserting this result in Eq. (5.65) and then in Eq. (5.64) yields the bound

$$\sup_{t\in\mathbb{R}} \big\|\langle\omega|\mathsf{P}_I(\mathsf{H})e^{-i\mathsf{H}t}|\alpha\rangle\big\| \leq \frac{1}{2\pi}\left(\int_I \big\|G_{\mathcal{G}_{S,S'}}\big(\omega,\alpha;\gamma_I(x)\big)\big\|^s\, d\gamma_I\right)^{\frac{1}{2-s}}. \tag{5.69}$$

The remaining steps are entirely similar to those exposed in [161] and [171]. Taking the expectation values on both sides, we note that $1/(2-s) < 1$ and Hölder's inequality yields $\mathbb{E}\big[|f|^{1/(2-s)}\big] \leq \big(\mathbb{E}\big[|f|\big]\big)^{1/(2-s)}$. Now Fubini's theorem gives

$$\mathbb{E}\Big[\sup_{t\in\mathbb{R}} \big\|\langle\omega|\mathsf{P}_I(\mathsf{H})e^{-i\mathsf{H}t}|\alpha\rangle\big\|\Big] \leq \frac{1}{2\pi}\left(\int_I \mathbb{E}\Big[\big\|G_{\mathcal{G}_{S,S'}}\big(\omega,\alpha;\gamma_I(x)\big)\big\|^s\Big]\, d\gamma_I\right)^{\frac{1}{2-s}}. \tag{5.70}$$

To progress further, we recall the M-L inequality, also called estimation lemma:

Proposition 5.6.1 (M-L inequality [172])**.** *Let f be a complex valued function, continuous on a contour γ and such that $|f(z)|$ is bounded for all $z \in \gamma$. Then we have*

$$\Big|\int_\gamma f(z)dz\Big| \leq \ell(\gamma)\, \max_{z\in\gamma} |f(z)|, \tag{5.71}$$

where $\ell(\gamma)$ is the length of the contour γ.

Returning to our proof, we note that if the fractional moments of the Green's function are bounded by an exponential, e.g. $Ce^{-d(\alpha,\omega)/\zeta}$, the M-L inequality implies

$$\mathbb{E}\Big[\sup_{t\in\mathbb{R}} \big\|\langle\omega|\mathsf{P}_I(\mathsf{H})e^{-i\mathsf{H}t}|\alpha\rangle\big\|\Big] \leq C_I\, Ce^{-\frac{d(\alpha,\omega)}{(2-s)\zeta}}, \tag{5.72}$$

where $C_I = (2\pi)^{-1}\big(2|I|\big)^{\frac{1}{2-s}}$ since $2|I|$ is the length of the smallest contour enclosing all poles within I, where $|I|$ the Lebesgue measure of I. This result extends the fractional moment criterion of Aizenman and Molchanov to arbitrary partitions of the system. □

5.6.2 Bounding the expectation of a fractional norm

In this section we establish Lemma 5.5.2, which we restate here for convenience.

Lemma 2. *Let Y be a normally distributed random variable with distribution function ρ. Let $\mathsf{A} \in \mathbb{C}^{n\times n}$ be a normal matrix. Then the following bound holds for any*

$0 < s < 1$,

$$\mathbb{E}_Y\Big[\big\|[Y\mathsf{I}+\mathsf{A}]^{-1}\big\|^s\Big] \leq \frac{(2n)^s}{1-s}\|\rho\|_\infty^s, \tag{5.73}$$

where $\|.\|$ *is the 2-norm.*

Proof. The lemma follows from the layer-cake integral for the expectation [154]. Since A is normal and finite, there exist a unitary matrix U and diagonal matrix D such that $Y\mathsf{I}+\mathsf{A} = \mathsf{U}(Y\mathsf{I}+\mathsf{D})\mathsf{U}^\dagger$. Now let $\mathrm{Sp}(\mathsf{A})$ be the spectrum of A and suppose Y is fixed. Then

$$\begin{aligned}\big\|[Y\mathsf{I}+\mathsf{A}]^{-1}\big\| &= \max_{\lambda\in\mathrm{Sp}(\mathsf{A})}|Y+\lambda|^{-1},\\ &= \Big(\min_{\lambda\in\mathrm{Sp}(\mathsf{A})}|Y+\lambda|\Big)^{-1}.\end{aligned} \tag{5.74}$$

Let $\mathbf{1}[x]$ be the indicator function, which equals 1 if assertion x is true and 0 otherwise. Then the expectation is upper bounded as follows

$$\begin{aligned}\mathbb{E}_Y\Big[\big\|[Y\mathsf{I}+\mathsf{A}]^{-1}\big\|^s\Big] &= \int_{-\infty}^{\infty}\big\|[Y\mathsf{I}+\mathsf{A}]^{-1}\big\|^s d\varrho,\\ &= \int_{-\infty}^{\infty}\int_0^{\|[Y\mathsf{I}+\mathsf{A}]^{-1}\|^s} 1dt\, d\varrho,\\ &= \int_{-\infty}^{\infty}\int_0^{\infty}\mathbf{1}\Big[\big\|[Y\mathsf{I}+\mathsf{A}]^{-1}\big\|^s > t\Big]dt\, d\varrho,\end{aligned} \tag{5.75}$$

where ϱ is the cumulative distribution function. By Fubini's theorem and on using Eq. (5.74) this is

$$\begin{aligned}\mathbb{E}_Y\Big[\big\|[Y\mathsf{I}+\mathsf{A}]^{-1}\big\|^s\Big] &= \int_0^{\infty}\int_{-\infty}^{\infty}\mathbf{1}\Big[\min_{\lambda\in\mathrm{Sp}(\mathsf{A})}|Y+\lambda| < t^{-1/s}\Big]d\varrho\, dt,\\ &= \int_0^{\infty}\min\Big(1, \int_{-\infty}^{\infty}\mathbf{1}\Big[\min_{\lambda\in\mathrm{Sp}(\mathsf{A})}|Y+\lambda| < t^{-1/s}\Big]d\varrho\Big)\, dt.\end{aligned} \tag{5.76}$$

Now let $\mathcal{I}_i = [a_i, a_{i+1}]$, $0 \leq i \leq n-1$ be n intervals such that $\min_{\lambda\in\mathrm{Sp}(\mathsf{A})}|Y+\lambda| = |Y+\lambda_i|$ for all $Y \in \mathcal{I}_i$. Then

$$\begin{aligned}\int_{-\infty}^{\infty}\mathbf{1}\Big[\min_{\lambda\in\mathrm{Sp}(\mathsf{A})}|Y+\lambda| < t^{-1/s}\Big]d\varrho &= \sum_{i=0}^{n}\int_{a_i}^{a_{i+1}}\mathbf{1}\big[|Y+\lambda_i| < t^{-1/s}\big]d\varrho,\\ &\leq \sum_{i=0}^{n}\int_{-\infty}^{\infty}\mathbf{1}\big[|Y+\lambda_i| < t^{-1/s}\big]d\varrho,\\ &= \sum_{i=0}^{n}\varrho\big(|Y+\lambda_i| < t^{-1/s}\big),\\ &\leq 2n\|\rho\|_\infty t^{-1/s},\end{aligned} \tag{5.77}$$

where, by virtue of the fact that ϱ is Hölder continuous[6], for any interval $[a,\, b]$, $\varrho([a,\, b]) \leq |a-b|\, K$ with $K = \sup_{a,\, b} \varrho([a,\, b])/|a-b| \leq 2\|\rho\|_\infty$. The last step of Eq. (5.77) is a rather crude upper bound which may be refined if more is known about the spectrum of M. Inserting this result in Eq. (5.76) gives

$$\begin{aligned}\mathbb{E}_Y\left[\left\|[Y\mathsf{I}+\mathsf{A}]^{-1}\right\|^s\right] &\leq \int_0^\infty \min\left(1, 2n\|\rho\|_\infty t^{-1/s}\right) dt, \\ &= \int_0^m 1dt + 2n\|\rho\|_\infty \int_m^\infty t^{-1/s} dt, \\ &= \frac{n^s}{1-s} 2^s \|\rho\|_\infty^s. \end{aligned} \tag{5.78}$$

We obtain the last line on choosing the m that minimises the bound. □

5.6.3 Proof of the extension lemma

In this section we prove the extension Lemma 5.5.3, which we restate here for convenience.

Lemma 5.5.3. (Extension lemma, based on Aizenman and Warzel [154]) *If there exists $s_{max} < 1$ such that for all s, $0 < s < s_{max}$,*

$$\mathbb{E}\left[\left\|G_{\mathcal{G}_{S,S'}}(\omega, \alpha;\, z)\right\|^s\right] < Ce^{-d(\alpha,\omega)/\zeta}, \tag{5.79}$$

then for all $\tau \in (0,1)$ we have

$$\mathbb{E}\left[\|G_{\mathcal{G}_{S,S'}}(\omega, \alpha;\, z)\|^\tau\right] \leq c[s_1]^{\tau/s_1} 2^{|S|\tau} \|\rho\|_\infty^\tau C^{\frac{s_1-\tau}{s_1}} e^{-\frac{(s_1-\tau)d(\alpha,\omega)}{s_1\zeta}}, \tag{5.80}$$

with $s_{max} < s_1 < 1$.

Proof. Let $0 < s_2 < s_{\max} < \tau < s_1 < 1$. Then since $\tau = s_1(\tau - s_2)/(s_1 - s_2) + s_2(s_1 - \tau)/(s_1 - s_2)$, it follows that

$$\begin{aligned}&\mathbb{E}\left[\|G_{\mathcal{G}_{S,S'}}(\omega, \alpha;\, z)\|^\tau\right] \\ &\qquad = \mathbb{E}\left[\|G_{\mathcal{G}_{S,S'}}(\omega, \alpha;\, z)\|^{s_1 \frac{\tau - s_2}{s_1 - s_2}} \|G_{\mathcal{G}_{S,S'}}(\omega, \alpha;\, z)\|^{s_2 \frac{s_1 - \tau}{s_1 - s_2}}\right].\end{aligned} \tag{5.81}$$

We use Hölder's inequality to separate the above expectation into a product involving two expectations. Let $q_1 = (s_1 - s_2)/(\tau - s_2)$ and $q_2 = (s_1 - s_2)/(s_1 - \tau)$ and

[6] We consider only on the case where ρ is Hölder continuous of order 1, which is the case of the normal distribution. The proof extends well to Hölder continuous distributions of higher order [161].

remark that $q_1^{-1} + q_2^{-1} = 1$. Thus

$$\begin{aligned}\mathbb{E}\Big[\|G_{\mathcal{G}_{S,S'}}(\omega,\alpha;\, z)\|^{\tau}\Big] &\leq \mathbb{E}\Big[\|G_{\mathcal{G}_{S,S'}}(\omega,\alpha;\, z)\|^{q_1 s_1 \frac{\tau-s_2}{s_1-s_2}}\Big]^{1/q_1} \times \\ &\qquad \mathbb{E}\Big[\|G_{\mathcal{G}_{S,S'}}(\omega,\alpha;\, z)\|^{q_2 s_2 \frac{s_1-\tau}{s_1-s_2}}\Big]^{1/q_2}, \\ &= \mathbb{E}\Big[\|G_{\mathcal{G}_{S,S'}}(\omega,\alpha;\, z)\|^{s_1}\Big]^{\frac{\tau-s_2}{s_1-s_2}} \times \\ &\qquad \mathbb{E}\Big[\|G_{\mathcal{G}_{S,S'}}(\omega,\alpha;\, z)\|^{s_2}\Big]^{\frac{s_1-\tau}{s_1-s_2}}. \end{aligned} \tag{5.82}$$

Now $\mathbb{E}\big[\|G_{\mathcal{G}_{S,S'}}(\omega,\alpha;\, z)\|^{s_2}\big] \leq Ce^{-d(\alpha,\omega)/\zeta}$ is exponentially bounded since $s_2 < s_{\max}$. Furthermore, $\mathbb{E}\big[\|G_{\mathcal{G}_{S,S'}}(\omega,\alpha;\, z)\|^{s_1}\big]$ is bounded as well. This follows from Theorem 2.1 of Ref. [154], based on results of Ref. [170]. These results give

$$\|G_{\mathcal{G}_{S,S'}}(\omega,\alpha;\, z)\|^{s_1} \leq c[s_1]\big(2^{|S|}\big)^{s_1}\|\rho\|_{\infty}^{s_1} \tag{5.83}$$

with $c[s_1] = 4^{1-s_1}k^{s_1}/(1-s_1)$ and k a finite universal constant. Then,

$$\mathbb{E}\Big[\|G_{\mathcal{G}_{S,S'}}(\omega,\alpha;\, z)\|^{\tau}\Big] \leq \Big(c[s_1]2^{|S|s_1}\|\rho\|_{\infty}^{s_1}\Big)^{\frac{\tau-s_2}{s_1-s_2}} C^{\frac{s_1-\tau}{s_1-s_2}} e^{-\frac{(s_1-\tau)d(\alpha,\omega)}{\zeta(s_1-s_2)}}. \tag{5.84}$$

Since we may choose s_2 to be arbitrarily small, we obtain for all $0 < \tau < 1$,

$$\mathbb{E}\Big[\|G_{\mathcal{G}_{S,S'}}(\omega,\alpha;\, z)\|^{\tau}\Big] \leq c[s_1]^{\tau/s_1}2^{|S|\tau}\|\rho\|_{\infty}^{\tau}C^{\frac{s_1-\tau}{s_1}} e^{-\frac{(s_1-\tau)d(\alpha,\omega)}{s_1\zeta}}. \tag{5.85}$$

This establishes the lemma. □

5.6.4 Conditional distribution of the configuration potentials

In this section we study the marginal and joint distribution of the configuration potentials.

We begin our study by determining the covariance between any two configuration potentials. To this end, we first introduce some notation. Let $\mathbf{B} = (B_1, \cdots, B_{|S'|})$ be the vector of the random B-fields at the sites comprised in S'. The $\{B_i\}_{i\in S'}$ are iid normal random variables with variance $\mathrm{Var}(B_i) = \sigma_B^2$. Let $\mathbf{v}_\alpha = (v_1^{(\alpha)}, v_2^{(\alpha)}, \cdots, v_{|S'|}^{(\alpha)})$ be the vector of coefficients $a_i^{(\alpha)} = \pm 1$ such that

$$Y_\alpha = \mathbf{v}_\alpha \,.\, \mathbf{B} = \sum_{i=1}^{|S'|} v_i^{(\alpha)} B_i, \tag{5.86}$$

i.e. $v_i^{(\alpha)} = 1$ when the spin at site i is up along z in the configuration α of S'

and $v_i^{(\alpha)} = -1$ otherwise. Because they are sums of the same random B-fields, the configuration potentials are strongly dependent. The following proposition quantifies the covariance between the configuration potentials.

Proposition 5.6.2. *Let $Y_\alpha = \mathbf{v}_\alpha \,.\, \mathbf{B}$, $Y_\beta = \mathbf{v}_\beta \,.\, \mathbf{B}$ and $D_{\alpha,\beta}$ be the Hamming distance between $\mathbf{v}_\alpha$ and $\mathbf{v}_\beta$. Then the covariance $\mathrm{Cov}(Y_\alpha, Y_\beta)$ is*

$$\mathrm{Cov}(Y_\alpha, Y_\beta) = (|S'| - 2D_{\alpha,\beta})\sigma_B^2. \tag{5.87}$$

Proof. We prove the proposition by expanding the configuration potentials in the definition of the covariance,

$$\begin{aligned}\mathrm{Cov}(Y_\alpha, Y_\beta) &= \mathbb{E}[Y_\alpha Y_\beta] - \mathbb{E}[Y_\alpha]\mathbb{E}[Y_\beta], \qquad (5.88)\\ &= \mathbb{E}\Bigg[\Big(\sum_{\substack{i\\ v_i^{(\alpha)}=v_i^{(\beta)}}} v_i^{(\alpha)}B_i + \sum_{\substack{i\\ v_i^{(\alpha)}\neq v_i^{(\beta)}}} v_i^{(\alpha)}B_i\Big)\Big(\sum_{\substack{i\\ v_i^{(\alpha)}=v_i^{(\beta)}}} v_i^{(\beta)}B_i + \sum_{\substack{i\\ v_i^{(\alpha)}\neq v_i^{(\beta)}}} v_i^{(\beta)}B_i\Big)\Bigg] - \mathbb{E}[Y_\alpha]\mathbb{E}[Y_\beta].\end{aligned}$$

Since the $v_i^{(\alpha,\beta)}$ coefficients are ± 1, the expectation of the product is of the form $\mathbb{E}[(a+b)(a-b)]$ and simplifies to

$$\begin{aligned}\mathrm{Cov}(Y_\alpha, Y_\beta) &= \mathbb{E}\Bigg[\Big(\sum_{\substack{i\\ v_i^{(\alpha)}=v_i^{(\beta)}}} v_i^{(\alpha)}B_i\Big)^2\Bigg] - \mathbb{E}\Bigg[\Big(\sum_{\substack{i\\ v_i^{(\alpha)}\neq v_i^{(\beta)}}} v_i^{(\alpha)}B_i\Big)^2\Bigg] - \mathbb{E}[Y_\alpha]\mathbb{E}[Y_\beta],\\ &= (|S'| - j_\alpha - j_\beta + 2l_{\alpha,\beta})\sigma_B^2 + (|S'| - j_\alpha - j_\beta)^2\mu^2\\ &\quad - (j_\alpha + j_\beta - 2l_{\alpha,\beta})\sigma_B^2 - (j_\alpha - j_\beta)^2\mu^2 - (|S'| - 2j_\alpha)\mu(|S'| - 2j_\beta)\mu,\\ &= (|S'| - 2D_{\alpha,\beta})\sigma_B^2, \qquad (5.89)\end{aligned}$$

where $j_\alpha = \#\{v_i^{(\alpha)} : v_i^{(\alpha)} < 0\}_{1\le i\le |S'|}$ is the number of negative entries in $\mathbf{v}_\alpha$ and $l_{\alpha,\beta} = \#\{v_i^{(\alpha)} : v_i^{(\alpha)} < 0,\ v_i^{(\alpha)} = v_i^{\beta}\}_{i\in S'}$ is the number of negative entries $v_i^{(\alpha)}$ such that $v_i^{(\alpha)} = v_i^{(\beta)}$. Finally, we observe that $\mathrm{Cov}(Y_\alpha, Y_\beta) \neq 0$ and Y_α and Y_β are dependent, unless $|S'|$ is even and $D_{\alpha,\beta} = |S'|/2$. In this special case and if both Y_α and Y_β are normally distributed, then they are independent. □

Lemma 5.6.1 (Conditional distributions of the configuration potentials)**.** *Let $\mathbb{S} = S \cup S'$ be a partition of the system and $\mathcal{Y} = \big\{Y_{\alpha_j} = \sum_{i\in S'} B_i(1 - 2\delta_{\downarrow_i,\alpha_j})\big\}_{1\le j\le 2^{|S'|}}$ the ensemble of random configuration potentials affecting S'. For a configuration potential $Y_\alpha \in \mathcal{Y}$, let $E_\alpha \subset \mathcal{Y}$ be an ensemble of $|S'|-1$ configuration potentials, excluding Y_α. Then the configuration potentials of $\{Y_\alpha\} \cup E_\alpha$ are marginally and jointly normal. Furthermore, the variance of the conditional distribution of Y_α knowing all configuration potentials of E_α is at least σ_B.*

Proof. In the situation of interest, all magnetic fields affecting S', $\{B_i\}_{i\in S'}$ are iid normal and are thus also jointly normal. Consequently, the configuration potentials, being linear superpositions of magnetic fields, are marginally and jointly normal.

Therefore, they form a multi-variate normal distribution (MVN) [173], denoted

$$\mathbf{Y} = \mathbf{C} \,.\, \mathbf{B} \sim \mathrm{MVN}(\mathbf{C} \,.\, \mathbb{E}[\mathbf{B}], \mathbf{C} \,.\, \mathrm{Cov}(\mathbf{B}) \,.\, \mathbf{C}^\dagger), \tag{5.90}$$

with $\mathbf{B}$ the random vector of the magnetic fields, $\mathbf{Y}$ the random vector of configuration potentials Y_α and $\mathbf{C} = \left(\mathbf{v}_{\alpha_1}, \cdots, \mathbf{v}_{\alpha_\ell}\right)^{\mathrm{T}}$ is the coefficient matrix. This establishes that $Y_\alpha | \, E_\alpha$ is normal. Thanks to the results of Proposition 5.6.2, the covariance matrix[7] $\mathbf{\Sigma}$ of $\{Y_\alpha\} \cup E_\alpha$ is known

$$\mathbf{\Sigma}_{\beta,\gamma} = (|S'| - 2D_{\beta,\gamma})\sigma_B^2, \qquad Y_\beta,\, Y_\gamma \,\in \{Y_\alpha\} \cup E_\alpha, \tag{5.91}$$

and the variance $\mathrm{Var}(Y_\alpha | \, E_\alpha) = \sigma^2_{Y_\alpha | \, E_\alpha}$ of Y_α knowing E_α follows as

$$\sigma^2_{Y_\alpha | \, E_\alpha} = \left((\mathbf{\Sigma}^{-1})_{\alpha,\alpha} \right)^{-1}. \tag{5.92}$$

A direct calculation shows that this is at least σ_B^2, which is the variance of a single magnetic field. This establishes the lemma. □

5.7 Localisation of sublattice magnetisation

Consider the situation where the SEP is dynamically localised on $\mathcal{G}_{S,S'}$. As we have seen, a finite amount of disorder is always sufficient for this to occur on finite systems. Furthermore, in the situation where sites of S' are well separated throughout the physical lattice $\mathcal{L}$, $\mathcal{G}_{S,S'}$ is the $|S'|$-hypercube and otherwise, $\mathcal{G}_{S,S'} \subseteq \mathcal{H}_{|S'|}$. In this section we show that SEP dynamical localisation implies localisation of the magnetisation of the sublattice S'. This is because, on the hypercube, the distance between two configurations is always greater than or equal to the difference between their number of up-spins. Thus, if the SEP is constrained to stay within a certain distance of its initial configuration, the number of up-spins is also constrained around its initial value.

5.7.1 Localisation of the magnetisation: simple arguments

To formalise these observations, let $|n\rangle = \sum_{\alpha_n} c_{\alpha_n} |\alpha_n\rangle$, $c_{\alpha_n} \in \mathbb{C}$, $\sum_{\alpha_n} |c_{\alpha_n}|^2 = 1$, be an arbitrary superposition of configurations α_n of S' with exactly n up-spins. Similarly let $|m\rangle$ be an arbitrary superposition of configurations of S' with exactly

[7] Unfortunately, conventions require that we denote both the self-energy and the covariance matrix using a sigma. To differentiate the two, we use a bold sigma for the covariance matrix.

m up-spins. Then

$$\mathbb{E}\Big[\sup_t \big\|\langle n|\mathsf{P}_I e^{-i\mathsf{H}t}|m\rangle\big\|\Big] = \sum_{\alpha_n,\,\alpha_m} c^*_{\alpha_n} c_{\alpha_m} \mathbb{E}\big[\sup_t \|\langle \alpha_n|\mathsf{P}_I e^{-i\mathsf{H}t}|\alpha_m\rangle\|\big]. \tag{5.93}$$

In the localised regime $\sup_t \|\langle \alpha_n|\mathsf{P}_I e^{-i\mathsf{H}t}|\alpha_m\rangle\| \leq Ce^{-d(\alpha_n,\,\alpha_m)/\zeta}$ and since on the hypercube $d(\alpha_n,\,\alpha_m) \geq |n-m|$, we have

$$\mathbb{E}\Big[\sup_t \big\|\langle n|\mathsf{P}_I e^{-i\mathsf{H}t}|m\rangle\big\|\Big] \leq C' e^{-|n-m|/\zeta}, \tag{5.94}$$

where

$$C' = \Big|C \sum_{\alpha_n,\,\alpha_m} c^*_{\alpha_n} c_{\alpha_m}\Big| \leq C. \tag{5.95}$$

This simple approach indicates that the fraction of up-spins present at any time in the sublattice S' is localised. Below we derive precise upper and lower bounds for the sublattice magnetisation as a function of the localisation length of S'.

5.7.2 Precise bounds on the magnetisation

In this section we derive bounds for the expected magnetisation M_t of S' at time t. To do so we find a lower bound for the disorder-averaged expected fraction of up-spins present in S' at time t, which is $\mathbb{E}\big[N^+(t)\big] = \mathbb{E}\big[\mathrm{Tr}[\mathsf{P}_I \mathsf{N}(t) \mathsf{P}_I\, \rho_{\mathbb{S}}]\big]$, with $\rho_{\mathbb{S}}$ the density matrix of the system. For simplicity we take it to be of the form $\rho_{\mathbb{S}} = |\psi_{S'} \otimes \varphi_{S'}\rangle\langle \psi_{S'} \otimes \varphi_{S'}|$. The up-spin fraction operator on S' is

$$\mathsf{N}(t) = e^{i\mathsf{H}t} \left(\sum_{n=0}^{|S'|} \lambda_m |m\rangle\langle m| \otimes \mathsf{I}_S \right) e^{-i\mathsf{H}t}, \tag{5.96}$$

where $\lambda_m = 2m/|S'|$ and $|m\rangle = \sum_{\alpha_m} |\alpha_m\rangle$ with α_m any configuration of S' with exactly m up-spins. Using cyclicality of the trace, the expected fraction of up-spins at t is therefore of the form

$$\mathbb{E}\big[N^+(t)\big] = \mathbb{E}\Big[\sum_m \lambda_m \mathrm{Tr}\big[\langle \psi_{S'} \otimes \varphi_{S'}|\mathsf{P}_I e^{i\mathsf{H}t}|m\rangle\langle m|e^{-i\mathsf{H}t}\mathsf{P}_I|\psi_{S'} \otimes \varphi_{S'}\rangle\big]\Big]. \tag{5.97}$$

Noting that $\langle \psi_{S'} \otimes \varphi_{S'}|\mathsf{P}_I e^{i\mathsf{H}t}|m\rangle = \big(\langle m|e^{-i\mathsf{H}t}\mathsf{P}_I|\psi_{S'} \otimes \varphi_{S'}\rangle\big)^\dagger$, we have

$$\mathbb{E}\big[N^+(t)\big] = \sum_m \lambda_m\, \mathbb{E}\Big[\big\|\langle m|e^{-i\mathsf{H}t}\mathsf{P}_I|\psi_{S'} \otimes \varphi_{S'}\rangle\big\|_F^2\Big], \tag{5.98}$$

with $\|\mathsf{A}\|_F^2 = \mathrm{Tr}[\mathsf{A}\mathsf{A}^\dagger]$ the Frobenius norm. Since for any matrix $\mathsf{A} \in \mathbb{C}^{m\times n}$ we have

$\|\mathsf{A}\|_2 \leq \|\mathsf{A}\|_F$, it follows that

$$\mathbb{E}\big[N^+(t)\big] \geq \sum_m \lambda_m \, \mathbb{E}\Big[\big\|\langle m|e^{-i\mathsf{H}t}\mathsf{P}_I|\psi_{S'}\otimes\varphi_{S'}\rangle\big\|^2\Big], \tag{5.99}$$

and using Jensen's inequality

$$\mathbb{E}\big[N^+(t)\big] \geq \sum_m \lambda_m \, \mathbb{E}\Big[\big\|\langle m|e^{-i\mathsf{H}t}\mathsf{P}_I|\psi_{S'}\otimes\varphi_{S'}\rangle\big\|\Big]^2. \tag{5.100}$$

Now the simplest initial state to consider for S' is $|\psi_{S'}\rangle = |\alpha_n\rangle$, where S' is in a single configuration α with exactly n up-spins. Then, expanding $|m\rangle$ on the configuration basis we obtain

$$\mathbb{E}\big[N^+(t)\big] \geq \sum_m \lambda_m \sum_{\alpha_m} \mathbb{E}\Big[\big\|\langle\alpha_m|\mathsf{P}_I e^{-i\mathsf{H}t}|\alpha_n\rangle\big\|\Big]^2. \tag{5.101}$$

In the localised phase, we know that for any two configurations α, ω and at any time $\mathbb{E}\big[\|\langle\omega|\mathsf{P}_I e^{-i\mathsf{H}t}|\alpha\rangle\|\big] \leq Ce^{-d(\alpha,\omega)/\zeta_0}$ for some positive ζ_0. To progress, we assume that there exists a localisation length ζ and time T such that for any $t > T$, the system saturates the localisation bounds on average, i.e. for any two configurations α, ω and $t > T$, we have $\mathbb{E}\big[\|\langle\omega|\mathsf{P}_I e^{-i\mathsf{H}t}|\alpha\rangle\|\big] = Ce^{-d(\alpha,\omega)/\zeta}$. Then we have

$$\mathbb{E}\Big[\big\|\langle\alpha_m|\mathsf{P}_I e^{-i\mathsf{H}t}|\alpha_n\rangle\big\|\Big]^2 = C^2 e^{-2d(\alpha_m,\alpha_n)/\zeta}. \tag{5.102}$$

It follows that

$$\mathbb{E}\big[N^+(t)\big] \geq C^2 \sum_m \lambda_m \sum_{\alpha_m} e^{-2d(\alpha_m,\alpha_n)/\zeta}. \tag{5.103}$$

Now let $\mathcal{N}(|S'|,n,m,d)$ be the number of configurations with m up-spins located at distance d from any configuration with n up-spins on the $|S'|$-hypercube. A combinatorial analysis of the hypercube shows that this is

$$\mathcal{N}(|S'|,n,m,d) = \begin{cases} \binom{n}{d/2+(n-m)/2}\binom{|S'|-n}{d/2-(n-m)/2}, & d+n-m \text{ even}, \\ 0, & \text{otherwise}. \end{cases} \tag{5.104}$$

This leads to the following bounds on the disorder-averaged fraction of up-spins

$$\begin{aligned} \mathbb{E}\big[N^+(t)\big] \geq n^+(\zeta) &= C^2 \sum_m \lambda_m \sum_{d=0}^{|S'|} \mathcal{N}(|S'|,n,m,d) e^{-2d/\zeta}, \\ &= \mathcal{F}(|S'|,n), \end{aligned} \tag{5.105}$$

where we defined $\mathcal{F}(|S'|,n)$ for latter convenience. We could not find an elegant form for this quantity, although it is straightforward to calculate for given values of

$|S'|$. In the strong localisation regime $\zeta \to 0$ we remark that

$$\lim_{\zeta\to 0} n^+(\zeta) = n/|S'|, \tag{5.106}$$

so that $\lim_{\zeta\to 0} \mathbb{E}\big[N^+(t)\big] = N^+(0)$, as expected of a strongly localised system. The bound on $\mathbb{E}\big[N^+(t)\big]$ gives a lower bound on the disorder-averaged magnetization $M(t)$ since $M(t) = \mathbb{E}\big[N^+(t)\big] - 1$. Now up-spins and down-spins can be exchanged in the entire analysis presented here. Exchanging up-spins with down-spins thus leads to a lower bound on the expected number of down-spins $\mathbb{E}\big[N^-(t)\big]$, which is

$$\mathbb{E}\big[N^-(t)\big] \geq n^-(\zeta) = \mathcal{F}(|S'|,\, |S'| - n). \tag{5.107}$$

Thus, the magnetization is bounded by

$$1 - n^-(\zeta) \leq M(t) \leq n^+(\zeta) - 1, \tag{5.108}$$

and in particular, on using Eq. (5.106), we have $\lim_{\zeta\to 0} M(t) = M(0)$.

The above demonstration extends straightforwardly to arbitrary incoherent superposition of configurations available to S', i.e. $\rho_{\mathbb{S}} = \sum_\alpha |c_\alpha|^2 |\alpha\rangle\langle\alpha| \otimes |\varphi_S\rangle\langle\varphi_S|$, $c_\alpha \in \mathbb{C}$ and $\sum_\alpha |c_\alpha|^2 = 1$. As per Eq. (5.100), the disorder-averaged fraction of up-spins is thus bounded by

$$\mathbb{E}\big[N^+(t)\big] \geq \sum_\alpha |c_\alpha|^2 \sum_m \lambda_m \sum_{\alpha_m} \mathbb{E}\Big[\big\|\langle\alpha_m|\mathsf{P}_I e^{-i\mathsf{H}t}|\alpha\rangle\big\|\Big]^2, \tag{5.109}$$

where α_m is any configuration of S' with m up-spins. Using our previous results for all configurations α_n with exactly n up-spins gives

$$\sum_m \lambda_m \sum_{\alpha_m} \mathbb{E}\Big[\big\|\langle\alpha_m|\mathsf{P}_I e^{-i\mathsf{H}t}|\alpha_n\rangle\big\|\Big]^2 \geq \mathcal{F}(|S'|, n). \tag{5.110}$$

Therefore the disorder-averaged fraction of up-spins is bounded as follows

$$\mathbb{E}\big[N^+(t)\big] \geq n^+(\zeta) = \sum_\alpha |c_\alpha|^2 \mathcal{F}\big(|S'|,\, |\alpha|\big), \tag{5.111}$$

where $|\alpha|$ is the number of up-spins in S' when it is in configuration α. Similarly, the disorder-averaged fraction of down-spins is bounded by

$$\mathbb{E}\big[N^-(t)\big] \geq n^-(\zeta) = \sum_\alpha |c_\alpha|^2 \mathcal{F}\big(|S'|,\, |S'| - |\alpha|\big), \tag{5.112}$$

and $1 - n^-(\zeta) \leq M(t) \leq n^+(\zeta) - 1$. Most importantly, using Eq. (5.106), we obtain

$$\lim_{\zeta\to 0} n^+(\zeta) = \sum_\alpha |c_\alpha|^2 \frac{|\alpha|}{|S'|} = N^+(0), \tag{5.113}$$

and similarly for $\mathbb{E}\big[N^-(t)\big]$. These results thus show that for any $\epsilon \geq 0$, there exists a localisation length ζ_0 such that for all $\zeta < \zeta_0$, the magnetisation M_t of S' is closer to its initial value than ϵ, $|M(t) - M(0)| \leq \epsilon$.

5.8 Localisation of sublattice correlations

In this section we calculate the realisation average of the two time correlation function for any two sites i and j of S' with I a bounded interval of energy

$$\tau_{i,j}(t) = \mathbb{E}\Big[\mathrm{Tr}[\mathsf{P}_I \sigma_z^i(t) \mathsf{P}_I \sigma_z^j \rho_{\mathbb{S}}]\Big], \tag{5.114}$$

where $\rho_{\mathbb{S}}$ is the density matrix of the system. For the sake of clarity, from now on we let $|\omega\rangle$ denote $|\omega\rangle \otimes \mathsf{I}_S$ and similarly for $|\alpha\rangle$. First, we remark that

$$\tau_{i,j}(t) = \mathbb{E}\Big[\mathrm{Tr}\big[\mathsf{P}_I e^{i\mathsf{H}t}(\mathsf{I}^i + \sigma_z^i) e^{-i\mathsf{H}t} \mathsf{P}_I \sigma_z^j \rho_{\mathbb{S}}\big]\Big] - \mathrm{Tr}[\sigma_z^j \rho_{\mathbb{S}}], \tag{5.115}$$

with I^i the identity matrix on site i and $\mathrm{Tr}[\sigma_z^j \rho_{\mathbb{S}}]$ is the initial expectation of σ_z^j, which is known. Now we consider the situation where $\rho_{\mathbb{S}} = |\alpha\rangle\langle\alpha| \otimes |\varphi_S\rangle\langle\varphi_S|$. Then

$$\begin{aligned}
&\mathbb{E}\Big[\mathrm{Tr}\big[\mathsf{P}_I e^{i\mathsf{H}t}(\mathsf{I}^i + \sigma_z^i) e^{-i\mathsf{H}t} \mathsf{P}_I \sigma_z^j \rho_{\mathbb{S}}\big]\Big] \\
&\quad = 2\,(-1)^{\delta_{\downarrow_j,\alpha}} \sum_{\omega:\uparrow_i} \mathbb{E}\Big[\mathrm{Tr}\big[\langle\alpha|\mathsf{P}_I e^{i\mathsf{H}t}|\omega\rangle\langle\omega|e^{-i\mathsf{H}t}\mathsf{P}_I|\alpha\rangle\big]\Big], \\
&\quad = 2\,(-1)^{\delta_{\downarrow_j,\alpha}} \sum_{\omega:\uparrow_i} \mathbb{E}\Big[\|\langle\omega|e^{-i\mathsf{H}t}\mathsf{P}_I|\alpha\rangle\|_F^2\Big],
\end{aligned} \tag{5.116}$$

where the sum runs over configurations ω with an up-spin at site i and $\delta_{\downarrow_j,\alpha} = 1$ if j is down in α and 0 otherwise. Then, $\|\mathsf{A}\|_2 \leq \|\mathsf{A}\|_F$ together with Jensen's inequality gives

$$\sum_{\omega:\uparrow_i} \mathbb{E}\Big[\|\langle\omega|e^{-i\mathsf{H}t}\mathsf{P}_I|\alpha\rangle\|_F^2\Big] \geq \sum_{\omega:\uparrow_i} \mathbb{E}\Big[\|\langle\omega|e^{-i\mathsf{H}t}\mathsf{P}_I|\alpha\rangle\|\Big]^2. \tag{5.117}$$

Now, in the localised phase, we know that for any two configurations α, ω and at any time $\mathbb{E}\big[\|\langle\omega|\mathsf{P}_I e^{-i\mathsf{H}t}|\alpha\rangle\|\big] \leq Ce^{-d(\alpha,\omega)/\zeta_0}$ for some positive ζ_0. To progress, we assume that there exists a localisation length ζ and time T such that for any $t > T$, the system saturates the localisation bounds on average, i.e. for any two configurations α, ω and $t > T$, we have $\mathbb{E}\big[\|\langle\omega|\mathsf{P}_I e^{-i\mathsf{H}t}|\alpha\rangle\|\big] = Ce^{-d(\alpha,\omega)/\zeta}$. Then we have

$$\sum_{\omega:\uparrow_i} \mathbb{E}\Big[\|\langle\omega|e^{-i\mathsf{H}t}\mathsf{P}_I|\alpha\rangle\|_F^2\Big] \geq \sum_{\omega:\uparrow_i} C^2 e^{-2d(\alpha,\omega)/\zeta} := \mathcal{K}(|S'|,\,|\alpha|), \tag{5.118}$$

where we have introduced $\mathcal{K}$ for later convenience. This quantity is explicitly given by

$$\mathcal{K}(|S'|,\,|\alpha|) = C^2\delta_{\uparrow_i,\alpha}\sum_{m=1}^{|S'|-1}\sum_{d=0}^{|S'|-1}\mathcal{N}(|S'|-1,|\alpha|-1,m-1,d)e^{-2d/\zeta} + C^2(1-\delta_{\uparrow_i,\alpha})\sum_{m=1}^{|S'|-1}\sum_{d=1}^{|S'|-1}\mathcal{N}(|S'|-1,|\alpha|,m-1,d-1)e^{-2d/\zeta}, \tag{5.119}$$

with $\delta_{\uparrow_i,\alpha}=1$ if α has an up-spin at site i and 0 otherwise and $|\alpha|$ is the number of up-spins in S' when it is in configurations α. We obtain this expression using the results of the previous section. Indeed, recall that $\mathcal{N}(|S'|,n,m,d)$ is the number of configurations with m up-spins at distance d from a configuration with n up-spins on the $|S'|$-hypercube, see Eq. (5.104). Then the number of configurations with m up-spins that have an up-spin at site i at distance d from a configuration with n up-spins with an up-spin at site i is $\mathcal{N}(|S'|-1,n-1,m-1,d)$. Similarly, the number of configurations with m up-spins that have an up-spin at site i at distance d from a configuration with n up-spins with a down-spin at site i is $\mathcal{N}(|S'|-1,n,m-1,d-1)$. We could not obtain an elegant form for the quantity $\mathcal{K}(|S'|,\,|\alpha|)$ although it is straightforward to evaluate for a given value of $|S'|$ and fixed configuration α. Finally, since $\mathcal{K}(|S'|,\,|\alpha|)\geq 0$ and for small ζ, $\mathcal{K}(|S'|,\,|\alpha|)\leq 1$, inserting Eq. (5.119) into Eq. (5.115) gives

$$\begin{cases}\tau_{i,j}(t)\leq 2\mathcal{K}(|S'|,\,|\alpha|)-1, & \text{if spin at site } j \text{ is up in } \alpha,\\ \tau_{i,j}(t)\geq -2\mathcal{K}(|S'|,\,|\alpha|)+1, & \text{otherwise.}\end{cases} \tag{5.120}$$

These bounds can be completed by another set of bounds obtained on repeating the procedure presented above but starting with

$$\tau_{i,j}(t) = \mathrm{Tr}[\sigma_z^j\rho_{\mathbb{S}}] - \mathbb{E}\Big[\mathrm{Tr}\big[\mathsf{P}_I e^{i\mathsf{H}t}(\mathsf{I}^i-\sigma_z^i)e^{-i\mathsf{H}t}\mathsf{P}_I\sigma_z^j\rho_{\mathbb{S}}\big]\Big]. \tag{5.121}$$

We obtain

$$\begin{cases}\tau_{i,j}(t)\geq -2\mathcal{Q}(|S'|,\,|\alpha|)+1, & \text{if spin at site } j \text{ is up in } \alpha,\\ \tau_{i,j}(t)\leq 2\mathcal{Q}(|S'|,\,|\alpha|)-1, & \text{otherwise,}\end{cases} \tag{5.122}$$

with

$$\mathcal{Q}(|S'|,\,|\alpha|) = C^2(1-\delta_{\uparrow_i,\alpha})\sum_{m=1}^{|S'|-1}\sum_{d=0}^{|S'|-1}\mathcal{N}(|S'|-1,|\alpha|-1,m-1,d)e^{-2d/\zeta} + C^2\delta_{\uparrow_i,\alpha}\sum_{m=1}^{|S'|-1}\sum_{d=1}^{|S'|-1}\mathcal{N}(|S'|-1,|\alpha|,m-1,d-1)e^{-2d/\zeta}. \tag{5.123}$$

Taken together Eqs. (5.120) and (5.122) guarantee that once our criterion for many-body dynamical localisation holds for a sublattice comprising $|S'|$ sites, then the correlation between any two spins of any such sublattice is localised in an interval centered on its initial value.

5.9 Summary

We have established a natural criterion characterising dynamical localisation in interacting many-body systems. Focusing on the XYZ Hamiltonian, which effectively does not conserve the number of particles in the system, we have shown explicitly that this criterion is fulfilled for a finite amount of disorder which scales at most exponentially with the system size. Furthermore, once fulfilled, the criterion leads to observable signatures of the localisation. In particular, we have bounded the magnetisation of any sublattice of a dynamically localised system and confirmed our predictions with TEBD simulations. Similarly, we have shown that the correlations between spins at the sites of the sublattice as well as the disorder-averaged magnetic linear response function are constrained in the localised regime.

Our proof relies on the path-sums representation of the system generalised Green's functions. As we have seen in Chapters 2 and 3, this representation is independent of the system Hamiltonian or system partition. For this reason, the proofs and results presented here in the specific case of the XYZ-Hamiltonian hold in a much more general setting. We hope that the path-sums representation, which allows the systematic manipulation of system Green's functions and generalised Green's functions, will contribute to the proof of localisation in infinite interacting many-body systems.

The bound for $\sigma_B^{\min}$ we obtain in Theorem 5.3.3 remains well above the critical disorder observed in simulations, in particular in the XXZ regime where $J_x = J_y$. To tighten the bound further will certainly require the explicit use of characteristic features of the Hamiltonian. Similarly it may not be possible to prove dynamical localisation of infinite interacting many-body systems without using specific properties that only *some* Hamiltonians exhibit. In particular, we believe that systems whose spectrum exhibits persisting gaps in the thermodynamic limit are well suited to proofs of dynamical localisation. Indeed in these situations, the moduli of the entries of the evolution operators are expected to *deterministically* exhibit an exponential decay as a function of distance on the configuration-space, i.e. even in the absence of disorder [81, 82, 80]. While this effect is too weak to cause localisation by itself, it might help control the divergences that appear when bounding the disorder required for the onset dynamical localisation. Interestingly, recent results establish deterministic exponential decay of functions of matrices over C^*-algebra [84]. This implies deterministic bounds for the norms of the generalised Green's functions, which are required to work with non-trivial system partitions $S \neq \emptyset$.

Chapter 6
The Method Generating Theorem

Mathematicians do not study objects, but relations between objects. Thus, they are free to replace some objects by others so long as the relations remain unchanged.

H. Poincaré

6.1 Introduction

Reconsider the results of Chapters 2 and 3. We have demonstrated that all the walks on a (di)graph $\mathcal{G}$ uniquely factorise into nesting products of simple paths and simple cycles, which we have shown are the prime elements of a near-algebra associated with $\mathcal{G}$. Then, we grouped walks that have common prime factors into families and summed over the members of each family. Because these members share a common structure — e.g. they could be of the form $a^k \odot b^l$ with a, b two prime walks and k, l two arbitrary integers — this sum is evaluated exactly, yielding a continued fraction of finite depth; e.g. $\sum_{k,l} a^k \odot b^l = \big(1 - a(1-b)^{-1}\big)^{-1}$. Consequently, the sum of weighted walks which corresponds to the desired matrix function $f\big(\mathsf{M}\big)$ is found to be equivalent to the sum of a few continued fractions, one for each family of walks generated by a simple path.

The factorisation of walks into products of primes that underpins the method of path-sums is not the only possible construction of this type on graphs. In particular, the important points in obtaining resummed expressions for series of walks are the *existence* and *uniqueness* of the factorisation of walks into primes. Indeed, provided both properties are verified, there is a unique way to group walks into families generated by the primes. Furthermore, we are free to construct different walk factorisations based on different definitions for the walk product, e.g. inducing different prime walks. Consequently, as long as the existence and uniqueness properties hold, we can construct as many representations of a matrix function as there are ways to define a walk product. In this chapter, we formalise the above observations with the Method Generating Theorem (MGT) and present three further methods to evaluate matrix functions. For the sake of conciseness we only discuss the case of the resolvent function $\mathsf{R}_\mathsf{M}(s) = (s\mathsf{I} - \mathsf{M})^{-1}$. Finally, we show in the last section that regardless of the type of primes one chooses to work with, a graph $\mathcal{G}$ is, up to an isomorphism, uniquely characterised by the primes it sustains.

Method	Walk product	Primes	Form of $\Sigma_{W_{\mathcal{G};\,\alpha\omega}}$
Power-series	Concatenation $\circ$	Edges	Infinite sum
Primitive series	Self-concatenation $\tilde{\circ}$	Primitive orbits	Infinite sum of fractions
Edge-sums	Dual-nesting $\bar{\odot}$	Edge-primes	Finite continued fraction
Path-sums	Nesting $\odot$	Simple paths & cycles	Finite continued fraction
Language equations	Incomplete nesting $\bigcirc$	Simple paths & cycles	Finite system of equations

Table 6.1: Techniques for evaluating matrix functions stemming from the Method Generating Theorem.

6.2 The method generating theorem

Theorem 6.2.1 (Method Generating Theorem)**.** *Let $\bullet$ be a walk product and* W[.] *a weight function. Let $S_{\mathcal{G}}$ be a subset of $W_{\mathcal{G}}$ such that any walk of $(S_{\mathcal{G}}, \bullet)$ uniquely factorises into products of prime walks and let $\mathcal{F}_\bullet(w)$ be the unique prime factorisation of walk w. Then for any subset $s_{\mathcal{G}} \subseteq S_{\mathcal{G}}$,*

$$\sum_{w \in s_{\mathcal{G}}} w = \sum_{w \in s_{\mathcal{G}}} \mathcal{F}_\bullet(w). \tag{6.1a}$$

Furthermore, if $S_{\mathcal{G}} = W_{\mathcal{G};\alpha\omega}$ and if $\mathrm{W}[\sum_{W_{\mathcal{G};\alpha\omega}} w]$ *is finite, then*

$$\mathsf{R}_{\mathsf{M}}(s) = s^{-1}\mathrm{W}[\sum_{W_{\mathcal{G};\,\alpha\omega}} s^{-\ell(w)}\mathcal{F}_\bullet(w)], \tag{6.1b}$$

with $\ell(w)$ the length of walk w.

Proof. The theorem follows from a walk counting argument. By hypothesis the factorisation a walks into products of prime walks always exists and is unique, therefore $W_{\mathcal{G}} = \{\mathcal{F}_\bullet(w);\, w \in W_{\mathcal{G}}\}$. Then $\Sigma_{\mathcal{G};\,\alpha\omega} = \sum_{w \in W_{\mathcal{G};\,\alpha\omega}} w = \sum_{w \in W_{\mathcal{G};\,\alpha\omega}} \mathcal{F}_\bullet(w)$, which is Eq. (6.1a). Supposing that $\mathrm{W}[\Sigma_{\mathcal{G};\,\alpha\omega}]$ exists, by virtue of Eq. (3.78b), any partition of the resolvent function is given by a sum over weighted walks, $\mathsf{R}_{\mathsf{M}}(s) = s^{-1}\mathrm{W}[\sum_{W_{\mathcal{G};\,\alpha\omega}} s^{-\ell(w)} w]$. Thus, weighting Eq. (6.1a) gives Eq. (6.1b). □

In spite of the apparent simplicity of the theorem, the MGT generates a rich variety of methods, see Table 6.1. For example, consider applying the MGT with the concatenation product: in this situation the prime elements of $(W_{\mathcal{G}}, \circ)$ are the graph edges (length 1 walks). Obviously $\mathcal{F}_\circ(w)$ always exist and is unique since it is just w in edge notation and Eq. (6.1b) is the ordinary power-series expression of the resolvent. The method of path-sums is another example of method that stems from

the MGT, in this case with the walk product being the nesting product. As seen in Chapters 2 and 3, Eq. (6.1b) now takes on the form of a continued fraction which always exists on any finite graph. The nature (series, fractions, etc.) as well as the convergence properties of the method so generated strongly depend on the extent to which the series of factorised forms $\mathrm{W}[\sum_{W_{\mathcal{G};\,\alpha\omega}} \mathcal{F}_\bullet(w)]$ lends itself to resummations. In the next three sections, we present three further methods for evaluating series of walks and matrix functions which stem from the MGT: primitive series, edge-sums and language equations which generate matrix functions through series of fractions, continued fractions and systems of equations, respectively.

6.3 Primitive series

A *primitive orbit* p' (also called *prime path* and *prime walk* [174]) is a cycle which is not a multiple of a shorter cycle, i.e. p' is primitive if and only if there exists no other cycle p such that $p' = p^k$. We denote the set of all primitive orbits off vertex α on $\mathcal{G}$ by $P_{\mathcal{G};\,\alpha}$. If $\mathcal{G}$ has at least two cycles with at least one vertex in common, then $P_{\mathcal{G};\,\alpha}$ is countably infinite. Primitive orbits are best known through their relations with matrix determinants [175] and the Ihara zeta function [174]. Here we show that primitive orbits are the prime elements induced by the self-concatenation walk product which we define. Then, by the MGT, we recast the statics of any partition of a resolvent as series of primitive orbits. We begin with the definition of a novel walk-product: the self-concatenation.

6.3.1 The self-concatenation product

Definition 6.3.1 (Self-concatenation product)**.** Let $w = (\alpha\eta_2 \cdots \eta_\ell\alpha)$ be a cycle of length ℓ off α. Then the operation of self-concatenation is defined by

$$\tilde{\circ} : W_{\mathcal{G}} \times W_{\mathcal{G}} \rightarrow W_{\mathcal{G}}, \tag{6.2a}$$

$$(w, w') \rightarrow w \,\tilde{\circ}\, w' = \begin{cases} w \circ w & \text{if } w = w', \\ 0 & \text{otherwise.} \end{cases} \tag{6.2b}$$

The walk $w \,\tilde{\circ}\, w$ of length 2ℓ consists of w concatenated with itself.

In the spirit of the path-algebra, the self-concatenation product induces an algebraic structure on cycle sets, the self-concatenation algebra:

Definition 6.3.2. The self-concatenation algebra $K\mathcal{G}_{\tilde{\circ}} = (\bigcup_{\alpha\in\mathcal{V}(\mathcal{G})} W_{\mathcal{G};\alpha\alpha}, +, \tilde{\circ})$ is a noncommutative K-algebra whose support set is the set of cycles on $\mathcal{G}$ and with the product of two cycles w, w' given by the self-concatenation product $w \,\tilde{\circ}\, w'$.

Proposition 6.3.1. *The primitive orbits are the irreducible and prime elements of* $K\mathcal{G}_{\tilde{\circ}}$*. Furthermore, every cycle* w *on* $\mathcal{G}$ *factorises uniquely as*

$$\mathcal{F}_{\tilde{\circ}}(w) = p^k, \tag{6.3}$$

where p is a primitive orbit and $k \in \mathbb{N}$.

Proof. Irreducibility: let $p \in P_{\mathcal{G}}$ and suppose p is reducible. Then, since $w \,\tilde{\circ}\, w' = w^2 \delta_{w,w'}$, there exists $p' \in P_{\mathcal{G}}$ and $k \in \mathbb{N}$ with $p = (p')^k \Rightarrow p \notin P_{\mathcal{G}}$, a contradiction. *Existence:* suppose that there exists a cycle w such that $\nexists p \in P_{\mathcal{G}}$ with $w = p^k$, $k \in \mathbb{N}$. Then w is a primitive orbit and $\mathcal{F}_{\tilde{\circ}}(w) = w$. Thus $\mathcal{F}_{\tilde{\circ}}(w)$ always exists. *Uniqueness:* suppose that there exists a cycle w, two primitive orbits p_1 and p_2 and two integers k_1 and k_2 such that $w = p_1^{k_1} = p_2^{k_2}$. Then, since $w \,\tilde{\circ}\, w \neq 0$, we have $p_1 \,\tilde{\circ}\, p_1 \,\tilde{\circ}\, \cdots \,\tilde{\circ}\, p_1 \,\tilde{\circ}\, p_2 \,\tilde{\circ}\, \cdots \,\tilde{\circ}\, p_2 \neq 0$ and therefore $p_1 \,\tilde{\circ}\, p_2 \neq 0 \Rightarrow p_1 = p_2$ and $k_1 = k_2$. Thus $\mathcal{F}_{\tilde{\circ}}(w)$ is unique. *Primality:* let w and w' be two cycles with $w \,\tilde{\circ}\, w' \neq 0$ and let $\mathcal{F}_{\tilde{\circ}}(w \,\tilde{\circ}\, w') = (p')^k$, $p' \in P_{\mathcal{G}}$. If $p | w \,\tilde{\circ}\, w'$, then $p|(p')^k$ and by the uniqueness of the factorisation $p = p'$. Since $w \,\tilde{\circ}\, w' \neq 0$, $w = w'$ and we have $p|w$. Thus p is prime. □

6.3.2 Primitive series for the resolvent

Having established the existence and uniqueness of the factorisation of cycles into primitive orbits, we recast the resolvent into a primitive series using the MGT.

Theorem 6.3.1 (Primitive series for the resolvent)**.** *Let $\mathsf{M} \in \mathbb{C}^{D\times D}$ such that $\rho(\mathsf{M}) < s$ and $\{\mathsf{M}_{\mu\nu}\}$ be an arbitrary partition of M. Then the statics of the partition of the resolvent $\mathsf{R}_{\mathsf{M}}(s)$ are given by the primitive series*

$$\big(\mathsf{R}_{\mathsf{M}}(s)\big)_{\alpha} = \frac{1}{s}\Big[1 + \sum_{p \in P_{\mathcal{G};\,\alpha}} \mathrm{W}[p]\,\big(s^{\ell}\mathsf{I} - \mathrm{W}[p]\big)^{-1}\Big], \tag{6.4}$$

with ℓ the length of the primitive orbit p.

Proof. On $K\mathcal{G}_{\tilde{\circ}}$, the factorised form of any cycle is $\mathcal{F}_{\tilde{\circ}}(w) = p^k$, Eq. (6.3). Then, according to the MGT, when the series for the resolvent exists, i.e. $\rho(\mathsf{M}) < s$ we have

$$\big(\mathsf{R}_{\mathsf{M}}(s)\big)_{\alpha} = s^{-1}\mathrm{W}[(\alpha) + \sum_{P_{\mathcal{G};\,\alpha}} \sum_{k>0} s^{-k\ell} p^k] = s^{-1}\Big[\mathsf{I} + \sum_{P_{\mathcal{G};\,\alpha}} \mathrm{W}[p]\big(s^{\ell}\mathsf{I} - \mathrm{W}[p]\big)^{-1}\Big], \tag{6.5}$$

where (α) is the trivial walk off α. Convergence of the original power-series for $\mathsf{R}_{\mathsf{M}}(s)$ is guaranteed when $\rho(\mathsf{M}) < s$ and so is the convergence of the primitive series. Additionally, if $\mathcal{G}$ has at least two cycles with at least one vertex in common, then the primitive series above has a countably infinite number of terms. Therefore, when $\rho(\mathsf{M}) \geq s$, convergence of the primitive series cannot be guaranteed. □

6.3.3 Prime counting on graphs

A consequence of the existence of primitive series is the "graph-theory prime number theorem", which counts the primitive orbits of a graph and is usually proven via the Ihara zeta-function [174].

Proposition 6.3.2 (Counting the primitive orbits of a graph)**.** *Let $\mathcal{G}$ be a digraph, A is adjacency matrix and α a vertex of $\mathcal{G}$. Then, the number $\pi_\alpha(\ell)$ of primitive orbits of length $\ell > 0$ off α on $\mathcal{G}$ is*

$$\pi_\alpha(\ell) = \sum_{n|\ell} \mu\big(\ell/n\big) \left(\mathsf{A}^n\right)_{\alpha\alpha}, \tag{6.6}$$

with $\mu(x)$ the Möbius function, defined as

$$\mu(n) = \begin{cases} 1, & \text{if } n \text{ is a square-free positive integer with an even number of prime factors,} \\ -1, & \text{if } n \text{ is a square-free positive integer with an odd number of prime factors,} \\ 0, & \text{otherwise.} \end{cases} \tag{6.7}$$

Remark 6.3.1. Usually, backtracks are omitted from the primitive orbits and one counts unrooted primitive orbits rather than rooted ones, i.e. $\ell^{-1}\pi_\alpha(\ell)$. The simple proof provided here extends to this situation upon replacing A with Hashimoto's edge adjacency operator $\mathsf{H}_{\text{Hashimoto}}$ [174].

Proof. First, we express the walk generating function $g_{\mathcal{G};\,\alpha\alpha}(z) = \sum_n z^n(\mathsf{A}^n)_{\alpha\alpha}$ as a primitive series. Since $\big(\mathsf{R}_{\mathsf{M}}(s)\big)_\alpha = s^{-1} g_{\mathcal{G};\,\alpha\alpha}(s^{-1})$, Theorem 6.3.1 yields

$$g_{\mathcal{G};\,\alpha\alpha}(z) = 1 + \sum_{p \in P_{\mathcal{G};\,\alpha}} \frac{z^\ell}{1 - z^\ell} = 1 + \sum_\ell \pi_\alpha(\ell) \frac{z^\ell}{1 - z^\ell}, \tag{6.8}$$

where ℓ is the length of the primitive orbit. Equating powers of z in the above expression with those of $g_{\mathcal{G};\,\alpha\alpha}(z) = \sum_n z^n(\mathsf{A}^n)_{\alpha\alpha}$, we obtain $(\mathsf{A}^n)_{\alpha\alpha} = \sum_{\ell|n} \pi_\alpha(\ell)$. Then the Möbius inversion formula [176] gives the Proposition. □

As noted by A. Terras in her book on zeta functions of graphs [174], the graph-theory prime number theorem is much easier to obtain than its number theory counterpart. This is because primitive orbits are not a good analogue to prime numbers: by Proposition 6.3.1 every cycle w is either a primitive orbit or the multiple of a unique primitive orbit. At the opposite, integers are generally divisible by *more than one* prime. Then, counting primitive orbits is really equivalent to counting integers that are not powers of other integers, $n \neq p^m$, $p, m \in \mathbb{N}^*$, a task much easier than counting primes. A good graph theoretic analogue to prime numbers are the simple cycles, since cycles are typically divisible by more than one simple cycle. We observe that counting the simple cycles is indeed very hard: it is in fact a long standing open problem [177], even on such simple graphs as $\mathbb{Z}^2$.

6.4 Edge-sums

We have seen that the the prime walks appearing in the path-sums are walks forbidden from visiting any vertex more than once. Edge-sums is the edge-equivalent of

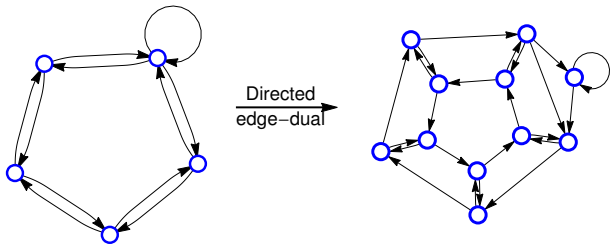

Figure 6.1: A digraph (left) and its directed edge-dual (right).

path-sums: it relies on prime walks that are forbidden from traversing any directed edge more than once. We call these walks, *edge-primes*.

The validity of edge-sums follows directly from that of path-sums thanks to the notion of directed edge-dual $\bar{\mathcal{G}}$ of a graph $\mathcal{G}$. The directed edge-dual is constructed as follows: i) for each *directed* edge of $\mathcal{G}$ draw a vertex in $\bar{\mathcal{G}}$; and ii) place an edge between two vertices of $\bar{\mathcal{G}}$ if the directed edges of $\mathcal{G}$ corresponding to these two vertices follow one another in $\mathcal{G}$. An example of graph and its directed edge-dual is represented in Figure 6.1. This construction implies that a walk on the directed edge-dual $\bar{w} \in W_{\bar{\mathcal{G}}}$ is the directed edge-dual of a unique non-trivial walk on $\mathcal{G}$. Thanks to this relation, we define the dual-nesting product directly from the nesting product.

Definition 6.4.1 (Dual-nesting)**.** Let $(w_1, w_2) \in W_{\mathcal{G}}$ and $(\bar{w}_1, \bar{w}_2) \in W_{\bar{\mathcal{G}}}$ their directed edge-duals. Then the dual-nesting of w_1 with w_2, denoted $w_1 \bar{\odot} w_2$, is the walk whose directed edge-dual is $\bar{w}_1 \odot \bar{w}_2$.

The directed edge-duals of the primes induced by $\bar{\odot}$ are simple paths and simple cycles on $\bar{\mathcal{G}}$. Since a simple path/cycle does not visit any vertex of $\bar{\mathcal{G}}$ more than once, the primes induced by $\bar{\odot}$ do not visit any directed edge more than once: there are the edge-primes. Furthermore, since for any $\bar{w} \in W_{\bar{\mathcal{G}}}$, the factorisation $\mathcal{F}_{\odot}(\bar{w})$ always exists and is unique, so is $\mathcal{F}_{\bar{\odot}}(w)$ for any $w \in W_{\mathcal{G}}$. These observations establish that edge-sums on $\mathcal{G}$ is path-sums on the directed edge-dual graph $\bar{G}$. Consequently, the edge-sum representation of the resolvent function is a continued fraction of finite depth over the edge-primes, we omit the details. If $\mathcal{G}$ is a loopless ordinary undirected connected graph, then the depth of this continued fraction is equal to the length of the longest simple path on $\bar{\mathcal{G}}$. This is necessarily larger than or equal to the length of the longest simple path on $\mathcal{G}$, which reflects the fact that there exists edge-primes which are not simple paths.

6.5 Language equations of matrix functions

Let Σ be a set of symbols, called an alphabet. Then a language L over Σ is any subset of the Kleene star of Σ, denoted Σ^*. The ensemble of rules satisfied by the words of L is the grammar of L [32]. Words of L are generated by this grammar through a set of equations, called the language equations [178, 179]. In this section

we obtain the language equations for the formal languages whose words are the walks on a graph. We do so by factoring walks into incomplete-nesting products of simple cycle and simple paths, incomplete-nesting being a walk-product we define. The connections between language theory and the theory of walk-sets are further explored in §6.6.

6.5.1 The incomplete-nesting product

Just as in the case of the nesting product, incomplete-nesting is more restrictive than concatenation; in particular, the incomplete-nesting of two walks will be non-zero only if they obey the following property:

Definition 6.5.1 (Almost canonical couple)**.** Consider $(a, b) \in W_{\mathcal{G}}^2$ with $b = \beta\,\beta_2 \cdots \beta_q\,\beta$ a cycle off β, and $a = \alpha_1\,\alpha_2 \cdots \beta \cdots \alpha_k$ a walk that visits β at least once. Let $\alpha_j = \beta$ be the last appearance of β in a. Then the couple (a, b) is almost canonical if and only if $\{\alpha_{1<i<j} \neq \beta\} \cap b = \emptyset$; that is, no vertex other than β or α_1 that is visited by a before α_j is also visited by b.

Definition 6.5.2 (Incomplete nesting product)**.** Let $w_1 = (\alpha\,\eta_2 \cdots \omega \cdots \eta_{\ell_1}\alpha)$ be a cycle of length ℓ_1 off α and $w_2 = (\omega\,\kappa_2 \cdots \kappa_{\ell_2}\,\omega)$ be a cycle of length ℓ_2 off ω such that the couple (w_1, w_2) is almost canonical. Then the operation of incomplete nesting is defined by

$$\begin{aligned} \bigcirc :\ W_{\mathcal{G}} \times W_{\mathcal{G}} &\rightarrow W_{\mathcal{G}}, && \text{(6.9a)} \\ (w_1,\, w_2) &\rightarrow w_1 \bigcirc w_2 = (\alpha\,\eta_2 \cdots \omega\,\kappa_2 \cdots \kappa_{\ell_2}\,\omega \cdots \eta_{\ell_1}\alpha). && \text{(6.9b)} \end{aligned}$$

The incomplete nesting of a couple $(w,\, w')$ that is not almost canonical is defined to be $w \bigcirc w' = 0$.

An almost canonical couple (a, b) differs from a canonical one in that the walk b is allowed to visit the first vertex of walk a. This changes the factorisation of walks, e.g. $(121, 212)$ is almost canonical and $12121 = 121 \bigcirc 212$; while $(121, 121)$ is canonical and $12121 = 121 \odot 121$. Because the first vertex α of a may be present in b, a set of cycles such as $W_{\mathcal{G};\,\alpha\alpha}$ will be factored into incomplete-nesting products of sets of walks that are allowed to visit α. These sets, in turn, depend on the set of cycles off α thereby constructing an equation giving $W_{\mathcal{G};\,\alpha\alpha}$ in terms of itself: it is the language equation for $W_{\mathcal{G};\,\alpha\alpha}$.

Definition 6.5.3. The incomplete-nesting algebra $K\mathcal{G}_{\bigcirc} = (W_{\mathcal{G}}, +, \bigcirc)$ is a noncommutative near K-algebra whose support set is the set of walks on $\mathcal{G}$ and with the product of two cycles w, w' given by the incomplete-nesting product $w \bigcirc w'$.

Proposition 6.5.1. *The set of irreducible and prime elements of $K\mathcal{G}_{\bigcirc}$ is exactly $\Pi_{\mathcal{G}} \cup \Gamma_{\mathcal{G}}$. Every walk w on $\mathcal{G}$ factorises uniquely into incomplete-nesting products of simple paths and simple cycles.*

Proof. The proofs that $K\mathcal{G}_{\bigcirc}$ is a near K-algebra and Proposition 6.5.1 are entirely similar to those given in §2.5.1 and §2.5.2, we omit the details. Note, the algorithm that factorises walks into incomplete-nesting products of primes is nearly identical to Algorithm 1. The only difference is that the new algorithm does not distinguish cycles visiting their first vertex more than once from cycles that do not. □

6.5.2 Language equations

Since all walks factorise uniquely into incomplete-nesting products of primes, the MGT gives a novel factorised forms for walk-sets and sums of walks: the language equations.

Theorem 6.5.1 (Language equations)**.** *The prime factorisation of $W_{\mathcal{G}}$ into incomplete-nesting products of sets of simple paths and simple cycles is achieved by the following relations:*

$$W_{\mathcal{G};\,\nu_0\nu_p} = \Big(\big((\,\Pi_{\mathcal{G};\,\nu_0\nu_p} \bigcirc W^*_{\mathcal{G}\setminus\{\nu_0,\cdots,\nu_{p-1}\};\,\nu_p}) \bigcirc \cdots \bigcirc W^*_{\mathcal{G}\setminus\{\nu_0\};\,\nu_1} \big) \bigcirc W^*_{\mathcal{G};\,\nu_0} \Big), \quad (6.10a)$$

$$W_{\mathcal{G};\,\mu_c\mu_c} = \Big(\big((\,\Gamma_{\mathcal{G};\,\mu_c} \bigcirc W^*_{\mathcal{G}\setminus\{\mu_1,\cdots,\mu_{c-1}\};\,\mu_c}) \bigcirc \cdots \bigcirc W^*_{\mathcal{G}\setminus\{\mu_1\};\,\mu_2} \big) \bigcirc W^*_{\mathcal{G};\,\mu_1} \Big), \quad (6.10b)$$

where $(\nu_0\,\nu_1\cdots\nu_{p-1}\,\nu_p) \in \Pi_{\mathcal{G};\,\nu_0\nu_p}$ and $(\mu_c\,\mu_1\cdots\mu_{c-1}\,\mu_c) \in \Gamma_{\mathcal{G};\,\mu_c}$.

Evaluating the incomplete-nesting products explicitly, we see that these equations involve the union $\cup$, the Kleene star $*$ and two-sided concatenations. The weighted equivalent to Theorem 6.5.1 produces a set of equations fulfilled by the desired matrix function. For the sake of conciseness, we present only the case of the resolvent function.

Theorem 6.5.2 (Language equations for the resolvent)**.** *Let $\mathsf{M} \in \mathbb{C}^{D\times D}$, $\{\mathsf{M}\}_{\mu\nu}$ be a partition of M and let $\mathcal{G}$ be the graph of this partition. Then the statics of the partition of the resolvent $\mathsf{R}_{\mathsf{M}}(s)$ fulfill the equations*

$$\big(\mathsf{R}_{\mathsf{M}}(s)\big)_{\alpha\omega} = \sum_{\Pi_{\mathcal{G};\,\alpha\omega}} \big(\mathsf{R}_{\mathsf{M};\,\mathcal{G}\setminus\{\alpha,\eta_2,\cdots,\eta_\ell\}}(s)\big)_{\omega} \mathsf{M}_{\omega\eta_\ell} \cdots \big(\mathsf{R}_{\mathsf{M}}(s)\big)_{\eta_2} \mathsf{M}_{\eta_2\alpha} \big(\mathsf{R}_{\mathsf{M}}(s)\big)_{\alpha}, \quad (6.11a)$$

$$\big(\mathsf{R}_{\mathsf{M}}(s)\big)_{\alpha} = \sum_{\Gamma_{\mathcal{G};\,\alpha}} \big(\mathsf{R}_{\mathsf{M};\,\mathcal{G}\setminus\{\eta_2,\cdots,\eta_\ell\}}(s)\big)_{\alpha} \mathsf{M}_{\alpha\eta_\ell} \cdots \mathsf{M}_{\eta_2\eta_3} \big(\mathsf{R}_{\mathsf{M}}(s)\big)_{\eta_2} \mathsf{M}_{\eta_2\alpha}. \quad (6.11b)$$

Remark 6.5.1 (Schützenberger methodology)**.** The process of weighting the language equations of Theorem 6.5.1 to obtain Theorem 6.5.2 is analogous to the Schützenberger methodology [178]. This methodology was devised to count the number of words in a language L defined through a formal grammar. It consists of weighting the letters of an alphabet by a variable x and the words of L by x^ℓ with ℓ their length. Introducing these weights into the language equations for L and solving them yields the generating function for the language. Clearly, this generating function is just the walk generating function on any graph $\mathcal{G}$ such that there exists two

vertices α and ω and a bijective map Θ with $\Theta(W_{\mathcal{G};\alpha\omega}) = L$ and is consequently the special case of Theorem 6.5.2 corresponding to $x^{-1}\mathsf{R}_{\mathsf{A}}(x^{-1})$, with A the adjacency matrix of $\mathcal{G}$.

Example 6.5.1 (Language equations on $\mathcal{P}_3$)**.** Consider the path-graph on three vertices with a loop on each vertex, denoted $\mathcal{P}_3$. We label the vertices of the graph 1, 2 and 3. Using Theorem 6.5.1 we obtain the language equations for $W_{\mathcal{P}_3;\,11}$, $W_{\mathcal{P}_3;\,22}$ and $W_{\mathcal{P}_3;\,12}$ as follows:

$$W_{\mathcal{P}_3;\,11} = \big\{(1)\big\} \cup \big\{(11) \circ W^*_{\mathcal{P}_3;\,11}\big\} \cup \big\{\big((121) \circ W^*_{\mathcal{P}_3;\,22}\big) \circ W^*_{\mathcal{P}_3\setminus\{2\};\,11}\big\}, \tag{6.12a}$$

$$W_{\mathcal{P}_3;\,22} = \big\{(2)\big\} \cup \big\{(22) \circ W^*_{\mathcal{P}_3;\,22}\big\} \cup \big\{(212) \circ W^*_{\mathcal{P}_3;\,11}\big\} \cup \big\{(232) \circ W^*_{\mathcal{P}_3;\,33}\big\}, \tag{6.12b}$$

$$W_{\mathcal{P}_3;\,12} = \big\{\big((12) \circ W^*_{\mathcal{P}_3\setminus\{1\};\,22}\big) \circ W^*_{\mathcal{P}_3;\,11}\big\}. \tag{6.12c}$$

Remark how $W_{\mathcal{P}_3;\,11}$ and $W_{\mathcal{P}_3;\,22}$ are given in terms of their Kleene stars. This is also true for $W_{\mathcal{P}_3;\,33}$ whose language equation is not shown here. The language equations for the resolvent are obtained upon weighting Eqs. (6.12). Theorem 6.5.2 gives

$$\mathsf{R}_{\mathcal{P}_3}(s)_1 = 1 + \mathsf{w}_{11}\mathsf{R}_{\mathcal{P}_3}(s)_1 + \mathsf{R}_{\mathcal{P}_3\setminus\{2\}}(s)_1\,\mathsf{w}_{12}\mathsf{R}_{\mathcal{P}_3}(s)_2\,\mathsf{w}_{21}, \tag{6.13a}$$

$$\begin{aligned}\mathsf{R}_{\mathcal{P}_3}(s)_2 = 1 + \mathsf{w}_{22}\mathsf{R}_{\mathcal{L}_2}(s)_1 + \mathsf{R}_{\mathcal{P}_3\setminus\{1\}}(s)_2\,\mathsf{w}_{21}\mathsf{R}_{\mathcal{P}_3}(s)_1\,\mathsf{w}_{12} \\ + \mathsf{R}_{\mathcal{P}_3\setminus\{3\}}(s)_2\,\mathsf{w}_{23}\mathsf{R}_{\mathcal{P}_3}(s)_3\,\mathsf{w}_{32},\end{aligned} \tag{6.13b}$$

where $\mathsf{w}_{\nu\mu} = \mathrm{W}[(\mu\nu)]$ is the weight of edge $(\mu\nu)$. Here again the statics of the resolvent are given in terms of themselves and other resolvent statics.

6.6 Unique characterisation of graphs

Graphs are pervasive mathematical objects and an essential tool in the study of large systems. Examples of applications abound where the analysis of complex networks is paramount, ranging from understanding the structure of social relations to evaluating the effects of medications on chains of protein reactions. Yet some basic tasks such as distinguishing or quantifying the similarities between two networks remain very difficult to perform and are the subject of active research in computer science.

A remarkable result of automata theory asserts that a network is, up to an isomorphism, uniquely determined by the set of all walks on it [32]. Thus, in principle, we can perfectly distinguish any two networks by comparing the walks they sustain. This result is seldom used however, for there are infinitely many walks on typical networks of interest. This difficulty is overcome by the fundamental result underlying the MGT and demonstrated in the thesis: there exists walk products such all the walks on any graph factorize uniquely into products of prime walks. This observation reduces the difficulty of comparing the infinitely many walks of two networks to comparing only their primes, of which there may be only a *finite* number, e.g. the simple paths and simple cycles.

To establish this result rigorously, it is first necessary to describe graphs and walks within the framework of language theory. Note, in this section we consider only undirected, i.e. ordinary, graphs. For clarity, we defer all the proofs to §6.6.1.

Definition 6.6.1 (Alphabet on a graph)**.** Let Σ be an alphabet and $\mathcal{G}$ a finite graph. We say that Σ is an alphabet on $\mathcal{G}$ if and only if there exists a map $\Theta : \mathcal{E}(\mathcal{G}) \to \Sigma$ assigning labels to edges. We call Θ the labeling function.

Definition 6.6.2 (Automaton)**.** An automaton $\mathbf{A} = (Q, \Sigma, \delta, i, T)$ is a machine with set of states Q, alphabet Σ, transition function δ, initial state i and final state T. This automaton recognizes a language L if for all words $w \in L$, one can reach T from i following transitions allowed by δ and labeled by letters of Σ.

Definition 6.6.3 (Minimal automaton)**.** The minimal automaton $\mathbf{A}$ recognising a language L is the automaton with the least number of states which recognises L.

Proposition 6.6.1 (Graphs as automata)**.** *Let $\mathcal{G}$ be a finite connected graph and α and ω two vertices of $\mathcal{G}$. Let Σ be an alphabet on $\mathcal{G}$ and Θ the corresponding labeling function. Then the finite non-deterministic automaton*

$$\boldsymbol{A}(\mathcal{G})_{\alpha\omega} = \Big(\mathcal{V}(\mathcal{G}),\, \Sigma,\, \mathcal{E}(\mathcal{G}),\, \alpha,\, \omega\Big), \tag{6.14}$$

recognizes the language $L \equiv \Theta\big(W_{\mathcal{G};\,\alpha\omega}\big)$. Furthermore, if Θ is bijective, then $\boldsymbol{A}(\mathcal{G})_{\alpha\omega}$ is the minimal automaton recognizing L.

Proposition 6.6.1 means that if we regard a walk-set $W_{\mathcal{G};\,\alpha\omega}$ as a formal language L, i.e. if we regard walks on $\mathcal{G}$ as words of L, then the graph $\mathcal{G}$ is the skeleton (the structure) of a finite state machine, $\mathbf{A}(\mathcal{G})_{\alpha\omega}$, which indicates whether a word w belongs to L. Equivalently $\mathbf{A}(\mathcal{G})_{\alpha\omega}$ determines whether a walk w can be made on $\mathcal{G}$. Now a remarkable result from automata theory dictates that the minimal automaton recognizing a language is unique up to an isomorphism [32]. This implies an important result linking graphs and their walk-sets: the skeleton of the minimal machine recognizing a language is uniquely determined by the walks on it.

Proposition 6.6.2 (Characterisation of graphs)**.** *Let $\mathcal{G}$ be a finite connected graph. Then $\mathcal{G}$ is, up to an isomorphism, the unique graph with walk-sets $\{W_{\mathcal{G};\,\alpha\omega}\}_{\alpha,\omega\in\mathcal{V}(\mathcal{G})}$. In other terms, $\mathcal{G}$ is uniquely determined by its walk-sets.*

Using this result to determine whether two graphs are isomorphic is hardly practical: it would entail comparing all the walks on the two graphs. But there are typically infinitely many possible walks on graphs of interest. To resolve this difficulty one needs to characterise uniquely the infinite set of all walks by finitely many objects. This is precisely what we achieve using prime factorisations.

Theorem 6.6.1 (Prime characterisation of graphs)**.** *Let $\mathcal{G}$ be a finite connected graph, $\bullet$ a walk product and $P_{\mathcal{G}}$ the set of all primes induced by $\bullet$. If the factorisation $\mathcal{F}_{\bullet}(w)$ of a walk $w \in W_{\mathcal{G}}$ into $\bullet$-products of primes always exists and is unique, then $\mathcal{G}$ is uniquely determined, up to an isomorphism, by the primes it sustains.*

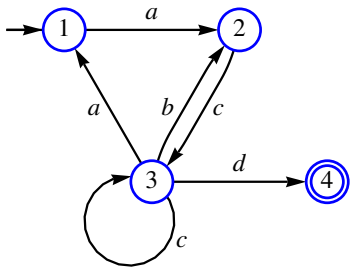

Figure 6.2: Non deterministic finite automaton **A** of Example 6.6.1.

We have seen that for the nesting, dual-nesting and incomplete nesting products, the number of primes on any finite graph is finite. Therefore, in principle it is possible to perfectly distinguish graphs by comparing finitely many prime walks.

Example 6.6.1 (Walk-sets as languages)**.** Let $\mathbf{A}_\mathcal{G}$ be the automaton $\mathbf{A}_\mathcal{G} = (Q,\, \{a,b,c,d\},\, \delta,\, 1,\, 4)$ of Fig. 6.2 with $\mathcal{G} = (Q,\delta)$ its skeleton. We first determine the grammar of $L \equiv \Theta(W_{\mathcal{G};14})$ through its language equations. To find these, we first obtain the unlabeled language equations for $W_{\mathcal{G};14}$. Following Theorem 6.5.1 these are

$$W_{\mathcal{G};14} = \big\{\big((1234 \circ W^*_{\mathcal{G};1}) \circ W^*_{\mathcal{G}\setminus\{1\};22}\big) \circ W^*_{\mathcal{G}\setminus\{1,2\};33}\big\}, \tag{6.15a}$$
$$W_{\mathcal{G};11} = \big\{1\big\} \cup \big\{\big(1231 \circ W^*_{\mathcal{G}\setminus\{2\};33}\big) \circ W^*_{\mathcal{G};22}\big\}, \tag{6.15b}$$
$$W_{\mathcal{G};22} = \big\{2\big\} \cup \big\{232 \circ W^*_{\mathcal{G};33}\big\} \cup \big\{2312 \circ W^*_{\mathcal{G};33}\big\}, \tag{6.15c}$$
$$W_{\mathcal{G};33} = \big\{3\big\} \cup \big\{33 \circ W^*_{\mathcal{G};33}\big\} \cup \{323 \circ W^*_{\mathcal{G};22}\} \cup \big\{(3123 \circ W^*_{\mathcal{G};11}) \circ W^*_{\mathcal{G}\setminus\{1\};22}\big\}. \tag{6.15d}$$

The labeling function is $\Theta(12) = \Theta(31) = a$, $\Theta(23) = \Theta(33) = c$, $\Theta(34) = d$ and $\Theta(x) = \lambda$ with (x) any trivial walk. Consequently, the labeled language equations are, written from right to left,

$$L = dc^+(bc^+)^*\, a\, E_1, \tag{6.16a}$$
$$E_1 = \lambda \cup ac^+E_2a, \qquad E_2 = \lambda \cup bE_3c \cup aaE_3c, \tag{6.16b}$$
$$E_3 = \lambda \cup cE_3 \cup c^+E_2b \cup c^+(bc^+)^*aE_1a, \tag{6.16c}$$

with the languages $E_x \equiv \Theta(W_{\mathcal{G};xx})$ and $c^+ = c^*c$. Eqs. (6.16) characterise the grammar of L, i.e. they represent the production rules for the words of L. The solutions of these language equations are provided by the unique factorisation of walk-sets into nesting-products of simple paths and cycles. Using Theorem 2.3.2 we find

$$L = dc^+(bc^+)^*a\big(ac^+(bc^+)^*a\big)^*, \tag{6.17a}$$
$$E_1 = \big(ac^+(bc^+)^*a\big)^*, \quad E_2 = (bc^+ \cup a^2c^+)^*, \quad E_3 = (c \cup cb \cup ca^2)^*. \tag{6.17b}$$

Since the edge ordering for any walk is preserved by Theorem 2.3.2, Eqs. (6.17)

remains valid for non-commuting letters.

6.6.1 Proofs for the unique characterisation of graphs

▶ We first prove Proposition 6.6.1.

Proof. $\boldsymbol{A}(\mathcal{G})_{\alpha\omega}$ *recognizes* $\Theta\big(W_{\mathcal{G};\,\alpha\omega}\big)$*:* let $Q \equiv \mathcal{V}(\mathcal{G})$, $\delta \equiv \mathcal{E}(\mathcal{G})$, and the initial state i and final state T be respectively α and ω. Any walk $w \in W_{\mathcal{G};\,\alpha\omega}$, starts on i and finishes on T. Furthermore, w only traverses edges $e \in \mathcal{E}(\mathcal{G})$, i.e. transitions allowed by δ with label $\Theta(e) \in \Sigma$, assuming Θ exists as in the proposition. The walk w only visits vertices of $\mathcal{V}(\mathcal{G})$, i.e. states of the set Q of states available to the automaton. Thus any word $\Theta(w) \in \Theta\big(W_{\mathcal{G};\,\alpha\omega}\big)$ is accepted by $\mathbf{A}(\mathcal{G})_{\alpha\omega}$ and $\Theta\big(W_{\mathcal{G};\,\alpha\omega}\big)$ is recognized by $\mathbf{A}(\mathcal{G})_{\alpha\omega}$.

$\boldsymbol{A}(\mathcal{G})_{\alpha\omega}$ *is minimal for* $L \equiv \Theta\big(W_{\mathcal{G};\,\alpha\omega}\big)$ *if* Θ *is bijective:* an automaton $\mathbf{A}$ is the minimal automaton recognizing a language if there exists no automaton $\mathbf{B}$ recognizing L with fewer states than $\mathbf{A}$ [32]. Suppose that there exists such an automaton $\mathbf{B}$ with $\mathcal{G}_{\mathbf{B}}$ its skeleton and suppose first that $\mathcal{G}_{\mathbf{B}}$ is a subgraph of $\mathcal{G}$. Then there exists $\eta \in \mathcal{V}(\mathcal{G})\backslash\mathcal{V}(\mathcal{G}_{\mathbf{B}})$. Since $\mathcal{G}$ is connected and undirected the set of walks $W_{\mathcal{G};\alpha\to\eta\to\omega}$ from α to ω visiting η is non-empty and since Θ is bijective, there exists no walk $w' \in W_{\mathcal{G}\backslash\{\eta\};\alpha\omega}$ such that $\Theta(w') = \Theta(w)$. Thus the automaton $\mathbf{B}$ does not recognize any word of $\Theta\big(W_{\mathcal{G};\alpha\to\eta\to\omega}\big) \subseteq L$ and, consequently, does not recognize L, a contradiction. Now suppose that $\mathcal{G}_{\mathbf{B}}$ is not a subgraph of $\mathcal{G}$. Since by hypothesis both $\mathbf{B}(\mathcal{G}_{\mathbf{B}})$ and $\mathbf{A}(\mathcal{G})_{\alpha\omega}$ recognize L and since $\mathbf{B}(\mathcal{G}_{\mathbf{B}})$ is the minimal automaton for L, it is isomorphic to a reduction of $\mathbf{A}(\mathcal{G})_{\alpha\omega}$, i.e. $\mathcal{G}_{\mathbf{B}}$ is isomorphic to a subgraph of $\mathcal{G}$. As seen before, this leads to a contradiction. □

▶ We now prove Proposition 6.6.2 and Theorem 6.6.1.

Proof. According to [32], the minimal automaton of a language is unique, up to an isomorphism. Furthermore, by Proposition 6.6.1, $\mathbf{A}(\mathcal{G})_{\alpha\omega}$ is the minimal automaton recognizing $\Theta\big(W_{\mathcal{G};\,\alpha\omega}\big)$ for any bijective labeling function Θ. This means that $\mathbf{A}$ is uniquely determined by $\Theta(W_{\mathcal{G};\,\alpha\omega})$ and since $\Theta(.)$ is bijective, it is also uniquely determined by $W_{\mathcal{G};\,\alpha\omega}$. Thus the skeleton $\mathcal{G}$ of $\mathbf{A}$ is uniquely determined by the walks it sustains. This proves Proposition 6.6.2. Finally, in the situation where $\forall\, w \in W_{\mathcal{G}},\ \exists!\mathcal{F}_{\bullet}(w)$, Theorem 6.6.1 follows upon noting that any walk $w \in W_{\mathcal{G}}$ has a unique factorisation into products of primes, i.e. the set of all walks between any two vertices of the graph is uniquely factorable into products of sets of primes. □

6.7 Summary

In this chapter we have demonstrated the Method Generating Theorem, which asserts that if there exists a walk product operation $\bullet$ such that the prime factorisation $\mathcal{F}_{\bullet}(w)$ of any walk w always exists and is unique, then there exists a universal representation of formal walk series and matrix functions that only involves the primes induced by the $\bullet$ product. Illustrating this result, we have presented three novel

representations that also give rise to methods for evaluating matrix functions: the primitive series, the edge-sums and the language equations. Finally, we have shown that regardless of the walk product, a graph is uniquely characterised by the primes it sustains.

The MGT offers remarkable freedom in the definition of walk products in spite of the stringent constraints it imposes on the structure of walk-sets. It is already surprising that walks on any digraph are uniquely factorable into prime elements, but it is striking that this can be achieved in several ways, all simultaneously valid. Additionally, the MGT shows that very little algebraic structure is required of $(W_{\mathcal{G}}, \bullet)$ in order to design new representations of formal walk series and matrix functions. Indeed, only the unique factorisation property is necessary. The weakness of this requirement is truly remarkable, e.g. in the case of the nesting product, unique factorisation holds at the individual walk level in spite of the product lacking a global identity element and being neither commutative nor associative nor even distributive with respect to addition. This stands in sharp contrast with the situation encountered in number theory where the uniqueness property is seemingly very fragile; a fact that was fully recognized during the 19th century with the first examples of number fields where uniqueness does not hold. This observation gave rise to the notion of ideal, a concept of paramount importance in ring theory and abstract algebra [39]. More recently, the study of unique factorisation and ideals was extended to rings with zero divisors [180, 181], some noncommutative rings [182, 183, 40] and nonassociative rings and algebras [184, 185]. So far, ideals of walks have not proven necessary since the uniqueness is so much more robust for walks than for numbers. Why this is so remains unclear. We propose that it is related to an intrinsic structure that walks possess and numbers do not.

Chapter 7
Summary & Future Directions

Our minds are finite, and yet even in those circumstances of finitude, we are surrounded by possibilities that are infinite, and the purpose of human life is to grasp as much as we can out of that infinitude.

A. N. Whitehead

We now summarise the work presented in this thesis, and indicate future directions in which each of the topics broached in the thesis could be further researched.

7.1 Prime factorisation on graphs and the MGT

Summary

In Chapter 2 we demonstrated that walks on digraphs factorise uniquely into nesting products of prime walks. We identified these primes with the simple paths and simple cycles of the digraph. We gave an algorithm factoring individual walks and obtained a recursive formula to factorise walk sets. Using these results we presented an universal continued fraction representation for characteristic series of walks on digraphs and weighted digraphs.

In Chapter 6 we presented the Method Generating Theorem. This Theorem asserts that if there exists a walk product operation $\bullet$ such that the prime factorisation $\mathcal{F}_\bullet(w)$ of any walk w always exists and is unique, then there exists a universal representation of formal walk series and matrix functions that only involves the primes induced by the $\bullet$ product. The method of path-sums is thus seen to be a member of wider family of methods for calculating matrix functions and which rely on different walk products. We illustrate the Method Generating Theorem with three novel methods for the computation of matrix functions: primitive-series, edge-sums and the language equations of matrix functions. Finally, we demonstrate that regardless of the walk product, if $\mathcal{F}_\bullet(w)$ always exists and is unique then any digraph is uniquely characterised, up to an isomorphism, by the primes it sustains.

Future directions

The prime factorisation of walks has found two potential applications beyond those in the realm of matrix computations: i) finding shortest paths between any two vertices of a graph; and ii) distinguishing and characterising graphs.

The first application relies on the observation that if a walk w passes through all the edges of the shortest path between two vertices α and ω on a graph $\mathcal{G}$, then this shortest path can be efficiently read off the prime factorisation of w. Most importantly, this remains true regardless of the order in which the edges of the shortest path are passed through by the walk. Thus, if we dispose of a sufficiently long random walk on $\mathcal{G}$ so as to guarantee with high probability that w traverses all the edges of $\mathcal{G}$, then we can recover the shortest path between any two vertices of $\mathcal{G}$. We must therefore elucidate the probability that a random walk of length ℓ misses an edge of the shortest path between two randomly chosen vertices. This question is currently under investigation in collaboration with researchers of the Statistics Department at the University of Oxford.

The second application consists of designing an algorithm characterising and distinguishing graphs based on the primes they sustain. Since the primes can be efficiently generated from random walks, we could compare graphs using a sample of primes extracted from long random walks. How large must this sample be in order to distinguish graphs with high probability and how long must the random walks be to recover a prime sample of fixed size are widely open questions.

7.2 The method of path-sums

Summary

In Chapter 3 we introduced the method of path-sums which expresses functions of matrices as continued fractions of finite depth. We presented explicit results for a matrix raised to a complex power, the matrix exponential, matrix inverse, and matrix logarithm. We introduced the generalised matrix powers which extend desirable properties of the Drazin inverse to all powers of a matrix. We presented specific formulas for the inverse and exponential of block tridiagonal matrices and evaluated the computational cost of path-sums for functions of tree-structured matrices. Finally, we demonstrated that our approach remains valid for a matrix with non-commuting matrix elements and obtained a generalised heredity principle for the quasideterminants of matrices with non-commuting entries.

Future directions

The accessibility and visibility of the method of path-sums would be greatly enhanced by the development and numerical analysis of an optimized, user-friendly, computer program implementing the method for arbitrary matrix functions. At the core of this program would be an algorithm producing the simple paths and simple cycles of a graph. This algorithm could be a probabilistic one based on factoring long random walks, as discussed in Section 7.1.

A better understanding of the error associated with truncated path-sums expressions is paramount, in particular for applications in physics. The relation between the speed of convergence of path-sums and the exponential decay of matrix func-

tions must be clarified by future research. In this respect, the results of Chapter 5 represent a breakthrough. Indeed, the demonstration of Anderson localisation establishes that for "sufficiently random" matrices M: i) the weight of a fully dressed simple path decays exponentially with its length, on average; and ii) this provokes the exponential localisation of functions of M, on average. In their current form, the arguments yielding these results do not extend to the deterministic case. They point however to a remarkable competition taking place in infinite matrices between the decay of simple path weights as a function of their length ℓ and the increase of the number of simple paths of length ℓ as ℓ grows. When the decay dominates, $f(\mathsf{M})$ is exponentially localised around the sparsity pattern of M. In the opposite situation, $f(\mathsf{M})$ is non-negligible everywhere and everywhere difficult to calculate. Physically, this would mean that the system approaches a phase transition, such as from insulator to conductor, or more generally any quantum phase transition [186].

Finally, we mention the extension of the method of path-sums to the calculation of functions of operators. In particular, we have developed a path-sum approach for solving fractional differential equations which we could not report here due to length concerns.

7.3 Quantum dynamics and many-body Anderson localisation

Summary

In the first part of Chapter 4, we derived the walk-sum lemma for the matrix-exponential relying solely on physical arguments. We considered a quantum system $\mathbb{S}$ to comprise two subsystems S and S' and described the dynamics of S as a superposition of walks undergone by S' on a graph $\mathcal{G}$. This graph is the discrete state space of S': vertices represent configurations of S' while edges represent physical processes allowed by the Hamiltonian and which cause changes in the instantaneous configuration of S'. A walk of S on $\mathcal{G}$ thus represents a succession of configurations of S', i.e. a walk is an history of S'. The weight of this walk carries information about the coupling between S and S' or equivalently, the influence on S of the history of S'. The method of walk-sums is thus the discrete equivalent to Feynman's path-integrals: the dynamics of S results from the superposition of all histories available to S'. This gives a physical interpretation for path-sums in the context of quantum dynamics: dressing vertices by cycles represents the dressing of S by virtual physical processes undergone by S'. Just as in quantum field theory, these processes give rise to a non-zero self-energy, which in the path-sum description is simply a sum over dressed simple cycles. In the second part of Chapter 4, we illustrated the method of walk-sums by solving single particle continuous time quantum random walks. We also investigated the dynamics of Rydberg-excited Mott insulators. In particular, we demonstrated the existence of transient crystals formed by the Rydberg-excitations.

In Chapter 5, we demonstrated dynamical localisation of a strongly interacting

many-body quantum spin system using the method of path-sums. First, we established a criterion describing many-body dynamical localisation. This criterion relies on the results of Chapter 4: considering the system as comprising two ensembles of sites S and S', the dynamics of S is equivalent to that of a single particle, the SEP, undergoing a quantum random walk on the configuration graph of S'. When applied to the SEP, the well known signature of one-body Anderson localisation yields the desired many-body criterion. Second, we showed that there always exists a finite amount of disorder such that this criterion is satisfied. To do so, we used results from Chapters 2 and 3 to describe the dynamics of the SEP with path-sums and identify certain technical properties of these path-sums. We also obtained bounds on the disorder required for the onset of one-body Anderson localisation. Finally, we demonstrated that our criterion for many-body dynamical localisation, when satisfied, yields several experimentally observable consequences. In particular, we demonstrated that the magnetisation of any finite ensemble of lattice sites is localised around its initial value and we obtained a similar result for the correlations between the particles at these sites.

Future directions

A major issue affecting the use of path-sums in physics is the lack of a sound, physically meaningful, criterion to decide a priori if the dynamics of a quantum system can effectively be simulated with the method. This is a key ingredient in the design of successful mathematical techniques for physics. For example, the existence of such a criterion for Time Evolving Block Decimation (TEBD) explains in part its widespread use in physics. Such a criterion must necessarily be related to factors determining the speed of convergence of truncated path-sum expressions, thereby providing yet another incentive to work on this subject. In this regard, the results of Chapter 5 are promising in the way they relate the weight of fully dressed simple paths with localisation of matrix functions.

Concerning the physics of Anderson localisation, the tools used in Chapter 5 permit an analytical exploration of the effects of decoherence and of statistical correlations between the random magnetic fields on the onset of localisation. This would contribute to the study of the interplay between disorder, decoherence and interactions in one-body and many-body systems. A largely unexplored territory.

Bibliography

[1] W. S. Bakr, J. I. Gillen, A. Peng, S. Fölling, and M. Greiner. A quantum gas microscope for detecting single atoms in a Hubbard-regime optical lattice. *Nature* **462**, 74–77 (2009).

[2] J. F. Sherson, C. Weitenberg, M. Endres, M. Cheneau, I. Bloch, and S. Kuhr. Single-atom-resolved fluorescence imaging of an atomic Mott insulator. *Nature* **467**, 6872 (2010).

[3] W. S. Bakr, A. Peng, M. E. Tai, R. Ma, J. Simon, J. I. Gillen, S. Fölling, L. Pollet, and M. Greiner. Probing the superfluid-to-Mott insulator transition at the single-atom level. *Science* **329**, 547–550 (2010).

[4] C. Weitenberg, M. Endres, J. F. Sherson, M. Cheneau, P. Schauß, T. Fukuhara, I. Bloch, and S. Kuhr. Single-spin addressing in an atomic Mott insulator. *Nature* **471**, 319324 (2011).

[5] M. Lewenstein, A. Sanpera, V. Ahufinger, B. Damski, A. Sen De, and U. Sen. Ultracold atomic gases in optical lattices: mimicking condensed matter physics and beyond. *Adv. Phys.* **56**, 243–379 (2007).

[6] R. P. Feynman. Simulating physics with computers. *Int. J. Theor. Phys.* **21**, 467 (1982).

[7] S. Lloyd. Universal quantum simulators. *Science* **273**, 1073 (1996).

[8] A. Steane. Multiple-particle interference and quantum error correction. *Proc. Roy. Soc. Lond. A* **452**, 2551 (1996).

[9] P. W. Shor. Algorithms for quantum computation: Discrete logarithms and factoring. *35th Ann. IEEE Symp. Found.* , 124 (1994).

[10] L. Grover. Quantum mechanics helps in searching for a needle in a haystack. *Phys. Rev. Lett.* **79**, 325 (1997).

[11] S. R. White. Density matrix formulation for quantum renormalization group. *Phys. Rev. Lett.* **69**, 28632866 (1992).

[12] J. I. Cirac and F. Verstraete. Renormalization and tensor product states in spin chains and lattices. *J. Phys. A - Math. Theor.* **42**, 504004 (2009).

[13] G. Vidal. Efficient classical simulation of slightly entangled quantum computations. *Phys. Rev. Lett.* **91**, 147902 (2003).

[14] F. Verstraete, V. Murg, and J. I. Cirac. Matrix product states, projected entangled pair states, and variational renormalization group methods for quantum spin systems. *Adv. Theor. Phys.* **57**, 143–224 (2008).

[15] E. Jeckelman. Density-matrix renormalization group methods for momentum- and frequency-resolved dynamical correlation functions. *Prog. Theor. Phys. Suppl.* **176**, 143–164 (2008).

[16] N. Shibata. Quantum hall systems studied by the density matrix renormalization group method. *Prog. Theor. Phys. Suppl.* **176**, 182–202 (2008).

[17] F. Verstraete and J. I. Cirac. Renormalization algorithms for quantum-many body systems in two and higher dimensions. *arXiv:cond-mat/0407066 [cond-mat.str-el]* (2004).

[18] Z.-C. Gu and X.-G. Wen. Tensor-entanglement-filtering renormalization approach and symmetry-protected topological order. *Phys. Rev. B* **80**, 155131 (2009).

[19] P. Flajolet and R. Sedgewick. *Analytic Combinatorics*. Cambridge University Press, Cambridge, 1st edition, (2009).

[20] N. Biggs. *Algebraic Graph Theory*. Cambridge University Press, Cambridge, 2nd edition, (1993).

[21] P. Flajolet. Combinatorial aspects of continued fractions. *Discrete Math.* **32**, 125–161 (1980).

[22] C. D. Godsil. *Algebraic Combinatorics*. Chapman & Hall, 1st edition, (1993).

[23] D. J. Aldous and J. A. Fill. *Reversible Markov Chains and Random Walks on Graphs*. (2003). Manuscript available electronically at http://www.stat.berkeley.edu/users/aldous/RWG/book.html.

[24] J. R. Norris. *Markov chains*. Cambrigde University Press, Cambridge, 1st edition, (1997).

[25] B. Bollobás. *Modern Graph Theory*. Springer, corrected edition, (1998).

[26] P. Blanchard and D. Volchenkov. *Random Walks and Diffusions on Graphs and Databases: An Introduction*. Springer, 2011 edition, (2011).

[27] T. J. Sheskin. *Markov Chains and Decision Processes for Engineers and Managers*. CRC Press, 1st edition, (2010).

[28] H. C. Berg. *Random walks in biology*. Princeton University Press, Princeton, revised edition, (1993).

[29] S. P. Borgatti, A. Mehra, D. J. Brass, and G. Labianca. Network analysis in the social sciences. *Science* **323**, 892–895 (2009).

[30] G. F. Lawler and V. Limic. *Random walk : a modern introduction*. Cambridge University Press, Cambridge, 1st edition, (2010).

[31] R. Burioni and D. Cassi. Random walks on graphs: ideas, techniques and results. *J. Phys. A - Math. Theor.* **38**, R45 – R78 (2005).

[32] M. V. Lawson. *Finite Automata*. Chapman & Hall/CRC, 1st edition, (2004). See in particular pp. 155-157.

[33] H. Dersken and J. Weyman. Quiver representations. *Notices Amer. Math. Soc.* **52**, 200–206 (2005).

[34] A. Savage. Finite-dimensional algebras and quivers. *arXiv:math/0505082v1 [math.RA]* (2005).

[35] J. Berstel and C. Reutenauer. *Rational Series and Their Languages*. Eatcs Monographs on Theoretical Computer Science, electronic edition, (2008). http://tagh.de/tom/wp-content/uploads/berstelreutenauer2008.pdf.

[36] I. M. Gel'fand, S. Gel'fand, V. Retakh, and R. Lee Wilson. Quasideterminants. *Adv. Math.* **193**, 56–141 (2005).

[37] H.-D. Ebbinghaus, J. Flum, and W. Thomas. *Mathematical Logic*. Springer, New York, 2nd edition, (1994).

[38] M. Auslander, I. Reiten, and S. O. Smalø. *Representation Theory of Artin Algebras*. Cambridge University Press, Cambridge, 1st edition, (1997).

[39] S. Lang. *Algebra*. Springer, 3rd edition, (2002).

[40] T. Y. Lam. *A first course in noncommutative rings*. Springer, 2nd edition, (2001).

[41] G. S. Staples. A new adjacency matrix for finite graphs. *Adv. Appl. Clifford Alg.* **18**, 979–991 (2008).

[42] R. Schott and G. S. Staples. *Operator calculus on graphs*. Imperial College Press, London, 1st edition, (2012).

[43] G. H. Hardy and E. M. Wright. *An introduction to the theory of numbers*. Oxford University Press, Oxford, 6th edition, (2008).

[44] L. C. Eggan. Transition graphs and the star-height of regular events. *Mich. Math. J.* **10**, 385–397 (1963).

[45] H. Bethe. Statistical theory of superlattices. *Proc. Roy. Soc. London Ser A* **150**, 552–575 (1935).

[46] R. J. Baxter. *Exactly solved models in statistical mechanics*. Academic Press, 1st edition, (1982).

[47] C. Cai and Z. Y. Chen. Rouse dynamics of a dendrimer model in the ϑ condition. *Macromolecules* **30**, 5104–5117 (1997).

[48] Z. Y. Chen and C. Cai. Dynamics of starburst dendrimers. *Macromolecules* **32**, 5423–5434 (1999).

[49] M. Droste and W. Kuich. *Semirings and Formal Power Series* in *Handbook of Weighted Automata,* pp. $3 - 28$. Springer, Berlin, Heidelberg, 1st edition, (2009).

[50] J. Sakarovitch. *Rational and Recognisable Power Series* in *Handbook of Weighted Automata,* pp. 105 − 174. Springer, Berlin, Heidelberg, 1st edition, (2009).

[51] N. J. Higham. *Functions of Matrices: Theory and Computation.* Society for Industrial and Applied Mathematics, Philadelphia, 1st edition, (2008).

[52] The On-Line Encyclopedia of Integer Sequences, 2013, *http://oeis.org/.*

[53] K. Ogata. *Discrete-Time Control Systems.* Prentice Hall, 2nd edition, (1995).

[54] G. Meurant. A review on the inverse of symmetric tridiagonal and block tridiagonal matrices. *SIAM. J. Matrix Anal. & Appl.* **13**, 707–728 (1992).

[55] R. K. Mallik. The inverse of a tridiagonal matrix. *Linear Algebra Appl.* **325**, 109–139 (2001).

[56] E. Kılıç. Explicit formula for the inverse of a tridiagonal matrix by backward continued fractions. *Appl. Math. Comput.* **197**, 345357 (2008).

[57] G. Grosso and G. P. Parravicini. *Solid State Physics.* Elsevier, 2nd edition, (2014). See in particular pp. 27-34.

[58] H. Richter. Zum Logarithmus einer Matrix. *Arch. Math.* **2**, 360–363 (1949).

[59] A. Wouk. Integral representation of the logarithm of matrices and operators. *J. Math. Anal. and Appl.* **11**, 131–138 (1965).

[60] S. L. Campbell and C. D. Meyer Jr. *Generalized Inverses of Linear Transformations.* Society for Industrial and Applied Mathematics, Philadelphia, (2009).

[61] N. J. Higham and L. Lin. On p^{th} roots of stochastic matrices. *Linear Algebra Appl.* **435**, 448–463 (2011).

[62] G. W. Cross and P. Lancaster. Square roots of complex matrices. *Linear and Multilinear Algebra* **1**, 289–293 (1974).

[63] A. Cayley. On certain results relating to quaternions. *Philos. Mag.* **26**, 141–145 (1845).

[64] E. Study. Zur Theorie der linearen Gleichungen. *Act. Math.* **42**, 1–61 (1920).

[65] A. Heyting. Die Theorie der linearen Gleichungen in einer Zahlenspezies mit nichtkommutativer Multiplikation. *Math. Ann.* **98**, 465–490 (1928).

[66] A. R. Richardson. Simultaneous linear equations over a division algebra. *P. Lond. Math. Soc.* **55**, 395–420 (1928).

[67] Ø. Ore. Linear equations in non-commutative fields. *Ann. Math.* **32**, 463–477 (1931).

[68] I. M. Gel'fand and V. S. Retakh. Determinants of matrices over noncommutative rings. *Funct. Anal. Appl.* **25**, 91–102 (1991).

[69] I. M. Gel'fand and V. S. Retakh. A theory of noncommutative determinants and characteristic functions of graphs. *Funct. Anal. Appl.* **26**, 231–246 (1992).

[70] I. M. Gel'fand and V. S. Retakh. Quasideterminants, i. *Sel. Math. - New Ser.* **3**, 517–546 (1997).

[71] D. Krob and B. Leclerc. Minor identities for quasideterminants and quantum determinants. *Comm. Math. Phys.* **169**, 1–23 (1995).

[72] P. Etingof, I. Gel'fand, and V. Retakh. Factorization of differential operators, quasideterminants, and nonabelian Toda field equations. *Math. Res. Lett.* **4**, 413–425 (1997).

[73] P. Etingof, I. Gel'fand, and V. Retakh. Nonabelian integrable systems, quasideterminants, and Marchenko lemma. *Math. Res. Lett.* **5**, 1–12 (1998).

[74] P. Etingof and V. Retakh. Quantum determinants and quasideterminants. *Asian J. Math.* **3**, 345–351 (1998).

[75] C. R. Gilson and S. R. Macfarlane. Dromion solutions of noncommutative Davey-Stewartson equations. *J. Phys. A - Math. Theor.* **42**, 235202 (2009).

[76] M. Hassan. Darboux transformation of the generalized coupled dispersionless integrable system. *J. Phys. A - Math. Theor.* **42**, 065203 (2009).

[77] B. Haider and M. Hassan. Quasideterminant solutions of an integrable chiral model in two dimensions. *J. Phys. A - Math. Theor.* **42**, 355211 (2009).

[78] U. Saleem and M. Hassan. Quasideterminant solutions of the generalized Heisenberg magnet model. *J. Phys. A - Math. Theor.* **43**, 045204 (2010).

[79] A. Iserles. How large is the exponential of a banded matrix? *New Zealand J. Math.* **29**, 177–192 (2000).

[80] M. Benzi, P. Boito, and N. Razouk. Decay properties of spectral projectors with applications to electronic structure. *SIAM Review* **55**, 3–64 (2013).

[81] M. Benzi and G. H. Golub. Bounds for the entries of matrix functions with application to preconditioning. *BIT* **39**, 417–438 (1999).

[82] M. Benzi and N. Razouk. Decay bounds and $O(n)$ algorithms for approximating functions of sparse matrices. *Electron. T. Numer. Ana.* **28**, 16–39 (2007).

[83] M. Cramer and J. Eisert. Correlations, spectral gap and entanglement in harmonic quantum systems on generic lattices. *New J. Phys.* **8**, 71 (2006).

[84] M. Benzi and P. Boito. Decay properties of functions of matrices over C*-algebras. *Linear Algebra Appl.* , 25 (2013). DOI: 10.1016/j.laa.2013.11.027.

[85] C. Cohen-Tannoudji, J. Dupont-Roc, and G. Grynberg. *Atom-Photon Interactions*. J. Wiley & Sons, 1st edition, (1998).

[86] G. Niestegge. An approach to quantum mechanics via conditional probabilities. *Found. Phys.* **38**, 241–256 (2008).

[87] Y. Aharonov, P. G. Bergman, and J. L. Lebowitz. Time symmetry in the quantum process of measurement. *Phys. Rev.* **134**, B1410B1416 (1964).

[88] Y. Aharonov and L. Vaidman. Complete description of a quantum system at a given time. *J. Phys A - Math. Gen.* **24**, 2315 (1991).

[89] Y. Aharonov, L. Davidovich, and N. Zagury. Quantum random walks. *Phys. Rev. A* **48**, 1687 (1993).

[90] C. Moore and A. Russell. Quantum walks on the hypercube. *Proc. 6th Int. Workshop Rand. Approx. in Computer Science, LNCS 2483, Springer* , 164 (2002).

[91] C. Moore and A. Russell. Quantum random walks hit exponentially faster. *Proc. 7th Int. Workshop Rand. Approx. in Computer Science, LNCS 2764, Springer* , 354 (2003).

[92] E. Farhi and S. Gutmann. Quantum computation and decision trees. *Phys. Rev. A* **58**, 915 (1998).

[93] A. M. Childs, R. Cleve, E. Deotto, E. Farhi, S. Gutmann, and D. A. Spielman. Exponential algorithmic speedup by quantum walk. *Proc. 35th ACM Symposium on Theory of Computing* , 59–68 (2003).

[94] N. Shenvi, J. Kempe, and K. Birgitta Whaley. Quantum random-walks search algorithm. *Phys. Rev. A* **67**, 052307 (2003).

[95] A. Childs, E. Farhi, and S. Gutmann. An example of the difference between quantum and classical random walks. *Quantum Information Processing* **1**, 35 (2002).

[96] J. Kempe. Quantum random walks - an introductory overview. *Contemporary Physics* **44**, 307 (2003).

[97] A. Ahmadi, R. Belk, C. Tamon, and C. Wendler. On mixing in continuous-time quantum walks on some circulant graphs. *Quantum Information and Computation* **3**, 611 (2003).

[98] H. B. Perets, Y. Lahini, F. Pozzi, M. Sorel, R. Morandotti, and Y. Silberberg. Realization of quantum walks with negligible decoherence in waveguide lattices. *Phys. Rev. Lett.* **100**, 170506 (2008).

[99] A. Peruzzo, M. Lobino, J. Matthews, N. Matsuda, A. Politi, K. Poulios, X. Zhou, Y. Lahini, N. Ismail, K. Worhoff, Y. Bromberg, Y. Silberberg, M. Thompson, and J. O'Brien. Quantum walks of correlated photons. *Science* **329**, 1193515 (2010).

[100] J. O. Owens, M. A. Broome, D. N. Biggerstaff, M. E. Goggin, A. Fedrizzi, T. Linjordet, M. Ams, G. D. Marshall, J. Twamley, M. J. Withford, and A. G. White. Two-photon quantum walks in an elliptical direct-write waveguide array. *New. J. Phys.* **13**, 075003 (2011).

[101] J. C. F. Matthews, K. Poulios, J. D. A. Meinecke, A. Politi, A. Peruzzo, N. Ismail, K. Wörhoff, M. G. Thompson, and J. L. O'Brien. Simulating quantum statistics with entangled photons: a continuous transition from bosons to fermions. *arXiv:1106.1166v1 [quant-ph]* (2011).

[102] L. Sansoni, F. Sciarrino, G. Vallone, P. Mataloni, A. Crespi, R. Ramponi, and R. Osellame. Two-particle bosonic-fermionic quantum walk via integrated photonics. *Phys. Rev. Lett.* **108**, 010502 (2012).

[103] N. Goldman, A. Kubasiak, A. Bermudez, P. Gaspard, M. Lewenstein, and M. A. Martin-Delgado. Non-Abelian optical lattices: Anomalous quantum Hall effect and Dirac fermions. *Phys. Rev. Lett.* **103**, 035301 (2009).

[104] A. Bermudez, L. Mazza, M. Rizzi, N. Goldman, M. Lewenstein, and M. A. Martin-Delgado. Wilson fermions and axion electrodynamics in optical lattices. *Phys. Rev. Lett.* **105**, 190404 (2010).

[105] O. Boada, A. Celi, J. I. Latorre, and M. Lewenstein. Dirac equation for cold atoms in artificial curved spacetimes. *New J. Phys.* **13**, 035002 (2011).

[106] T. Kitagawa, M. S. Rudner, E. Berg, and E. Demler. Exploring topological phases with quantum walks. *Phys. Rev. A* **82**, 033429 (2010).

[107] L. Mazza, A. Bermudez, N. Goldman, M. Rizzi, M. A. Martin-Delgado, and M. Lewenstein. An optical-lattice-based quantum simulator for relativistic field theories and topological insulators. *New. J. Phys.* **14** (2012).

[108] R. C. Busby and W. Fair. Quadratic operator equations and periodic operator continued fractions. *J. Comput. Appl. Math.* , 377–387 (1994).

[109] R. Vescovo. Inversion of block-circulant matrices and circular array approach. *IEEE T. Antenn. Propag.* **45**, 1565–1567 (1997).

[110] J. Anandan and Y. Aharonov. Geometry of quantum evolution. *Phys. Rev. Lett.* **65**, 1697–1700 (1990).

[111] V. Giovannetti, S. Lloyd, and L. Maccone. Quantum limits to dynamical evolution. *Phys. Rev. A* **67**, 052109 (2003).

[112] A. F. Andreev and I. M. Lifshitz. Quantum theory of defects in crystals. *Sov.Phys.-JETP* **29**, 1107–1113 (1969).

[113] G.V. Chester. Speculations on Bose-Einstein condensation and quantum crystals. *Phys. Rev. A* **2**, 256–258 (1970).

[114] A. J. Leggett. Can a solid be "superfluid"? *Phys. Rev. Lett* **25**, 1543–1546 (1970).

[115] E. Kim and M. H. W. Chan. Probable observation of a supersolid helium phase. *Nature* **427**, 225–227 (2004).

[116] V. W. Scarola, E. Demler, and S. Das Sarma. Searching for a supersolid in cold-atom optical lattices. *Phys. Rev. A* **73**, 051601(R) (2006).

[117] L. Pollet, J. D. Picon, H. P. Büchler, and M. Troyer. Supersolid phase with cold polar molecules on a triangular lattice. *Phys. Rev. Lett.* **104**, 125302 (2010).

[118] L. Bonnes and S. Wessel. Supersolid polar molecules beyond pairwise interactions. *Phys. Rev. B* **83**, 134511 (2011).

[119] T. Keilmann, I. Cirac, and R. Roscilde. Dynamical creation of a supersolid in asymmetric mixtures of bosons. *Phys. Rev. Lett.* **102**, 255304 (2009).

[120] D. Jaksch, J. I. Cirac, P. Zoller, S. L. Rolston, R. Côté, and M. D. Lukin. Fast quantum gates for neutral atoms. *Phys. Rev. Lett.* **85**, 2208 (2000).

[121] I. Ryabtsev, D. Tretyakov, and I. Beterov. Applicability of Rydberg atoms to quantum computers. *J. Phys. B: At. Mol. Phys.* **38**, S421 (2005).

[122] M. Müller, I. Lesanovsky, H. Weimer, H. P. Büchler, and P. Zoller. Mesoscopic Rydberg gate based on electromagnetically induced transparency. *Phys. Rev. Lett.* **102**, 170502 (2009).

[123] M. Saffman, T. G. Walker, and K. Molmer. Quantum information with Rydberg atoms. *arXiv:0909.4777v3 [quant-ph]* (2010).

[124] M. Müller H. Weimer, I. Lesanovsky, P. Zoller, and H. P. Büchler. A Rydberg quantum simulator. *Nature Phys.* **6**, 382–388 (2010).

[125] H. Weimer H., R. Löw, T. Pfau, and H. Büchler. Quantum critical behavior in strongly interacting Rydberg gases. *Phys. Rev. Lett.* **101**, 250601 (2008).

[126] S. Ji, C. Ates, and I. Lesanovsky. Two-dimensional Rydberg gases and the quantum hard squares model. *Phys. Rev. Lett* **107**, 060406 (2011).

[127] I. Lesanovsky. Many-body spin interactions and the ground state of a dense Rydberg lattice gas. *Phys. Rev. Lett.* **106**, 025301 (2011).

[128] H. Weimer and H. Büchler. Two-stage melting in systems of strongly interacting Rydberg atoms. *Phys. Rev. Lett.* **105**, 230403 (2010).

[129] J. Schachenmayer, I. Lesanovsky, A. Micheli, and A. J. Daley. Dynamical crystal creation with polar molecules or Rydberg atoms in optical lattices. *New J. Phys.* **12**, 103044 (2010).

[130] T. Pohl, E. Demler, and M. D. Lukin. Dynamical crystallization in the dipole blockade of ultracold atoms. *Phys. Rev. Lett.* **104**, 043002 (2010).

[131] M. Viteau, M. G. Bason, J. Radogostowicz, N. Malossi, D. Ciampini, O. Morsch, and E. Arimondo. Rydberg excitations in Bose-Einstein condensates in quasi-one-dimensional potentials and optical lattices. *Phys. Rev. Lett.* **107**, 060402 (2011).

[132] T. F. Gallagher. *Rydberg Atoms*. Cambridge Monographs on Atomic, Molecular and Chemical Physics. Cambridge University Press, (2005).

[133] T. Wilk, A. Gaëtan, C. Evellin, J. Wolters, Y. Miroshnychenko, P. Grangier, and A. Browaeys. Entanglement of two individual neutral atoms using Rydberg blockade. *Phys. Rev. Lett.* **104**, 010502 (2010).

[134] J. Stanojevic and R. Côté. Many-body dynamics of Rydberg excitation using the Ω-expansion. *arXiv:0801.2396v1* (2008).

[135] R. Heidemann, U. Raitzsch, V. Bendkowsky1, B. Butscher, R. Löw, L. Santos, and T. Pfau. Evidence for coherent collective Rydberg excitation in the strong blockade regime. *Phys. Rev. Lett.* **99**, 163601 (2007).

[136] A. Gaëtan, Y. Miroshnychenko, T. Wilk, A. Chotia, M. Viteau, D. Comparat, P. Pillet, A. Browaeys, and P. Grangier. Observation of collective excitation of two individual atoms in the Rydberg blockade regime. *Nat. Phys.* **5**, 115 – 118 (2009).

[137] G. G. Batrouni and R. T. Scalettar. Phase separation in supersolids. *Phys. Rev. Lett.* **84**, 1599–1602 (2000).

[138] P. Sengupta, L. P. Pryadko, F. Alet, M. Troyer, and G. Schmid. Supersolids versus phase separation in two-dimensional lattice bosons. *Phys. Rev. Lett.* **94**, 207202 (2005).

[139] P. W. Anderson. Absence of diffusion in certain random lattices. *Phys. Rev.* **109**, 1492–1505 (1958).

[140] B. Kramer and A. MacKinnon. Localization: theory and experiment. *Rep. Prog. Phys.* **56**(12), 1469 (1993).

[141] D. Hundertmark. A short introduction to Anderson localization. *Analysis and Stochastics of Growth Processes and Interface Models, Oxford Scholarship Online Monographs* , 194–219 (2007).

[142] I. V. Gornyi, A. D. Mirlin, and D. G. Polyakov. Interacting electrons in disordered wires: Anderson localization and low-T transport. *Phys. Rev. Lett.* **95**, 206603 (2005).

[143] D. M. Basko, I. L. Aleiner, and B. L. Altshuler. Metal insulator transition in a weakly interacting many-electron system with localized single-particle states. *Ann. Phys.* **321**(5), 1126 – 1205 (2006).

[144] V. Oganesyan and D. A. Huse. Localization of interacting fermions at high temperature. *Phys. Rev. B* **75**, 155111 (2007).

[145] M. Žnidarič, T. Prosen, and P. Prelovšek. Many-body localization in the Heisenberg XXZ magnet in a random field. *Phys. Rev. B* **77**, 064426 (2008).

[146] A. Karahalios, A. Metavitsiadis, X. Zotos, A. Gorczyca, and P. Prelovšek. Finite-temperature transport in disordered Heisenberg chains. *Phys. Rev. B* **79**, 024425 (2009).

[147] T. C. Berkelbach and D. R. Reichman. Conductivity of disordered quantum lattice models at infinite temperature: Many-body localization. *Phys. Rev. B* **81**, 224429 (2010).

[148] O. S. Barišić and P. Prelovšek. Conductivity in a disordered one-dimensional system of interacting fermions. *Phys. Rev. B* **82**, 161106 (2010).

[149] C. Monthus and T. Garel. Many-body localization transition in a lattice model of interacting fermions: Statistics of renormalized hoppings in configuration space. *Phys. Rev. B* **81**, 134202 (2010).

[150] I. L. Aleiner, B. L. Altshuler, and G. V. Shlyapnikov. A finite-temperature phase transition for disordered weakly interacting bosons in one dimension. *Nature Physics* **6**(11), 900–904 (2010).

[151] A. Pal and D. A. Huse. Many-body localization phase transition. *Phys. Rev. B* **82**, 174411 (2010).

[152] E. Khatami, M. Rigol, A. Relaño, and A. N. García-García. Quantum quenches in disordered systems: Approach to thermal equilibrium without a typical relaxation time. *Phys. Rev. E* **85**, 050102 (2012).

[153] C. Albrecht and S. Wimberger. Induced delocalization by correlations and interaction in the one-dimensional Anderson model. *Phys. Rev. B* **85**, 045107 (2012).

[154] M. Aizenman and S. Warzel. Localization bounds for multiparticle systems. *Commun. Math. Phys.* **290**, 903–934 (2009).

[155] B. Bauer and C. Nayak. Area laws in a many-body localized state and its implications for topological order. arXiv:1306.5753 [cond-mat.dis-nn], (2013).

[156] B. L. Altshuler, Y. Gefen, A. Kamenev, and L. S. Levitov. Quasiparticle lifetime in a finite system: A nonperturbative approach. *Phys. Rev. Lett.* **78**, 2803–2806 (1997).

[157] E. Canovi, D. Rossini, R. Fazio, G. E. Santoro, and A. Silva. Quantum quenches, thermalization, and many-body localization. *Phys. Rev. B* **83**, 094431 (2011).

[158] G. Carleo, F. Becca, M. Schiró, and M. Fabrizio. Localization and glassy dynamics of many-body quantum systems. *Scientific reports* **2** (2012).

[159] V. Chulaevsky and Y. Suhov. Multi-particle Anderson localisation: Induction on the number of particles. *Math. Phys. Anal. Geom.* **12**, 117–139 (2009).

[160] E. Abrahams, P. W. Anderson, D. C. Licciardello, and T. V. Ramakrishnan. Scaling theory of localization: absence of quantum diffusion in two dimensions. *Phys. Rev. Lett.* **42**, 673 (1979).

[161] D. Hundertmark. On the time-dependent approach to Anderson localization. *Math. Nachr.* **214**, 25–38 (2000).

[162] S. Al-Assam, S. R. Clark, D. Jaksch, and TNT Development Team. TNT Library Alpha Version, http://www.tensornetworktheory.org, (2012).

[163] D. Forster. *Hydrodynamic fluctuations, broken symmetry, and correlation functions.* Addison-Wesley, 3rd edition, (1990).

[164] M. Aizenman and S. Molchanov. Localization at large disorder and at extreme energies: An elementary derivation. *Commun. Math. Phys.* **157**, 245 (1993).

[165] M. Aizenman, J. H. Schenker, R. M. Friedrich, and D. Hundertmark. Finite-volume fractional-moment criteria for Anderson localization. *Commun. Math. Phys.* **224**, 219–253 (2001).

[166] H. Finner. A generalization of Hölder's inequality and some probability inequalities. *Ann. Probab.* **20**, 1893–1901 (1992).

[167] W. Kirsch. A Wegner estimate for multi-particle random hamiltonians. arXiv:0704.2664v1 [math-ph], (2007).

[168] H. Bercovici B. Sz Nagy, C. Foias and L. Kérchy. *Harmonic Analysis of Operators on Hilbert Space*. Springer, 2nd edition, (2010).

[169] K.-J. Engel, R. Nagel, S. Brendle, and M. Campiti. *One-Parameter Semigroups for Linear Evolution Equations*. Springer, 1st edition, (2000).

[170] M. Aizenman, A. Elgart, S. Naboko, J. H. Schenker, and G. Stolz. Moment analysis for localization in random Schrödinger operators. *Invent. Math.* **163**(2), 343–413 (2006).

[171] R. Del Rio, S. Jitomirskaya, Y. Last, and B. Simon. Operators with singular continuous spectrum, IV. Hausdorff dimensions, rank one perturbations, and localization. *J. Anal. Math.* **69**, 153–200 (1996).

[172] E. B. Saff and A. D. Snider. *Fundamentals of Complex Analysis for Mathematics, Science, and Engineering*. Prentice Hall, 1st edition, (1993).

[173] D. W. Wichern R. A. Johnson. *Applied Multivariate Statistical Analysis*. Pearson Higher Ed USA, 6th edition, (2007).

[174] A. Terras. *Zeta Functions of Graphs: A Stroll through the Garden*. Cambridge University Press, Cambridge, 1st edition, (2011).

[175] R. Band, J. M. Harrison, and C. H. Joyner. Finite pseudo orbit expansions for spectral quantities of quantum graphs. *J. Phys. A - Math. Theor.* **45**, 325204 (2012).

[176] T. M. Apostol. *Introduction to Analytic Number Theory*. Springer, (2010).

[177] R. Bauerschmidt, H. Duminil-Copin, J. Goodman, and G. Slade. Lectures on self-avoiding walks. In D. Ellwood, C. Newman, V. Sidoravicius, and W. Werner, editors, *Lecture notes, in Probability and Statistical Physics in Two and More Dimensions*, CMI/AMS Clay Mathematics Institute Proceedings, 2011.

[178] N. Chomsky and M. P. Schützenberger. The algebraic theory of context-free languages. *Comput. Prog. Form. Sys.* **35**, 118–161 (1963).

[179] E. L. Leiss. *Language Equations*. Springer, New York, reprint of the original 1st ed. 1999 edition edition, (2012).

[180] S. Galovich. Unique factorization rings with zero divisors. *Math. Mag.* **51**, 276–283 (1978).

[181] A. G. Agargün, D. D. Anderson, and S. Valdes-Leon. Unique factorization rings with zero divisors. *Commun. Algebra* **27**, 1967–1974 (1999).

[182] P. M. Cohn. Noncommutative unique factorization domains. *Trans. Amer. Math. Soc.* **109**, 313–331 (1963).

[183] A. W. Chatters, M. P. Gilchrist, and D. Wilson. Unique factorization rings. *P. Edinburgh Math. Soc.* **35**, 255–269 (1992).

[184] B. Brown and N. H. McCoy. Prime ideals in nonassociative rings. *Trans. Amer. Math. Soc.* **89**, 245–255 (1958).

[185] P. J. Zwier. Prime ideals in a large class of non associative rings. *Trans. Amer. Math. Soc.* **158**, 257–271 (1971).

[186] S. Sachdev. *Quantum Phase Transitions.* Cambridge University Press, 2nd edition, (2011).